Monitoring Biomass of Mangrove Species Using Remote Sensing Data for Implementation of REDD+ Policies in Vietnam

March 2018

Pham Tien Dat

Monitoring Biomass of Mangrove Species Using Remote Sensing Data for Implementation of REDD+ Policies in Vietnam

Graduate School of Systems and Information Engineering

University of Tsukuba

March 2018

Pham Tien Dat

Monitoring Biomass of Mangrove Species Using Remote Sensing Data for Implementation of REDD+ Policies in Vietnam

Pham Tien Dat

201530148

March 2018

A Dissertation Submitted to

The Graduate school of Systems and Information Engineering,

The University of Tsukuba

in Partial Fulfillment of the Requirements

for the Degree of Doctor of Philosophy in Policy and Planning Sciences

Abstract

Climate change is one of the main concerns and the biggest challenges for all scientists to deal with. The “reducing emissions from deforestation and forest degradation” (REDD+) activities and “blue carbon” programs under the United Nations Framework Convention on Climate Change (UNFCCC) are expected to offer the reliable methods for monitoring, reporting, and verification (MRV) for providing reference levels (or baselines), and protect biodiversity and ecosystem services. Mangroves play an important role in the global carbon cycle by reducing greenhouse gas (GHG) emissions, and mitigating climate change impacts. However, these forests have been lost worldwide, resulting in the systematic loss in carbon stocks. Additionally, the roles of mangrove forests remain poorly quantitatively characterized as compared to other forest ecosystems, due to the practical difficulties and the cost-effectiveness in measuring and monitoring mangrove forests biomass and their carbon stocks. Without a quantitative method for effectively monitoring the carbon stocks in the mangrove ecosystems, sensible policies and actions for conserving mangroves in the context of climate change can be hard to be made.

This thesis presents a novel technology to retrieve biomass of mangrove species and monitor their changes using optical and SAR remote sensing data combined with different machine learning techniques and to promote the implementation of the REDD+ mechanism and blue carbon projects by introducing the willingness to pay (WTP) concept to mangrove ecosystem services. The present thesis selected Hai Phong City located on the northern coast of Vietnam, where the mangroves are distributed within zones I and II of the four mangrove zones in Vietnam as a case study.

This thesis first determines the relationship between biophysical parameters of specific mangrove species and remote sensing data and then attempt to estimate above-ground biomass (AGB) of these species using multiple linear regression models delivered from dual-polarization HH and HV backscatters of ALOS-2 PALSAR-2 imagery. In the second part, the present thesis investigates the applicability of machine learning techniques and remotely sensed data for estimating AGB and carbon stocks of mangrove species. For the improvement of model performance, this thesis test the usability of selected machine learning techniques with an integration of optical and SAR data for the AGB estimation of mangrove forests. In the last part, the thesis shows a case study at Cat Ba Biosphere Reserve for monitoring mangrove forests change between 2010 and 2015, and attempt to evaluate the economic values of mangrove ecosystem services and the social benefits of mangrove restoration in the context of climate change by estimating WTP using contingent valuation method (CVM).

The results of this research show that a high correlation was observed between the means backscattering coefficients (σ^0) of dominant mangrove species at dual polarizations HH and HV and various biophysical parameters, apart from tree density. The sensitivity of (σ^0) at HV polarization is higher than that of (σ^0) at HH polarization. I investigated the use of machine learning techniques for the estimation of AGB of *Sonneratia caseolaris* in a coastal area of Hai Phong city. The performance of the model was assessed using root-mean-square error (RMSE), mean absolute error (MAE), coefficient of determination *(*R^2), and leave-one-out cross-validation. The multi-layer perceptron neural networks (MLPNN) model performed well (R^2= 0.776) and outperformed the machine learning techniques. The MLPNN model-estimated AGB ranged between 2.78 and 298.95 Mg ha^{-1} (average 55.8 Mg ha^{-1}), below-ground biomass ranged between 4.06 and 436.47 Mg ha^{-1} (average 81.47 Mg ha^{-1}), and total carbon stock ranged between 3.22 and 345.65 Mg C ha^{-1} (average 64.52 Mg C ha^{-1}). I also investigated the usability of machine learning techniques with an integration of ALOS-2 PALSAR-2 (L-band HH, HV) and Sentinel-2 multispectral data for the estimation of AGB of mangrove plantation at a coastal area of Hai Phong. The Support Vector Regression (SVR) model showed a satisfactory result (R^2 = 0.596) and estimated AGB ranged between 36.22 and 230.14 Mg ha^{-1} (average = 87.67 Mg ha^{-1}). I conclude that ALOS-2 PALSAR-2 data can be accurately used with MLPNN model for estimating mangrove forest biomass and an integration of ALOS-2 PALSAR-2 and Sentinel-2 data can be accurately used with SVR model for estimating the AGB of mangrove plantations in tropical areas. The findings provide useful information and understanding of the spatial distribution of AGB and carbon stocks for different mangrove species.

CVM was employed to estimate household WTP for mangrove restoration, drawing upon data from a survey of 205 respondents in a coastal commune of the biosphere reserve. The results showed that gender, education level, occupation, the participation of respondents in mangrove restoration activities, and the attitude of respondents toward future climate scenarios were significant factors influencing their WTP for a mangrove restoration project. The estimation yielded a mean WTP at 192,780 VND (US$8.64) and 712.3 million VND (US$31,943) as the total annual benefit for the villagers in the study area. The current work can provide significant comment regarding Payment for Ecosystem Services (PES) for developing regional and national blue carbon trading markets. This will support provincial decision making on mangrove conservation and management. The results of this study may promote the implementation of mangrove conservation and restoration strategies in climate change mitigation approaches such as REDD+ and blue carbon programs.

Keywords: *Blue carbon, climate change, contingent valuation method, mangrove species, mangrove restoration, machine learning, ALOS PALSAR, Sentinel-2, REDD+, willingness to pay.*

Acknowledgements

First of all, I would like to express my sincere thanks to my former academic supervisor Prof. Kunihiko Yoshino for his comments and suggestions about this research. I am also highly thankful to Prof. Naoko Kaida for supervising me during the last year of the doctoral program and for her valuable advices and suggestions on the CVM for mangrove ecosystem services valuation.

Furthermore, I would like to thank to all committee members Prof. Kenlo Nasahara, Prof. Akinobu Murakami and Dr. Tuan Phung-Duc for their useful comments on the Ph.D. thesis. I really appreciate their time for reading entire this thesis.

Big thanks go to the MEXT (Ministry of Education, Culture, Sports, Science, and Technology), Japanese Government for financial support to pursue my Ph.D. degree at the Graduate School of Systems and Information Engineering, University of Tsukuba, Japan. Moreover, I have received lots of assistance in my daily life, which made me feel very happy and enjoy studying and living in Japan.

My gratitude and thanks go to Prof. Dr. Phan Nguyen Hong and Prof. Dr. Nguyen Hoang Tri who gave me very nice advice in choosing a case study and recommended useful books for this thesis. I extend thanks for help and kind support to Associate Prof. Dieu Tien Bui at University College of Southeast Norway in machine learning techniques for my Ph.D. study.

The Center for Agricultural Research and Ecological Studies (CARES), Vietnam National University of Agriculture (VNUA), Vietnam are thanked for providing useful data, textbooks and references for this thesis. I would like to thank Prof. Dr. Tran Duc Vien, who is a former rector of VNUA and a director of CARES and to my colleagues at CARES for their support during fieldwork.

I am also thankful to the chairpersons of the People's Committee in the four coastal districts in Hai Phong city, and the headmen, People committees, farmers' association, and the Security Guard Groups of Dai Hop, Kien Thuy district; Bang La, Do Son district; Vinh Quang, Tien Lang district and Phu Long – Cat Ba Biosphere Reserve, Cat Hai district who assisted me during this Ph.D. study. Without their help, I could not have undertaken the surveys successfully or gained worthwhile results.

Finally, I would love to thank to my family, who always encouraged me during the time I have been studying in Japan. Last but not least, special thanks to my wife and my daughter who are always with me, love and encouragement makes me do my best and have more confidence to study. From the bottom of my heart, I would love to say thank all of you, without your love and encouragement I could complete well the Ph.D. degree. I love you all and highly appreciate your support and encouragement.

Table of Contents

List of Tables

List of Figures

List of Papers

Peer-reviewed Publications

1. **Tien Dat Pham**, Dieu Tien Bui, Kunihiko Yoshino, Nga Nhu Le, 2018. Optimized Rule-Based Logistic Model Tree Algorithm for Mapping Mangrove Species Using ALOS PALSAR Imagery and GIS in the Tropical Region. *Environmental Earth Sciences*, Springer Berlin Heidelberg. **(Accepted)**
2. Sasan Vafaei, Javad Soosani, Kamran Adeli, Hadi Fadaei, Hamed Naghavi, **Tien Dat Pham,** Dieu Tien Bui, 2018. Improving Accuracy Estimation of Forest Aboveground Biomass Based on Incorporation of ALOS-2 PALSAR-2 and Sentinel-2 Imagery and Machine Learning: A Case Study at the Hyrcanian Forest Area (Iran). *Remote Sensing*, **10**(2), 172; http://dx.doi.org/10.3390/rs10020172
3. **Tien Dat Pham**, Kunihiko Yoshino, Naoko Kaida, 2018. Monitoring Mangrove Forest changes in Cat Ba Biosphere Reserve using ALOS PALSAR Imagery and a GIS-based Support Vector Machine Algorithm. In: Tien Bui D., Ngoc Do A., Bui HB., Hoang ND. (eds) *"Advances and Applications in Geospatial Technology and Earth Resources".* GTER 2017. Springer, Cham. http://dx.doi.org/10.1007/978-3-319-68240-2_7
4. **Tien Dat Pham**, Kunihiko Yoshino, 2017. Aboveground biomass estimation of mangrove species using ALOS-2 PALSAR imagery in Hai Phong City, Vietnam. *Journal of Applied Remote Sensing*, **11**(2): 026010, http://dx.doi.org/10.1117/1.JRS.11.026010 .
5. **Tien Dat Pham**, Kunihiko Yoshino, Dieu Tien Bui, 2017. Biomass estimation of *Sonneratia caseolaris* (l.) Engler at a coastal area of Hai Phong city (Vietnam) using ALOS-2 PALSAR imagery and GIS- based multi-layer perceptron neural networks. *GIScience & Remote Sensing*, **54**(3): 329-353. http://dx.doi.org/10.1080/15481603.2016.1269869
6. **Tien Dat Pham**, Kunihiko Yoshino, 2016. Characterization of mangrove species using ALOS-2 PALSAR in Hai Phong city, Vietnam. *IOP Conference Series Earth and Environmental Science* 06/2016; **37**(1):012036., http://dx.doi.org/10.1088/1755-1315/37/1/012036
7. **Tien Dat Pham**, Kunihiko Yoshino, 2016. Impact of Mangrove Management Systems on Mangrove Change in the Northern coast of Vietnam. *Tropics*, **24**(4): 141-151: http://doi.org/10.3759/tropics.24.141
8. **Tien Dat Pham**, Kunihiko Yoshino, 2015. Mangrove Mapping and Change Detection Using Multi-temporal Landsat imagery in Hai Phong city, Vietnam. *The International Symposium on Cartography in Internet and Ubiquitous Environments 2015*, March 17th to 19th, 2015. Tokyo, Japan. http://ubimap.csis.u-tokyo.ac.jp/index.php/top-ciu2015
9. Mohamed Kefi, **Tien Dat Pham**, Kenichi Kashiwagi, Kunihiko Yoshino, 2016. Identification of irrigated olive growing farms using remote sensing techniques. *Euro-Mediterranean Journal for Environmental Integration* 12/2016; **1**(1), http://dx.doi.org/10.1007/s41207-016-0004-7

Under review

1. **Tien Dat Pham**, Naoko Kaida, Kunihiko Yoshino, Xuan Huu Nguyen, Hao Thi Nguyen. Willingness to Pay for Mangroves restoration in the context of climate change in the Cat Ba Biosphere Reserve, Vietnam. **(Under review in Marine Policy).**
2. **Tien Dat Pham**, Dieu Tien Bui, Kunihiko Yoshino, Nga Nhu Le. Estimating Aboveground Biomass of Mangrove Plantation in the Northern Coast of Vietnam using machine learning techniques with an integration of ALOS-2 PALSAR-2 and Sentinel-2A data. (**Under review in International Journal of Remote Sensing).**

List of Abbreviations

ALOS	Advanced Land Observing Satellite
ASL	Above Sea Level
CARES	Centre for Agricultural Research and Ecological Studies
CVM	Contingent Valuation Method
DEM	Digital Elevation Model
ESA	European Space Agency
GIS	Geographic Information System
GEF	Global Environment Facility
GHG	Greenhouse Gas
GPS	Global Position System
MARD	Ministry of Agriculture and Rural Development
MERC	Mangrove Ecosystem Research Centre
NDVI	Normalized Difference Vegetation Index
REDD	Reducing Emissions from Deforestation and Forest Degradation
SRTM	Shuttle Radar Topographic Mission
PALSAR	Phased Array type L-band Synthetic Aperture Radar
PES	Payment for Ecosystem Services
UNEP	United Nations Environment Programme
UNFCCC	United Nations Framework Convention on Climate Change
VHR	Very High Resolution satellite images
VNUA	Vietnam National University of Agriculture
WGS84	World Geodetic System 1984
WTP	Willingness to Pay

Chapter 1

Introduction

Chapter 1 provides general information on the motivation and necessaries for current Ph.D. work. This chapter shows the research questions, the research objectives and frameworks. The following parts are thesis contribution to the scientific literature and structure of this thesis.

1.1. Background

1.1.1. Climate change and global carbon cycle

Climate change is a global environmental issue that has significant impacts on human and natural ecosystems. This phenomenon has resulted in an increased temperature in many regions, increasing number of climate extremes such as droughts, wildfires, rising sea level, tropical storms [1, 2] (Fig. 1.1). Global climate change is widely recognized as the biggest challenge facing the planet. Most scientists believe that the main cause of the current global warming problem is due to the greenhouse gases (GHG) effects, of which carbon dioxide (CO_2) is the most significant one. More importantly, human activities particularly fossil fuel burning and deforestation has released billion of tons of CO_2 into the atmosphere, resulting in unbalance of the global carbon cycle [3]. However, according to the IPCC 2007, the number of the flux of CO_2 in and out of terrestrial and ocean zones are much larger than those from fossil fuels and land-use change as shown in Figure 1.2. Therefore, in order to better understanding the global climate change and designing mitigation policies to reduce emissions form deforestation and forest degradation (REDD), it is necessary to determine and examine the amount of CO_2 released from human activities and the carbon uptakes and storage by land and ocean ecosystems. Scientists use forest carbon stock estimates from Earth observation data. One of the parameters for these estimates is 'biomass volume', which describes how many

cubic meters of wood (or biomass) are estimated per hectare. The biomass volume includes above-ground and below-ground biomass that are important variables to understand the global carbon cycle.

Forest biomass is defined by the United Nations Framework Convention on Climate Change (UNFCCC) as a crucial climate variable needed to reduce uncertainties in our knowledge of the global climate change. To improve the reliable methods for measuring, reporting, and verification (MRV) of the global biomass under the REDD mechanism, which was introduced in the UNFCCC Committee of the Parties (COP-13) Bali Action Plan, it is required to implement relies fundamentally on developing systems to monitor carbon emissions due to loss of biomass from deforestation and forest degradation. At the COP-14 in Poznan in 2008, REDD was further expanded to REDD+ which includes forest conservation, sustainable management, and enhancement of carbon stocks. However, there is a lack of information on the global forest biomass that has resulted in the greatest uncertainties concerning the global carbon budget.

All these statements mentioned above highlight an urgent need for estimating global forest biomass based on an accurate, timely, and cost-effective method. However, up-to-date there is no existing global observation program for forest biomass. Therefore, a quantitative biomass estimation model is needed for supporting the REDD+ mechanism and blue carbon program.

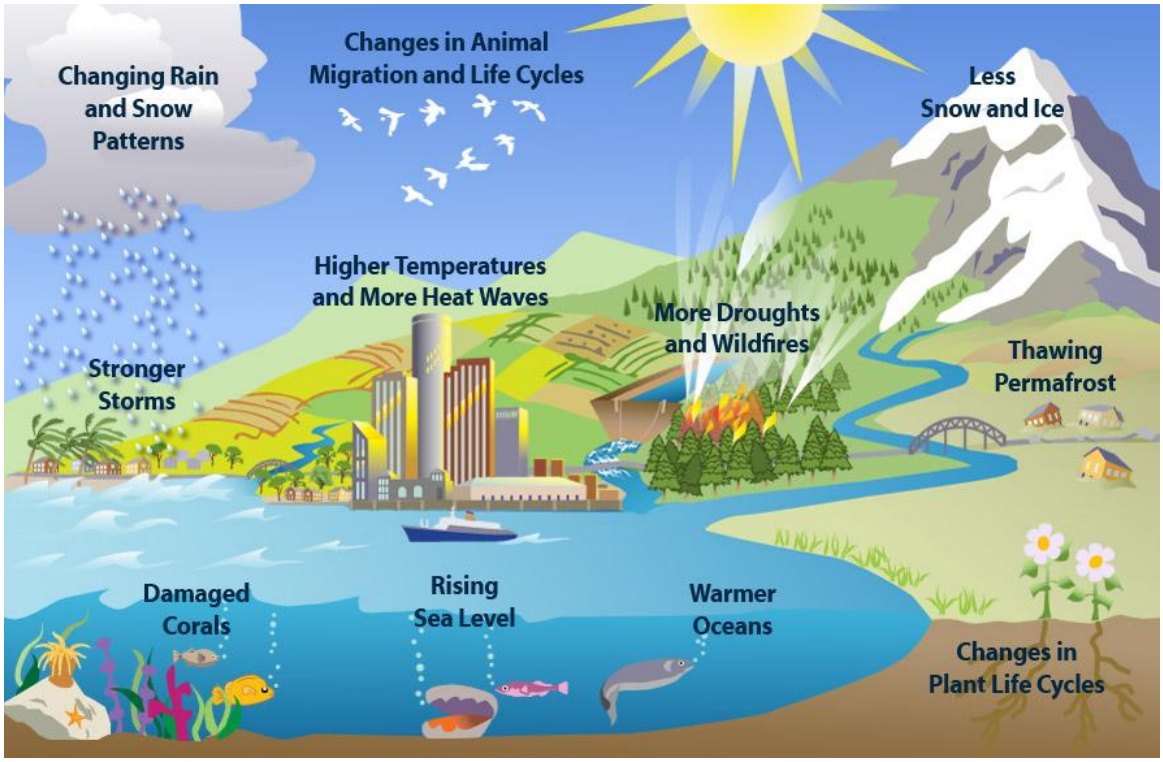

Source: Collin, 2007

Figure 1.1. Effects of climate changes on human and natural ecosystems

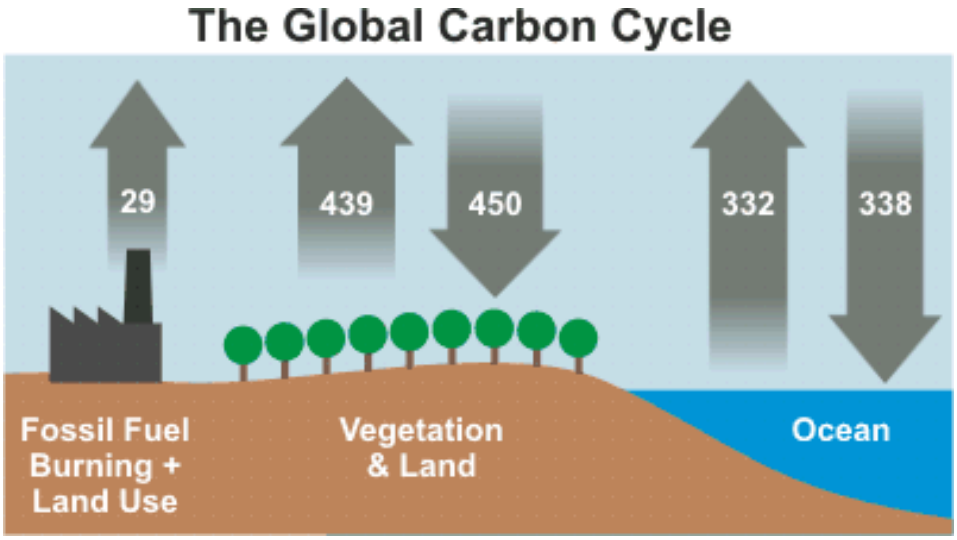

Source: IPCC AR4

Figure 1.2. A comparison of human CO_2 and the natural CO_2 emission
(Numbers represent flux of carbon dioxide in gigatons)

1.1.2. Significance of mangrove forests in global carbon cycle and climate change

Mangrove forests, which appear in the inter-tidal zones along the coast in most tropical and semi-tropical regions, are considered to be the most important ecosystems on earth as they play a crucial role in global carbon cycle [4, 5] and can reduce damage from the effects of Tsunami. The most obvious evidence can be found from the Indian Ocean tsunami in Dec, 2004 [6]. These forests absorb and store carbon dioxide from the atmosphere and can act as highly efficient carbon sinks in tropical climates [7], as well as sequester carbon in both above and below-ground biomass as well as their sediment [8].

Mangrove forests are the most productive of ecosystems and their ecosystems stabilize coastlines, clean water, protect the land from erosion, in many cases promote coastal accretion, and provide a natural barrier against storms, cyclones, tidal bores and other potentially damaging natural forces (Fig 1.3). For centuries, mangroves have contributed significantly to the socio-economic lives of coastal dwellers. In addition, they are a source of timber for fire-wood and provide building materials, charcoal, tannin, food, honey, herbal medicines, and other forest products [9, 10].

***Storm Washi* (31/7/2005) attacked the coast of Do Son, Hai Phong city**

Storm *Vincente* (18/9/2005) attacked Do Son, Hai Phong city

Source: Thai V.D., 2005

Figure 1.3. Tropical cyclones attacked the coast of Vietnam

Despite of their benefits and services, mangroves are under severe threat. High population growth, and migration into coastal areas, has led to an increased demand for their products. The situation is further exacerbated by weak governance, poor planning and uncoordinated economic development in the coastal zones. Globally more than 3.6 million hectares of mangrove has been lost since 1980. Asia has suffered the greatest loss of 1.9 million hectares [11]. Mangrove forests that are logged or converted to shrimp aquaculture, however, release parts of the stored carbon into the atmosphere (Figure 1.4)

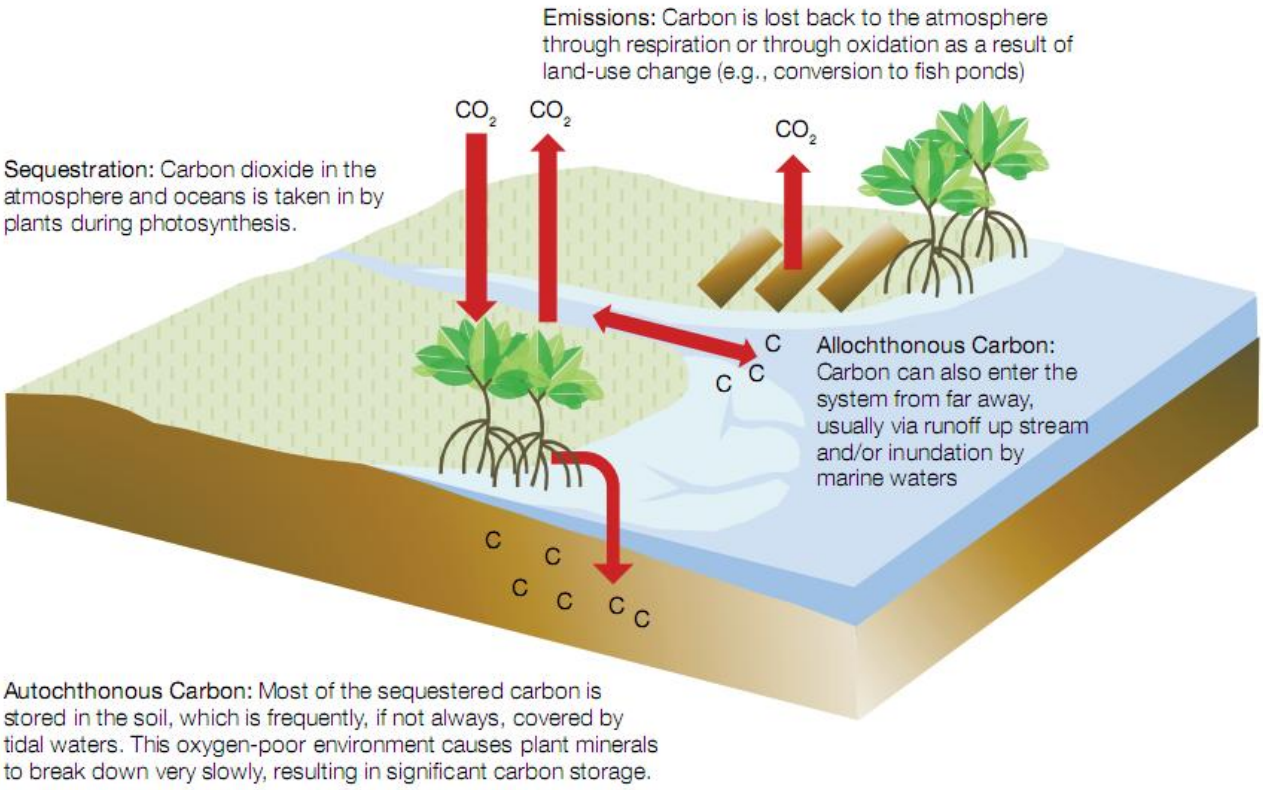

Source: ***http://thebluecarboninitiative.org/***

Figure 1.4. Mangrove loss and their carbon stock change

Like many other countries in Southeast Asia, the mangrove area in Vietnam has decreased markedly. In Vietnam, it is estimated that mangrove forest accounted for about 400,000 hectares in the early 20th century. However, this has decreased dramatically during the last 50 years [12]. In Northern parts of Vietnam, from Mong Cai to Do Son, throughout the periods 1964-1997, mangrove area decreased by 17,094 ha. In the Red River plain, the loss of mangrove was 4,640 ha from 1975 to 1991 followed by a decrease of 7,430 ha in 1993 [13]. The coastal zone of Southern Viet Nam witnessed little change in mangroves (from 250,000 ha to 210,000 ha) during 1950 - 1960; yet, the figure was reduced to 92,000 ha of mangroves in 1975 due to the spraying of military herbicides by the American forces (1962 – 1972) [10]. Therefore, the reliable and cost-effective for the estimation of mangrove plantation biomass is highly necessary to support monitoring, reporting, and verification (MRV) work as part of the REDD+ program and Blue Carbon projects in developing nations.

According to current literature, this is the first time an estimation of biomass for mangrove species has been conducted for this coastal area. Accordingly, a function of mangrove ecosystems

in the study area can be established and it may help to elucidate the spatial distribution patterns of biomass in tropical and sub-tropical regions. This work also promotes the implementation of REDD+ mechanism and Payment for Ecosystem Services (PES) strategies, thus providing practical significances for developing regional and national blue carbon trading markets and guiding mangrove management and conservation.

1.2. Research questions

This research aims to answer the following questions:

1. What are the characteristics of mangrove species in Hai Phong City?
2. What are the relationships between biophysical parameters of mangrove species in Hai Phong and remote sensing data?
3. How to effectively map the spatial distribution of mangrove species and analyze their changes using machine learning techniques?
4. How to map the AGB of mangrove species using parametric and non-parametric approaches?
5. How to promote the implementation of REDD+ and blue carbon projects for mangrove ecosystem services?
6. What are the social benefits to support PES strategies in the coastal zone?

1.3. Research objectives

The overall objective of this research is to monitor biomass of mangrove species in Hai Phong city on the Northern coast of Vietnam using satellite remote sensing data and machine learning techniques towards REDD+ mechanism and blue carbon program in Vietnam. There are four specific objectives in this research:

1. To determine the relationship between biophysical parameters of specific mangrove species and remote sensing data;
2. To investigate the applicability of machine learning techniques and remotely sensed data for estimating biomass of mangrove species;
3. To examine the implementation of REDD+ and blue carbon projects based on willingness to pay (WTP) estimation for the economic values of mangrove ecosystem services;

4. To suggest better policies for sustainable mangrove conservation and management in Vietnam.

1.4. Research framework

Hai Phong is a coastal city located in the north of Vietnam. Over 95% of mangroves on the northern coast are distributed in Hai Phong, Quang Ninh, Thai Binh and Nam Dinh [14]. This city is vulnerable to rising sea levels and tropical cyclones due to the impacts of climate change. Mangrove conservation and restoration have been implemented in Hai Phong in the context of climate change issues; however, weak policies and practices have resulted in mangrove conversion into shrimp aquaculture and mangrove degradation. Thus, monitoring mangrove change is crucial for coastal environmental management towards REDD+ mechanism and Blue carbon programs. Modeling plays a vital role in understanding the driving forces of land cover change [15] and the current status of mangrove forest biomass. Therefore, modeling associated with field survey data and machine learning techniques are expected to provide the reliable and cost-effective methods to determine the biophysical characteristics of mangrove species in Hai Phong. The lack of available research on modeling mangrove forest biomass towards REDD+ and blue carbon programs motivates the present research. In addition, the policy recommendations are also provided in this research to facilitate better mangrove conservation and management. The integrated research framework is shown in Figure 1.5.

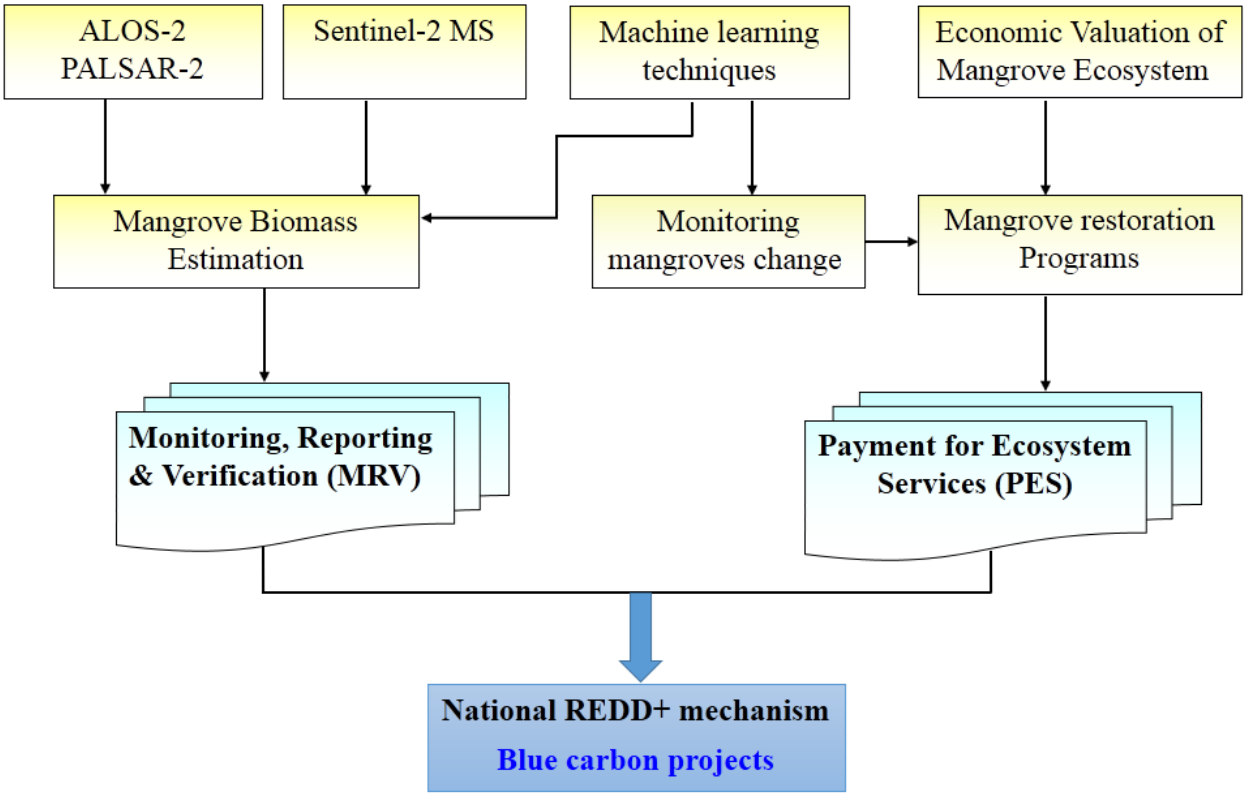

Figure 1.5. Research framework

1.5. Thesis contribution

This thesis is the first attempt to develop reliable and accurate models for estimating forest biomass of specific mangrove species in Hai Phong city, Vietnam using SAR and optical data combined with machine learning techniques. This study provides an alternative approach that may allow rapid estimation of mangrove forests biomass in the tropics in large areas where accessibility is limited. The novel methods used in this study can be replicated for other mangrove forest species with similar characteristics, stand structures and various biophysical parameters. The use of machine learning techniques together with an integration of SAR and optical data provides a promising tool for the preliminary design of national and regional levels biomass assessment and monitoring mangrove forest biomass changes. More importantly, this research will support decision making on mangrove conservation and management.

1.6. Structure of this thesis

There are eight chapters in this thesis. Chapter 1 outlines the motivation of current work and depicts the significant roles of mangrove forest in global carbon cycle. Chapter 1 also provides the general information about mangrove degradation and deforestation in Vietnam in general and on the

Northern coast in particular. The research background, objectives, research framework and thesis contribution to the scientific literature are given in Chapter 1.

Chapter 2 comprises the literature review of the research including the mangroves distribution in Vietnam. This chapter reviews current methods used for forest biomass estimation using various satellite remote sensing data from SAR, optical, multispectral and LiDAR data. This chapter also compares different mangrove mapping and change detection approaches based on satellite remotely sensed data and GIS applications.

Chapter 3 represents the reasons why we chose Hai Phong city as a study site. This chapter also mentions the materials and different methods used in this research.

Chapter 4 illustrates the results of the characteristics of different mangrove species in the study area, determines the relationship between biophysical parameters of specific mangrove species and attempts to estimate their aboveground biomass using multiple linear regression models delivered from dual-polarization HH and HV backscatters of ALOS-2 PALSAR-2 imagery

Chapters 5 shows the applicability of multi-layer perceptron neural networks (MLPNNs) for estimating AGB and carbon stocks of *S. caseolaris* in the coastal area of Hai Phong using dual-polarization HH and HV backscatters of ALOS-2 PALSAR-2 imagery, and compares the performances of selected machine learning techniques for the estimation of AGB for *S. caseolaris.*

Chapter 6 attempts to improve the accuracy for the estimation of AGB at a mangrove forests plantation consisted of several species and tests the usability of selected machine learning techniques with an integration of optical and SAR data for the AGB estimation of mangrove forest plantation in the coastal area of Hai Phong.

Chapter 7 shows a case study at Cat Ba Biosphere Reserve for monitoring mangrove forests change between 2010 and 2015, and attempt to know the economic valuation of mangroves, and the social benefits of mangrove restoration by estimating the WTP using the Contingent Valuation Method (CVM) for mangrove ecosystem services. We analyze households' participation in mangrove plantation programs and the awareness of local people in Cat Ba of mangrove restoration in the context of climate change. The last part of chapter 7 contains the policy recommendations and suggestions for sustainable mangrove management practices for Hai Phong city.

Finally, Chapter 8 summarizes the main findings of current work and presents the future works.

Chapter 2

Literature review

Chapter 2 reviews the spatial distribution of mangrove forests in Vietnam and the mangrove biomass estimation using optical, synthetic aperture radar (SAR), multispectral, and LiDAR data. This chapter presents the different methods used from linear to non-linear models such as machine learning techniques for the estimation of forests biomass. The following sections compare the advantages and disadvantages of various methodologies for estimating the AGB of forest biomass and mangrove forests in the world and in Vietnam. The last section highlights the limitation and uncertainties for the use of remote sensing data for retrieving forest biomass. It is noted that the literature review on economic valuation for mangrove restoration is presented in Chapter 7.

2.1. Mangroves Distribution in Vietnam

Phan Nguyen Hong [9, 16] has categorized the mangroves in Viet Nam into 4 zones based on geographical factors, field surveys and satellite images (Fig 2.1).

Zone I (northeast coastal zone): stretches from Ngoc Cape to Do Son cape. Zone I is topographically favorable for the establishment of mangroves. Due to the island system in Bai Tu Long Bay and Ha Long Bay, monsoon and storm induced waves are mitigated. Main rivers are high slope with strong currents, bringing alluvia to bays and estuaries and therefore, facilitating the colonization of some mangrove species on tidal flats. The rainfall is large and lasts for months – a favorable condition for the growth of mangrove trees (particularly during regeneration stages). Nevertheless, the temperature declines greatly during winter (when the monsoon occurs), making some mangrove species of Southeast Asian and South Asian origin inadaptable. As a result, this area supports only some cold tolerant species. The timber trees are about 8-12m size. Many shrubs are found. Dominant species are *Avicennia marina*, *Rhizophora stylosa*, *Kandelia obovata*,

Aegiceras corniculatum, and *Bruguiera gymnorrhiza*. On the mud flat, only flooded at high tide, two dominant species are present are *Excoecaria agallocha* and *Scyphiphora hydrophyllacea*. In brackish water, *Sonneratia caseolaris* is present. There are 18 true mangroves and 36 associate mangroves present in this area. Particularly, two mangrove species namely a shrubby species *Myoporum bontioides* and a grassy succulent one *Scaevola hainanense* originating from Hainan Island (China) are distributed only in this area.

Zone II (the coastal zone of northern plain): stretches from Do Son cape to Lach Truong cape. This area comprises deposited alluvia from the Red river and Thai Binh river. The thick and slightly sloping river system with large water flow helps create vast mud flats rich in alluvia, suitable for brackish water mangrove species. Yet, due to the large open space, the area suffers much influence from tropical depression and storms from the East Sea and monsoon that causes large waves. During the stormy season, heavy rain and spring tide are common, mangroves in this area include brackish water or wide ranged salinity tolerant species such as *Acanthus ilicifolius*, *K. obovata*, and *Aegiceras corniculatum* that distribute from the river mouth upstream. [17] investigated around 11 true mangrove species and 34 associate mangrove species. The coastal inhabitants have known how to plant *K. obovata*, forming seadyke protection forest belts. For a certain period, these forests were cut down for sedge cultivation for export and then for shrimp farming. Recently, with the sponsorship of some NGOs, a fairly large area of mangroves has been restored, creating a green belt that helps protect the shoreline. In this area, there exists the Xuan Thuy RAMSAR site which was upgraded to a National Park in 2003. The National Park previously saw wave buffering plantation; thanks to strict protection work and the presence of alluvia rich mud flats, some mangrove species have been seen regenerating, creating semi-natural forests.

Figure 2.1. Map of mangrove distribution in Vietnam

Zone III (the coastal central zone): stretches from Lach Truong cape to Vung Tau cape. Topographical conditions here (short and sloping rivers, little alluvia, many places with rocky mounts running along the coast, long-lasting heavy rain, floods, high tide, sea level rise …) are not suitable for mangroves. Thus, mangroves are not found along the coast in this area. Thin mangrove bands are distributed inside river mouths, and along ponds and lagoons. Due to the difference in climatic conditions and the influence of the northeast monsoon in winter from Hai Van Pass northward, only cold tolerant mangrove species exist. Species composition is almost the same from Da Nang southward; however, there is a change in species composition. Many species from the South have migrated and been transferred here such as *Rhizophora apiculata*, *Rhizophora mucronata*, and *Avicennia officinalis, A. alba*. Some species commonly found in the North such as *R. stylosa, A. corniculatum* and *K. obovata* are sparsely distributed.

Zone IV (the coastal zone of southern Vietnam): stretches from Vung Tau Cape to Nai Cape- Ha Tien. Compared with the above three zones, zone IV has more favorable natural conditions for the establishment and development of mangroves. The presence of the long and wide river system (Sai Gon - Dong Nai) and branches of the Mekong River that flow through the vast plain area enriches the alluvia in this zone.

There is no winter in this area; it is hot all the year round with a fairly abundant rainfall. Storms are rarely found. The irregular semi-diurnal regime of the East Sea facilitates air intake for mangrove plant organs lying in mud, and thereby the mangroves grow rapidly. However, topographically, the Sai Gon-Dong Nai river system flows into the estuaries, narrowing mud flats with little alluvia; consequently, mangrove trees are not big in size. Mangrove species are fairly large in quantity: 32 true and 42 associate mangrove species. This area is dominated by *Avicennia alba* and *Sonneratia alba* – pioneer species on newly accreted tidal flats, and *A. officinalis*; on stabilized land there exists *Ceriopstagal*, and *Rhizophora apiculata, Excoecaria aglalocha* and *Phoenix paludasa*can be observed on high land rarely flooded by tide. In brackish water area, *Nypafruticans,* S*onneratia caseolaris* and two grassy species (*Acanthus ilicifolius* and *Cryptocoryne ciliata*) form a below-canopy layer.

The coastal zone of Mekong River Delta and Ca Mau Peninsula has river mouths, receiving a large amount of alluvia; as a result, the tidal flats are large, particularly Southwest of Ca Mau Cape which is close to the mangrove dispersion centre - Indonesia and Malaysia and therefore, mangroves are more abundant in species (34 true and approximately 50 associate mangrove species). Predominant species are *A. alba,* and *A. officinalis, R. apiculata, R. mucronata* and *Bruguiera parviflora*. Along the east coast, in addition to dominant *R. apiculata*, some high salinity tolerant

species such as *A. marina*, and *B. cylindrical* are also common. On high riverside land rarely flooded by tide or flooded shallowly/little by high tide, *Phoenix paludosa* has developed robustly (thanks to asexual reproduction), forming a pure population in many places. High land area adjacent to the sea is dominated by *Excoecaria agallocha*. Mixed with this species is *Ceriops decandra*. In the coastal area of the west of the Gulf of Thailand, due to low tidal amplitude (0.5-1.0m) and small amount of alluvia and high salinity, only *A. alba* forest belt can be seen. Dependent on the features of tidal flats, some other species are found to grow sparsely, namely *R. mucronata, R. sexangula* and *A. officinalis*.

2.2. Biomass estimation using remotely sensed data

Remote sensing data could offer an alternative approaches to estimate biomass or carbon dynamic of forests. Remote sensing becomes more popular in estimating biomass due to the abilities of capturing spatial information and repeatable monitoring in remote regions [18]. Remote sensing techniques have numerous advantages in estimating above-ground biomass (AGB) over traditional field-survey measurement methods and provide the potential to assess AGB at various scales [19].

Numerous researches paid their attention on developing methods to estimate above-ground biomass (AGB) based on the relationship between biophysical parameters of forests or plantation such as: DBH (diameter at breast height), basal area, tree height, crown cover, age and the response value of the electromagnetic radiation [20-30]. Remote sensing such as optical, SAR, hyperspectral and LiDAR techniques have been used for estimating AGB for tropical forest in general and mangroves in particular.

2.2.1. Biomass estimation using optical sensor data

In fact, remotely sensed data can be used in directly estimating AGB with different approaches such as multiple regression model, machine learning, and neural network [24, 31-33], and directly estimating from canopy parameter such as crown diameter using multiple regression or canopy reflectance models [34-36]. The AGB estimation could be estimated based on different spatial resolutions (high, medium, and coarse) of optical remote sensing data.

2.2.1.1. High spatial resolution data

High spatial resolution images can be space-borne such as IKONOS and Quick Bird with spatial resolution of less than 5 meter (spatial resolution of panchromatic images of IKONOS and Quick Bird are 0.83 and 0.61m). Spatial information such as forest canopy structures and tree crown size were extracted from the high spatial resolution [30, 37, 38]. These images have been used as reference data for validating or assessing the accuracy of medium or low spatial resolution data

[19]. Proisy et al. (2007) used a linear regression based on the three main textural indices yielded accurate predictions of mangrove total aboveground biomass [39]. An empirical regression models was developed by Thenkabail et al. (2004) to estimate wet and dry biomass of oil palm plantations in Africa using IKONOS images based on field plot data [26]. An automated tree crown analysis algorithm was developed by Palace et al (2008) to calculate crown width using IKONOS panchromatic images in tropical forests of Amazon. These data were used to develop an allometric equation of DBH, as a function of crown width with R^2 of 57% [40]. Leboeuf et al. (2007) using QuickBird images to develop a shadow fraction as a predictive variable for estimating biomass and its linear regression as the independent variable. Biomass for the sample plots were calculated with allometric functions and used to fit the model, with R^2 ranging between 0.41 and 0.87 [41].

However, there are several drawbacks of using high spatial resolution involved. The first drawback is that impacts of forest canopy and topography may lead difficulty in developing models for estimating AGB. The second drawback is that the high spectral resolution data lack of a shortwave infrared imagery, which often plays an important role in estimating AGB. The last ones is the cost of purchasing high spatial resolution imagery which is much more expensive and requires much more time to analyze than medium spatial resolutions imagery. Two important factors may influence the extensive applications of high spatial resolution images for estimating AGB in a large region [19].

2.2.1.2. Medium spatial resolution data

There are numerous optical sensors, which have medium spatial resolution ranging from 10 to 100 m. However, the time-series Landsat data are the most frequently used in a wide variety of applications including AGB estimation at local and regional scales [24, 31, 34, 42-48]. A combination of medium and low spatial resolution developed by Hame et al. (1997) and Tomppo et al. (2002) to achieve better results in estimating biomass [49, 50]. A combination of remotely sensed data at different scale of Landsat and Wide Field Sensor (WiFS) was used to estimate the tree volume and AGB in the Northern Europe [50].

There are numerous methods used for estimating AGB using medium spatial resolution data. The most frequently used approaches are multiple regression [24, 43, 44]; multiple regression and artificial neural network models [27, 51]; linear or non-linear regression models [31, 45, 49, 51]; non-linear regression models and *K* nearest-neighbor [50]; *K* nearest-neighbor [52, 53] and tree-based models [54].

AGB have been successfully estimated in previous research at different scales. The use of neural networks were potential using Landsat TM data for the AGB estimation in tropical rain

forest [55]. Landsat TM also used in Finland and Sweden to estimate tree volume and AGB using the *K* nearest-neighbor [50, 52]. Steininger found that the ability of AGB estimation in tropical secondary forests using Landsat TM data may influence by data saturation [31]. The impact of shadows resulted from canopy and topography may lead to low accuracy of AGB estimation [27, 31]. To improve the accuracy of AGB estimation using Landsat data, Liu and Zhu (2015) developed six empirical model by using seasonal NDVI time-series. The results showed that using the time-series of NDVI provides a more accurate AGB estimation and less saturation than using a single NDVI [47]. Vegetation indexes such as NDVI, EVI have been widely used to remove variability resulted from canopy geometry, soil background, and other environmental conditions when measuring different biophysical parameters. Liu, et al. [56] reported the potential use of annual NDVI for estimating aboveground biomass of desert grassland and no significant relationship between AGB and soil organic carbon contents. The impacts on reflectance caused by atmospheric conditions and shadows can partially reduce by using vegetation indexes, especially regions where vegetation stand structures are complex [57]. Recently, the successful operation of Landsat 8 OLI imagery offers a new primary data source for AGB estimation. The Landsat 8 OLI dataset with large swath width of 185km is crucial especially in the regions where high spatial resolution data remain a challenge [48]. Texture parameters derived from Landsat 8 OLI dataset provides an important tool for updating AGB maps and texture metrics provide higher accuracy in estimating AGB when compared to the used of spectral vegetation indexes [58]. Ahmadian, et al. [59] pointed out that Landsat 8 OLI can produce more precise results and outperform than Landsat 7 ETM+ for estimating vegetation biomass, indicating that the saturation levels of Landsat 7 ETM+ occurred earlier than Landsat 8 OLI. Nevertheless, not all texture measures are able to extract biomass information since the characteristics of objects vary with texture imagery used. Therefore, selecting an appropriate window size and an image band is important. A small window size such as 3 x 3 may increase the noise content on the texture image whilst a large window size, conversely, such as 31 x 31 can lead to too much smoothing of textural variation and could not extract information from image. Thus, identification of appropriate window sizes and image bands is difficult for a scientific research topics and more research is needed to develop a guideline on how to select suitable image textures for estimating biomass [27].

2.2.1.3. Low spatial resolution data

In remote sensing field, satellite data with spatial resolution greater than 100 m is often called a low spatial resolution. Several satellite sensors provide coarse spatial resolution data in which common data used are NOAA Advanced Very High Resolution Radiometer (AVHRR) and

MODIS (Moderate Resolution Imaging Spectroradiometer) [60]. These data are often utilized at national, continental, and global scales. Boyd (1999) found that MIR (middle infrared reflectance) may be more sensitive than visible and near-infrared reflectance in terms of forest properties changes [61]. Barbose et al. (1999) used AVHRR NDVI to estimate biomass density and evaluate burned areas and biomass, and atmospheric emissions in Africa as well as assess forest woody biomass in six European nations [62]. The large number of spectral bands in MODIS data may be potential for improvement of AGB estimation at the continental and global scales.

The literature review shows that few studies have been done for estimating AGB using low spatial resolution data due to the common occurrence of mixed pixels and the significant difference between the size of field measurement and pixel size in the image, such as NOAA and MODIS (spatial resolution of 1.1km and 250 m, respectively), caused difficulty for choosing remote sensing derived variables and sampling data. Thus, a combination of multi-scales data would be applied in estimating AGB. A combination of AVHRR and Landsat TM data, for instance, was used by Hamme et al. (1997) to estimate biomass of coniferous forest [49]. Combining TM and IRS-1C Wide Field Sensors (WiFS) data for estimation of tree stem volume and AGB in inland and Sweden is other example of AGB estimation [50]. The spatiotemporal patterns of above ground biomass was also estimated using a combination of Landsat TM and MODIS images in China [63].

Several methods used for AGB estimation based on a combination of low spatial resolution and other medium spatial resolution data such as Landsat, IRS-1C WiFS. Dong et al. (2003) applied regression models using NDVI of AVHRR data while Hame et al. (1997) used linear regression model based on a combination of Landsat TM and IRS-1C WiFS. Tomppo et al. (2002) used K nearest-neighbour method [49, 50, 64]. Yan et al. (2015) used a linear fitting method based on different degrees of slope to understand the trends and fluctuation of AGB in China [63].

2.2.2. Biomass estimation using SAR data

2.2.2.1.Advantages of using SAR data for estimating biomass

In remote sensing field, SAR (Synthetic Aperture Radar) offers unique benefits that bring it advantages over optical sensors as follows [65]:

1. Day and nighttime capability (SAR is independent of intensity and sun illumination angle);

2. Data acquisition at all weather conditions (penetration capability through clouds which are the main problem of optical sensors, especially in the tropics;
3. Penetration capability through vegetation, soil sand, and snow;
4. Sensitivity to surface roughness, dielectric properties and moisture;
5. Sensitivity to wave polarization and frequency;
6. Capability through volumetric studies;
7. Capability research studies from inaccessible regions.

2.2.2.2.Wavelength and polarization of SAR data

SAR data can be achieved at different wavelengths including X, C, L, and P bands with different polarizations, which have a variety range of azimuth resolutions. Each band has own characteristics and capability related to forest stand parameter [66]. Short wavelengths such as X-band (3.75 – 2.5 cm) and C-band (7.5 – 3.75 cm) could strongly interact with the surface of the canopy whilst long wavelength such as L-band (30 – 15 cm) and P-band (68cm) could penetrate into the canopy and reflect information on branches and stems. [67-74]. The longer wavelengths could provide a high and close relationship between biomass and other biophysical parameters than short wavelengths [65, 66].

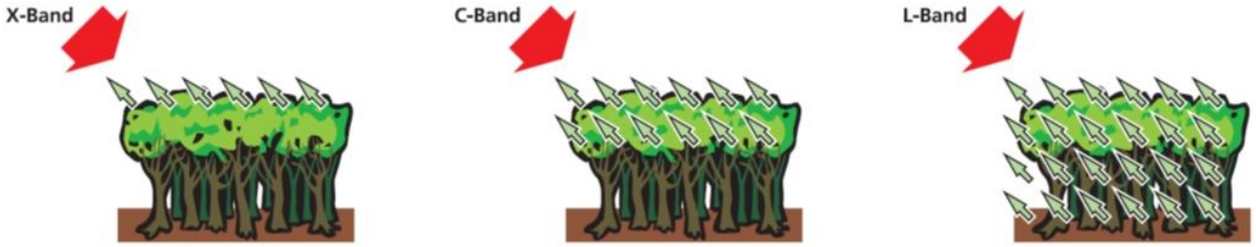

X band: 3.75 – 2.5 cm C band: 7.5 – 3.75 cm L band: 30 – 15 cm

Source: European Space Agency (ESA)

Figure 2.2. Wavelength illustration of multi-frequency radar system through vegetation

Polarization of SAR play an important role in understanding interactions between electromagnetic waves and the reflectors. There are two ways of emitted signal in horizontal (H) or vertical (V) polarizations. Thus, a combination of two single polarization is resulted in four SAR data polarization: (1) HH signal emits and backscatters at horizontal polarization; (2) HV signal emits horizontal polarization and backscatters at vertical polarization; (3) VH signal emits vertical polarization and backscatters at horizontal polarization; and (4) VV signal emits and reflects at vertical polarization [75].

Different SAR data have used in their own applications in numerous research studies. The longer wavelength SAR L and P bands and the HV polarization have proven to be the most sensitive to AGB [25, 71, 76, 77]. Ghasemi et al (2011) found that the co-polarized (HH and VV) data at the longer wavelengths such as P-band were sensitive to surface condition change [75] whilst Ranson and Sun (1994) pointed out that cross-polarizations (HV and VH) backscattering data were less influenced by the surface condition [78]. Thus, they seem to be better than co-polarized for estimating biomass since volume scattering is mainly from the crown [66]. Le Toan et al. (1992) pointed out that cross-polarized backscattering intensity of L-band were the best sensitivities to forest biomass [79]. A short wavelength, C-band, for instance, would be applicable for small and lower biomass sites such as grassland, bogs, and young forest plantation. P-band with long wavelength of 68 cm gives low backscattering for the ground surface sites covered by shrubs, brush, or juvenile trees whilst C-band with a short wavelength of 6 cm at the same surface would not be appropriate because it saturates often at 10kg/m^2 [78]. The limitation of a short wavelength could be overcome by using a longer wavelength such as L-band. The L and P-bands saturates often at 100t/ha for a complex and mixed forest structure and this saturation number boosts to roughly 250t/ha for simple and a few dominant species. Thus, a combination of C and L bands for biomass estimation would be the most suitable for deciduous forests [78].

2.2.2.3. Drawbacks of using SAR data

The saturation is the main and common problem of SAR data. The level of saturation depends on the wavelength (C, L, or P bands) and polarizations (HH, HV, VH, and VV), and the characteristics of ground conditions and the structure of forest sand. Shugart et al. (2010) pointed out that L-band saturates at around 100-150t/ha [80] whilst P-band could be sensitive for biomass estimation at a saturation level of 100-300t/ha [81]. A combination of ecosystem and radar backscattering modeling used for forest biomass estimation was achieved a good results when AGB was limited to 15kg/m^2[82]. Several studies have been proven that L-band would be the most suitable for AGB with the trunk and branches due to minimal sensitive to the environmental conditions [25, 76, 77, 83].

Previous studies indicated that SAR data plays a crucial role in AGB estimation, especially in the areas where cloud conditions occur frequently. Nevertheless, SAR image processing requires more skills, specific software and scientific knowledge as well as time consuming due to many steps involved such as: pre-processing, noise removal etc… In addition, SAR data, which usually obtained through airborne sensor, may be more costly than space-borne sensors. SAR data were

also captured in limited areas, where AGB estimation in regional and global scales has not been used extensively due to the constraints of cost and labor [19].

2.2.2.4.Biomass estimation methods using SAR data

There are two common widely used approaches for estimation biomass using SAR data. Backscatter coefficient extracted from SAR data is the most preferred approach and interferometry technique is based on interference of waves.

2.2.2.4.1. Backscattering coefficient extraction of biomass estimation

The most common method for biomass estimation using regression analysis based on backscattering coefficient extraction value and field survey biomass measurement. The detailed list of research studies and these techniques is summarized in Table 2.1

Table 2.1. Methods used for AGB estimation using backscatters

Research study	Sensor/SAR dataset	Study site	Model
Le Toan, et al. [79]	AirSAR	Landes forest, France	Regression Model
Ranson and Guoqing [78]	AirSAR	Maine, USA	Regression Model
Ranson, et al. [82]	AirSAR	Maine, USA	Regression Model
Luckman, et al. [76]	ERS-1, JERS-1 and SIR-C	Tapajos, Brazil	Forest Backscatter model
Kurvonen, et al. [77]	ERS-1, JERS-1 and SAR	Scandinavian forest, Finland	Backscattering model
Kuplich, et al. [84]	JERS-1	Tapajos, Brazil	Regression Model
Fransson, et al. [85]	ERS-1/2, SPOT SX	Kattbole, Sweden	Regression Model
Santos, et al. [86]	JERS-1	Amazonia, Brazil	Regression Model
Sun, et al. [25]	SIR-C	Siberia	Regression Model
Austin, et al. [87]	JERS-1 SAR	New South Wales, Australi	Regression Model
Jha, et al. [88]	ENVISAT ASAR	Western Ghats, Karnataka, India	Regression Model
Hyde, et al. [89]	LiDAR, SAR/inSAR, ETM+, QB	Sierra Nevada, California, USA	Regression Model
Navulur [90]	ENVISAT ASAR, Landsat ETM+	Dudhwa National Park, India	Regression Model
Amini and Tetuko Sri Sumantyo [91]	ALOS AVNIR-2, PRISM, JERS-1 SAR	Northern forests of Iran	Neural Network

Yu, et al. [92]	SRTM, Landsat ETM, NED	Maine, USA	Biomass transformation algorithms
Gama, et al. [73]	OrbiSAR-1	Sao Polo State, Brazil	Regression Model
Alappat, et al. [93]	E-SAR	Chandrapur Forest Division, Maharashtra, India	Regression Model
Sandberg, et al. [72]	E-SAR (L & P band) BIOSAR-I	Sweden	Linear Regression
Englhart, et al. [69]	ALOS PALSAR, TerraSAR-X	Central Kalimantan, Borneo, Indonesia	Regression Model
Antropov, et al. [94]	ALOS PALSAR	Central Finland	Semi-empirical forest model
Carreiras, et al. [21]	ALOS PALSAR	Mozambique, Africa	BagSGB model
Ghasemi, et al. [95]	ALOS PALSAR	Temperate deciduous forest	Wavelet analysis
Hame, et al. [96]	ALOS PALSAR	Lao PDR, Laos	Regression Analysis, probability model
Hamdan, et al. [23]	ALOS PALSAR	Matang Forest, Malaysia	Regression Model
Avtar, et al. [20]	ALOS PALSAR	Kampong Cham province, Cambodia	Empirical models
Thumaty, et al. [71]	ALOS PALSAR	Madhya Pradesh state, India	Empirical models
Pham and Yoshino [97]	ALOS-2 PALSAR-2	Hai Phong, Vietnam	Regression Model
Pham, et al. [98]	ALOS-2 PALSAR-2	Coastal area, Hai Phong city, Vietnam	Machine learning

2.2.2.4.2. Biomass estimation using Interferometry (InSAR)

A technique based on interference, where two waves superimpose leading to a wave of greater or lower amplitude, is call interferometry. An utilization technique in geodesy and remote sensing fields, which refers to Interferometric synthetic aperture radar (InSAR), uses at least two SAR images in the phrase of the waves [65]. This technique could overcome the saturation problem of backscatters approach [74, 85] and provides more accurate results than the single-image used [99]. Table 2.2 summaries the list of studies using interferometry technique.

Table 2.2. Methods for AGB estimation using interferometry technique

Research study	Sensor/SAR dataset	Study site	Model
Pulliainen, et al. [99]	ERS1/2	Finland	Interferometry, Empirical model
Santos, et al. [100]	Airborne SAR	Rapajos River region, Para state, Brazil	Interferometry, regression analysis
Lucas, et al. [101]	AirSAR, LiDAR	Queensland, Australia	Water Cloud Model

Neumann [102]	Polarimetric SAR interferometry	Oberpfaffenhofen, Germany	Inversion model Polarimetric decomposition
Wollersheim, et al. [103]	POLSAR data	Petawawa Research Forest, Ontaria, Canada	Polarimetric Analysis
Peregon and Yamagata [104]	ALOS PALSAR	Western Siberia	Water Cloud model
Kubota, et al. [74]	X-band Interferometric SAR	Tropical rainforest in Peninsular Malaysia	Rectangular prisms method

Accuracy for AGB estimation would be improved by using interferometry. Using InSAR technique could improve accuracy in estimating AGB in comparison to the backscatter approach for X and P-bands [100], L-band [105]. In addition, this technique would be suitable for logged tropical forest using X-band [74].

2.3. Biomass estimation for mangrove forests

Understanding the structure and biomass of tropical forest is necessary to quantify its carbon pools [106]. Carbon pools of mangrove forests which is called as '*blue carbon'* refers to the carbon sequestration, which is a process of capturing carbon dioxide from atmosphere and the carbon stored within their sediments [107, 108]. Like tropical forest, the structure and biomass of mangrove forests must be known in assessing their blue carbon stocks. The biomass of mangrove forests has been studies for the past 30 years [109-114] and numerous studies established their allometric equations to predict and improve the AGB estimation from *in-situ* measurement [115] and inventory data on stem weights, trees height and diameter at beast height (DBH) of mangroves [112, 116]. There are several methods used to estimate AGB of mangrove forests such as regression models [115, 117] and machine learning [33]. However, these studies are based on small-scale, plot-based research and would be influenced by site selection biases. In addition, other factors such as tidal inundation, high dense mangrove forests with aboveground root systems could lead to difficulty in estimating the structure and biomass of these forests on a large scale disturbance in the field [4, 118]. Time consuming and labor constraints during the field measurement, particularly in the high density of mangrove trees associated with their roots, as well as impacts of tidal inundation are considerable factors resulted in a lack of updated information on the structure and biomass of mangroves. Thus, remote sensing technology would be valuable and effective to assess the biomass of mangrove forests in such a large scale.

2.3.1. Biomass estimation for mangrove forests using optical data

Optical remotely sensed data especially very high-spatial resolution (VHR) data may play a crucial role in assessing AGB of mangroves. Recent studies have been used VHR optical data such as IKONOS [39] and Quick-Bird [22] for AGB estimation in mangrove forests. Proisy et al. (2007) attempted to predict and map the biomass of mangrove from canopy grain in the coastline of French Guiana using texture analysis of IKONOS images. This research argued that using 120 m the windows size (30 pixels) from 4-m NIR data provided acceptable results for AGB estimation of young mangrove species [39]. Hirata et al. (2014) pointed out the use of Quick-Bird and multispectral optical data to estimate AGB of four mangrove species in the coastal zone of Southern Ranong Province, Thailand. The results of regression analysis showed that biomass derived from field survey and estimated biomass from QuickBird data reached to R^2 = 0.65. Nevertheless, stand AGB of mangrove species based on the QuickBird data was underestimated due to a lack data availability on the mangrove species biomass and crowns of large trees [22]. Thus, more research need to be undertaken to clarify the potential and limitations of optical data for AGB estimation derived from very high resolution data in the future.

2.3.2. Biomass estimation for mangrove forests using SAR data

SAR plays an important role in monitoring mangrove dynamics since it can penetrate clouds, which often occur in the tropics, and acquire data throughout the year [19]. The dependence between both multifrequency and multipolariation of SAR backscattering coefficient and parameters of mangrove forests was found by Mougin et al. (1999) in French Guiana. This research indicated that the biophysical parameters of three mangrove species (the gray mangrove namely *Laguncularia racemosa*, the white namely *Avicennia germinans,* and the red mangroves namely *Rhizophore* spp.) such as: tree height, DBH, tree density, and basal area were highly correlated with HV polarization of P-band. The biomass of mangrove forests at the study site could be accurately estimated up to roughly 240 t DM ha^{-1} since HV backscattering of P-band saturated at around 160t DM ha^{-1} [119]. Proisy et al. (2000) found that the polarimetric radar signatures at the P-bands were the most sensitive to different mangrove species along the coast of French Guiana. Moreover, the polarization ratio of the polarimetric parameters would be useful to discriminate between different stages of mangrove forests. This research also pointed out that the backscattering coefficients of HV polarization at L and P-bands reached the highest correlations with most of mangrove parameters [120]. However, correlation coefficients of different regression models were limited in this research. Recent research using L-band ALOS PALSAR to estimate AGB of Matang mangroves, Malaysia found that HV backscatter gave the best correlation coefficient between

polarimetric of ALOS PALSAR backscattering and AGB for three dominant *species R. apiculata, A. alba and B. parviflora*. The saturation of using HV backscattering coefficients for estimating AGB of mangroves started at exceedingly 100 Mg ha^{-1} and the error of the estimation took place largely when AGB exceeded 150 Mg ha^{-1} [23].

The most common method used to estimate AGB of mangrove forests was regression analysis. This method was investigated by several authors used for different case studies in French Guiana [119, 120], Malaysia [23] and Vietnam [97, 121, 122].

2.3.3. Biomass estimation using LiDAR and data fusion

LiDAR (Light Detection and Ranging) is an active airborne sensors that utilized a pulsed laser to measure ranges and examine the surface of the Earth [123, 124]. The LiDAR data have important roles in estimating AGB since LiDAR pulses can penetrate certain vegetation canopy [125], especially in the tropics where frequent cloud conditions occur. Recent studies have indicated the potential of LiDAR data together with SAR data to map height and biomass of mangrove forests [126]. Several studies found the potential use of LiDAR data for estimating the canopy height of temperate mixed forest [127, 128], and mangrove forests such as the SRTM (Shuttle Radar Topography Mission) elevation data which was calibrated using LiDAR and DEM (Digital Elevation Model) [126] or LANDSAT ETM+ and height calibration equations [129].

It should be noted that direct biomass estimation methods using airborne LiDAR can offer higher accuracy in tree extraction [130], estimating tree height [131], and AGB estimation than those from radar and optical data [132] since LiDAR can characterize both horizontal and vertical canopy structure [133]. However, LiDAR are still captured in limited and small areas and may be more costly than data obtained from space-borne for a large area. Analyzing data derived from LiDAR requires more skills, knowledge and specific software [19]. In addition, LiDAR has limited spectral information due to one wavelength of laser point intensity [133].

2.3.4. Biomass estimation using Hyperspectral data

Spaceborne hyperspectral sensors are anticipated to offer relatively higher spectral data by providing a large number of spectral bands from space. It is widely recognized that they can be the best in estimating vegetation biomass comparing with other multispectral sensors. Sibanda, et al. [134] reported that hyperspectral data can provide slightly higher accuracies in estimating grass biomass than the Sentinel 2 multispectral imager (MSI) data. However, hyperspectral data are mainly airborne and captured in small and limited areas.

Compared with LiDAR metrics, spaceborne hyperspectral sensors are anticipated to offer relatively higher spectral data by providing a large number of spectral bands from visible to near infrared (NIR) or shortwave infrared (SWIR) range. It is widely recognized that they can be potential in classifying vegetation cover and estimating vegetation biomass comparing with other multispectral sensors. Sibanda et al. (2016) reported that hyperspectral data can provide slightly higher accuracies in estimating grass biomass than the Sentinel-2 multispectral imager (MSI) data. However, Vaglio Laurin et al. (2014) claimed that hyperspectral data alone had limited prediction ability in estimating forest biomass (R^2=0.36). In addition, hyperspectral data are mainly spaceborne and captured in small and limited areas (Lu, 2006). Integration of LiDAR and hyperspectral or multi-source data can improved biomass estimation significantly with a relative high accuracy (Anderson et al., 2008; Vaglio Laurin et al. 2014; Luo et al., 2017). In the summary, integration of LiDAR and hyperspectral or multi-source data can improved biomass estimation significantly with a relative high accuracy [135].

2.4. Biomass estimation of mangrove forests in Vietnam

Mangrove forests play important role in defending against the impacts of tropical cyclones and protecting coastal area. These forests also can help reduce wave which occurs during storms in the coastal zone of Vietnam [136, 137]. However, there is a lack of available and updated data on the current status of mangrove area in Vietnam [138]. Mangrove mapping and change detection have been done only in some specific regions of Vietnam such as Ca Mau Peninsula in the South [139-141] and Hai Phong, Quang Ninh in the North [14, 142, 143]. In addition, research on the AGB estimation of mangrove forests in Vietnam is still extremely limited. In fact, few research studies have attempted to estimate the biomass and carbon stocks of mangrove plantation in Nam Dinh province located in the Northern coast of Vietnam [144] and in Quang Ninh province in the north, and two provinces namely Ca Mau and Kien Giang in the South [122]. The common methods used to calculate AGB and carbon stock in Vietnam were field survey measurement and associated with remotely sensed data [122, 145] and SNV [138].

2.5. Limitation and Uncertainties

2.5.1. Limitation of remote sensing technologies in estimating AGB

In remote sensing field, two difficult and important tasks involved are radiometric and atmospheric correction because of complex atmospheric conditions. In order to overcome this issue, many scientists have attempted to develop different approaches for radiometric and atmospheric condition for specific case studies [146-152].

In mountainous areas, terrain factors such as slope and aspect could be positively influenced vegetation surface, leading to invalid relationships between biomass and reflectance for optical data [153], biomass and backscattering coefficient for SAR data [65]. Thus, it is needed to remove topographic effects on vegetation reflectance. Numerous methods attempt to reduce these effects by applying band ratio [154], radiance models [155], and regression models such as PCA (Principle Component Analysis) [156], topographic correction methods for optical data [157, 158], and SAR data [159] or integration of DEM and remote sensing data [160].

Another important factor may affect the AGB estimation could be from different spatial, spectral, and radiometric resolutions of satellite remote sensing data. Landsat 5 TM, for instance, with 30m spatial resolution would contain several mixed pixels that have information for different forest species in a single pixel. Furthermore, the spectral resolution of Landsat 5 TM have six bands ranging from visible, near-infrared and short-wave infrared as well as one thermal band could limit to distinguish certain forest types. In addition to spectral resolution, radiometric resolution also needs to be considered such as 8 bit for Landsat 5 TM since digital number (DN) value saturates the AGB estimation because of similarities forest stand structures and topographic factors. The hyperspectral imagery could improve these limitation in estimating AGB due to a wide range number of spectral bands with narrow wavelengths [19].

Each remotely sensed sensor has own characteristics in reflecting land surfaces, thus integration of different satellite remotely sensed data would enhance the information extraction process. Data fusion of multi-sensors or multi-resolution data bring a variety of benefits of the strengths of each single imagery for improvement of visual interpretation and quantitative analysis. Several research studies have attempted the use of data fusion for AGB estimation based on the integration of different optical sensors such as: SPOT HRV and Landsat TM [161], SPOT multispectral and Panchromatic bands [162, 163]. In addition, an integration of SAR and optical data such as: Landsat TM and ALOS PALSAR could provide higher accuracy in assessing tropical forest biomass [164]. More research multi-sensors data fusion is needed for exploring the improvement of AGB estimation for tropical forest and mangrove forests. Despite the advantages of using data fusion, the time and labour constraints involved in image processing should take into considerations, especially in a large area [19].

2.5.2. Uncertainties

In the remotely sensed data, five types of uncertainties were found by Dungan (2006) including: positional, spatial support, parametric, structural (model), and variables [165] whilst three primary sources of errors were highlighted by Friedl et al. (2001) such as: errors of data processing, errors

of image acquisition process, and errors introduced though instrument resolution and the scale of an ecological process on the ground [166]. The uncertainties issue listed is also found in SAR remotely sensed data. In addition, there are several other limitations using SAR data such as: (1) very high cost for data acquisition, (2) temporal data acquisition, (3) limited SAR sensors, (4) limited area coverage, (5) limited global scale dataset [65]. SAR data processing requires high skillful interpreters, knowledge and specific software [19].

For AGB estimation, the collection of AGB sampling data may be contributed to the important uncertainties sources. Other sources would be the atmospheric correction, the geometric correction, the selection of appropriate variables, and algorithms used in the models to estimate AGB. The level of uncertainties and accuracy assessment of AGB models could be measured by the coefficient of determination (R^2) and root-mean-squared error (RMSE) [167]. The higher goodness of fit between the sampling data and the model predicted expresses a low RMSE or high R^2. In order to improve the accuracy of AGB estimation, it is necessary to understand and identify the uncertainties sources. Another solution is to develop an allometric equation for each forest type. This method, nevertheless, requires a wide range of samples compared to other approaches. In fact, the AGB estimation approach based on forest type has not been extensively utilized due to the difficulty in data collection of AGB. Thus, in order to reduce the uncertainties come from different sources in estimating AGB, more research is needed in the future [19]. Different new SAR data such as ALOS-2 PALSAR-2 with better spatial resolution, Sentinel-1, ect… would offer further possibilities of improvement for AGB estimation in future.

2.6. Conclusions and future perspectives

Biomass estimation in tropical forest and mangroves is facing numerous issues due to accessibility conditions and labor constraints. Remote sensing based techniques provide an alternative approach in assessing biomass and carbon dynamic over traditional field-survey measurement methods and would offer the potential to assess AGB at various scales. High spatial resolution data such as aerial photograph and spaceborne such as: IKONOS, QuickBird images could provide higher accuracy in estimation AGB at a local scale. Nevertheless, the shadow problem, the huge data storage and the cost of data acquisition are the drawbacks of HSR data and limit its application for a large scale. Medium spatial-resolution data would offer the potential for assessing AGB at a regional scale; however, mixed pixel and data saturation associated with Landsat imagery for instance are the primary problems in AGB estimation in complex biophysical conditions of study sites. The low spatial-resolution data, such as MODIS would be used at a national or global scale, but have not yet been utilized extensively due to difficulty in the link between low spatial-resolution data and

field survey measurements. Combining multi-resolution and multi-source data may improve the accuracy of assessing AGB at the continental and global scale. Several methods often used to estimate AGB using optical remotely sensed data such as linear or non-linear regression model, neural network, or *K* nearest-neighbor. A combination of image texture analysis and spectral signatures would improve accuracy of AGB estimation. The integration of GIS and remote sensing will also be helpful in assessing AGB when multi-source data are available. Model-based development among a variety optical remotely sensed data used such as spectral mixture techniques and neural network could offer other direction for AGB estimation. A lack of sufficient and high reliable AGB sampling plots is a core issue in developing AGB models and in assessing accuracy of the AGB estimation results.

SAR-based remote sensing data may offer other approaches for AGB estimation and would overcome the disadvantages of optical remotely sensed data. Long wavelength such as L and P-bands, cross-polarization in SAR would be more sensitive to biomass. A combination of texture SAR image analysis and backscattering coefficients, interferometry and polarimetric analysis of SAR data will be useful in improving AGB estimation results. The most common method used to estimation is regression analysis due to an effective and easy used technique for assessing AGB for both tropical and mangrove forests. Development of model-based approaches using machine learning, semi-empirical models, Water Cloud model, or interferometric Water Cloud model would provide other direction for AGB estimation using SAR. LiDAR seems to be the most appropriate sole sensor for assessing AGB. A combination between SAR and optical would be the potential choice because of reasonable cost and time of data processing whilst an integration of multi-temporal optical, microwave (SAR/inSAR/Pol-InSAR) and LiDAR would be the best choice for estimating AGB.

Identifying the major uncertainties during the development of AGB estimation models plays an important role to improve accuracy of AGB estimation. Several potential interventions would be (1) improvement of atmospheric calibration; (2) selection of appropriate vegetation indexes and image textures to minimize the impacts of environmental conditions and shadows caused by canopy; (3) the integration of optical and SAR data to minimize the data saturation of optical remotely sensed sensor images; (4) the combination of multi-data sources and (5) using data fusion to minimize the mixed pixel problem. Thus, research studies in future need to pay more attention on the integration of multi-data sources which can engage the benefits of using different remote

sensing data (optical, SAR, and LiDAR) and the development of an appropriate approaches in assessing AGB to reduce uncertainties and improve the accuracy assessment.

Chapter 3

Materials and methodology

This chapter highlights the reasons for selecting Hai Phong city as the study site and sampling area. The following sections describe materials and briefly present different methods used in this research including methods for the estimation of the AGB and carbon stocks of mangrove species, and contingent valuation method (CVM) to estimate WTP for mangrove restoration in the context of climate change issue.

3.1. Study site

On the northern coast of Vietnam, 95% of the mangrove is located within the four provinces of Hai Phong, Quang Ninh, Nam Dinh and Thai Binh. From 1990 to 2007, mangrove loss was about 2,700 hectares of which Hai Phong contributed over 1,000 hectares [14].

Hai Phong is located between 20º30' to 20º01' N latitude and 106º23' to 107º08' E longitude. This city belongs to the Northern coastal zone of Vietnam and lies within the tropical monsoons belt of Asia. It borders Quang Ninh province to the north, Hai Duong province to the west, Thai Binh province to the south, and the Gulf of Tonkin to the east. It is about 120 km from the capital Hanoi. The length of the sea coast of Hai Phong is 125 km including the length of coast surrounding the offshore islands (Fig 3.1).

The mangroves of Vietnam were categorized into four main zones based on geographical factors, field survey and satellite imagery [16]. Mangrove forests in Hai Phong include zone I the northeast coastal zone stretching from Ngoc Cape to Do Son cape and zone II the Northern plain coastal zone stretching from Do Son cape to Lach Truong cape [9]. This city is vulnerable to rising sea levels associated with climate change and tropical cyclones, which are forecasted to become more prevalent and stronger as climate change intensifies.

Mapping mangrove forests and assessing their changes play an important role in coastal environmental management and in dealing with climate change impacts in Hai Phong city.

Although mangrove conservation and management have been implemented in the city; however, weak policies and over-expansion of shrimp aquaculture have led to mangrove deforestation and degradation [168].

In Hai Phong, there are two-mangrove plantations programs implemented by the State and NGOs. With the efforts of international organizations including: the Japanese Red Cross (JRC) and the Action for Mangrove Reforestation [169], and the State reforestation program, mangroves had been planted in all five coastal districts in Hai Phong. However, the mangrove forests have decreased significantly and the current situation varies considerably among these coastal districts. In a few communes within the five districts, mangrove is well protected while in the rest of the communes mangrove forest has degraded.

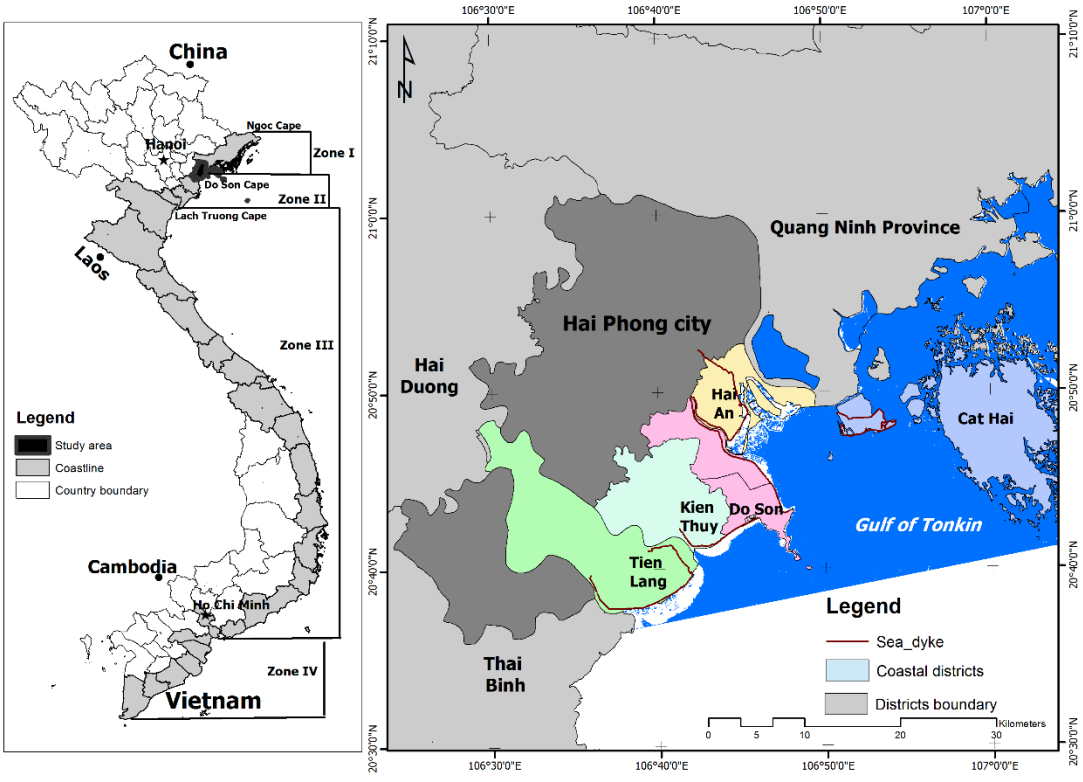

Figure 3.1. Location map of study area

3.2. Materials

3.2.1. Satellite imagery

Satellite remote sensing images relying on both medium and high spatial resolution were used to obtain comprehensive coverage and analysis of the current as well as historical situation. The used images were acquired from SAR and optical sensors including ALOS PALSAR data and Sentinel-2 MSI (Table 3.1).

Table 3.1. Acquired satellite remote sensing data

Satellite Sensor	Date of acquisition	Spatial resolution	Processing Level	Polarizations/ Band used
ALOS PALSAR	2010/8/25	12.50 m	1.5	HH, HV
ALOS-2 PALSAR-2	2015/7/31	6.25 m	1.5	HH. HV
Sentinel-2 MSI	2015/8/10	10 m	1C	Band 2, Band 3, Band 4, Band 8

Source: JAXA, Japan and ESA.

ALOS PALSAR and ALOS-2 PALSAR-2 data level 1.5 were acquired from the Remote Sensing Technology Centre (RESTEC) of Japan. The ALOS PALSAR data was acquired in the same period during summer time for the years 2010 and 2015 to avoid seasonal and tidal effects. As terrain can significantly impact the results of image classification [170], the ALOS PALSAR data were geometrically corrected and geocoded using the Advanced Spaceborne Thermal Emission and Reflection Radiometer (ASTER), Global Digital Elevation Model (GDEM) [171] as suggested by JAXA to correct inherent SAR geometry effects. The ALOS-2 PALSAR-2 imagery was geocoded and re-sampled to similar pixel spacing of 12.5 m for the ALOS PALSAR.

3.2.2. Spatial data

The spatial data were collected from CARES and field survey. These data are listed in Table 3.2. The spatial data included in this research are either vector data or raster data. In vector data, the basic units of spatial information are points, lines and polygons.

Table 3.2. Spatial data entered in the study

Feature	Source/type	Importance for research
Map of dyke system	Topographic maps/ vector	❖ The dykes represent an important and often the only constituent of coastal protection
Infrastructure (roads, rivers)	Topographic maps/ vector	❖ Spatial analysis
Land elevation	ASTER GDEM	❖ Needed as input for deforestation modeling
Map of administrative units (e.g. districts and province boundaries)	Topographic maps/ vector	❖ To enable area specific analysis and statistics

3.2.3. Field survey data

The field data at the Hai Phong coast was conducted several times in July, August 2010 and July 2015 with the help and permission of the local authorities. The former dataset was used for

mapping mangrove species for 2010 and the latter dataset was to generate a mangrove species map for 2015. We collected ground-truth points (GTP) using GPS (Global Positioning Systems) at five coastal districts in Hai Phong (Fig. 3.1) to create training data for supervised classification and assess the accuracy of the post classification of the mangrove cover maps in 2010 and 2015. The field data collection for measuring biophysical parameters to estimate mangrove forest biomass of specific mangrove species in Hai Phong was described briefly in 3.3 and more details are found in Chapters 4, 5 and 6. Additionally, a questionnaire survey was conducted during September and October 2016 in Cat Ba Biosphere Reserve. The details of questionnaire design and survey method are shown in Chapter 7.

3.3. Methods

3.3.1. Field Data collection

The fieldwork was conducted in July and August 2015, which was the same time as the ALOS-2 PALSAR-2 and Sentinel-2 data acquisition with the help of the Vietnam National University of Agriculture and permission from local authorities. The fieldwork did not cause any damage to the mangrove ecosystem. Specific biophysical parameters of the two dominant mangrove species were measured for a total of sixty sampling plots in three coastal districts of Hai Phong city (Fig. 3.1). Sampling plots were randomly selected to capture all possible ages of mangrove species across the study sites. In addition, key informant interviews with heads of villages and chairmen of farmer's associations were conducted to understand how the mangrove species plantation programs have progressed over the years.

3.3.2. Methods used

In this research, we used both linear and nonlinear regression models such as machine learning algorithms to estimate mangrove forests biomass. The methods used for the estimation of biomass for specific mangrove species are briefly described below and clearly shown in the following chapters Chapter 4, 5, and Chapter 6. The details of mangrove forests mapping and their change detection using GIS-based Support Vector Machine algorithm is presented in Chapter 7.

3.3.2.1. Linear regression models

The literature shows that the conventional methods such as linear regression and multi-linear regression models are widely used in forest biomass estimation as shown in many case studies. The main purpose of using linear regression model was to check the potential application for the study area and to compare the results of other previous works. In this study, we employed stepwise

multi-linear regression (MLR) models to generate predicted AGB model for specific mangrove species using backscattering coefficients σ^0 for HH and HV as the independent variables.

3.3.2.2. Multi-layer Perceptron Neural Network

An artificial neural network (ANN) consists of a large number of highly interconnected nodes using mathematical algorithms to model non-linear complex problems such as forest biomass modeling. Although, various ANN algorithms have been developed, multi-layer perceptron neural networks (MLPNNs) are the most widely used in environmental modeling [172, 173] including land-use and land-cover classification [174], forest monitoring and mapping [174, 175], and forest biomass estimation [98].

The structure of a common MLPNN consists of three layers: input, hidden, and output layers. In the input layer, the number of neurons is equal to the number of input images used whereas the number of neuron in the hidden layer must be determined beforehand based on the study area data. The output layer contains one neuron; in this case, the values for AGB. The MLPNN's performance is influenced by connection weights between the input and hidden layers, and between the hidden layer and the output. The main difficulties in designing an MLPNN model is to determine the number of neurons in hidden layer. Too many neurons will lead to over-fitting. In contrast, a network with an insufficient number of neurons will have difficulty in learning. An MLPNN model, which is too simple or too complex, will result in poor prediction performance.

This thesis addresses this problem by using selected input variables such as multi-polarization generated from HH and HV backscatter coefficients with different weights for each variable. These weights are adjusted and updated accordingly in the training phase based on a back-propagation algorithm [176] with the intention of minimizing the difference between the AGB value produced from the MLPNN model and the AGB inventories.

3.3.2.3. Support Vector Machines

Support Vector Machine (SVM) is one of the most common machine learning techniques using statistical learning theory [177, 178]. The SVM has been widely used in environmental modeling and outperforms the conventional methods [179-181]. The SVM technique has been successful utilized in classifying land-use and land-cover (LULC) [182], mapping LULC [183], quantifying urban land cover types [184], and estimating forest biomass [185, 186]. The SVM models consist of a wide range number of vectors that have functions in separating different objects (classification) or minimizing the mean error (regression). The SVM can produce high estimated predictions even

with small numbers of training set [187]. The support vector machine regression (SVR) has shown great capabilities to predict biophysical plant parameters [188, 189].

For an application such as forest biomass estimation, SVR function is defined as follows (Equation 3.1):

$$\mathrm{AGB} = \sum_{i=1}^{n} \alpha_i k(x_i; x) + b \quad (3.1)$$

Where k (x_i;x) represents the kernel function with the training vector xi, α denotes the Lagrange multiplier and b is the bias term in the regression.

The accuracy of forest biomass estimation is measured by the loss function. SVR uses a new type of loss function called ε-insensitive loss function proposed by Vapnik [190]. Main issues have to be taken into accounts while using ε-SVR for the mangrove forest AGB estimation applications. As the performance of the SVR model is significantly influenced by the selection of the kernel functions, different kernel functions such as polynomial, sigmoid, and radial basis function (RBF) are used in the SVR models. In this study, we selected the RBF kernel in this study, because it is the most widely used in estimating forest biomass in previous studies [185, 186, 191]. Additionally, the performance of the SVR models depend on the choices of kernel parameters such as the capacity (C), epsilon (ε), and gamma (γ). However, according to current literature a few studies investigate SVR using different kernel parameters as related to forest biomass estimation. This thesis addresses this problem by testing and evaluating a potential application of SVR with different kernel parameters for biomass modeling in the study area. The findings of the application of SVR model for mangrove biomass estimation are shown in Chapter 6.

3.3.2.4. Random Forest

Random Forests (RF) is an ensemble method combined by multiple individual regression trees proposed by Breiman [192], showing both for classification and regression functions. The RF has been shown its ability to produce the high accuracy, the robustness outliers and noise, fast computation speed, capability estimation of the important input explanatory variables [193, 194].

In the RF method, different algorithms were developed to realize an ensemble of tree models, of which "*bagging*", a bootstrap aggregating technique [195] is widely used including the following steps:

(1) Given the training dataset of size *k*, bagging generates *n* new training datasets D*i* (*i* = 1, 2,…, *n*) – as the same size as the original dataset - by randomly selection data with replacement from the original dataset. This is called a bootstrap sample.

(2) The bootstrap samples are then used to build decision trees *ntree*, which means the number of trees, to be optimized in the modeling process applied in different field of studies [196].

A random subset of the predictors (*mtry*) which means the number of features to split the nodes is used to determine the best split at each node of the tree to construct a decision tree model [192].

(3) The prediction at a target point x results from averaging the predictions of all trees.

About two-thirds of the total samples from the original dataset is included in a bootstrap sample as *'in bag'* data while one-third of the remaining data set is excluded from the bootstrap sample – known as *'out-of-bag'* (OOB) data used to evaluate the ensemble [197].

In this study, different model parameters were adopted to investigate different states of RF methodology. To determine the values that give the most accurate prediction of the forest AGB, a training dataset using LOO cross-validation technique was used to optimize the parameters *ntree* and *mtry* and to minimize the RMSE of prediction.

3.3.2.5. Gaussian processes

Gaussian processes (GP) is a machine learning technique in Bayesian inference of which the GP regression is a probabilistic approximation to nonparametric kernel-based regression [198]. The GP regression was applied in this study to determine whether and how much improvement could be achieved for the combined Sentinel-2 and ALOS-2 PALSAR-2 data. In the GP regression model, a relation between the input (e.g., explanatory variables) $x = [x_1, \ldots, x_B] \in R^B$ and the output variable (i.e., the AGB value) $y \in R$ depicts as the form in Equation 3.3:

$$\hat{y} = f(x) = \sum_{i=1}^{n} \alpha_i K(x_i, x) \quad (3.3)$$

Where $\{xi\}N_{i=1}$ are the explanatory variables used in the training phase, α_i is the weight assigned to each one of them, and K is a kernel function (evaluating the similarity between the plots test and all N training samples [199, 200].

A scaled Gaussian kernel function was used using Equation 3.4

$$K(x_i, x_j) = v \exp\left(-\sum_{b=1}^{B} \frac{\left(x_i^{(b)} - x_j^{(b)}\right)^2}{2\sigma_b^2}\right) \quad (3.4)$$

Where υ is a scaling factor, B is the number of input explanatory variables), and σ_b is a dedicated parameter controlling the spread of the relations for each particular input variable b. Model parameters (υ, σ_b) and model weights α_i can be automatically optimized by maximizing the marginal likelihood in the training set [189, 198].

3.3.3. Contingent Valuation Method

Contingent valuation method (CVM) is widely used to estimate willingness to pay (WTP) for environmental conservation and ecosystem services [201-205]. CVM is a survey-based approach, in which an individual independently states his or her WTP for the conservation of environmental services in a particular location [206]. There are two main kinds of WTP questions: direct or open-ended, and dichotomous choice. The latter was employed in this study; a single-bounded dichotomous choice WTP question was used, incorporating five bids. Dichotomous choice (DC) questions help avoid some biases in answers (such as outliers) but require complicated statistical treatment [207].

In this study, CVM was employed to estimate WTP for the restoration of the mangrove forest in the CBBR [206]. The DC consists of two formulas: a single-bound (SB) model, which offers one question as to whether a bid is "accepted" or "rejected," and a double-bound (DB) model which presents two bids to a respondent. The respondent who has accepted the first bid is offered a higher bid in a second round, and the one that has rejected is offered a lower bid. The DB model has been widely used because the additional information provides clearer bounds for the respondent in determining their WTP. However, several studies have pointed out that the DB format can induce some biases and inconsistencies through the existence of bound effects [208-210]. To avoid these potential problems, a single-bound dichotomous choice model was considered the appropriate empirical analysis method to determine household WTP in this study.

3.3.4. Questionnaire design and survey method

Semi-structured interviews and focus group discussions were conducted in July 2015 with 20 headmen of the people's committee in three districts of Do Son, Kien Thuy, and Tien Lang. Moreover, interviews with the women's union, farmers and political party member associates were also conducted to collect information on mangrove plantation, mangrove conservation and management programs. The main household survey was conducted in September 2016 in Cat Ba Biosphere Reserve in Hai Phong. A total of 205 household responses were collected, all of which were usable. All respondents were asked to answer the questionnaire, which consisted of four main parts. The details of questionnaire design are presented in Chapter 7. The household questionnaire (see Appendix 1) was used based on the annual income of each household, and were selected randomly from rich, medium, and poor households.

3.3.5. Statistical analysis

The questionnaire data were analyzed by Microsoft Excel compiled and coded using the Stata 14 software (Stata Corp). The details of statistical analysis for the household interview are shown in Chapter 7.

3.4. Scope and Limitations of the study

Due to time and budget constraints, the study was carried out in four coastal districts in Hai Phong of which the biomass measurement was conducted in Bang La commune, Do Son district, Dai Hop commune, Kien Thuy district, and Vinh Quang commune, Tien Lang district during summer time in 2015 while the questionnaire survey was conducted in Cat Ba Biosphere Reserve, Cat Hai district in September in 2016. The findings of this research can be generalized for the mangrove situation in Hai Phong and other mangrove forested area with similar biophysical characteristics in North Vietnam.

Chapter 4

Characteristics of mangrove species and their biomass

Chapter 4 presents the findings on the characteristics of specific mangrove species in Hai Phong City (Vietnam) and the estimation of above-ground biomass of these species using ALOS-2 PALSAR-2 data and linear regression models. These findings was accepted for publication in Science Citation Index (SCI/SCIE) scientific journal entitled the Journal of Applied Remote Sensing and partly results of this chapter also was shared during the 8th IGRSM International Conference and Exhibition on Geospatial & Remote Sensing (IGRSM 2016), 13–14 April 2016, Kuala Lumpur, Malaysia and was published in IOP conference series on Earth and Environmental Science 06/2016.

4.1 Introduction

Mangrove forests are productive and important ecosystems that appear in the inter-tidal zones along the coast in most tropical and semi-tropical climates. They play an important role in protecting land from erosion, mitigating the effects of tropical cyclones [136], and reducing damage from the effects of storm surge [6]. Moreover, their ecosystems can stabilize coastlines, clean water, and act as highly efficient carbon sinks in the tropics [113]. For centuries, mangroves have contributed significantly to the socio-economic lives of coastal dwellers by providing building materials, charcoal, tannin, food, honey, herbal medicines, and other forest products [9].

Unfortunately, mangroves are under serious threat from rapid population growth, aquaculture expansion, and human migration into coastal areas. Globally more than 3.6 million hectares of mangroves have been lost since 1980, with Asia having suffered the greatest loss at 1.9 million hectares [11]. The mangrove areas in Vietnam have decreased dramatically over the last 50 years [12]. On the northern coast of Vietnam, throughout the period 1964–1997, the mangrove area

decreased by 17,094 ha – a loss that was largely due to the over-expansion of shrimp aquaculture [168].

Numerous studies on mangrove biomass estimation have been conducted over the past 30 years [109-114]. Several studies have used allometric equations to predict and improve AGB estimation from *in-situ* measurements [115] and inventory data on stem weights, tree heights, and diameters at breast height (DBH) of mangroves [112, 116]. There are several methods used to estimate the above-ground dry-weight biomass mangrove forests, such as regression models [115, 117] and machine learning [33]. However, these studies are based on small-scale, plot-based research and would be influenced by site selection. In addition, factors such as tidal inundation and area of dense mangrove forests with above-ground root systems can lead to difficulty in estimating the structure and biomass of these forests [4, 118]. Current methods also rely on field measurements, which can be time consuming, and costly, particularly in areas of dense mangrove forests. These factors result in a lack of updated information on the structure and biomass of mangroves. Thus, the development of accurate models to estimate the biomass of mangrove species in such regions is necessary to support mangrove management and conservation programs.

Satellite remote sensing data has been widely utilized for monitoring mangrove forests. Throughout the world, many studies have utilized various satellite remote sensing data for mapping mangrove forests, including optical imagery [211-215] and SAR (Synthetic Aperture Radar) data [212, 216]. SAR plays an important role in monitoring the biophysical parameters of mangrove forests since its microwave energy can penetrate clouds that occur constantly in the tropics, and acquire data throughout the year [19]. Zhu, et al. [217] and Pham, et al. [218] reported that the AGB estimation of mangrove forests is most accurate when conducted at the individual species level. However, the AGB estimation using SAR for specific mangrove species has been rarely carried out. Thus, this study attempted to estimate the AGB of *S. caseolaris* and *K. obovata* (two dominant mangrove species in the study area) using ALOS-2 PALSAR-2 data.

Biomass estimation of mangrove forests in Vietnam is still limited. Existing studies are restricted to specific regions, such as the Ca Mau Peninsula in South Vietnam [139-141], Hai Phong and Quang Ninh provinces in North Vietnam [14, 142, 143]. In addition, several studies have been attempted to estimate the biomass and carbon stocks of mangrove plantation in Nam Dinh province located on the Northern coast of Vietnam [144] and in Quang Ninh province in North Vietnam, and in two provinces namely, Ca Mau and Kien Giang, in South Vietnam [122]. However, in Vietnam few studies have used remotely sensed data to characterize mangrove species and estimate their biomass. Despite the availability of SAR data captured for mangrove forests in Vietnam from ALOS and ALOS-2 PALSAR-2, only a few studies have been conducted to estimate

biomass of mangroves using radar backscatter coefficients, and the spatial distribution of mangrove forest biomass in Vietnam is limited and not well documented.

The objective of this research is to investigate the biophysical parameters of specific mangrove species present in Hai Phong and to estimate the AGB of these species using ALOS-2 PALSAR-2 data for year 2015. This involves comparing the biophysical parameters of different mangrove species, determining the relationship between ALOS-2 PALSAR-2 data and field measurements, and developing multiple regression models to estimate the AGB of mangrove species using ALOS-2 PALSAR-2 imagery in Hai Phong. Therefore, the results of the study will reveal the potential use of ALOS-2 PALSAR-2 data for estimating the biomass of mangrove forests species in the tropics.

4. 2. Methods

4.2.1 Study site

This study was conducted in the mangrove forests of Hai Phong city, which is located between 20°30' N and 20°01' N latitude and between 106°23' E and 107°08' E longitude. This city is located on the Northern coast of Vietnam about 120 km from the capital, Hanoi and lies within the belt of tropical monsoons of Asia. It is bordered by the Quang Ninh province to the north, the Hai Duong province to the west, the Thai Binh province to the south, and the Gulf of Tonkin to the east. The length of the sea coast of Hai Phong is 125 km including the length of coast surrounding the offshore islands (Fig. 4.1). This city is exposed to rising sea levels and possible tropical storms associated with climate change [174]. The vast majority of mangrove forests in North Vietnam is distributed in Hai Phong and the surrounding provinces [14]. Mangrove forests in this city are under serious threat from over-expansion of shrimp aquaculture [168]. Field measurements have been conducted in the mangrove forest area of three coastal districts of Hai Phong: Do Son, Kien Thuy, and Tien Lang (Fig. 4.1).

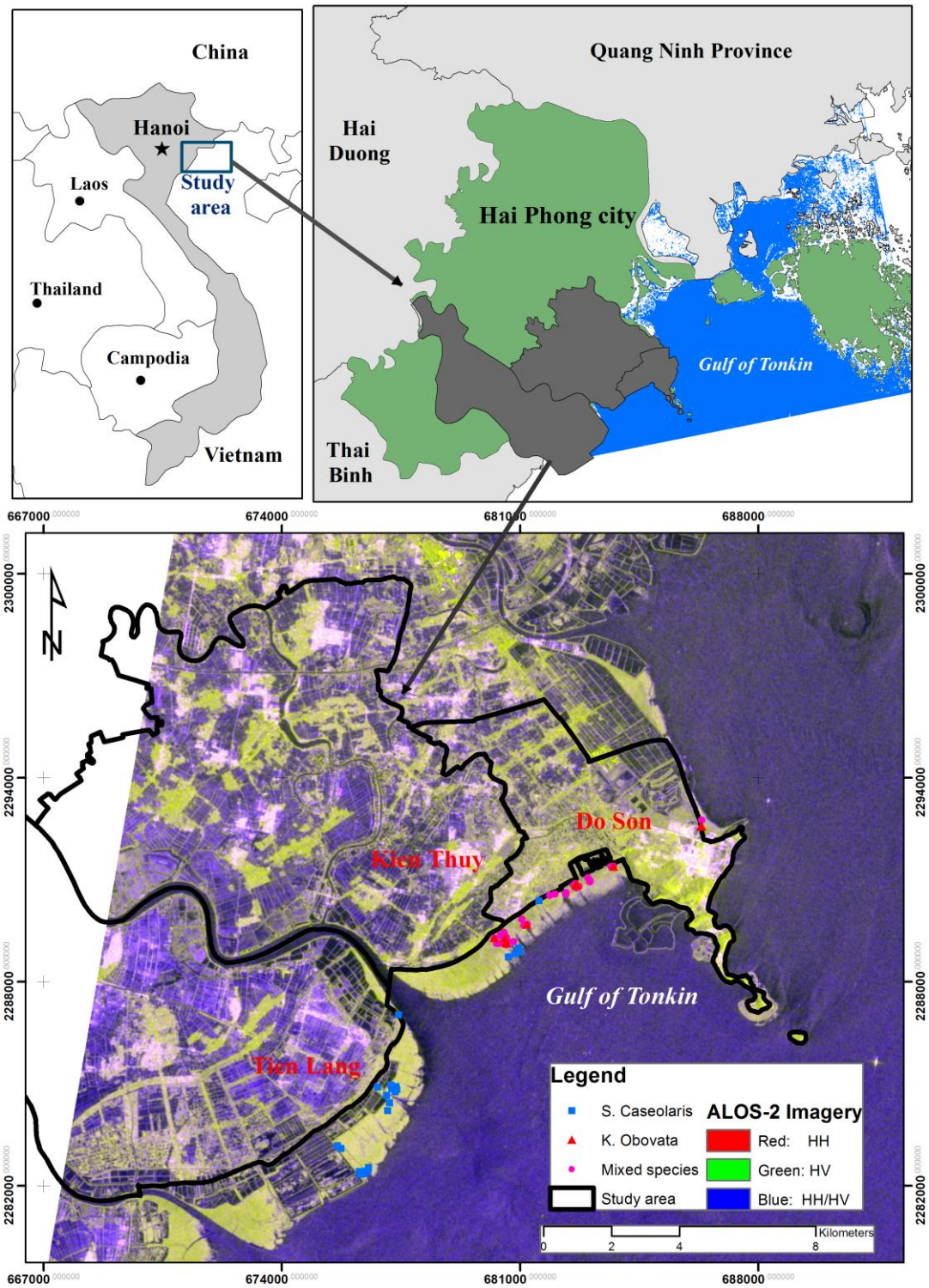

Source: ALOS-2 PALSAR-2 acquired on 31 July 2015

Figure 4.1. Location map of the study area.

4.2.2 ALOS-2 PALSAR-2 imagery processing.

ALOS-2 PALSAR-2 data level 1.5 were provided by the Remote Sensing Technology Centre (RESTEC) of Japan. ALOS-2 PALSAR-2 data were acquired at approximately 5:30 am local time

on July 31, 2015 as shown in Table 4.1. There was almost no rainfall during the date of data acquisition.

Table 4.1. Acquired satellite remote sensing data.

Satellite sensor	Date of acquisition	Level of process	Spatial resolution	Polarizations
ALOS-2 PALSAR-2	2015/7/31	1.5	6.25 m	L band (HH, HV)

Source: JAXA, Japan

The DN (digital number) was converted to the normalized radar backscattering coefficient using equation (4.1)

$$\sigma^0 \text{ [dB]} = 10 \log_{10} (\text{DN})^2 + \text{CF} \quad (4.1)$$

where σ^0 is backscattering coefficient, DN is digital number of the amplitude image, and CF is calibration factor = –83 dB for both HH and HV polarizations [219].

The DN of each pixel was transformed into the backscattering coefficient (σ^0) in decibels (dB) after applying the Frost filter with a 5 × 5 moving window kernel to reduce the speckle noise of the data [220]. Several studies have pointed out that backscatter can be significantly affected by the tidal level [221, 222]. A high tidal level may result in inundation or flooding in the study area. Thus, to minimize the effects of tidal level, we carefully conducted field work by choosing the early morning to conduct field measurements when the ground surface was not flooded, during days without precipitation. ALOS-2 PALSAR-2 data were acquired at approximately 5:30 am local time when the tidal level was at its lowest point, at around 0.2 meters, on July 31, 2015 as shown in Table 4.1. There was almost no rainfall during the date of data acquisition. The ALOS-2 PALSAR-2 data were acquired at a similar time in July 2015 as when the field measurements were taken. However, it is noted that specific mangrove species associated with pneumatophores such as *S. caseolaris* were often inter-planted at high tidal inundation levels in the river mouth or sea to effectively protect dyke systems and mitigate damage from storm surges [223]. Thus, the standing water underneath tree canopies and extensive prop root systems can affect the backscatter from the SAR sensor. The ENVI 5.2 software was employed for SAR imagery processing.

4.2.3 Field data collection

The fieldwork was conducted in July 2015, which was the same time as the ALOS-2 PALSAR-2 data acquisition with the help of the Vietnam National University of Agriculture and permission from local authorities. The fieldwork did not cause any damage to the mangrove ecosystem.

Specific biophysical parameters of the two dominant mangrove species were measured for a total of sixty sampling plots in three coastal districts of Hai Phong city (Fig. 4.1). Sampling plots were randomly selected to capture all possible ages of mangrove species across the study sites. In addition, key informant interviews with heads of villages and chairmen of farmer's associations were conducted to understand how the mangrove species plantation programs have progressed over the years.

Biophysical parameters data were collected from 60 sampling plots, representing the two dominant mangrove stand types. From the collection of sampling plots, 12 plots were of *K. obovata*, 23 plots were of *S. caseolaris*, and 25 were of mixed species. All living *S. caseolaris* stands with diameters of 5 cm and above were recorded. It is noted that *K. obovata* stands in the study area are small trees with diameters less than 5 cm. Thus, we measured the crown depth, crown diameter, and tree height in order to calculate the AGB for *K. obovata* using the allometric equation adapted from [224]. The description of field data of mangrove species is shown in Table 4.2.

Table 4. 2. Mean values for biophysical parameters of mangrove species in study area

Stand type	Number of plots (*n*)	Biophysical parameters						
		Stem height (m)	Stem DBH (cm)	Density (stems/ ha)	Stand age (years)	Crown-area (m)	Crown-volume (m)	Total dry biomass (Mg ha^{-1})
S. caseolaris	23	7.5	19.9	869	15.78	-	-	40.4
K. obovata	12	2.75	-	4600	12.83	1.51	2.54	100.84
Mixed species	25	2.84 - 7.61	16.05	178 - 3096	15.96	1.47	2.44	86.29

It is noted that the mixed mangroves consist of the two dominant species at the study site. The mean tree height was about 2.84 and 7.61 m for *K. obovata* and *S. caseolaris*, respectively. The mixed species had stand densities varying from 1800 to 4050 ha^{-1}, with a mean of 3096 trees ha^{-1} for *K. obovata* and densities varying from 43 to 444 ha^{-1}, with a mean of 178 trees ha^{-1} for *S. caseolaris.*

We also measured the height of pneumatophores of *S. caseolaris* by establishing a sub-plot size of 1 m × 1 m to measure their maximum and minimum heights and counted the number of roots in each plot. The four corners of each sampling plot were established in the field using Garmin Global

Positioning Systems (GPS) eTrex Legend HCx, with a plot size of 30 m × 30 m to access the ALOS-2 PALSAR-2 pixel size of 6.25 m × 6.25 m. Photos and locations of the plots were also recorded using GPS during the field survey. Figure 4.2 shows the techniques used to measure biophysical parameters of *K. obovata*, *S. caseolaris* and their roots at the sub-plot. The diameter at breast height (DBH) of the *S. caseolaris* was typically measured at 1.3 meter above ground. It is noted that this measurement is not always a straightforward process because of anomalies in the stem structure. Thus, we measured different locations for irregular mangrove tree configurations to minimize the possible sources of errors. For instance, if the mangrove tree was forked at or below 1.3 m then we measured just below the fork. If the fork was very close to the ground, we measured the object as two trees, and if the tree was leaning, the DBH was taken according to the tree height parallel to the trunk [41].

(a) (b)

(c)

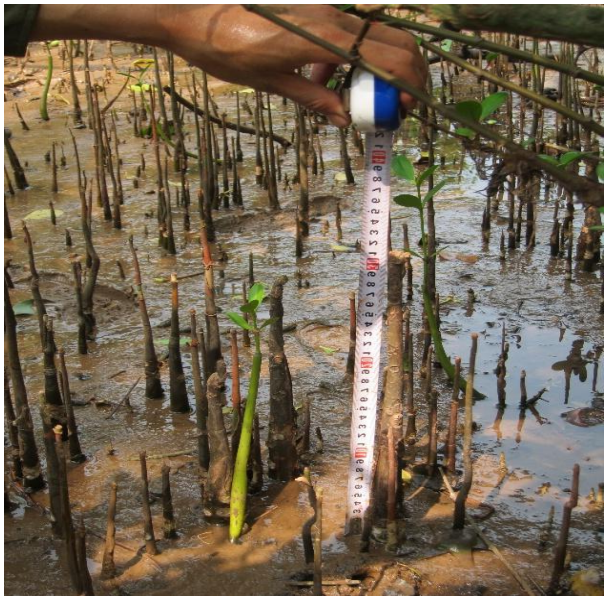

(d)

Source: photos took by Pham T.D. in July 2015

Figure 4.2. Measurement of biophysical parameters of *K. obovata* (a & b), *S. caseolaris* (c) and their roots (d).

The aboveground biomass of *S. caseolaris* was calculated using the allometric equation (4.2) [116]

$$Ws = a.\ \rho.\ (D^2H)^b \quad (4.2)$$

where *W*s is tree dry-weight (kg), *D* is diameter at breast height (DBH) (cm), *H* is tree height (m), ρ is wood density (ρ = 0.340 for *S. caseolaris*) [116], and *a* and *b* are constants, equal to 0.251 and 0.0825, respectively, for *S. caseolaris*.

The biomass of *K. obovata* was calculated using the following allometric equation from [224]. The crown area of *K. obovata* was calculated based on the crown diameters and crown depth since the crown area was considered an ellipse (Eq. 4.3).

$$\text{Crown area} = (W_1.W_2/2)^2.\ \pi \quad (4.3)$$

where W_1 is the widest length of the tree canopy through its centre, and W_2 is the canopy width perpendicular to W_1. The AGB of *K. obovata* was calculated using the allometric equation (4.4) [224],

$$\text{Tree volume} = \text{Crown area. Crown depth.} \quad (4.4)$$

Tree height is measured from the sediment surface to the highest point of the canopy.

4.2.4 Statistical analysis

The mean of the HH and HV backscattering coefficients σ^0 were calculated for each sampling plots with moving window size of 3 × 3 pixels to minimize the positional inaccuracies of GPS and geo-coding. We used a logarithmic equation to analyze the relationship between σ^0 and various biophysical parameters of mangrove species. Correlation analysis was used to examine the relationship between biophysical parameters of two mangrove species and backscatter coefficients σ^0. We used stepwise multi-linear regression (MLR) models to analyze the relationship between the dependent variables (biophysical parameters) and the independent variables (σ^0 for HH and HV). Previous studies that applied the MLR approach achieved good results [20, 69, 79, 225]. In this research, different MLR models were generated for *K. obovata, S. caseolaris*, and a mixture of both species. These models were used for the AGB estimation of mangrove species using ALOS-2 PALSAR-2 data.

4.2.5. Validation

We used the root-mean-square error (RMSE), and coefficient of determination (R^2) to assess and validate the AGB estimation models with the leave-one-out (LOO) cross-validation method. This technique was used to eliminate bias in estimating the AGB of mangrove species using regression models [226]. This technique allows each sample to be excluded while a model is developed with the remaining samples and used to predict the excluded samples. These statistical measures are widely used in biomass modeling to evaluate discrepancies between field-based data (AGB inventories) and predicted AGB data [227, 228]. RMSE (Eq. 4.4) and R^2 (Eq. 4.5) are standard metric for measuring errors of regression models. Lower RMSE and higher R^2 values correspond to better model results [33, 218],

$$\text{RMSE} = \sqrt{\sum_{i=1}^{n} \frac{(\hat{y}_i - y_i)2}{n}} \tag{4.4}$$

$$R^2 = 1 - \frac{\sum_{i=1}^{n}(y_i - \hat{y}_i)^2}{\sum_{i=1}^{n}(y_i - \bar{y})^2} \tag{4.5}$$

where $\hat{y}_i$ and y_i are the predicted and observed biomass for the i^{th} plot, respectively; n is the total number of validation plots, and $\bar{y}$ is the observed mean values of biomass.

4.3 Results and discussion

4.3.1 Characteristics of mangrove species in Hai Phong

We observed three kinds of mangrove forests at the study site during fieldwork in July 2015. The two dominant mangrove species are *K. obovata* and *S. caseolaris* (Fig. 4.3).

K. obovata *S. caseolaris* Mixed mangrove forest

Source: photos took by Pham T.D. in July 2015

Figure 4.3. Mangrove forest communities in the study area.

We compared the characteristics of dominant mangrove species in Hai Phong based on backscattering coefficient values for HH and HV polarizations. The results are shown in Table 4.3.

Table 4.3. Backscatter coefficients of mangrove species of Hai Phong in July 2015.

	HH			HV		
	Max	Min	Mean	Max	Min	Mean
***K. obovata* (*n* =12)**	-10.4	-12.9	-11.7	-16.7	-19.7	-17.9
***S. caseolaris* (*n* =23)**	-7.9	-13.7	-9.7	-14.1	-20.2	-16.1
Mixed species (*n* = 25)	-8.1	-13.4	-11.3	-14.3	-19.8	-17.9

As can be seen from Table 4.3, the means of HH and HV backscatter coefficients of *K. obovata* are lower than *S. caseolaris*. In fact, *K. obovata* has HH values between −12.9 dB and −10.4 dB and HV values between −19.7 dB and −16.7 dB. Higher HH values between −13.7 dB and −7.9 dB and HV values between −20.2 dB and −14.1 dB were observed for *S. caseolaris*. The mean backscattering coefficients at HH and HV polarizations of the two dominant mangrove species differ compared to those of Malaysia [23] and Indonesia [229]. These differences are likely due to differences in the mangrove species. The dominant species found in the Matang mangroves in

Malaysia are *R. apiculata*, *A. alba*, and *B. parviflore* [23] while the three dominant mangrove species found in Indonesia are *Rhizophora*, *Bruguiera* spp., and *Ceriops* [229].

4.3.2 Comparison of biophysical parameters of mangrove species

A correlation matrix summarizing the relationship among various biophysical parameters of the two mangrove species *K. obovata* and *S. caseolaris* are shown in Tables 4.4 and 4.5. These tables show that apart from tree density, all biophysical parameters of the two mangrove species are well correlated. Data regarding the ages of trees for the two species were acquired with the help of security guard teams from different communes during the fieldwork.

Table 4.4. Pearson's correlation matrix of different biophysical parameters of *S. caseolaris*

	Height (m)	Age (years)	DBH (cm)	Tree density	Biomass (Mg ha^{-1})
Height (m)	1				
Age (years)	0.79**	1			
DBH (cm)	0.66**	0.71**	1		
Tree density	0.09	-0.01	-0.19	1	
Biomass (Mg ha^{-1})	0.86**	0.76**	0.69**	0.30	1

**Correlation is significant at the 0.01 level, *Correlation is significant at the 0.05 level

Table 4.5. Pearson's correlation matrix of different biophysical parameters of *K. obovata*

	Height (m)	Crown diameter (m)	Crown area (m^2)	Age (years)	Tree density	Biomass (Mg ha^{-1})
Height (m)	1					
Crown diameter (m)	0.75**	1				
Crown volume (m^2)	0.89**	0.95**	1			
Age (years)	0.73**	0.75**	0.79**	1		
Tree density	-0.31	-0.18	-0.20	-0.08	1	
Biomass (Mg ha^{-1})	0.86**	0.88**	0.92**	0.85**	-0.05	1

**Correlation is significant at the 0.01 level, *Correlation is significant at the 0.05 level

A strong positive relationship was observed between the biophysical parameters of *S. caseolaris* and *K. obovata* and their above-ground biomass, with the exception of tree density. A possible explanation for this might be that tree density is a conditional parameter and depends on the species of the seedlings used. In addition, low correlations are observed with tree density, reflecting a decrease in the number of trees in the region. During the typhoon season, it is common for trees to fall due to storm activity, primarily in the case of trees at the juvenile stage at which their pneumatophores have not grown enough, and due to *Chthamalus stellatus*, which occurs frequently in the sea of Hai Phong and Quang Ninh [230].

The ALOS-2 PALSAR-2 data with HH and HV polarizations were analysed to examine how they relate with the different biophysical parameters of the two mangrove species. The results are shown in Tables 4.6 and 4.7. The L-Band backscattering (σ^0) HH and HV polarizations show a positive relationship with the biophysical parameters of both mangrove species at the study site. However, the sensitivity of σ^0 for HV polarization is higher than that of σ^0 for HH polarization. This is likely due to an increase in the volume of scattering with growth for both mangrove species. In contrast, the backscattering coefficient (σ^0) for HH polarization is slightly less sensitive than that for HV polarization for *K. obovata*.

Table 4.6. Relationship between HH and HV polarization and the various biophysical parameters for *S. caseolaris* (*n*=23).

	HH (σ^0)	HV (σ^0)	Height (m)	Age (years)	DBH (cm)	Biomass (Mg ha^{-1})
HH (σ^0)	1					
HV (σ^0)	0.88**	1				
Height (m)	0.43	0.60**	1			
Age (years)	0.48*	0.56**	0.79**	1		
DBH (cm)	0.35	0.42	0.66**	0.71**	1	
Biomass (Mg ha^{-1})	0.59**	0.74**	0.86**	0.76**	0.69**	1

**Correlation is significant at the 0.01 level, *Correlation is significant at the 0.05 level

Table 4.7. Relationship between HH and HV polarization and the various biophysical parameters for *K. obovata* (*n*=12).

	HH (σ^0)	HV (σ^0)	Height (m)	Age (years)	Crown diameter (m)	Crown area (m^2)	Biomass (Mg ha^{-1})
HH (σ^0)	1						
HV (σ^0)	0.77**	1					
Height (m)	0.60**	0.61**	1				
Age (years)	0.81**	0.76**	0.74**	1			
Crown diameter (m)	0.58**	0.51**	0.72**	0.75**	1		
Crown area (m^2)	0.61**	0.57**	0.88**	0.80**	0.94**	1	
Biomass (Mg ha^{-1})	0.79**	0.67**	0.79**	0.88**	0.89**	0.91**	1

***Correlation is significant at the 0.01 level, *Correlation is significant at the 0.05 level*

This research has also determined the relationship between the biophysical parameters of the dominant mangrove species of Hai Phong city in 2015 and the backscattering coefficients for HH and HV polarizations (Tables 4.6 and 4.7). A high correlation was observed between the means backscattering coefficients for HH and HV polarizations and the various biophysical parameters, apart from tree density for the two mangrove species. The HV polarization showed a higher correlation than HH for *S. caseolaris* where the volumetric scattering might strengthen the cross-polarization. The co-polarization HH data also showed high correlation which can be explained by strong surface scattering [120].

To examine the relationship between the plots of biomass and backscatter coefficients of the ALOS-2 PALSAR-2 L-band for HH and HV polarizations for each mangrove species, scatterplots were generated for these species (Figures 4.4, 4.5 and 4.6).

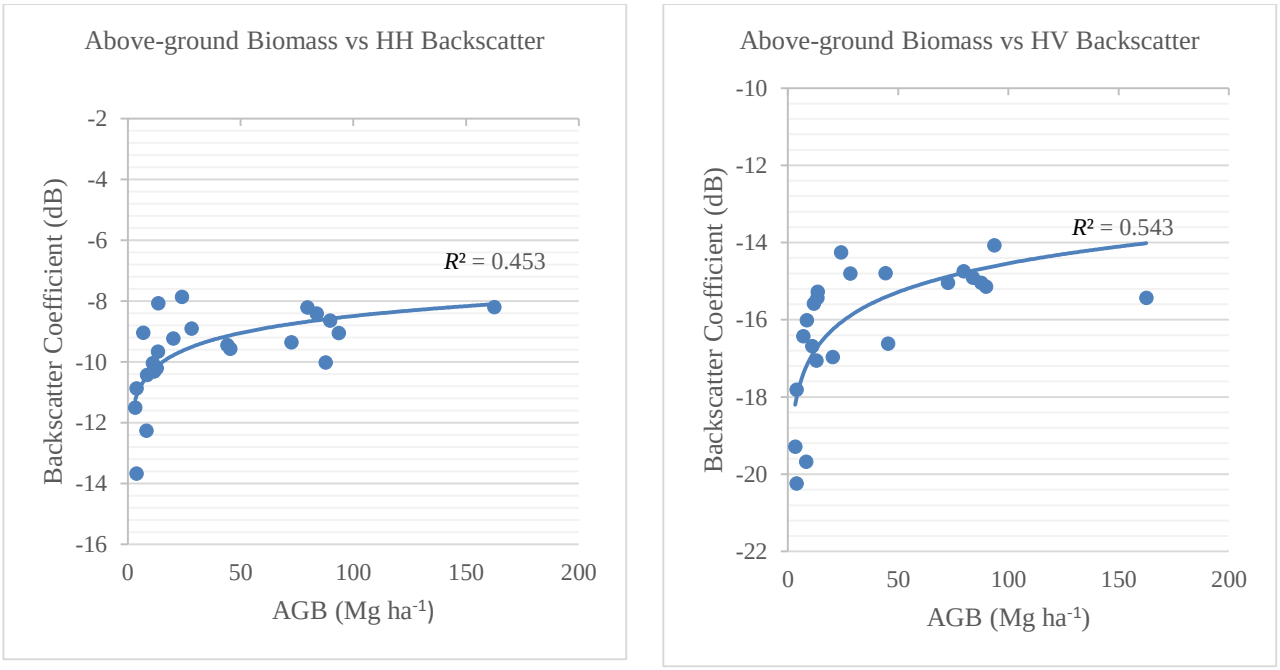

Figure 4.4. The AGB (Mg ha^{-1}) versus L-HH and HV backscatter coefficients (dB) of *S. caseolaris*

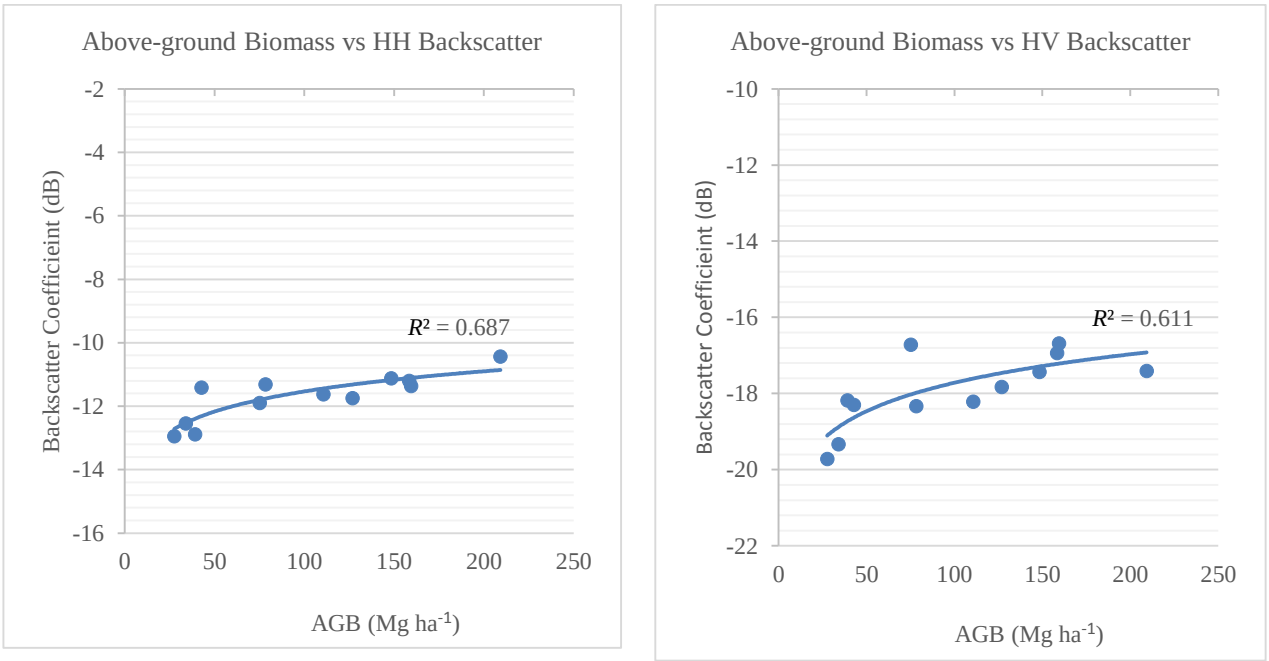

Figure 4.5. The AGB (Mg ha^{-1}) versus L-HH and HV backscatter coefficients (dB) of *K. obovata.*

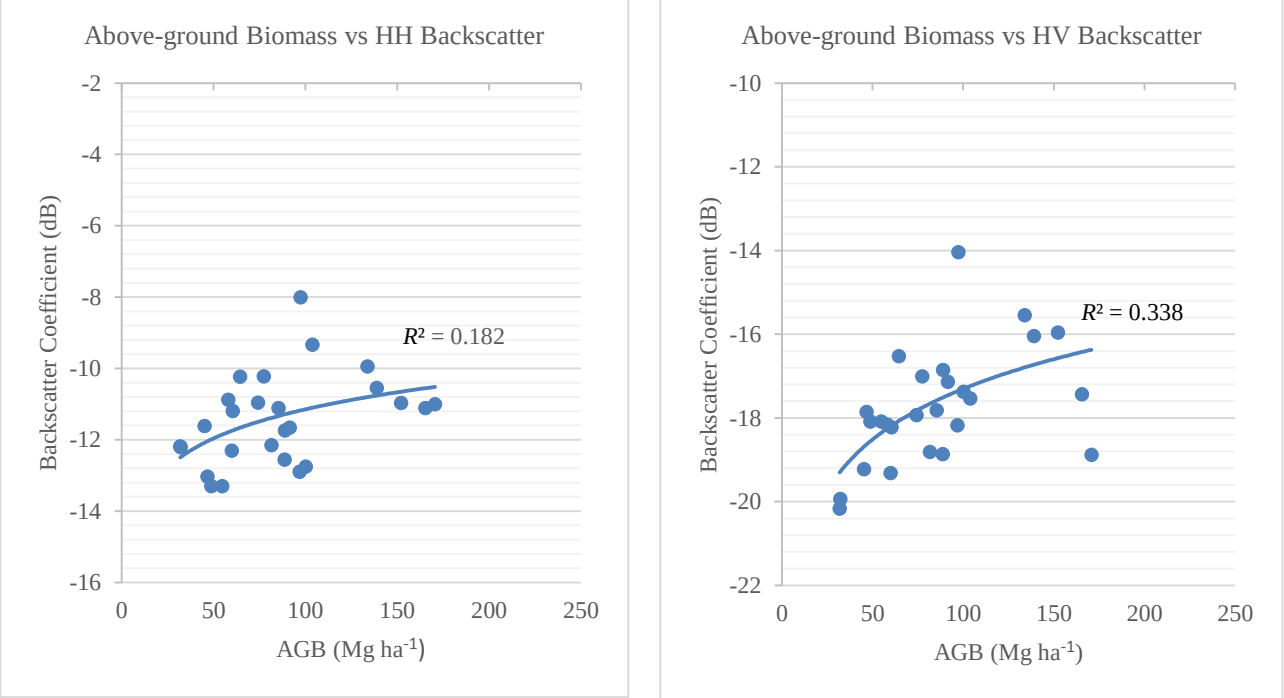

Figure 4.6. The AGB (Mg ha^{-1}) versus L-HH and HV backscatter coefficients (dB) of mixed species

The scatterplots show that the L-HV backscatter coefficient gave a better correlation with the AGB than that of the HH backscatter for *S. caseolaris.* However, the L-HH backscatter was likely more sensitive to the AGB of *K. obovata* than the HV backscatter coefficients. In terms of mixed species, a weak correlation was observed by both L-HH and HV backscatter coefficients and the AGB. The responses observed between the HH and HV backscatter coefficients and the biomass for mixed species likely contained no significant correlation due to the complicated nature of the extensive root systems of the mixed species [216].

As the biomass increases in the mangrove communities, the radar backscatter coefficients increase to about 100–120 Mg ha^{-1}, and saturation was observed [216]. However, the L-HH and HV backscatter decrease when the level of the aboveground biomass increases above 100–120 Mg ha^{-1} for some mangrove species with extensive prop root systems, such as pneumatophores of *S. caseolaris*, *A. marina*, and *L. racemose*. Figure 4.6 shows that the saturation level of *S. caseolaris* is less than 100 Mg ha^{-1}; while Figure 4.6 shows the scatterplots of the mixture of the two species, reflecting that the saturation level of mixed species was lower than 100 Mg ha^{-1}. Figure 4.5 presents the saturation level of *K. obovata* at approximately 150 Mg ha^{-1}. These results are consistent with previous studies [23, 231].

4.3.3 Aboveground biomass estimation of mangrove species at the sampling plots

Table 4.8 and Figure 4.7 provide the distribution of the AGB of different mangrove species in the sampling plots during the year 2015. The estimation of the AGB for *S. caseolaris* ranged between 2.75 and 161.51 Mg ha^{-1}, and for *K. obovata* the AGB ranged from 27.6 to 209.20 Mg ha^{-1}.

Table 4.8. Summary of AGB measured for different species in all sample plots.

	Min (Mg ha^{-1})	Max (Mg ha^{-1})	Mean (Mg ha^{-1})	Std (Mg ha^{-1})
S. caseolaris (n=23*)*	2.75	161.51	40.47	41.57
K. obovata (n=12*)*	27.60	209.20	100.84	60.43
Mixed species *(n*=25*)*	31.88	170.65	86.29	39.75

As can be seen in Fig. 4.7, the number of sampling plots occupied by *K. obovata* is 12 while *S. caseolaris* occupied 23 of the 60 total sample plots. At the study site, most the plots measured AGB in 2015 at less than 100 Mg ha^{-1}. This situation is similar to mangrove forests in Malaysia [23]. The plots covered by *K. obovata* and mixed species have higher biomass than those of *S. caseolaris,* since the stand density of the former species was much higher than that of the latter species.

It is noted that the range for L-HH and HV backscatter coefficients of *S. caseolaris* were higher than those of *K. obovata* while a lower biomass level of *S. caseolaris* was observed. A possible explanation is that pneumatophores are associated with this species, resulting in lower saturation levels than *K. obovata*. In addition, *S. caseolaris* species are often inter-planted in high tidal inundation levels in the river mouth or sea to effectively protect dyke systems and to reduce damage from storm surge [223]. Thus, the water levels associated with *S. caseolaris* forest could lead to an increase in the L-HH and HV backscatter [221, 222].

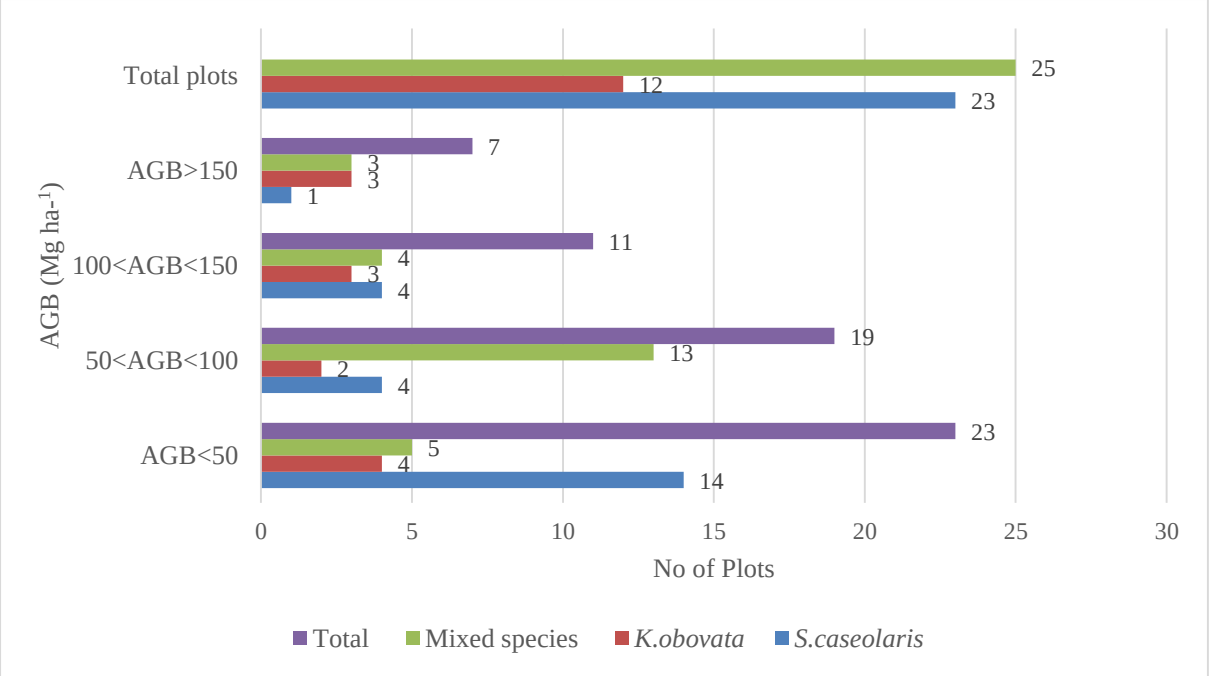

Figure 4.7. Variation of AGB for mangrove species in all sample plots.

Our study illustrates how the above-ground biomass of different mangrove forests varies considerably according to species and geographical locations. Different mangrove types at different stand-ages respond in different ways to the SAR signal. The AGB of *K. obovata* shows a range of 27.6 to 209.2 ± 60.4 Mg ha^{-1} with an average of about 100 Mg ha^{-1}. This value is around two times higher than that of the *K. obovata* plantation in Nam Dinh province, Vietnam [144]. These differences may be explained by the differences in the stand-age of mangrove plantation [232]. The mean of stand-age in the study area for *S. caseolaris* was about 16 years old while the mean was 13 years old for *K. obovata* (Table 4.2). These values are, respectively, 7 and 4 years higher than the mangrove forests plantation in Nam Dinh province. This research has confirmed that the stand-age affects the above-ground biomass of the *K. obovata* mangrove plantation. In addition, the AGB of *S. caseolaris* is estimated to range from 2.8 to 161.5 ± 41.6 Mg ha^{-1} with an RMSE of 35.5 Mg ha^{-1}. Thus, further study with more focus on the estimation of mangrove species is suggested.

Referring to Fig. 4.7, the findings show the spatial distribution pattern of the AGB for the two mangrove species of Hai Phong city for the year 2015. Most the plots contained AGB less than 100 Mg ha^{-1}, followed by the group of plots with AGB ranging from 100 to 150 Mg ha^{-1}. Several regions of the Do Son and Dai Hop districts were covered by areas with AGB over 150 Mg ha^{-1}.

This is likely due to successful mangrove conservation by the community-based forest management, in cooperation with the local authority in these coastal districts of Hai Phong [168].

4.3.4 Biomass modeling and estimations using ALOS-2 PALSAR-2 data

To predict the above-ground biomass of the two mangrove species and mixed species, multi-linear regression models were created: Model 1 (*S. caseolaris*-based biomass), Model 2 (*K. obovata*-based biomass), and Model 3 for mixed species. Table 4.9 shows the three models with their R^2 value.

Table 4. 9. Multi-linear regression models based on the biomass of the two mangrove species

No	Mangrove species	Polarization	Beta Coefficients	R^2	R^2 *Adj*	Regression Model
1	*S. caseolaris*	HH HV	0.135 0.620	0.547	0.502	Y(biomass) = 4.808 + 0.049 σ^0HH + 0.184 σ^0HV
2	*K. obovata*	HH HV	0.603 0.416	0.644	0.554	Y(biomass) = 4.758 + 0.191 σ^0HH + 0.031 σ^0HV
3	Mixed species	HH HV	0.085 0.527	0.342	0.285	Y(biomass) = 3.397 + 0.013 σ^0HH + 0.076 σ^0HV

The estimated coefficients of HH and HV polarizations have significant impact on the AGB estimation of the mangrove species. Both L-HH and HV backscatter coefficients contributed to the total aboveground biomass of the two mangrove species at a statistical significance level of 5%. However, the standardized beta coefficient of HV backscatter was higher than that of HH backscatter, indicating a stronger effect for the total AGB of *S. caseolaris* [233]. In contrast, a stronger effect for the L-HH backscatter coefficient on the total AGB for *K. obovata* was observed. These were consistent with the relationship between the AGB and the backscatter coefficients of L-band at HH and HV polarizations for the mangrove species (Fig. 4.4 and 4.5).

Models 1 and 2 provide higher R^2 values than Model 3 and, therefore, have the greatest potential to provide useful estimates of mangrove species at the study site. In contrast, Model 3 for mixed species is not suitable for mixed species. The R^2 values of the two MLR models are about 0.547 and 0.644 for *S. caseolaris* and *K. obovata*, respectively. The overall RMSE (root-mean-square-error) is 35.5 Mg ha^{-1} for *S. caseolaris* and 41.3 Mg ha^{-1} for *K. obovata.* These values are slightly higher than those for the mangrove forests in Matang, Malaysia. This is likely due to a combined estimation of AGB for the entire mangrove communities in Malaysia [23].

Validation

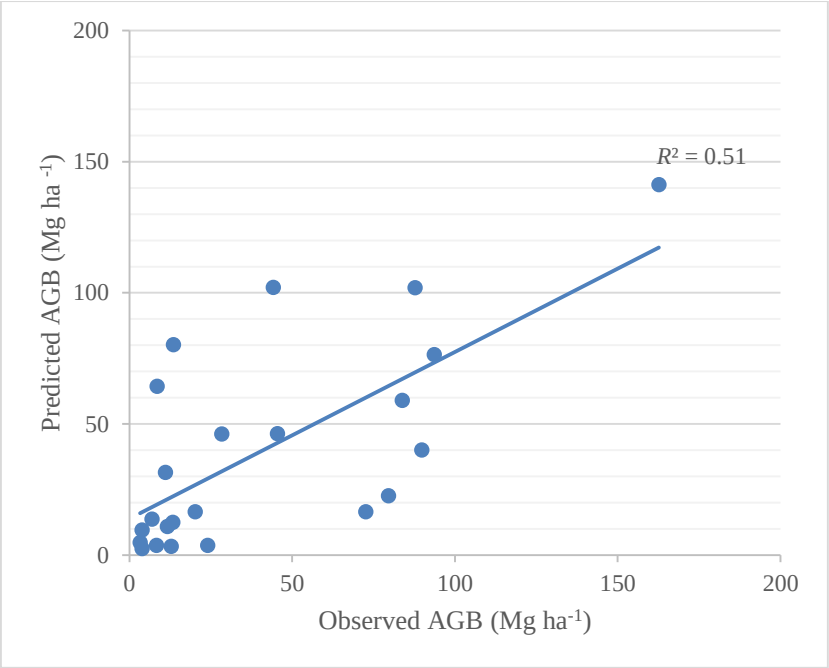

Figure 4.8. Validation results of AGB for *S. caseolaris* using MLR and LOO cross-validation

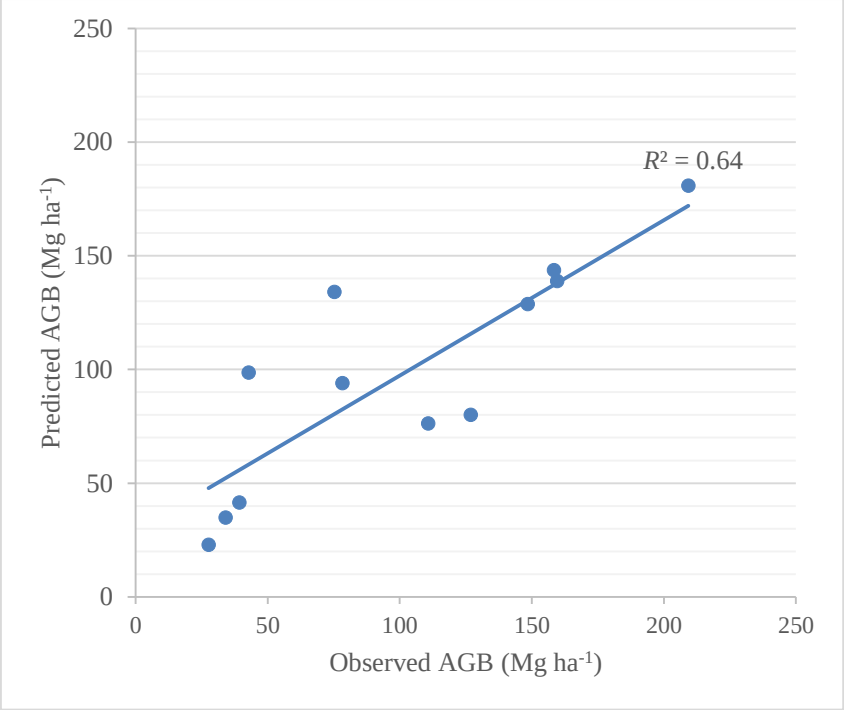

Figure 4.9. Validation results of AGB for *K. obovata* using MLR and LOO cross-validation.

Figures 4.8 and 4.9 show scatterplots of the predicted vs. observed AGB, in consideration of the accuracy of the estimated AGB by the MLR models of the two mangrove species at the study site.

The value of the coefficient of determination (R^2) using MLR models with LOO cross-validation were 0.51 and 0.64 for *S. caseolaris* and *K. obovata*, respectively. A lower value of R^2 was observed for the pure planted *S. caseolaris* forest due to its pneumatophores and tidal inundation level. The sensitivity of the estimated AGB from the L-band HH and HV polarizations decreases as the mangrove forest biomass increases due to the saturation of the SAR signal. A high variation of error was observed in the high biomass plots where the AGB was greater than 100 Mg ha^{-1} for *S. caseolaris* and 150 Mg ha^{-1} for *K. obovata* [216]. More research is, therefore, needed to investigate the sensitivity of ALOS-2 PALSAR-2 for other mangrove species in the tropics.

The findings show that for the ALOS-2 PALSAR-2 backscatter coefficients at HH and HV polarizations, the L-band in high sensitive mode was sensitive to the AGB exceeding 100 Mg ha^{-1} for *S. caseolaris* and 150 Mg ha^{-1} for *K. obovata* (Fig. 4.4 and 4.5). This means that the errors by the MLR models 1 and 2 with LOO cross-validation were observed to increase significantly when the AGB exceeded 150 Mg ha^{-1}. The saturation levels of the two mangrove species of Hai Phong were consistent with previous studies [23, 231].

Based on the findings, the above-ground carbon stock and total carbon emissions of each mangrove species can be derived. This work is essential for carbon monitoring and, thus, plays an important role in national forest-monitoring systems towards implementing the United Nations' Reduce Emission from Deforestation and Forest Degradation (REDD+) program in developing countries and the coastal blue carbon projects [107, 108].

4.4 Conclusions

This chapter has been undertaken to investigate the characteristics of different mangrove species and estimate their aboveground biomass using SAR data during the year 2015 in Hai Phong city, Vietnam. This research illustrates the use of ALOS-2 PALSAR-2 in high sensitive mode to characterize the distribution of mangrove species and determine the relationship between the biophysical parameters of different species and backscattering coefficients for HH and HV polarizations. The findings demonstrate that ALOS-2 PALSAR-2 can be useful in estimating the above-ground biomass of mangrove species. The validation results show a satisfactory correlation between model estimates and field-based measurements, with R^2 = 0.51 and 0.64 and RMSE = 35.5 Mg ha^{-1} and 41.3 Mg ha^{-1} for *S. caseolaris* and *K. obovata*, respectively. Although the saturation level of the AGB for two mangrove species is above 100 Mg ha^{-1}, the use of L-band ALOS-2 PALSAR-2 in high sensitive mode can provide an alternative approach that should allow

rapid estimation of the AGB for different mangrove species in the tropics in large areas where accessibility is limited.

The development of the aboveground biomass estimation for different mangrove species provides an alternative method to derive biomass in a cost-effective and timely way. The technique and methods developed can be replicated for other mangrove forest species with similar characteristics, stand structures, and various biophysical parameters. The MLR approach using ALOS-2 PALSAR-2 data can be used as a practical guide for other regions of Vietnam for the preliminary design of regional and local level biomass assessment. This research has been conducted on the mangrove forests of Hai Phong city, Vietnam. Further research is needed to determine the biomass of other mangrove species and extend this work for the entire mangrove forests of Vietnam. This will support provincial decision making on mangrove conservation and management.

Chapter 5

Biomass and carbon stocks estimation of mangrove species using machine learning techniques

Chapter 5 presents the findings on the characteristics of specific mangrove species in Hai Phong City (Vietnam) and the estimation of its above-ground biomass and carbon stocks of Sonneratia caseolaris (l.) Engler *at a coastal area of Hai Phong city (Vietnam) using ALOS-2 PALSAR-2 imagery and GIS- based multi-layer perceptron neural networks.*

5.1. Introduction

The mangrove forest biome, commonly referred to as "mangroves" collectively, is the most important ecosystem within coastal inter-tidal zones in many tropical and semi-tropical regions. It plays a vital role in reducing damage from tsunamis [6], protecting land from erosion, and mitigating the effects of typhoons [136]. In addition, this ecosystem can act as a highly efficient carbon sink in the tropics [7], because mangroves can sequester carbon in both above and below-ground biomass as well as within sediment [8].

Despite the large carbon storage potential in mangrove biomass and soils, mangroves are under serious threat from high population growth, aquaculture expansion, timber harvesting, and other human activities [234]. In Southeast Asia, mangroves have declined markedly suffering from the greatest loss of 1.9 million hectares [11]. Vietnam has experienced severe mangrove loss over the last 50 years [12]: on the northern coast in particular, mangrove area decreased by 17,094 ha from 1964 to 1997, largely due to over-expansion of shrimp farming [235].

Numerous studies have estimated mangrove biomass during the past 30 years [109-111, 113, 114]. Several studies established allometric equations to estimate the above-ground biomass (AGB) from *in-situ* measurements [115], as well as forest inventory from biophysical parameters

of mangrove trees such as stem weight, tree height and diameter at breast height (DBH) [112, 116]. The computational methods involved have included regression models [115, 117] and machine learning [33]. However, these studies were influenced by site selection biases and other factors such as tidal inundation [4, 118]. Current methods used can be time consuming, and costly, particularly in areas of dense mangrove forests, resulting in a lack of up-to-date information on spatial distribution of biomass and carbon stock. Thus, it is necessary to develop accurate and low-cost models to estimate mangrove biomass in order to support coastal zone management programs.

A variety of remote sensing data have been widely used for mapping and monitoring mangrove forests including optical imagery [211-215] and synthetic aperture radar (SAR) data [216, 236]. SAR sensors have been largely found to be more effective in monitoring mangrove dynamics as they can penetrate clouds, a common occurrence in the tropics [19]. Estimation of mangrove forests AGB is most accurate when conducted at the individual species level [217]. However, estimation of AGB using remote sensing data for specific mangrove species, *i.e. Sonneratia caseolaris*, has rarely been conducted. Thus, this study attempted to estimate the biomass and carbon stock of *S. caseolaris* (a dominant mangrove species in the study area) using ALOS-2 PALSAR-2 imagery.

Biomass and carbon stock estimation of mangrove forests in Vietnam is still limited. Existing studies are restricted to specific regions, such as Ca Mau Peninsula in the south [141] and Hai Phong, Quang Ninh in the North [14, 142]. Several studies have attempted to estimate the biomass and carbon stock of mangrove plantation in the northern coast of Vietnam [144], in Quang Ninh province in the north, in Ca Mau and Kien Giang in the South [122], and in the Mekong Delta region [237]. However, the spatial distribution of mangrove forest biomass and carbon stock in Vietnam is limited and not well documented. Thus, there is a need to quantify and assess these variables using a practical and cost-effective approach.

Recently introduced machine learning algorithms have been shown to be effective for modeling mangrove biomass and species distribution using remote sensing data [238, 239]. However, there are several difficulties involved in implementing machine learning algorithms as long as traditional modeling techniques. The recent development of open-source software tools such as WEKA and Python has led to the wide use of machine learning [240, 241]. Machine learning has become more common for the estimation of mangrove forest biomass due to its potential to produce better models than traditional modeling methods. Therefore, the investigation of machine learning algorithms for the estimation of mangrove forest biomass is highly necessary to support monitoring, reporting, and verification (MRV) work as part of the United Nations' Reducing Emission from Deforestation and Forest Degradation (REDD+) program in developing countries.

Our study developed a prediction model using SAR remote sensing imagery and multi-layer perceptron neural networks (MLPNNs) to estimate the biomass of a high-density mangrove species in the coastal area of Hai Phong city, Vietnam. According to current literature, this is the first time an estimation of AGB for *S. caseolaris* has been carried out in this area. Our work will allow further investigation into the functional condition of mangrove ecosystems in the study area and may help elucidate the spatial distribution patterns of biomass in tropical and sub-tropical climates. Our results also promote the implementation of REDD+ and payment for ecosystem services (PES) strategies by providing practical tools for developing regional and national blue carbon trading markets and guiding mangrove management and conservation.

Among various machine learning methods, artificial neural networks (ANNs) have great potential for nonlinear mapping, adaptive learning, and forecasting environmental problems, because they require no statistical assumptions on data distribution and have performed well in recent studies [242, 243]. Many studies have used ANNs in modelling non-linear relationship problems such as drought [243], surface irrigation systems [244-246], and shallow landslide hazards [180]. However, ANNs have seldom been utilized for estimating mangrove forest biomass. More importantly, the ability of available machine learning techniques to estimate mangrove AGB has not been quantitatively assessed.

This study used ALOS-2 PALSAR-2 data to investigate the applicability of MLPNNs for estimating the AGB of *S. caseolaris* in a coastal area of Hai Phong city, Vietnam. We also compared the MLPNNs' performance with other machine learning techniques. Our results demonstrate that the use of ALOS-2 PALSAR-2 imagery and MLPNNs for estimating mangrove forest biomass has the potential to support improved coastal conservation and management. We note that the data visualization and processing were carried out using ENVI 5.2 and ArcGIS 10.2 software, while the modeling process was conducted using Weka 3.7 software.

5.2. Study area and data

5.2.1 Description of study area

We conducted this study in the mangrove forests of Vinh Quang village, which belongs to the Tien Lang district of Hai Phong city (Fig. 5.1). The coastline in this part of northern Vietnam consists of high tidal mudflats formed by a large quantity of alluvial sediment from the Red River. This area is vulnerable to rising sea levels and tropical storms, which often take place during the wet season from May to October [247]. Part of the coastline is protected by the dominant mangrove

species *S. caseolaris* [142, 236], which plays an important role in wave reduction [137] and contributes to the socio-economic lives of local residents by providing forest products [9].

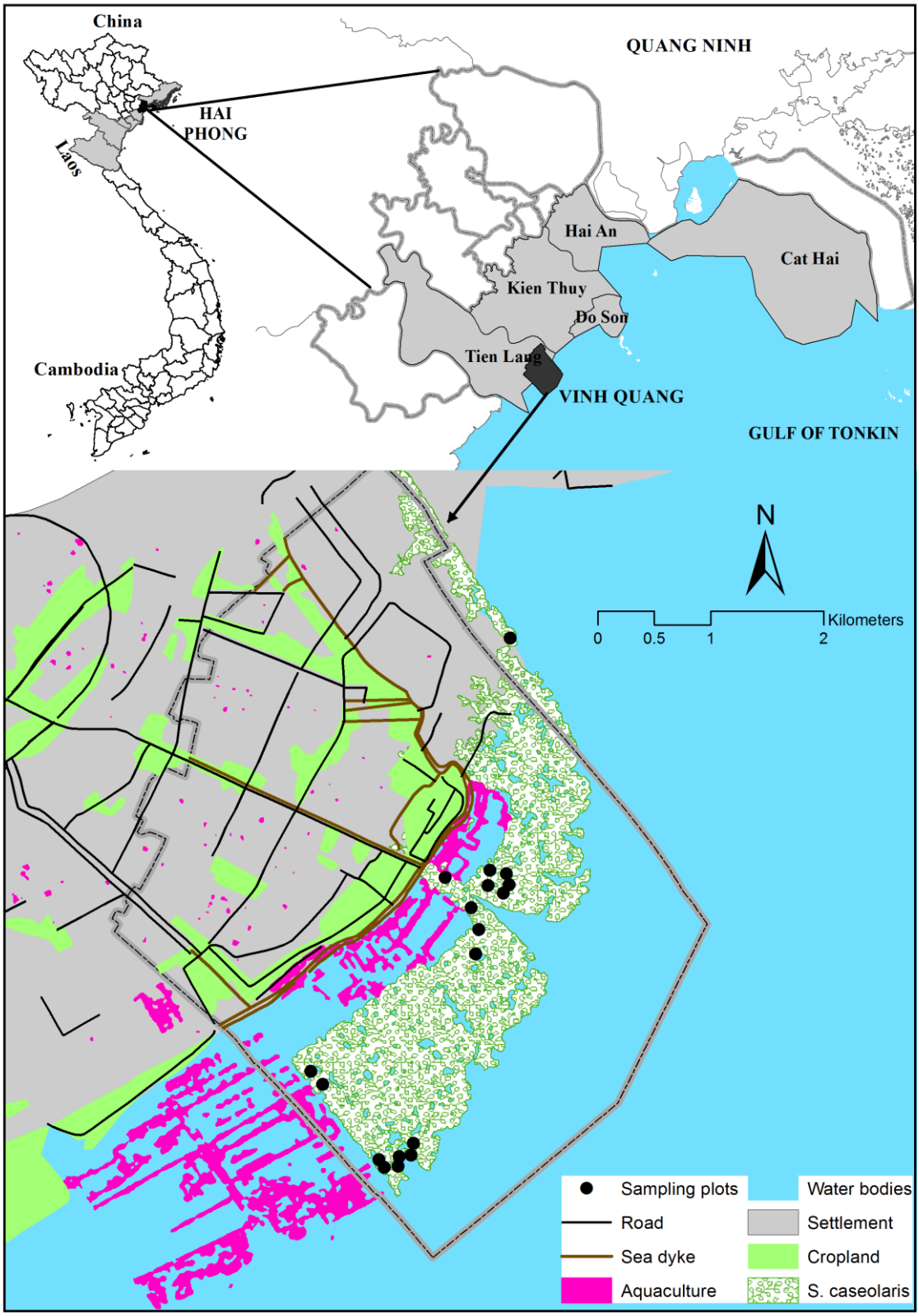

Figure 5.1. Map of the study area at Vinh Quang coast, Tien Lang district, Hai Phong city

5.2.2 Data collection and processing

5.2.2.1 SAR image collection and processing

We used ALOS-2 PALSAR-2 satellite imagery (level 1.5, in high-sensitive polarimetric mode), acquired from the Remote Sensing Technology Centre (RESTEC) of Japan to estimate the biomass of *S. caseolaris* (Table 5.1).

Table 5.1. Acquired satellite remote sensing data.

Satellite sensor	Date of acquisition	Level of process	Pixel Spacing	Polarizations
ALOS-2 PALSAR-2	2015/7/31	1.5	6.25 m	L band (HH, HV)

Source: JAXA, Japan

The digital number (DN) was converted to normalized radar sigma-zero using Eq. 5.1

$$\sigma^0 \text{ [dB]} = 10 \log_{10} (\text{DN})^2 + \text{CF} \quad (5.1)$$

where σ^0: backscattering coefficient; DN: digital number of the amplitude image; CF: calibration factor which = –83 dB for both HH and HV polarizations [219]. The CF used to process ALOS-2 PALSAR-2 is similar to ALOS PALSAR [248].

The DN of each pixel was transformed into backscattering sigma naught (σ^0) in decibel (dB) after applying Frost filters with moving windows of 5 x 5 in order to reduce speckle noise of SAR data [220]. In order to minimize effects from tidal height, we also carefully took the time to conduct field work into consideration [249].

We employed ENVI 5.2 software for SAR imagery processing and *S. caseolaris* identification, as illustrated in Figure 5.2.

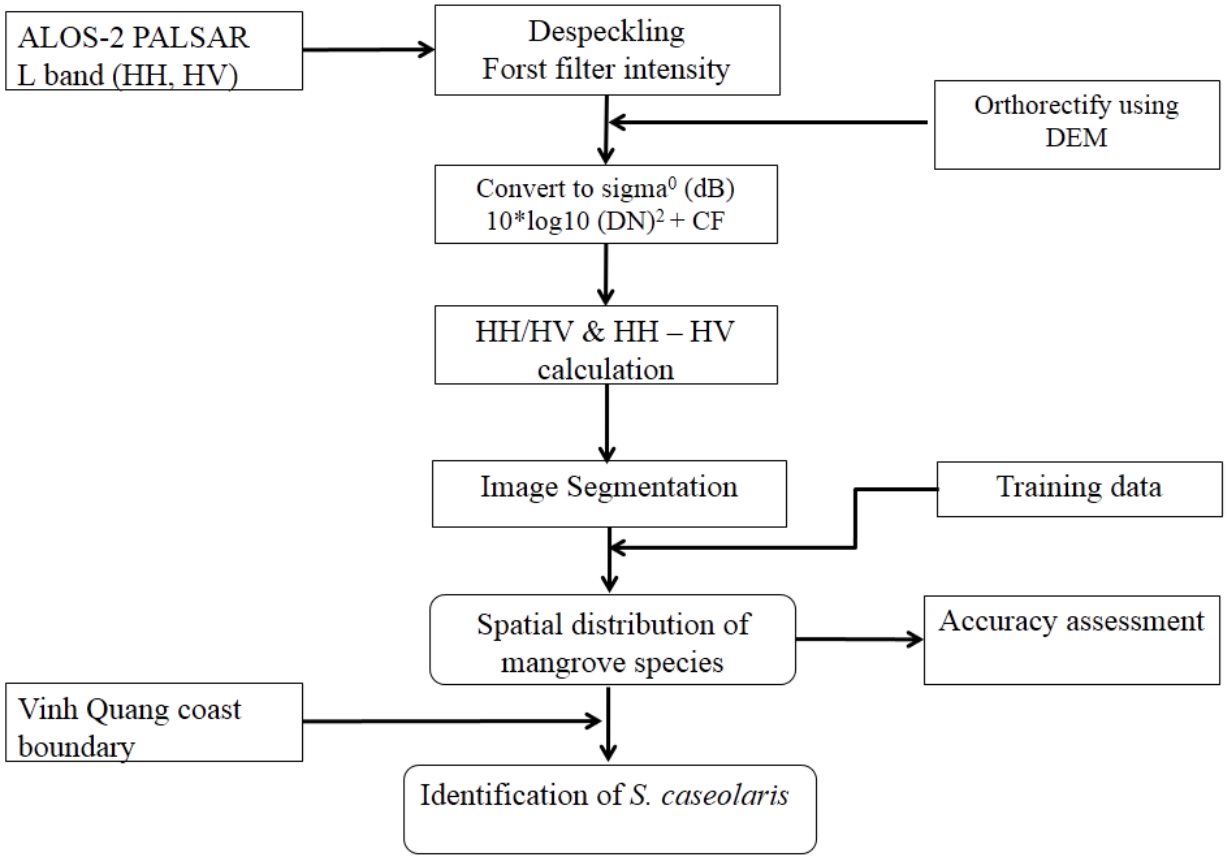

Figure 5.2. Flowchart used to identify *S. caseolaris* using ALOS-2 PALSAR-2 imagery.

5.2.2.2 Field data collection

We conducted field survey measurements along the Vinh Quang coast in July 2015 with help and permission from local authorities. We selected plots using a stratified random sampling method in which strata were determined based on a pre-survey involving local people to ensure the range of biomass values would be valid for the entire mangrove forest. A total of eighteen sampling plots were measured for specific biophysical parameters such as diameter at breast height (DBH), tree height, and tree density. In addition, interviews with village heads, chairmen of farmer's associations, and women's reunions were conducted to understand the history of mangrove plantation programs in the area.

We also measured the height of *S. caseolaris* pneumatophores by establishing 1 x 1 m sub-plots to measure their maximum and minimum height along with a root count. The four corners of each sampling plot were established in the field using a Garmin Global Positioning Systems (GPS) eTrex Legend HCx unit, with a plot size of 30 x 30 m to access the ALOS-2 PALSAR-2 pixel size of 6.25 x 6.25 m (Fig. 5.3). The field data were divided into two sets: the first was used to estimate

mangrove AGB using machine learning algorithm models, while the second was used for model validation. Photos and locations of the plots were also recorded using GPS during the field survey. Figure 5.3 shows the techniques used to measure biophysical parameters of *S. caseolaris* and their roots in a sub-plot.

Source: photos took by Pham T.D. in July 2015

Figure 5.3. Measurement biophysical parameters of *S. caseolaris* and their roots.

The above-ground biomass (AGB) and below-ground biomass (BGB) of *S. caseolaris* were calculated using the allometric equation 5.2 and 5.3 [116].

$$AGB = a.\ \rho.\ (D^2H)^b;\ BGB = 0.199.\ \rho^{0.90}.\ D^{2.22} \quad (5.2\ \&\ 5.3)$$

where AGB and BGB: tree weight (kg); D: diameter at breast height (DBH) (cm); H: tree height (m); ρ: wood density (ρ = 0.340 applied for *S. caseolaris*) [116]; a = 0.251 and b = 0.0825 are constant for *S. caseolaris.*

A ratio of 0.47 was applied in order to convert above-ground and below-ground biomass to carbon stocks [108].

5.3. Method used

5.3.1 Multi-Layer perceptron neural networks

An artificial neural network is defined as a large number of highly interconnected nodes which can be suitably used for modeling non-linear complex problems such as forest biomass modeling. Although various network structures and algorithms have been proposed, multi-layer perceptron neural networks (MLPNNs) may be the most widely used in environmental modeling [173] including land-use and land-cover classification [174], forest monitoring and mapping [174, 175], mangrove species classification [238], mangrove mapping [250], and characterization of mangrove ecosystems [251]. Therefore, we used MLPNNs in this study.

The structure of a common MLPNN consists of three layers: input, hidden, and output layers. In the input layer, the number of neurons is equal to the number of input images used (Fig. 5.4) whereas the number of neuron in the hidden layer must be determined beforehand based on the study area data. The output layer contains one neuron; in this case, the values for AGB. The MLPNN's performance is influenced by connection weights between the input and hidden layers, and between the hidden layer and the output. These weights are adjusted and updated accordingly in the training phase based on a back-propagation algorithm [176] with the intention of minimizing the difference between the AGB value produced from the MLPNN model and the AGB inventories.

Table 5.2. Performance of MLPNN with different numbers of neurons in the hidden layer.

Number of neurons in hidden layer	R^2	RMSE	MAE
1	0.510	0.403	0.296
2	0.029	0.685	0.526
3	0.177	0.694	0.514
4	0.357	0.591	0.448
5	**0.776**	**0.299**	**0.237**
6	0.480	0.573	0.388
7	0.274	0.766	0.441
8	0.286	0.746	0.44
9	0.325	0.700	0.418
10	0.196	0.839	0.479
11	0.238	0.714	0.431
12	0.194	0.855	0.525
13	0.151	0.872	0.513
14	0.303	0.764	0.403
15	0.174	0.890	0.509

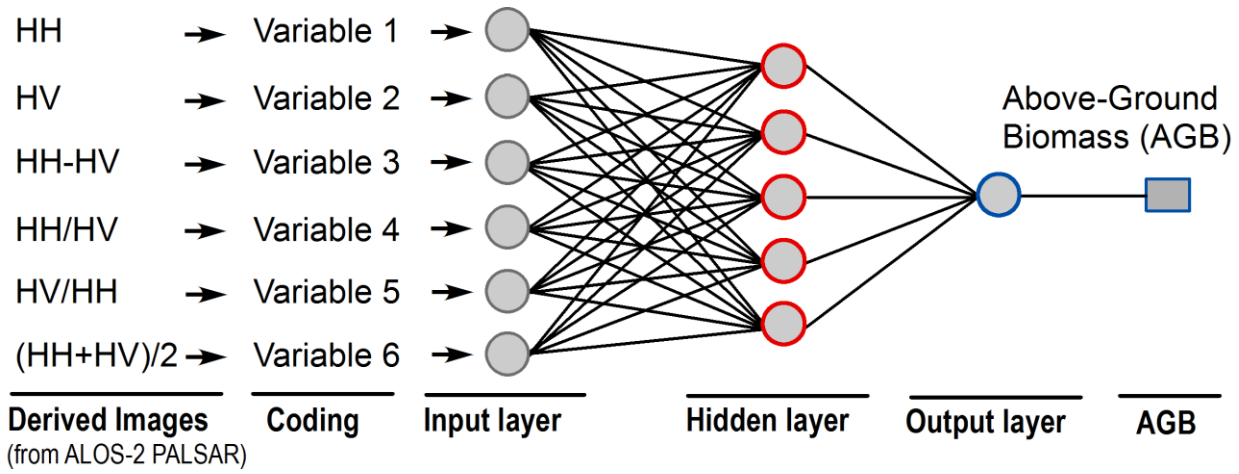

Figure 5.4. Structure of the MLPNN model for estimating the AGB in this study.

To design the MLPNN model for this study, it was necessary to determine the optimal number of hidden neurons. For this purpose, we used a test suggested by Tien Bui, et al. [180] by varying the numbers of neurons of the MLPNN versus the root-mean-square error (RMSE) using the training data with leave-one-out cross-validation techniques. Table 5.2 shows that the ANN model with 5 neurons in the hidden layer produced the best performance (the highest R^2, and the lowest RMSE and mean absolute error, MAE); therefore the hidden layer with 5 neurons was selected for use in this study. The final structure of the MLPNN model for this study is shown in Fig. 5.4. The learning rate, momentum, and training iteration were selected as 0.3, 0.2, and 500, respectively [252]. The activation function is the logistic sigmoid as suggested by Şenkal and Kuleli [253].

5.3.2 Performance assessment

We used root-mean-square error (RMSE), mean absolute error (MAE), and coefficient of determination (R^2) to assess and compare the performance of the biomass estimation models. These statistical measures are widely used in biomass modeling to evaluate discrepancies between measured data (AGB inventories) and predicted AGB data [227, 228].

RMSE (Eq. 5.4) is a standard metric for measuring errors of regression models, but it is strongly influenced by large values and outliers [254]. Therefore MAE (Eq. 5.5) is suggested for use with RMSE for determining the variation of model errors [255]. Lower RMSE and MAE values mean a better model. In addition, a smaller difference between RMSE and MAE means a smaller variance of errors. R^2 is estimated using Eq. 5.6; higher R^2 values also mean a better model [33].

$$\text{RMSE} = \sqrt{\sum_{i=1}^{n} \frac{(\hat{y}_i - y_i)2}{n}} \quad (5.4)$$

$$\text{MAE} = \frac{1}{n}\sum_{i=1}^{n} |\hat{y}_i - y_i| \quad (5.5)$$

$$R^2 = 1 - \frac{\sum_{i=1}^{n}(y_i - \hat{y}_i)^2}{\sum_{i=1}^{n}(y_i - \bar{y})^2} \quad (5.6)$$

where $\hat{y}_i$ and y_i are the predicted and observed biomass for the i^{th} plot, respectively; n is the total number of validation plots, and $\bar{y}$ is the observed mean values of biomass.

To select the best model among different machine learning methods, we used Akaike's Information Criterion (AIC) and Bayesian Information Criterion (BIC) to determine which regression model gives the most accurate estimates [256-258]. Both AIC and BIC provide simple and effective methods for selecting and comparing regression models [259, 260]. Kelloway [261] reported that lower AIC values indicated a better-fitting model.

AIC and BIC have been widely used for selecting and comparing different regression models related to the estimation of forest structures and biomass in recent studies [262-264]. We calculated AIC and BIC using equations (5.7) and (5.8). Models were ranked from the lowest to the highest AIC and BIC scores; the model with the lowest AIC and BIC values was considered the best.

$$\text{AIC} = n.\log(\frac{SSE}{n}) + 2K \quad (5.7)$$

$$\text{BIC} = n.\log(\frac{SSE}{n}) + \log(n).K \quad (5.8)$$

Where *SSE* is the sum of squares errors; n is the number of sampling plots; and K is the number of parameters; $K = p + 1$ where p is the number of predictors.

5.4. Results and Discussion

5.4.1 Field survey results

A total of 1508 mangrove trees were recorded in the 18 sampling plots. We chose only 18 plots because plot collection is time-consuming and there were labor constraints during the field measurement. Two factors in particular that resulted in a small number of sampling plots were the high density of the mangrove forests and their pneumatophores in the study area, and the considerable impact of tidal inundation.

Despite the limited sample plots, we consider our analyses reliable due to the use of machine learning techniques such as MLPNN and leave-one-out cross-validation. These approaches emphasize that small datasets exist in many real-world problems; data-mining methods work well

in such circumstances because they do not require statistical distribution assumptions. These issues were discussed in detail in Wisz, et al. [265] and Patel Patel, et al. [266]. The effects of sample sizes were discussed in Wisz, et al. [265].

Tree counts ranged from 42 to 126 trees per plot, while tree density averaged 79 (Table 5.3). Total AGB in each 900 m^2 plot ranged from 620 to 14,634 kg (median = 4447 kg). BGB estimated in each plot ranged from 823 to 29,492 kg (median = 6472 kg). The overall ratio of BGB/AGB was 1.46, calculated using the average BGB (Mg ha^{-1}) and AGB (Mg ha^{-1}) of all 18 recorded sampling plots. This number is comparable to that reported by Komiyama, et al. [113].

Table 5.3. Characteristics of *S. caseolaris* in the study site

Plot ID	Tree Density (No./900 m^2)	DBH (cm)	Age (years)	Tree height (meter)	AGB (kg/900 m^2)	Root Weight (kg/900 m^2)	BGB (kg/900 m^2)	AGB (Mg ha^{-1})	BGB (Mg ha^{-1})
1	57	10.67	17	5.71	542.91	7.709	823.444	6.887	9.149
2	45	13.22	17	6.42	699.36	9.309	1045.777	8.496	11.620
3	72	11.98	10	6.06	890.00	8.787	1345.252	11.049	14.947
4	83	11.49	10	6.08	956.30	6.992	1414.689	11.686	15.719
5	110	11.81	10	4.85	1085.77	5.093	1992.168	13.347	22.135
6	98	12.06	10	5.33	1094.05	6.663	1859.210	13.517	20.658
7	42	18.79	17	5.67	1099.30	7.655	2131.574	12.844	23.684
8	48	23.07	17	6.56	2077.34	11.480	3843.674	24.015	42.707
9	65	21.18	17	6.67	2442.24	11.006	4302.659	28.328	47.807
10	84	19.02	17	10.30	3846.09	15.965	4378.573	44.181	48.651
11	54	31.58	17	6.33	3976.38	12.977	8679.311	45.412	96.437
12	56	28.84	23	12.40	6409.29	26.660	7356.972	72.552	81.744
13	126	20.42	23	11.00	6955.34	18.150	7689.924	79.592	85.444
14	105	26.11	17	8.64	7264.79	22.896	11066.636	83.812	122.963
15	115	26.25	17	8.17	7632.43	18.383	12261.683	87.680	136.241
16	63	29.25	22	13.40	7928.94	31.490	8538.093	89.744	94.868
17	117	21.82	22	12.50	8162.52	28.125	8271.390	93.620	91.904
18	89	43.75	23	8.00	14535.88	8.800	29492.032	162.598	327.689
Average	79	21.18	17	8.10	4311.052	14.341	6471.837	49.409	71.909

5.4.2 Modeling results, assessment, and comparison

Since the sample size was small, the leave-one-out (LOO) cross-validation technique was used for building prediction models. This is an effective technique that has ability to eliminate bias in estimations of model performance [226]. This technique allows each sample to be excluded while a model is developed with all remaining samples and used to predict the excluded sample. Accordingly, a total of 18 sub-models were developed using the MLPNN techniques; the final MLPNN model was generated by averaging the 18 sub-models.

The performance of the final MLPNN model is shown in Table 5.4. The RMSE value (0.299) is significantly lower than the standard deviation of the AGB inventories (0.425) indicating that

the model performed well with the data. The MAE (0.237) is slightly lower than the RMSE indicating that the error variation is small. The R^2 value (0.776) indicates a satisfactory result. Overall, the MLPNN model performed well in this study area.

As the purpose of this study was to estimate the AGB of *S. caseolaris* in coastal Vietnam, the usability of the MLPNN model should be assessed and confirmed in its effectiveness. We selected the support vector regression (SVR), radial basis function neural network (RBFNN), Gaussian process (GP), and random forests (RF) models for comparison. SVR was selected because it outperforms various machine learning models in estimating AGB [33] whereas the others are widely used soft computing models with high performance in many fields [187, 243, 267].

Table 5.4. Machine learning models with LOO cross-validation for AGB estimation in this study

No	Machine learning model	RMSE	MAE	R^2
1	Multi-layer Perceptron Neural Networks (MLPNN)	0.299	0.237	0.776
2	Support vector regression (SVR)	0.359	0.268	0.596
3	Radial Basis Function Neural Networks (RBFNN)	0.388	0.333	0.612
4	Gaussian Process (GP)	0.379	0.345	0.483
5	Random Forests (RF)	0.402	0.364	0.372

Table 5.5. Comparison of MLPNN, SVR, RBFNN, GP, and RF models using AIC and BIC

	MLPNN	SVR	RBFNN	GP	RF
AIC	-29.473	-22.745	-20.101	-20.510	-18.151
BIC	-23.240	-16.512	-13.868	-14.278	-11.918

SVR is a regression version of the popular support vector machines that was developed based on statistical learning theory [268]. In this study, we used SVR with the radial basis function kernel [269] and the SMO algorithm [267]. Accordingly, the best values for the kernel width (0.195) and the regularization (2.75) were found using the grid search method. For RBFNN [270], the best structure (6 input neurons, one hidden layer with 10 clusters, and one output) was found based on a test suggested in Hong, et al. [271]. For GP, the radial basis function [272] was used with gamma of 4.185 as the best value for the study area. The RF [192] model with 60 trees had the highest performance for this study area.

The modeling results for estimating the AGB of *S. caseolaris* using the four machine-learning models (SVR, RBFNN, GP, and RF) with the leave-one-out cross-validation technique are shown in Table 5.6. Among the four machine-learning models, the SVR model had the highest

performance: RMSE, MAE, and R^2 were 0.359, 0.268, and 0.596, respectively. However, the performance of the SVR model was clearly lower than the MLPNN model in this study (Table 5.4). In contrast to the SVR model, the RF model had the lowest performance: RMSE, MAE, and R^2 were 0.402, 0.364, and 0.372, respectively. In addition, the MLPNN model had the lowest AIC and BIC values among the five machine learning models (Table 5.5). Therefore, we conclude that the MLPNN model achieved the best performance in this study for estimating the AGB of *S. caseolaris*.

5.4.3 Generation of the AGB map and its analysis

Since the MLPNN model was the best suited for the data, we used it to estimate the AGB of *S. caseolaris* for the study area; the results were then converted to a GIS format for use in ArcGIS 10.2. The resulting map visualized five classes (Fig. 5.5) showing that the AGB ranged between 2.78 and 298.95 ± 1.99 Mg ha^{-1}, with an average of 55.80 ± 1.99 Mg ha^{-1}; the highest biomass was located in the Northeast region. These results showed that the estimation of AGB spatial distribution generated by the MLPNN model was consistent with the measured mean, though the AGB range was higher than the actual distribution range (Table 5.3). This was likely due to the saturation level of the L-band ALOS-2 PALSAR-2 sensor in estimating the biomass of mangrove forests. The estimated biomass of *S. caseolaris* was mainly distributed in the high tidal zones. The experimental results matched our field observations, as this species can grow well in high tidal inundation level due to its pneumatophores (Fig. 5.4 c & d).

Our estimate of the mangroves' BGB (using the previously-defined 1.46 BGB/AGB ratio) yielded a range between 4.06 and 436.47 ± 2.91 Mg ha^{-1}, with an average of 81.47 ± 2.91 Mg ha^{-1}. The total biomass of *S. caseolaris* in the study area, derived by a combination of AGB and BGB, ranged from 6.85 to 735.42 Mg ha^{-1}, with an average of 137.27 Mg ha^{-1}. Using the 0.47 conversion factor between total biomass and carbon stock [108], we estimated that the total carbon stock of *S. caseolaris* in the study area ranged from 3.22 to 345.65 Mg C ha^{-1}, with an average of 64.52 Mg C ha^{-1}. This number is different from the results reported by Hamdan, et al. [273] and Vu, et al. [122] probably because these studies calculated the carbon stock of Matang mangroves in Malaysia and Quang Ninh province, Vietnam, based solely on AGB. We therefore suggest further study with more focus on carbon stock estimation derived from both AGB and BGB. In addition, our estimate is much lower than that for mangrove ecosystems in the Mekong Delta region since they belong to a biosphere reserve and protected area [237].

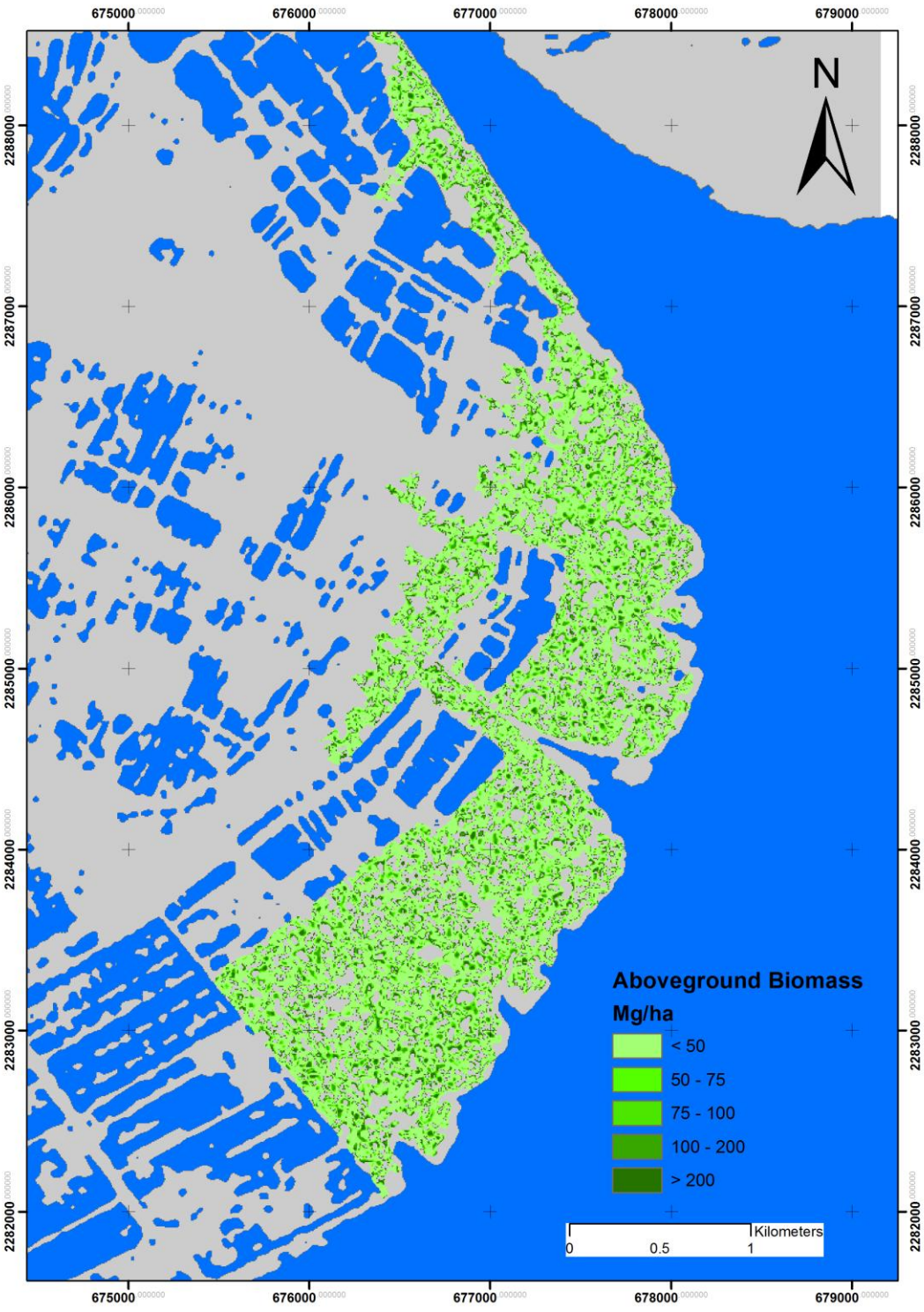

Figure 5.5. Spatial distribution pattern of biomass in the study area.

Previous studies have found that polarimetric radar signatures at long wavelengths such as the L- and P-bands were most sensitive to different mangrove species along the coast of French Guiana. This research pointed out that the backscattering coefficients of HV polarization at L- and P-bands reached the highest correlations with most mangrove parameters [120]. However, the

correlation coefficients of different regression models were limited. Recent studies using ALOS PALSAR to estimate the AGB of Matang mangroves in Malaysia found that HV backscatter gave the best correlation coefficient between polarimetric ALOS PALSAR backscattering and AGB for the three dominant species *R. apiculata, A. alba* and *B. parviflora,* though the accuracy of the model (R^2 = 0.427) was relatively low [23]. Multi-linear regression is the most commonly used method for estimating the AGB of mangrove forests in previous studies [22, 23, 39]. However, the performance of this model was relatively low with an R^2 value less than 0.6. Thus, the development of more accurate models for estimating mangrove biomass is necessary to promote the implementation of MRV strategies and developing national REDD+ mechanisms. Our results suggest that a combination of multi-polarizations generated in MNPNN can perform better than traditional models (R^2 = 0.776).

Prior studies reported that the saturation level of AGB in mangrove forests was at over 100 Mg ha^{-1} [216], and 150 Mg ha^{-1} [23] because of differences in the root systems and tidal inundation level of different tropical mangrove species. Therefore, MLPNNs likely over-estimate biomass at low observed values and under-estimate at high observed values. This may explain why errors occur largely at very high biomass values. The biomass of plots containing dense large mangrove trees with high DBH is likely under-estimated using machine learning algorithms. Despite these limitations of SAR data, our findings show that the ALOS-2 PALSAR-2 L-band, with high sensitive mode and backscattering coefficients at HH and HV polarizations, was sensitive to AGB, exceeding 100 Mg ha^{-1} for *S. caseolaris*. This means that the backscattering coefficients at HH and HV polarizations remain stable when the AGB of *S. caseolaris* reaches over 100 Mg ha^{-1}. The saturation level of mangrove species of Hai Phong is slightly lower than that of mangrove forests in Malaysia due to differences in stand age, growth stage, and species [23]. Backscattering in HH and HV polarizations of ALOS-2 PALSAR-2 increased when biomass was below 100 Mg ha^{-1}. Backscattering in HH and HV polarizations increased when biomass was below 100 Mg ha^{-1}. The backscattering was then saturated after the biomass of mangrove species increased further. This is likely due to an increased extinction of radar signals caused by the mangrove canopy [67].

Data saturation, which occurs in both optical and SAR sensor data, is an important factor influencing the accuracy of biomass estimation. Previous studies have reported that data saturation is one of the major problems resulting in low performance by optical data sensors when estimating AGB for areas with high biomass or high canopy density. The saturation level of optical sensors such as Landsat TM reaches about 100-150 tons ha^{-1} in complex moist tropical forests [51].

Saturation is also a common problem for SAR sensors when estimating biomass in a study area with complex forest stand structure [28, 231]. A short wavelength such as C-band at 6 cm saturates

often at 10kg/m^2 while long wavelengths such as L- and P-bands saturate often at 100 tons ha^{-1} for a complex and mixed forest structure; this saturation number rises to roughly 250 tons ha^{-1} for simple forests with a few dominant species [78]. Shugart, et al. [80] pointed out that the L-band saturation point is at around 100-150 tons ha^{-1} while P-band could be sensitive for biomass estimation at a saturation level of 100-300 tons ha^{-1}, depending on the forest types [81]. The saturation level of the ALOS-2 PALSAR-2 sensor for AGB estimation of *S. caseolaris* in this study was around 100 Mg ha^{-1}, which is consistent with the results reported by Lucas, et al. [216] and Hamdan, et al. [23]. More research is therefore needed to reduce the data saturation problem through the use of multi-source data or data fusion [135, 164].

5.4.4. Biomass estimation using remotely sensed data and machine learning methods

LiDAR (Light Detection and Ranging) is an active remote sensing sensors that utilized a pulsed laser to measure ranges and examine the surface of the Earth [124]. LiDAR data have an important role in estimating AGB since LiDAR pulses can penetrate certain vegetation canopy [125], especially in tropical areas where frequent cloud conditions occur. Several studies have used LiDAR data for estimating the canopy height of mixed forest [127, 128] and mangrove forests, in combination with Shuttle Radar Topography Mission data (SRTM) [126] or together with LANDSAT ETM+ imagery [129].

Direct biomass estimation methods using airborne LiDAR can offer higher accuracy in tree extraction [130], estimating number of trees and tree height [131], and AGB than methods using radar and optical data [132] because LiDAR can characterize both horizontal and vertical canopy structure [133]. Recent studies have indicated the potential of using LiDAR data with SAR data to map height and biomass of mangrove forest [126], and hyperspectral imagery for both AGB and BGB [135]. However, LiDAR data are still captured in small and geographically limited areas and may be more costly than data obtained from space-borne resources for a large area. Analyzing data derived from LiDAR requires more skills, knowledge, and specific software [19]. In addition, LiDAR has limited spectral information due to the one wavelength of laser point intensity [133].

Compared with LiDAR metrics, space-borne hyperspectral sensors offer a broader data set by providing a large number of spectral bands from visible to near infrared (NIR) or shortwave infrared (SWIR). These have great potential for classifying vegetation cover and estimating vegetation biomass comparing to other multispectral sensors. For example, Sibanda, et al. [134] reported that hyperspectral data can provide slightly higher accuracies in estimating grass biomass than Sentinel-2 multispectral imager (MSI) data. However, Vaglio Laurin, et al. [262] claimed that

hyperspectral data alone had limited prediction ability in estimating forest biomass (R^2 = 0.36). In addition, hyperspectral data are mainly space-borne and captured in small and geographically limited (Lu, 2006).

With the launch of new space-borne satellite sensors such as Rapid Eye, Sentinel, Terra SAR-X, and ALOS-2 PALSAR-2 (with high spatial, temporal, and spectral resolution), the issue of limited areas associated with airborne remote sensing can be overcome by encouraging new approaches to developing more accurate models for AGB estimation. The development of data mining and machine learning methods for biomass estimation has real potential in this regard, resulting in an increased use of machine learning methods for forest biomass estimation.

Several machine learning methods have been used for AGB estimation in the last few years, including *k*-NN, ANN, SVR, and RF [33, 185, 274, 275]. Machine learning models have shown their ability to estimate forest biomass by using optical and SAR sensors and by data fusion of multi-source data. These approaches have been also compared to other parametric approaches, showing that in most cases, machine learning methods have outperformed conventional methods [275]. Recently, several studies showed the potential of the stochastic gradient boosting (SGB) algorithm for AGB estimation by using both optical sensors from medium resolution [276] to high resolution [274], and SAR data [277].

Other recent approaches using machine learning and remote sensing consider data from multi-sensors in order to improve performance. For example, Shataee Joibary [278] studied the application of non-parametric models (*k*-NN, SVR, RF, and ANN) for the estimation of forest volume and basal area based on airborne LiDAR and Landsat TM data. The results show that SVR performed better than the other models when LiDAR and Landsat TM data were combined. More recently, another study in southwest Thailand [33] used GeoEye-1 and ASTER with the SVM model for mangrove biomass estimation, showing a promising result (R^2 = 0.66). Integration of LiDAR and hyperspectral or multi-source data can therefore improve biomass estimation significantly with relatively high accuracy [135, 262, 279]. Thus, the use of machine learning techniques in combination with multi-source data or data fusion should be investigated further in order to acquire more precise biomass maps.

5.5. Concluding remarks

This chapter investigated the applicability of using ALOS-2 PALSAR-2 data with the MLPNN model for estimating the AGB of *S. caseolaris* in the coastal area of Hai Phong city, Vietnam, and compared performance of the MLPNN with other machine learning algorithms. Our findings show that the MLPNN model produced more accurate biomass estimates than other machine learning

models. AGB and BGB for this species were estimated from 2.78 to 298.95 Mg ha^{-1} (with an average of 55.8 Mg ha^{-1}) and 4.06 to 436.47 Mg ha^{-1}(with an average of 81.47 Mg ha^{-1}), respectively, using leave-one-out cross-validation with an RMSE of 0.299, an MAE of 0.237, and R^2 of 0.776. The total carbon stock in the study area was estimated between 3.22 to 345.65 Mg C ha^{-1} (with an average of 64.52 Mg C ha^{-1}). Our study also illustrated the use of ALOS-2 PALSAR-2 data in high sensitive mode together with machine learning algorithms for characterizing the spatial distribution of mangrove biomass and determined the relationship between the biophysical parameters of a dominant mangrove species and backscattering coefficients at HH and HV polarizations. We conclude that ALOS-2 PALSAR-2 can be used with MLPNN in estimating mangrove biomass and carbon stock. Despite the limitations caused by saturation levels of AGB for *S. caseolaris* over 100 Mg ha^{-1}, the use of L-band ALOS-2 PALSAR-2 in high sensitive mode with machine learning provides an alternative approach that may allow rapid estimation of biomass for different mangrove species and their carbon stock in the tropics where accessibility is limited in large areas.

Our results show that MNPNN models provide an alternative method to derive mangrove biomass in a cost-effective and practical way. The machine learning algorithms and methods used in this research can be replicated for other mangrove forest species with similar characteristics, stand structures, and other biophysical parameters. Our approach, using ALOS-2 PALSAR-2 in high sensitive mode together with machine learning algorithms, can be used as a practical guide for the preliminary design of regional and local biomass assessment in other regions of Vietnam. Further research is needed to determine the biomass of other mangrove species and extend this work for entire mangrove forests in Vietnam. The findings will provide useful information regarding the spatial distribution of biomass for *S. caseolaris* and its carbon stock. This will support provincial decision-making on mangrove conservation and management.

Chapter 6

Data integration for mangrove forest biomass estimation

Chapter 6 describes a novel machine learning technique to estimate mangrove forest biomass using data integration of ALOS-2 PALSAR-2 and Sentinel-2 optical sensors at a mangrove plantation consisted of several species in Hai Phong, Vietnam.

6.1. Introduction

Mangroves are considered to be one of the most important ecosystems that grow exclusively in the inter-tidal zones along the coast of the tropical and semi-tropical climates. Their ecosystems provide a wide range of functions in reducing damage caused by the effects of tsunamis [6], protecting land from erosion, and mitigating the effects of tropical typhoons [136]. They can sequester highly efficient carbon in the tropics [7] and are considered a key component of *Blue Carbon* which helps to understand the carbon stocks in dealing with climate change impacts [8, 280].

Despite the large potential carbon stocks in mangrove ecosystems, they have been lost in the past 50 years worldwide due to high population growth, rapid urbanization, aquaculture expansion, and other human activities [234, 281]. Among regions of the world, the mangroves of Southeast Asia have suffered the greatest loss of more than 100,000 ha from 2000 to 2012 [282]. For the case of Vietnam, the mangrove area has decreased dramatically by 400,000 hectares in the early 20th century [12]. Particularly, in North Vietnam, between 1964 and1997, mangrove area decreased by 17,094 ha, largely due to over-expansion of shrimp farming [235].

Various studies have been conducted for estimating the above-ground biomass (AGB) of mangroves during the last 30 years [22, 109-111, 113, 114]. Several studies established their allometric equations to estimate the AGB from field measurements [115] and others using forest

inventory data on as stem weights, trees height, and diameter at breast height (DBH) [112, 116]. However, these studies were influenced by site selection biases and tidal inundation depth and waves [4, 118]. Additionally, forest inventory approach requires detailed field measurements that can be time-consuming, and costly, particularly in areas of dense and mixed mangrove forests such as in mangrove plantations, resulting in a lack of up-to-date information and statistical data on the spatial distribution of mangrove forest biomass. Thus, development of accurate and low-cost models to estimate the AGB of mangrove plantations is necessary to support conservation strategies in climate change mitigation programs such as the United Nations' Reducing Emissions from Deforestation and Forest Degradation (REDD+) program and Blue Carbon projects [283, 284].

Remotely sensed data have been widely used for mapping the spatial distribution of mangrove forests including optical data [143, 211, 213, 214], Synthetic Aperture Radar (SAR) data [212, 216, 285], and light detection and ranging (LiDAR) data [286]. Compared to optical sensors, SAR sensors have been largely found to be more effective in monitoring their disturbance dynamics because they can penetrate clouds, which often occur in the tropical area [19]. The AGB estimation of mangrove forests is considered most accurate when conducted at the individual species level [98, 217]. However, mangrove plantations have often planted several species together in the river mouth or sea to effectively protect dyke systems and mitigate damage from natural disaster [223], resulting in difficulties to estimate its AGB with high accuracy and low-cost. Furthermore, the AGB estimation using remotely sensed data for mangrove plantation has been rarely conducted. Thus, this study attempted to estimate the AGB in a mangrove forest plantation using an integration of ALOS-2 PALSAR-2 and Sentinel-2 data.

Information on biomass and its spatial distribution of mangrove forests in Vietnam is still limited. Several studies existed are restricted to specific regions, such as Ca Mau Peninsula in South Vietnam [139-141], and Hai Phong, Quang Ninh in the North [14, 142]. Few studies have attempted to estimate the AGB of mangrove plantation in North Vietnam [144], in Quang Ninh province in North Vietnam, and Ca Mau and Kien Giang provinces in South Vietnam [122], in the Mekong Delta regions [237], and Can Gio region [287]. SAR data captured for mangrove forests in Vietnam are available from ALOS and ALOS-2 sensors, however, only a few studies have been conducted to estimate their biomass, resulting in the limited spatial distribution of mangrove forest biomass in Vietnam. Thus, it is necessary to quantify and assess these variables in a mangrove plantation using a practical and cost-effective method.

The literature review shows that methods used to estimate the AGB of mangroves are diversified, from simple regression models [115, 117], multi-linear regression models [97] to

sophisticated machine learning methods [33, 98, 287]. Compared to parametric methods, machine learning algorithms have been shown to be effective for modeling mangrove biomass using satellite remotely sensed data [238, 239, 288]. The open-source software tools such as WEKA, R, and Python have been widely used in machine learning approach [240, 241]. Non-parametric statistical models such as Random Forest (RF) algorithm [185, 287], Artificial Neuron Networks (ANN) [98], and Support Vector Machines (SVM) [191] have become more common for estimating the AGB with remote sensing dataset because of its potential to outperform than parametric models. Therefore, the investigation of machine learning algorithms for the estimation of mangrove plantation biomass is highly necessary to support monitoring, reporting, and verification (MRV) work as part of the REDD+ program and Blue Carbon projects in developing nations.

Previous studies show that an integration of multi-source data such as SAR and optical images may improve the accuracy of forest biomass estimation [133, 289]. A combination of SAR and optical data can be achieved by two-way: data fusion of both SAR and optical into a new dataset such as principal component analysis (PCA) or wavelet transforms and incorporated all sensors as extra bands [133]. However, a limited number of studies have been conducted to develop a model for estimating the AGB of mangrove forests using an integration of SAR and optical data for mitigating the impacts of data saturation from these data in the mangrove AGB estimation. In this study, we selected an integration of ALOS-2 PALSAR-2 and Sentinel-2 data because L-band ALOS-2 PALSAR-2 has longer wavelengths can penetrate into mangrove forest canopies while Sentinel-2 has multispectral bands, reflecting forest stand structures such as biomass volume. Thus, we attempted to develop a prediction model that uses an integration of ALOS-2 PALSAR-2 and Sentinel-2 data together with machine learning techniques for estimating the AGB in a mangrove plantation at the Do Son and Kien Thuy coastal area of Hai Phong city, Vietnam. According to current literature, this is the first time an estimation of the AGB of mangrove plantation has been conducted for this coastal area. Accordingly, a function of mangrove ecosystems in the study area can be established and it may help to elucidate the spatial distribution patterns of biomass in tropical and sub-tropical regions. This work also promotes the implementation of REDD+ and Payment for Ecosystem Services (PES) strategies, thus providing practical significances for developing regional and national blue carbon trading markets and guiding mangrove management and conservation.

We selected support vector machines for this work because among numerous number of machine learning techniques, the support vector machines (SVM) have widely been used as an effective method for nonlinear mapping and complex classification problems such as land-use, land cover mapping [182], land cover change detection [290], and shallow landslide hazards [180].

However, SVM has seldom been utilized for estimating mangrove forest biomass. In addition, the ability of available machine learning algorithms for estimating mangrove forest biomass has not been quantitatively assessed. More importantly, there is a lack of quantitative comparison of available machine learning techniques for estimating above-ground biomass of mangrove plantation. Investigation of SVM for mangrove biomass estimation is highly necessary to acquire more accurate biomass estimation for mangrove plantation in the tropics. Thus, the current research work attempted to fill this gap in the literature.

The objective of this study are to investigate the usability of SVM for estimating the AGB in a mangrove plantation using a combination of ALOS-2 PALSAR-2 and Sentinel-2 data in a coastal area of Hai Phong city and to compare the performance of the SVM with other machine learning techniques for estimating the AGB in the mangrove plantation. Our findings demonstrate that the integration of ALOS-2 PALSAR-2 and Sentinel-2 data combined with SVM for estimating mangrove forest biomass has the potential to support improved mangrove conservation and management in the tropics.

6.2. Study area and satellite remote sensing data

6.2.1 Study area

We conducted this study in a mangrove plantation of Bang La and Dai Hop villages, which belongs to Do Son and Kien Thuy districts, Hai Phong city (Fig. 6.1). The coast of two communes located on North Vietnam consists of high tidal mudflats and formed by a large quantity of alluvial sediment from the Red River. The mixture of *K. obovata* and *S. caseolaris* mangrove stands planted since 1999 and was supported by Japanese Red Cross [223] because the coastal area of two communes is vulnerable to rising sea level and tropical storms which often takes place during wet season from May to October [247]. The vast majority of mangrove forests in North Vietnam is distributed in Hai Phong and the surrounding provinces [14]. Mangrove forests in the study site are well protected due to a cooperation by community-based forest management and local authority [291]. Mangrove plantation plays an important role in reducing damage from the effects of storm surge and contributing to the socio-economic lives of dwellers by providing forest products [9]. Field measurements were conducted in the mangrove plantation of two coastal districts of Hai Phong, Do Son and Kien Thuy (Fig. 6.1).

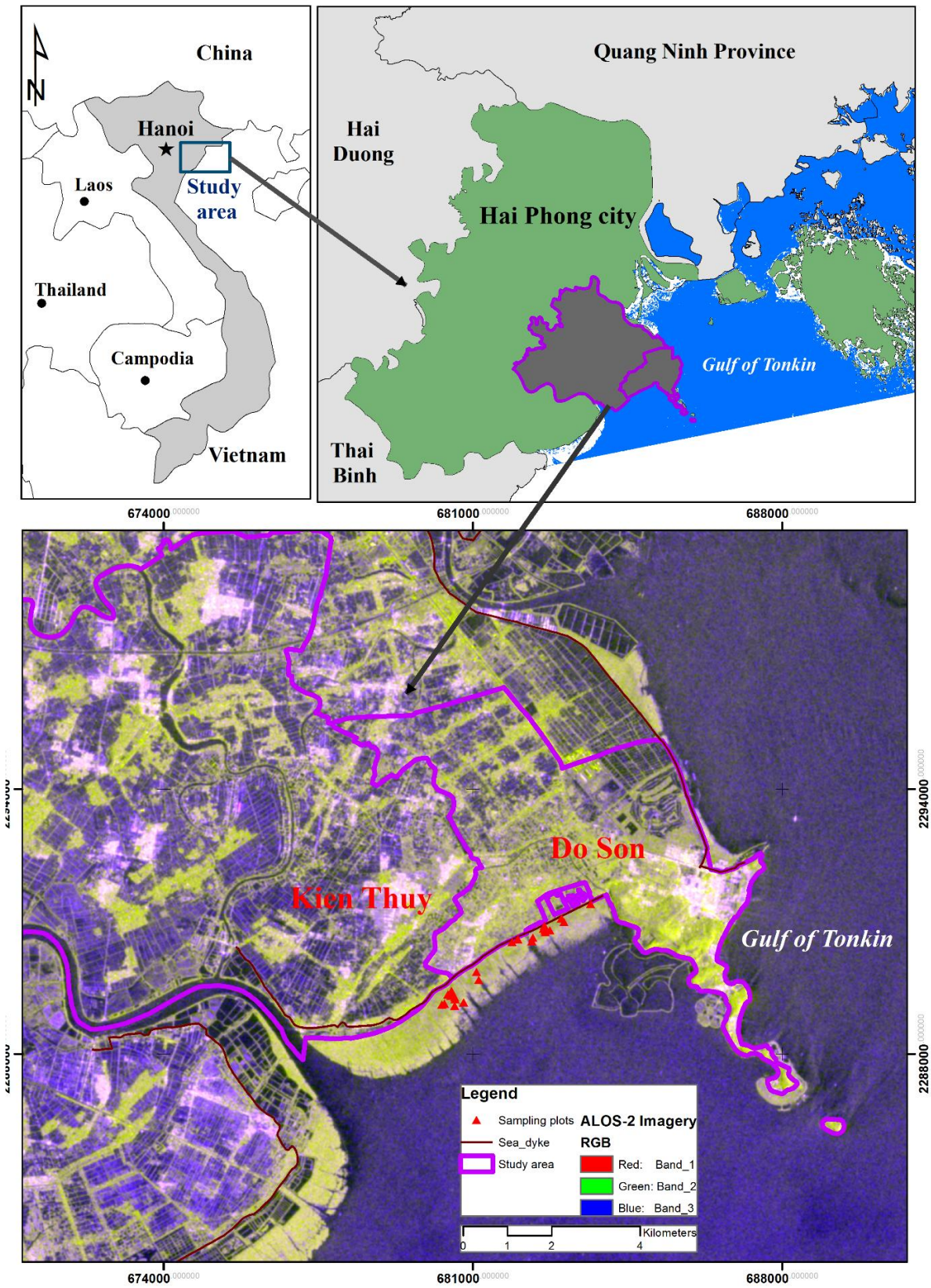

Source: ALOS-2 PALSAR-2 acquired on 31 July 2015

Figure 6.1. Map of the study area at Do Son and Kien Thuy districts, Hai Phong city.

6.2.2 Satellite remote sensing data collection and processing

6.2.2.1 Images collection and processing

ALOS-2 PALSAR-2 L-band (HH and HV) with high sensitive polarimetric mode and Sentinel-2 multispectral (MS) data were used to estimate biomass of mangrove plantation at Do Son and Kien Thuy coastal districts of Hai Phong city (Table 6.1). The ALOS-2 PALSAR-2 and Sentinel-2 MS data were acquired at a similar time in July and August 2015 as when the field measurements were taken.

Table 6.1. Acquired satellite remote sensing data.

Satellite sensor	Date of acquisition	Level of process	Spectral/ Polarizations used
ALOS-2 PALSAR-2	2015/7/31	1.5	L band (HH, HV)
Sentinel-2 MS	2015/8/10	1C	Band 2, Band 3, Band 4, Band 8

Source: JAXA, Japan and ESA.

ALOS-2 PALSAR-2 data level 1.5 was acquired from the Remote Sensing Technology Centre (RESTEC) of Japan. The DN (Digital Number) was converted to normalized radar sigma-zero using Eq. 6.1

$$\sigma^0\,[\mathrm{dB}] = 10 \log_{10} (\mathrm{DN})^2 + \mathrm{CF} \qquad (6.1)$$

where σ^0 is backscattering coefficient; DN is digital number of the amplitude image; CF is the Calibration Factor and CF = –83 dB for both HH and HV polarizations [219]. The CF used to process ALOS-2 PALSAR-2 is similar to ALOS PALSAR [248].

The DN of each pixel was transformed into backscattering sigma naught (σ^0) in decibel (dB) after applying the Frost filters with a 5 x 5 moving windows kernel in order to reduce speckle noise of SAR data [220]. In order to minimize effects from tidal level, we also carefully took the time to conduct field work into consideration [221, 222].

The Sentinel-2 Level-1C imagery acquired on 10 August 2015 from the European Space Agency (ESA). The Sentinel-2 data was geo-coded in the UTM/WGS84 projection at top of atmosphere (TOA) reflectance with a sub-pixel multispectral registration [292]. The Sentinel-2 Level-1C data were processed to Level-2A using the ESA's Sen2Cor algorithm to obtain the atmospheric correction of TOA Level-1C input data http://step.esa.int/main/third-party-plugins-2/sen2cor/. The ENVI 5.2 software was employed for SAR imagery processing while the SNAP toolbox was used to process Sentinel-2 imagery. We note that the modeling process was conducted using Weka 3.7 software.

6.2.2.2. Image transformation of ALOS-2 PALSAR-2 and Sentinel-2 multispectral data

Image transformation for SAR and optical data has been widely and extensively utilized to map and estimate AGB of mangrove forest in previous studies [23, 98, 217, 293-295]. The image transformation for ALOS-2 PALSAR-2 was used as suggested by Pham, et al. [98] including a combination of multi-polarizations such as HH/HV, HV/HH, HH-HV, and (HH+HV)/2. The most common image transformation for multispectral data is the vegetation index because each index has a sensitivity to different biophysical parameters such as canopy, biomass, and carbon stock of mangrove forests. In this study, six vegetation indexes as shown in Table 6.2 were selected for an AGB estimation model as suggested by previous studies [185, 191, 293].

6.2.2.3. Principal Component Analysis

Principal Component Analysis (PC) has successfully used for modeling vegetation biomass using optical data in previous studies [295, 296]. PC consists a number of input bands, thus, it can be more effective than using a single spectral band. The PC bands tend to provide better biophysical information on mangrove forests. In this study, PC1 and PC2 transformation were generated for four multispectral bands (Blue, Green, Red, and NIR) and six vegetation indices, respectively (Table 6.2).

To generate predictor variables for a model of AGB estimation, we chose a total of 32 variables, including 6 variables of ALOS-2 data (HH, HV, HH/HV, HV/HH, HH-HV, and ½(HH+HV), 4 multispectral bands (Blue, Green, Red, and NIR-infrared), 6 vegetation indices (Table 6.2), 4 PC1 combination bands generated from 4 multispectral bands, 6 PC2 combination bands generated from six vegetation indices, and 6 simple ratios (e.g. Band 2 /Band 3).

For all survey plots, spectral reflectance values of bands 2, 3, 4 and 8 were extracted from the Sentinel-2 image (Table 6.1). Due to the large plot sizes (900 m^2), the band ratio variables were used to obtain the average pixel values in each plot. The selection of predictor variables is always subjective, and there are an infinite possible number of variables that could have been examined. We chose these 32 variables because they are easily accessible to practitioners and simple to compute.

Table 6. 2. List of vegetation indices used.

Vegetation Index	Acronyms	Formula	References
Ratio Vegetation Index	RVI	$\frac{\text{NIR}}{\text{RED}}$	[297]
Normalized Difference Vegetation Index	NDVI	$\frac{\text{NIR} - \text{RED}}{\text{NIR} + \text{RED}}$	[298]
Enhanced Vegetation Index-2	EVI-2	$2.5(\frac{\text{NIR} - \text{RED}}{\text{NIR} + 2.4\ \text{RED} + 1})$	[299]
Soil Adjusted Vegetation Index	SAVI	$(1 + L)(\frac{\text{NIR} - \text{RED}}{\text{NIR} + 2.4\ \text{RED} + 1})$ L = 0.5 in most conditions	[300]
Modified Soil Adjusted Vegetation Index	MSAVI	$\frac{(2\text{NIR} + 1) - \sqrt{(2NIR + 1)^2 - 8(NIR - RED)}}{2}$	[301]
Difference Vegetation Index	DVI	NIR - RED	[302]

The procedures for estimating the AGB of mangrove plantation using machine learning techniques and an integration of ALOS-2 PALSAR-2 and Sentinel-2 data are shown in Fig 6.2.

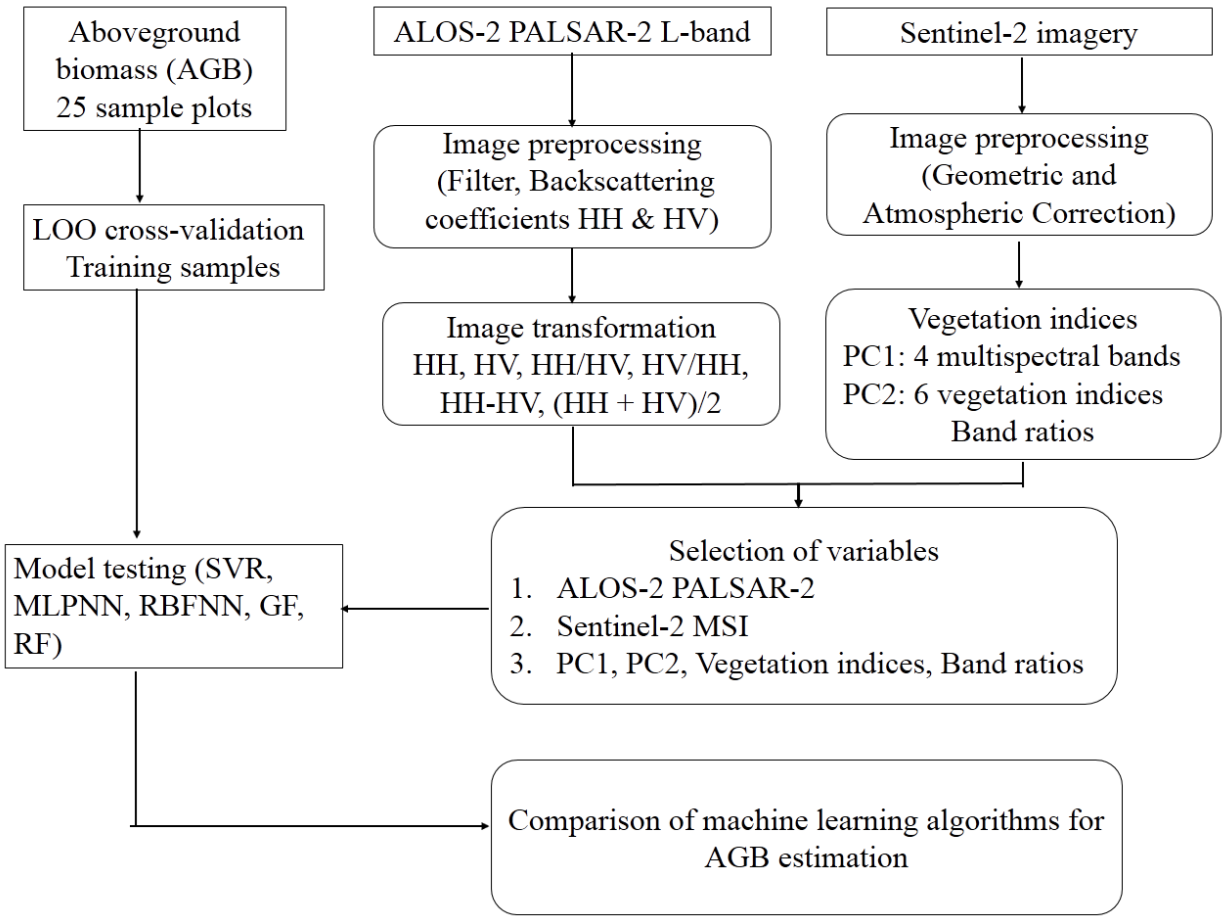

Figure 6.2. A flowchart used for estimating the AGB of mangrove plantation using machine learning techniques with an integration of ALOS-2 PALSAR and Sentinel-2 data.

6.2.2.4 Field data collection

The field survey measurement at the Bang La and Dai Hop coastal area was conducted in July and August 2015, which was the same time as the ALOS-2 PALSAR-2 and Sentinel-2 data acquisition with the help and permission from the local authorities. Plots were selected using a stratified random sampling method in which each strata was determined based on pre-survey with the help of local people to ensure the range of biomass values and would be valid for the entire mangrove forest plantation. A total of twenty-five sampling plots were measured specific biophysical parameters such as diameter at breast height (DBH), tree height, tree density.

Biophysical parameters data were collected from 25 sampling plots, representing the two dominant mangrove stand types: *K. obovata* and *S. caseolaris*. All living *S. caseolaris* stands with diameters of 5 cm and above were recorded. It is noted that *K. obovata* stands in the study area are small trees with diameters less than 5 cm. Thus, we measured the crown depth, crown diameter, and tree height in order to calculate the AGB for *K. obovata* using the allometric equation adapted from Fourqurean, et al. [224]. The mangrove forest plantation consists of the two dominant species at the study site. The mean tree height was about 2.84 and 7.61 m for *K. obovata* and *S. caseolaris*, respectively. The mangrove plantation had stand densities varying from 1800 to 4050 ha^{-1}, with a mean of 3096 trees ha^{-1} for *K. obovata* and densities varying from 43 to 444 ha^{-1}, with a mean of 178 trees ha^{-1} for *S. caseolaris*.

We also measured the height of pneumatophores of *S. caseolaris* by establishing a sub-plot size of 1x 1 m to measure their maximum and minimum heights and counted the number of roots in each plot. The four corners of each sampling plot were established in the field using Garmin Global Positioning Systems (GPS) eTrex Legend HCx, with a plot size of 30 m x 30 m to access the ALOS-2 PALSAR-2 pixel size of 6.25 m x 6.25 m, and the Sentinel-2 pixel size of 10 m x 10 m (Fig. 6.3). Photos and locations of the plots were also recorded using GPS during the field survey. Figure 6.3 depicts the techniques to measure the biophysical parameters of *S. caseolaris* and *K. obovata* and their roots at the sub-plot.

(a) (b)

(c) (d)

Source: Photos took by Pham T.D. in July 2015

Figure 6. 3. Measurement of biophysical parameters of *K. obovata* (a & b), *S. caseolaris* (c) and their roots (d) for the study area.

The AGB of *S. caseolaris* was calculated using the allometric equation (6.2) [116]

$$Ws = a \,.\rho.\, (D^2H)^b \quad (6.2)$$

where *W*s is tree dry-weight (kg), *D* is diameter at breast height (DBH) (cm), *H* is tree height (m), ρ is wood density (ρ = 0.340 for *S. caseolaris*) [116], and *a* and *b* are constants, equal to 0.251 and 0.0825, respectively, for *S. caseolaris*.

The AGB of *K. obovata* was calculated using the following allometric equation from Fourqurean, et al. [224]. The crown area of *K. obovata* was calculated based on the crown diameters and crown depth since the crown area was considered an ellipse in Eq. 6.3.

$$\text{Crown area} = (W_1.\, W_2/2)^2\, \pi, \quad (6.3)$$

where W_1 is the widest length of the tree canopy through its centre, and W_2 is the canopy width perpendicular to W_1. The AGB of *K. obovata* was calculated using the allometric equation (6.4) [224],

Tree volume = Crown area. Crown depth. (6.4)

6.3. Method used

6.3.1 Support Vector Machines

Support Vector Machine (SVM) is one of the most common machine learning methods using statistical learning theory. The SVM has been widely used in environmental modeling and derived outperforms than conventional methods [179-181]. This machine learning technique has been successful utilized in classifying land-use and land-cover (LULC) [182], mapping LULC [183], mapping mangrove forests [303, 304], and monitoring mangrove change detection [305]. The SVM models consist of a wide range number of vectors that have functions in separating different objects (classification) or minimizing the mean error (regression). To overcome the linear limitations, different kernel functions such as polynomial, sigmoid, and radial basis function (RBF) are used in the SVM models. The performance of the SVM model is influenced by the selecting the kernel functions. However, RBF kernel may be the most commonly used in estimating forest biomass and was selected in this study.

6.3.2 Performance assessment

To assess and compare the performance of different machine learning techniques for estimating the mangrove forest biomass, Root-mean-square-error (RMSE), Mean absolute error (MAE), and coefficient of determination (R^2) were used. These statistical criteria are widely utilized in modeling forest biomass to evaluate the discrepancies between the observed data (the AGB inventories) and the predicted AGB data [227, 228].

RMSE (Eq. 6.5) is considered as a standard metric for measuring errors of regression models; however, it is strongly affected by large values and outliers [254]. Therefore, MAE (Eq. 6.6) is suggested use together with RMSE for determining the variation of the model errors [180]. Lower RMSE and MAE values indicate the better regression model. Furthermore, a smaller difference between RMSE and MAE reflects a smaller the variance of the errors. R^2 is estimated using Eq. 6.7; and higher the R^2 values also mean a better model [33, 98].

$$\text{RMSE} = \sqrt{\sum_{i=1}^{n} \frac{(\hat{y}_i - y_i)2}{n}} \quad (6.5)$$

$$\text{MAE} = \frac{1}{n}\sum_{i=1}^{n} |\hat{y}_i - y_i| \quad (6.6)$$

$$R^2 = 1 - \frac{\sum_{i=1}^{n}(y_i - \hat{y}_i)^2}{\sum_{i=1}^{n}(y_i - \bar{y})^2} \quad (6.7)$$

where $\hat{y}_i$ and y_i are the predicted and observed biomass for the i^{th} plot, respectively; n is the total number of validation plots, and $\bar{y}$ is the observed mean values of biomass.

6.4. Results and Discussion

6.4.1 Field survey results

All mangrove forests stands were recorded in the 25 sampling plots in the mangrove plantation of the study area. The mixed species had stand densities varying from 1800 to 4050 ha^{-1}, with a mean of 3096 trees ha^{-1} for *K. obovata* and densities varying from 43 to 444 ha^{-1}, with a mean of 178 trees ha^{-1} for *S. caseolaris* (Table 6.3). The average age of mangrove plantation in the study area is 16 years old. The average tree heights are 2.84 and 7.61 meters for *K. obovata* and *S. caseolaris*, respectively. Total above-ground biomass in each 900 m^2 plot ranged from 2,869 to 15,359 kg (median = 7766 kg).

Table 6. 3. Characteristics of mangrove plantation in the study site.

		S. caseolaris				*K. obovata*						
Plot ID	Age (year)	Tree height (m)	DBH (cm)	Tree density (No./900 m^2)	AGB (kg/ 900 m^2)	Tree height (m)	Crown Area (m^2)	Crown Volume (kg/m^2)	Tree density (No./900 m^2)	AGB (kg/900 m^2)	Total AGB (kg/ 900 m^2)	Total AGB (Mg ha^{-1})
1	17	8.86	11.61	30	493.21	3.19	0.64	0.66	3600	2376.00	2869.21	31.88
2	17	7.67	24.20	4	216.71	2.88	0.67	0.99	2700	2673.00	2889.71	32.11
3	17	6.25	17.99	19	502.42	2.02	1.35	1.98	1800	3564.00	4066.42	45.18
4	17	8.58	11.00	19	275.69	2.92	0.87	1.09	3600	3924.00	4199.69	46.66
5	17	6.50	17.23	30	760.49	3.78	0.81	1.01	3600	3636.00	4396.49	48.85
6	17	6.71	18.68	14	422.52	4.02	0.93	1.43	3150	4504.50	4927.02	54.74
7	17	6.67	14.46	18	340.32	2.70	1.08	1.81	2700	4887.00	5227.32	58.08
8	17	6.25	14.15	36	618.12	2.60	1.44	2.65	1800	4770.00	5388.12	59.87
9	17	8.20	8.49	38	332.29	3.40	0.78	1.26	4050	5103.00	5435.29	60.39
10	17	6.33	17.34	12	300.51	2.16	2.10	3.06	1800	5508.00	5808.51	64.54
11	17	7.50	23.25	9	444.64	2.48	1.15	1.73	3600	6228.00	6672.64	74.14
12	17	5.80	7.92	9	50.85	2.16	1.89	3.07	2250	6907.50	6958.35	77.32
13	17	8.71	9.24	40	429.60	2.45	1.17	1.92	3600	6912.00	7341.60	81.57
14	17	6.20	22.16	8	305.42	2.45	1.08	1.82	4050	7371.00	7676.42	85.29
15	17	7.07	10.51	8	89.78	2.87	1.12	2.19	3600	7884.00	7973.78	88.60

16	17	6.50	10.62	11	116.60	2.50	1.71	2.92	2700	7884.00	8000.60	88.90
17	17	10.88	21.87	8	494.56	3.76	1.25	2.61	3150	8221.50	8716.06	96.85
18	17	11.75	21.89	10	664.22	2.26	2.67	3.60	2250	8100.00	8764.22	97.38
19	17	9.60	16.24	10	323.57	4.52	1.28	2.76	3150	8694.00	9017.57	100.20
20	5	5.33	10.44	16	137.65	2.22	2.31	4.09	2250	9202.50	9340.15	103.78
21	17	11.00	28.82	9	923.80	3.32	1.69	3.09	3600	11124.00	12047.80	133.86
22	17	7.00	12.99	14	227.98	2.71	2.10	3.41	3600	12276.00	12504.00	138.93
23	17	10.00	23.73	11	730.23	3.54	1.71	3.60	3600	12960.00	13690.20	152.11
24	10	6.00	18.79	7	192.88	1.91	2.48	4.08	3600	14688.00	14880.90	165.34
25	10	5.00	7.54	13	58.76	2.19	2.45	4.25	3600	15300.00	15358.80	170.65
AVG	16	7.61	16.05	16	378.11	2.84	1.47	2.44	3096	7387.92	7766.03	86.29

6.4.2 Modeling results, assessment, and comparison

We employed the leave-one-out (LOO) cross-validation technique for building prediction models as the number of sampling plots was small. This is an effective technique that allows each sample to be excluded while a model is developed with all remaining samples and used to predict the excluded samples. This technique has the ability to eliminate bias in estimations of model performance [226] and has been widely used in previous studies [33, 97, 98]. As a result, the SVM model was used to build a total 25 sub-models and then the final SVM model was generated by averaging the 25 sub-models.

In order to produce better performance, machine learning techniques generally require a large number of input data. In this study, four multispectral bands (MS) of Sentinel-2 imagery (Blue, Green, Red, NIR) along with six vegetation indexes (Table 6.2) were used as input variables to PC1 and PC2. Additionally, six simple ratios (e.g. Blue/Green) and six variables of ALOS-2 data (HH, HV, HH/HV, HV/HH, HH-HV, and ½(HH+HV) were used as input variables. A total of 32 variables generated from ALOS-2 PALSAR-2, Sentinel-2 MS data, vegetation indices and PCA were used as inputs to the model.

Various different combinations of inputs were tested using training data and LOO cross-validation techniques. Table 6.4 shows that the optimal number of variables for this study was achieved by using nine variables including HH, HV, HV/HH, HH-HV, NIR, PC1-Blue, PC1-Green, PC1-Red, and PC1-NIR (Table 6.4). The SVR model with nine variables produced the best performance (the highest R^2, and the lowest RMSE and MAE). Therefore, nine variables were selected as input variables in the SVR model.

Table 6. 4. Performance of SVR model and LOO cross-validation with different number of input variables

Number of variables	R^2	RMSE	MAE
4 variables from MS bands	-0.165	0.211	0.174
6 variables from PALSAR-2 data	0.112	0.435	0.346
8 variables (4 MS bands + 4 PC1)	0.052	0.208	0.171
9 variables (HH, HV, HV/HH, HH-HV, NIR, and 4 PC1)	0.596	0.187	0.123
10 variables (4 MS bands + 6 vegetation indices)	-0.174	0.378	0.300
16 variables (4 MS bands + 6 ratios + 6 SAR variables)	0.382	0.281	0.184
22 variables (4 MS bands + 6 ratios + 6 SAR variables + 6 vegetation indices)	0.290	0.297	0.188
32 variables (4 MS bands + 6 ratios + 6 SAR variables + 6 vegetation indices + 4 PC1+ 6 PC2)	0.304	0.297	0.196

As shown in Table 6.4, the best AGB model was generated from a support vector regression with 9 variables. This model had a coefficient of determination *(R^2)* of 0.596, showing a satisfactory correlation between model estimation and field-based measurements.

Our results suggest that the PC1 generated from multispectral bands was the most important variable for predicting the AGB of mangrove plantation. A similar finding was made by Lu, et al. [57] and Wicaksono, et al. [295]. The next important variables were multi-polarizations generated from ALOS-2 PALSAR-2 imagery which was also observed by Pham, et al. [98].

It is noted that among four spectral bands, the near-infrared (NIR) spectrum is more sensitive to the AGB of mangrove forest than the visible bands. This result was similar finding reported by Jachowski, et al. [33]. An explanation for this is that NIR reflectance has the strongest relationship with forest characteristics such as wood volume compared to the visible reflectance [287].

Vegetation indices were likely less important in mangrove biomass estimation than the PC derived from multispectral bands. This is similar to Lu, et al. [57] observation that vegetation indices generated from NIR and RED reflectance such as SAVI and NDVI were weakly correlated with AGB.

This research also found that the band ratios generated from Sentinel-2 data played a less important role in biomass estimation of mixed mangrove forest than those derived from both HH and HH polarizations from ALOS-2 PALSAR-2 image. A further in-depth study is recommended to improve understanding of significances of image transformation such as vegetation indices derived from MIR and NIR bands of Sentinel-2 data and other multi-polarizations transformation

derived from full polarized ALOS-2 PALSAR-2 (HH, HV, VH, and VV) data in mangrove forest plantations.

6.4.3. Model comparison

The performance of the final SVM model is shown in Table 5. The R^2 of 0.596 shows a satisfactory result compared to previous studies reported by Goh, et al. [289] (R^2 = 0.46*)*, Zhao, et al. [306] *(*R^2= 0.28-0.44*)*, and Aslan, et al. [307] *(*R^2 = 0.46*)*. These studies attempted to develop a model for estimating the AGB using the integration of optical data such as Landsat TM [306], Landsat-8 OLI [307], SPOT-5 [289] and ALOS PALSAR data. Our result shows that an integration of Sentinel-2 and ALOS-2 PALSAR-2 combined with SVM model can provide better results in terms of R^2, RMSE, and MAE. Thus, we conclude that overall the SVM model performs well in this study area.

Table 6. 5. Machine learning models with LOO cross-validation for the AGB estimation of mangrove plantation in this study.

No	Machine learning model	RMSE	MAE	R^2
1	Support vector regression (SVR)	0.187	0.123	0.596
2	Multilayer Perceptron Neural Networks (MLPNN)	0.293	0.214	0.345
3	Radial Basis Function neural network (RBFNN)	0.228	0.183	0.276
4	Gaussian Process (GP)	0.245	0.172	0.529
5	Random Forests (RF)	0.328	0.257	0.030

As the purpose of this study was to estimate the AGB of mangrove plantation in the coastal area of Hai Phong city (Vietnam), the usability of the SVM model should be assessed and confirmed its effectiveness. For this purpose, we selected the Multilayer Perceptron Neural Networks (MLPNN), Radial Basis Function neural network (RBFNN), Gaussian process (GP), and Random Forests (RF) model for comparison. MLPNN was selected because it outperforms various machine learning techniques in estimating mangrove forest biomass [98] while RF was selected as it provides the highest accuracy for modelling and mapping mangrove biomass change [287] whereas the others are the most widely used soft computing models that showed high performance in many fields [185, 187, 243].

SVR is a regression version of the popular support vector machines that was developed based on statistical learning theory [268]. In this study, the SVR with the radial basis function kernel [269] and the SMO algorithm [267] was used. Accordingly, the best values for the kernel width

(0.346) and the regularization (398) were found through using the grid search method. For RBFNN [270], the best structure (6 input neurons, one hidden layer with 9 clusters, and one output layer) was found based on a test suggested by Hong, et al. [271]. The MLPNN model with five neurons in the hidden layer produced the best performance was used as suggested by Pham, et al. [98]. For GP, the radial basis function [272] was used and gamma of 0.352 was found as the best value for the study area. Regarding RF [192], the model with 500 trees had the highest performance for this study area.

The modeling results of estimating the AGB of mangrove plantation using the five machine-learning models (SVR, MLPNN, RBFNN, GP, and RF) with the LOO cross-validation technique are shown in Table 6.5. It could be seen that among the five machine-learning models, the SVR model had the highest performance: R^2, RMSE, and MAE were 0.596, 0.187, and 0.123, respectively. In contrast to the SVR model, the RF model had the lowest performance: R^2, RMSE, and MAE were 0.030, 0.328, and 0.275, respectively. Therefore, we conclude that the SVR model achieved the best performance for estimating the AGB of mangrove plantation in this study.

6.4.4 Generation of the AGB map and its analysis

Since the SVR model is the best suited for the data, the model was selected for estimating the AGB of mangrove plantation for the study area. The results were converted to a GRID format to open in ArcGIS 10.3 software. The AGB map was visualized by five classes (Fig. 6.4), showing a range of 36.22 and 230.14 Mg ha^{-1} (average = 87.67 Mg ha^{-1}) and the highest biomass was found in front of the sea and the river mouth. The results were consistent with previous studies reported by Phan and Vu [223] that in the mangrove plantation forest, *S. caseolaris* species are often inter-planted in high tidal inundation levels together with *K. obovata* in the river mouth or sea to effectively protect dyke systems and to reduce damage from storm surge. The results revealed that the estimation of the spatial distribution of the AGB generated by the SVR model is consistent with the actual measured mean, however, the AGB range was higher than the actual distribution range (Table 6.3). This was likely due to the saturation level of L-band ALOS-2 PALSAR-2 and Sentinel-2 sensors for estimating biomass of mangrove forests. The estimated biomass of mangrove plantation was mainly distributed in the high tidal zones of the river mouth. The predicted AGB results matched the field observation, reflecting that two mixed species are often planted together and *S. caseolaris* can grow well in the high tidal inundation level due to their pneumatophores (Fig. 6.3d).

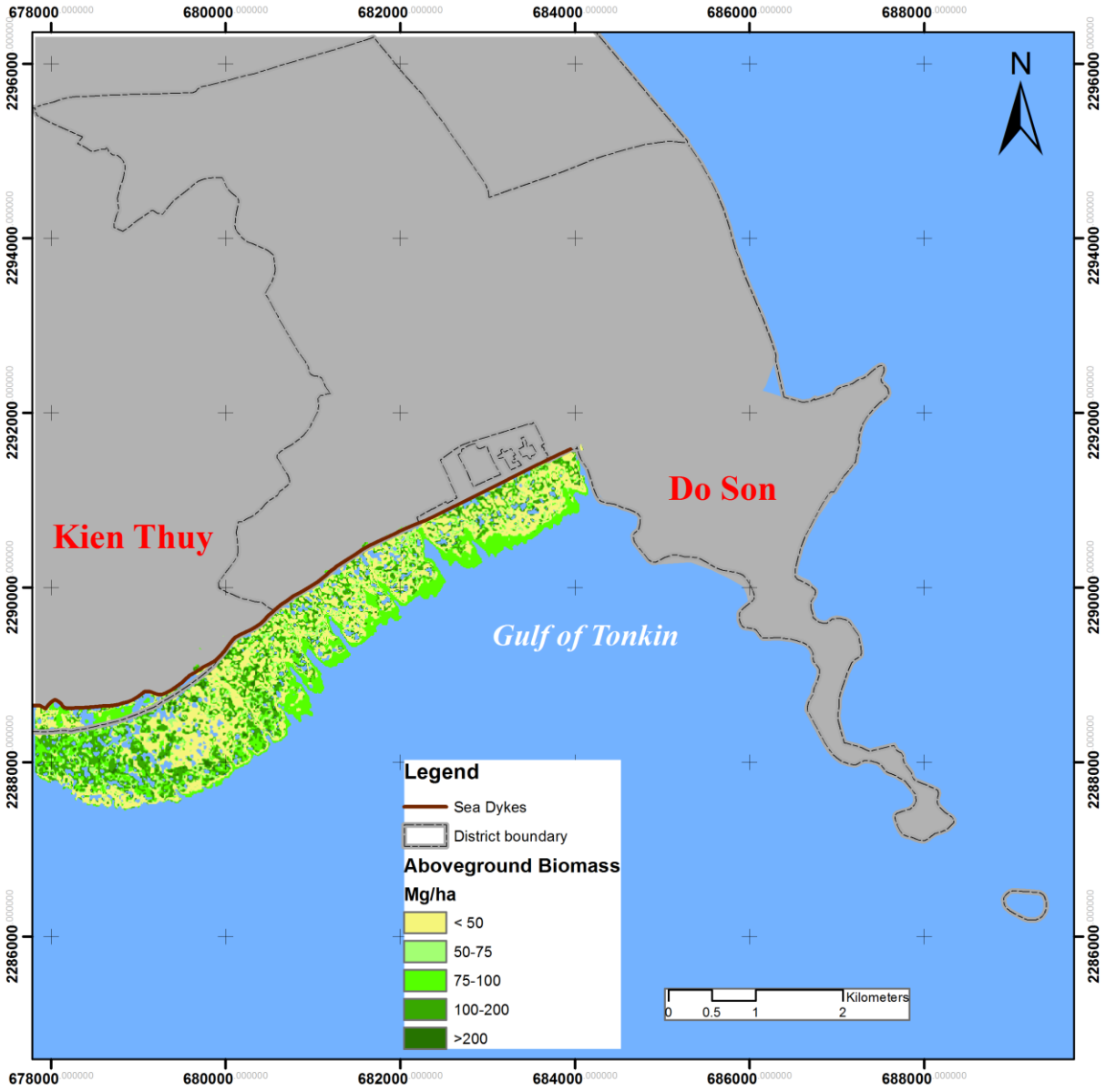

Figure 6.4. Spatial distribution pattern of the AGB in the study area.

Previous studies reported that using SAR data at the long wavelength such as L and P-bands was found the most sensitive to different mangrove species, of which the HV-polarized can produce better correlations with biophysical mangrove parameters [120, 225]. However, mangrove forest plantations have their own stand structures and species compositions, resulting in different data saturation problem in both optical and SAR data. For optical data such as Landsat TM, ETM+, and Landsat 8 OLI, data saturation has resulted in low performance when estimating the AGB in high biomass and high canopy density. The saturation level of optical sensors reaches about 100-150 Mg ha^{-1} in complex moist tropical forests [51], around 152-159 Mg ha^{-1} in mixed and pine forests [308]. Several studies have indicated that the saturation level of the AGB estimation in mangrove forests using SAR data was at over 100 Mg ha^{-1} [216], and 150 Mg ha^{-1} [23] because of the root

systems and tidal inundation level of different mangrove species in the tropical and sub-tropical climates. This study showed that the AGB estimation using SVR model likely over-estimate at low observed values and under-estimated at high values. This may explain why the errors occur largely at very high biomass value over 150 Mg ha^{-1} and at low biomass very less than 50 Mg ha^{-1} (Fig. 6.4).

Mangrove plantations often consist of several species, which contain dense large mangrove trees with high DBH such as *S. caseolaris*, resulting in underestimation and small high-density trees such as *K. obovata*, resulting in overestimation using machine learning algorithms. Despite these limitations of the SVR model, our findings show that the integration of ALOS-2 PALSAR-2 and Sentinel-2 MS data was sensitive to the AGB exceeding 100 Mg ha^{-1} for mixed species in a mangrove plantation, showing that the backscattering coefficients at HH and HV polarizations and multispectral data remain stable when the AGB of mixed species reaches over 100 Mg ha^{-1}. The saturation level of mangrove plantation in two coastal district of Hai Phong is slightly lower than that of mangrove forests in Malaysia due to the differences in species composition [23]. Backscattering in HH and HV polarizations of ALOS-2 PALSAR-2 increased when biomass was below 100 Mg ha^{-1}. The backscattering was then saturated after the biomass of mangrove species increased further. This is most likely due to an increased extinction of radar signals caused by mangrove canopy [67]. The results of this work were consistent with the conclusion of previous studies [23, 216]. To acquire a more precise biomass map, combining the advantages of different machine learning techniques, multi-source data should be exploited in the future [54, 309]. More research should be undertaken to investigate the usability of multi-source data combined with the machine learning approach for different mangrove species and geographical locations.

Multi-linear regression is considered to be the most commonly used method for estimating the AGB of mangrove forest in previous studies [22, 23, 97]. However, the performance of this model was relatively low with an R^2 ranged from 0.43 to 0.65. A number of machine learning algorithms have been used for estimating the AGB in the last few years such as *k*-nearest neighbor (*k*-NN), GP, MLPNN, SVR, and RF [33, 98, 185, 274, 275, 287]. Machine learning approaches have shown their ability to estimate the AGB by using optical and SAR data, compared to other parametric methods, showing that in most cases, machine learning approaches have outperformed conventional methods [275, 310]. However, a limited number of studies have been attempted to develop a model using the integration of multi-source data combined with machine learning techniques. Our findings show that an integration of ALOS-2 PALSAR-2 and Sentinel-2 data generated in the SVR model can be used for estimating the AGB of mangrove forests with a promising result (R^2 = 0.596). Thus, a combination of SAR and optical data or multi-source data

combined with machine learning approaches should further investigate to improve the accuracy of the AGB estimation in mangrove forests [135, 262, 279].

6.5. Conclusions

This chapter was undertaken to investigate the applicability of the SVM model for estimating the AGB in a mangrove plantation using an integration of ALOS-2 PALSAR-2 and Sentinel-2 data at the Do Son and Kien Thuy coastal area of Hai Phong city, Vietnam and compared performance of the SVM with other machine learning algorithms. Our findings show that the SVM model produced better estimations of the AGB for mangrove plantation than MLPNN, RBFNN, GP, and RF. The AGB of mangrove forest plantation in the study site was estimated between 36.22 and 230.14 Mg ha^{-1} (average = 87.67 Mg ha^{-1}) using LOO cross-validation with R^2 of 0.596. The findings demonstrate that an integration of ALOS-2 PALSAR-2 and Sentinel-2 data together with machine learning approach can be used for estimating the AGB of mangrove plantations. Despite the limitations caused by the saturation of satellite signals, our findings show significant promise for the use of a combination of L-band ALOS-2 PALSAR-2 and Sentinel-2 together with machine learning techniques as an effective tool for modeling mangrove forest biomass to support the REDD+ program and blue carbon projects.

The model development of this research using the SVR model for estimating the AGB in a mangrove plantation can provide an alternative method to derive biomass in a cost-effective and practical way. The machine learning algorithms and methods used in this research can be used for other mangrove plantations with similar characteristics, stand structures and various biophysical parameters. Our approach using an integration of ALOS-2 PALSAR-2 and Sentinel-2 MS together with machine learning algorithms can be used as a practical guide for other mangrove forest regions of Vietnam for the regional and local levels biomass assessment. More research focusing on the integration of optical and SAR data combined with machine learning approach is needed to increase the estimation accuracy of the mangrove AGB and extend this work for entire mangrove forests of Vietnam. The findings provide useful information and understanding of the spatial distribution of the AGB in a mangrove plantation. This will support provincial decision making on mangrove plantation monitoring and management.

Chapter 7

Mangroves change and their ecosystem services valuation

Chapter 7 presents the findings on mangroves mapping and their changes detection using multi-temporal ALOS PALSAR data from 2010 to 2015 and valuing the mangrove ecosystem services based on willingness to pay for mangrove restoration in the Cat Ba Biosphere Reserve, Vietnam. The first part of chapter 7 was published as a book chapter in the book entitled "Advances and Applications in Geospatial Technology and Earth Resources" published by Springer. The second part of this chapter was submitted for consideration for publication and currently under review in Marine Policy.

7.1. Mangroves change mapping and detection

7.1.1. Introduction

Mangroves are found in most tropical and semi-tropical regions along the sheltered coastlines such as river estuaries or tidal marshes [311]. They are considered to be the most important ecosystems on earth [5] as they play a vital role in mitigating the impact of climate change in tropical climates [7] by sequestering carbon in both above and below-ground biomass as well as their sediment [8].

Despite their significant roles in providing habitats for marine species and serving the local communities with ecological and economic services, mangroves have been lost in the past 50 years worldwide due to high population growth, rapid urbanization, aquaculture expansion and other human activities [4]. Among regions of the world, Asia has suffered the greatest loss of 1.9 million hectares of mangroves [11]. Like many other countries in Southeast Asia, the mangroves in Vietnam have been cleared for coastal development, aquaculture expansion, and fuel production in the early 21st century [12]. Thus, mapping the spatial distribution of mangrove forests is important in order to support coastal zone management and planning programs.

Satellite remotely sensed data and various techniques have been applied for mapping mangrove forests including optical data [213, 215] and synthetic aperture radar (SAR) data [142, 216]. Pixel-based classification methods are most frequently used for mapping mangrove forests in Vietnam [312-314]. Béland, et al. [315] used Landsat imagery to investigate the land cover changes from mangrove to aquaculture in the Red River Delta using Tasselled Cap Transformation. Pixel-based approaches were employed by previous studies conducted in the Mekong Delta by Tong, et al. [312] and Thu and Populus [313]. Recent studies reported that object-based classification approaches have been successfully applied in mapping mangrove forests and assessing their changes based on optical sensors such as Landsat images [141] and SPOT-5 data [316]. These studies have been conducted in specific regions, such as Ca Mau Peninsula in South Vietnam [139, 141, 314]. However, only a few studies in Vietnam have been used SAR data to map the spatial distribution of mangrove forests and assess their changes despite the fact that SAR can penetrate clouds, which occur constantly in the tropical area and acquire data throughout the year [19]. As a result, the spatial distribution of the mangroves in Vietnam is still limited and not well documented. Thus, there is a need to map and assess their spatial distribution in Vietnam using SAR data and suitable methodology.

Recently, machine learning techniques have been shown as an effective tool for mapping Land-use and Land-cover (LULC) [174, 183, 317, 318], mapping mangrove forests and their distribution using remotely sensed data [238, 319]. Recent studies have demonstrated that support vector machines (SVM) classifier is one of the most popular machine learning algorithms in LULC classification [290, 320] as it can provide high accuracy and require a small number of the training data [187]. We selected a support vector machine algorithm for mapping mangroves and assessing their changes because, among numerous number of machine learning techniques, the support vector machine (SVM) has been widely used for nonlinear mapping and complex classification problems such as land cover change detection [290]. However, the SVM classifier has rarely been used for monitoring mangroves changes using SAR data in the tropics.

The overall goal of this study was to map the spatial distribution of mangrove forests in the Cat Ba Biosphere Reserve, Vietnam and to evaluate their changes using ALOS PALSAR data and a GIS-based support vector machine classifier. Such studies are crucial for monitoring mangroves changes at a regional scale and play an important role in conserving mangrove resources in Vietnam. This study has demonstrated the potential use of ALOS PALSAR data combined with machine learning algorithms for mapping the spatial distribution mangrove forests and assessing their changes in the tropical area.

7.1.2. Study area and spatial data

7.1.2.1. Study area

Cat Ba is the largest island in the Cat Ba Archipelago in Hai Phong City, located in the north of Vietnam. The Cat Ba Biosphere Reserve consists of six communes and one town (Fig. 7.1.1). The core ecosystem of the island is tropical forest including tropical evergreen forest in the lowlands, limestone forest in the mountains, and mangrove forests along the coast. Cat Ba Island has been recognized by United Nations Educational, Scientific and Cultural Organization (UNESCO) as a biosphere reserve since 2004. The total area of the Cat Ba Biosphere Reserve is about 26,241 hectares. The biosphere is a well-known destination for tourists from not only all parts of Vietnam, but also from around the world. The number of tourists has significantly increased over the last decade [321] with around annual 500,000 recently [322].

The Cat Ba Biosphere Reserve is under serious threat from deforestation and forest degradation. The tropical forest of the reserve decreased by around 660 hectares while the mangrove forest decreased by almost 50% from 1990 to 2001 [323]. The mangrove forest area in the reserve declined largely due to over-expansion of shrimp aquaculture [168].

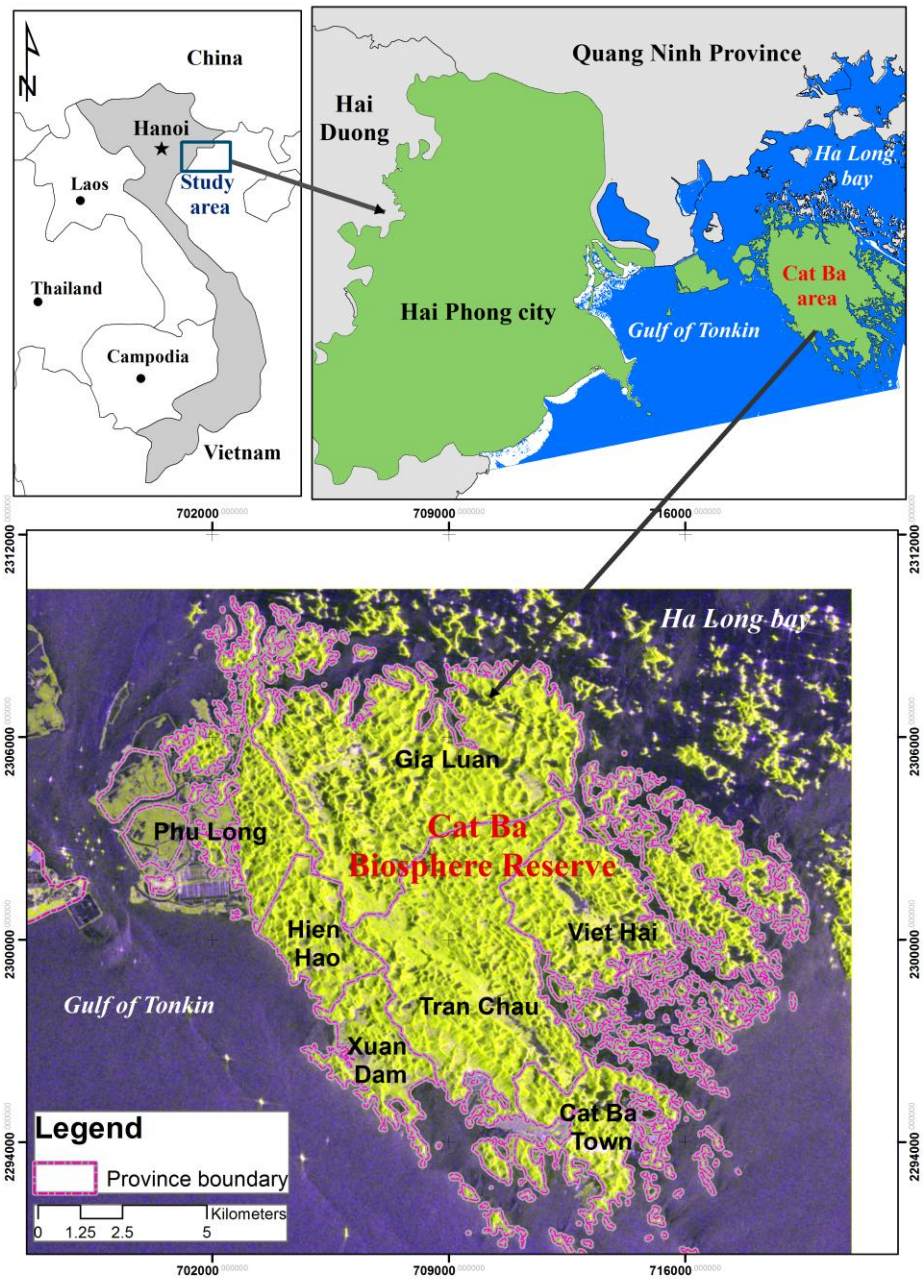

Source: ALOS-2 PALSAR-2 acquired on July 31, 2015

Figure 7.1.1. Map of the study area in the Cat Ba Biosphere Reserve, Vietnam.

7.1.2.2. SAR data used

The Advanced Land Observing Satellite (ALOS) Phased Arrayed L-band SAR (PALSAR) images acquired in 2010 and 2015 were used to map the spatial distribution of mangrove forests and assess their changes. The images used were acquired by ALOS PALSAR and ALOS-2 PALSAR sensors (Table 7.1.1).

Table 7.1.1. Acquired SAR remote sensing data in the study area.

Satellite sensor	Date of acquisition	Pixel spacing	Processing level	Polarizations
ALOS PALSAR	2010/8/25	12.50 m	1.5	HH, HV
ALOS-2 PALSAR-2	2015/7/31	6.25 m	1.5	HH. HV

Source: JAXA, Japan.

ALOS and ALOS-2 PALSAR-2 data level 1.5 were acquired from the Remote Sensing Technology Centre (RESTEC) of Japan. The ALOS PALSAR data was acquired in the same period during summer time for the years 2010 and 2015 to avoid seasonal and tidal effects. Since terrain can significantly influence backscatters and image projection, the ALOS PALSAR data were orthorectified using the Advanced Spaceborne Thermal Emission and Reflection Radiometer (ASTER), Global Digital Elevation Model (GDEM) [171]. Two images then were geocoded and projected into the Universal Transverse Mercator (UTM) coordinate system, Zone 48 North based on the World Geodetic System datum (WGS84). The DN (Digital Number) was converted to normalized radar sigma-zero using Eq. 7.1

$$\sigma^0 \text{ [dB]} = 10 \log_{10} (\text{DN})^2 + \text{CF} \quad (7.1)$$

where σ^0 is backscattering coefficient, DN is a digital number of the amplitude image, and CF is the Calibration Factor and CF = –83 dB for both HH and HV polarizations [219]. The CF used to process ALOS-2 PALSAR-2 is similar to ALOS PALSAR [248]. The DN of each pixel was transformed into backscattering sigma naught (σ^0) in decibel (dB).

The ALOS PALSAR images were moderately despeckled using the Frost filter with a 5 x 5 moving window kernel to retain textural information [220]. To minimize the blurring effect on filtered images, image pixels were then averaged to 30-meter resolution, allowing the detection of small-area forest disturbances and comparability to Landsat-based datasets [324] as suggested by Neha, et al. [325].

Since surface moisture and tidal height can affect radar backscatters, we also carefully took the time to conduct field work into consideration to minimize effects of surface moisture and tidal height [222, 225, 249, 326].

7.1.2.3 Field data collection

The field data at the Cat Ba Biosphere Reserve was conducted several times in July and August 2010 and July 2015 with the help and permission from local authorities. The former dataset was used for mapping mangroves for 2010 and the latter dataset was used to generate a mangroves cover map for 2015. During the field survey, we collected ground-truth points (GTP) using Global Positioning Systems (GPS) to create training data for supervised classification and assess the accuracy of the post classification of the mangrove cover maps in 2010 and 2015. All GTPs data were transformed into a GIS format to select the training and validation datasets for SAR images classification. We also took photos for different land-cover types and mangrove species during the field survey for two periods. A total of five land-cover types (forest, mangrove, settlement, aquaculture, and water bodies) and two dominant mangrove species namely *Rhizophora stylosa* and *Avicennia marina* are found in the Cat Ba Biosphere Reserve were recorded during the survey (Fig. 7.1.2).

Rhizophora stylosa *Avicennia marina*

Figure 7.1.2. Mangrove communities in the Cat Ba Biosphere Reserve

7.1.3. Method used

7.1.3.1. Support vector machine classifier

Support vector machine (SVM) is a supervised non-parametric statistical learning method and has been widely used in numerous applications in remote sensing. SVMs have been successfully utilized in classifying LULC [319], mapping LULC [183], mapping mangrove forests [303], and monitoring mangrove change detection [305]. The SVMs consist of a large number of vectors that

have functions in separating different objects. However, selecting an optimal SVM algorithms for classifying these objects is not an easy task [187]. To overcome this problem, different kernel functions such as polynomial, sigmoid, and radial basis function (RBF) are used in the SVM-based classification algorithms. The accuracy of the SVM-based methods is relatively influenced by the selecting the kernel functions [187, 320]. We chose the RBF kernel in this study because it is the most commonly used in satellite image classification and it generally requires only a few parameters as well as it can produce good results [327, 328]. Additionally, suggestions provided in the ENVI User' Guide [329] were also taken into consideration in choosing the RBF kernel function parameters. As a result, the γ parameter was set to a value equal to the inverse of the number of the polarizations used of the ALOS imagery (i.e., 0.166). The penalty parameter was set to its maximum value (i.e., 100), showing no misclassification during the training process while the pyramid parameter was set to a value of zero, showing the ALOS imagery to be processed at full resolution. It is noted that a classification probability threshold of zero was used, reflecting that all image pixels had to be classified into one class.

In order to produce better accuracy, the support vector machine supervised classification generally requires a large number of input data for the classification. In this study, we selected multi-polarizations generated from dual-polarization such as HH, HV, HH/HV, HV/HH, HH-HV, and ½(HH+HV) as suggested by Pham, et al. [98] as input bands for classifying ALOS PALSAR imagery using ENVI. The ALOS PALSAR imagery was classified using a supervised training method by applying pixel-based support vector machines algorithms. The ENVI 5.2 software was employed for SAR imagery processing.

7.1.3.2 Mangrove forest change detection

A pixel-based supervised classification using the SVM classifier was carried out on the ALOS PALSAR imagery using ENVI 5.2. Figure 7.1.3 shows the flowchart used for mapping mangrove species and monitoring their changes in the Cat Ba Biosphere Reserve, Hai Phong. Classification results for two periods were overlaid in ArcGIS 10.3 environment to detect mangrove forests changes.

It is noted that the GIS data and the statistical results were conducted in ArcGIS environment. The classification results were transformed into a GIS format for analyzing the mangrove forest changes in ArcGIS 10.3. Additionally, ancillary GIS data such as commune boundary were overlaid in the final classification results to analyze mangrove area statistics changes from 2010 to 2015 (Fig. 7.1.3).

7.1.3.3 Accuracy assessment

We used the confusion matrix to assess the performance of the SVMs for mapping mangrove forests. The confusion matrix table was generated by comparing error value for each class that is classified with its value in ground truth data (reference data). The confusion matrix table contains the same number of column and row and equals to the number of classes [60, 330].

The reliability of the mangrove forests classification using SVM algorithm was measured using Kappa coefficient (*K*) [60, 141, 142, 331]. The kappa coefficient was calculated using Equation 7.5.

$$\hat{k} = \frac{N\sum_{i=1}^{r} X_{ii} - \sum_{i=1}^{r} X_{i+} X_{+i}}{N^2 - \sum_{i=1}^{r} X_{i+} X_{+i}} \tag{7.5}$$

where r is the number of row in confusion matrix; X_{ii} is the number of rows i and column i; X_{i+} and X_{+i} are the totals of row i and column i, and N is the number of observations.

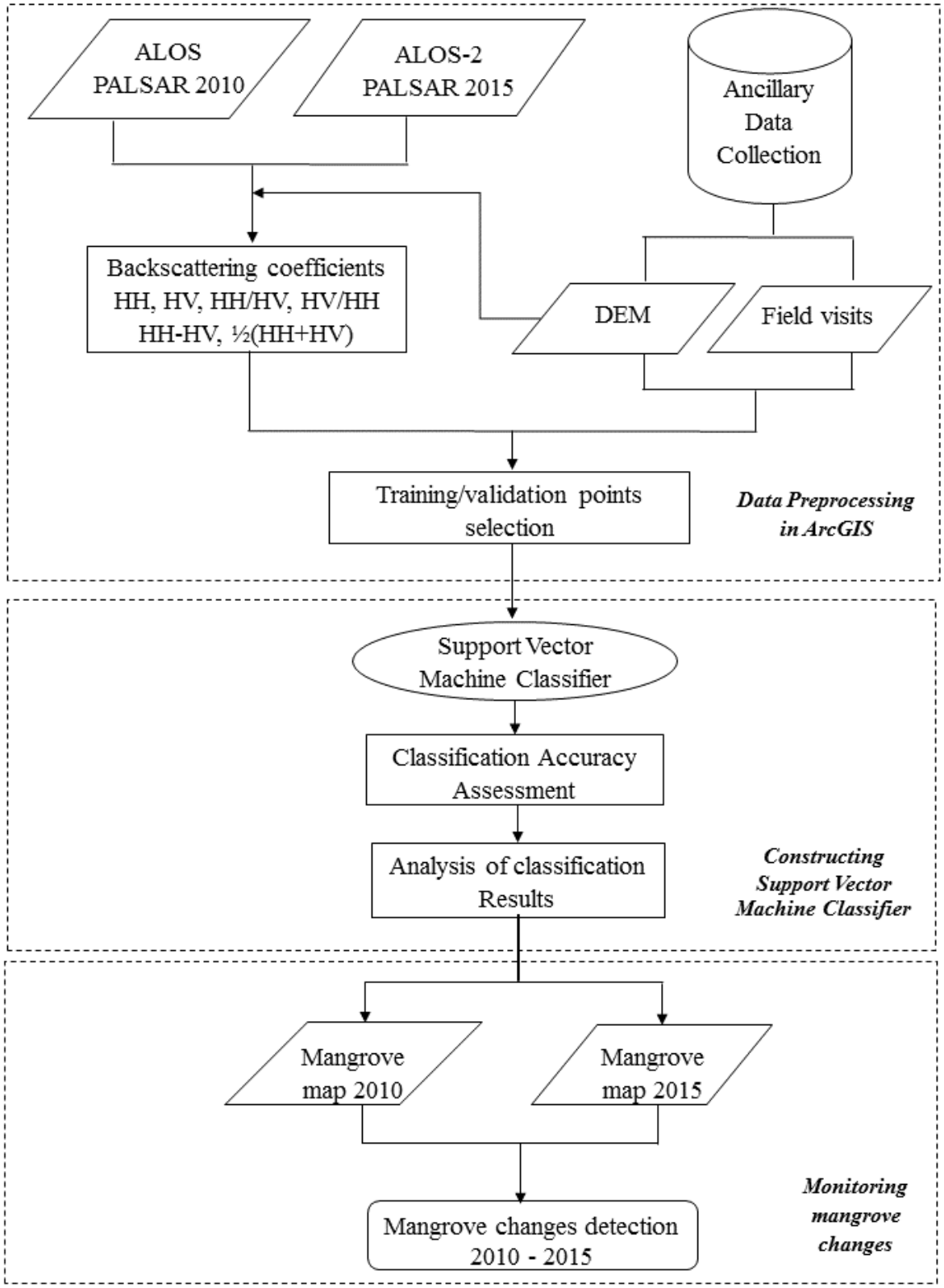

Figure 7.1.3. Flowchart used for mapping mangroves and monitoring their changes

7.1.4. Results and discussion

7.1.4.1 Mangrove forests mapping

The classification results using the SVM algorithm with radial functions were converted to a GIS format for use in ArcGIS 10.3. The land-cover maps for 2010 and 2015 visualized five classes including forest, mangrove, settlement, aquaculture, and water bodies. Figures 7.1.3 and 7.1.4 show the spatial distribution of mangroves in the Cat Ba Biosphere Reserve, Hai Phong for 2010 and 2015, respectively. Mangroves are found mostly in the coast and the river mouths of Phu Long commune, accounting for the vast majority of the total mangrove area of the Cat Ba Biosphere Reserve. Also, a small grove of mangroves on the shore is found in Gia Luan and Xuan Dam communes.

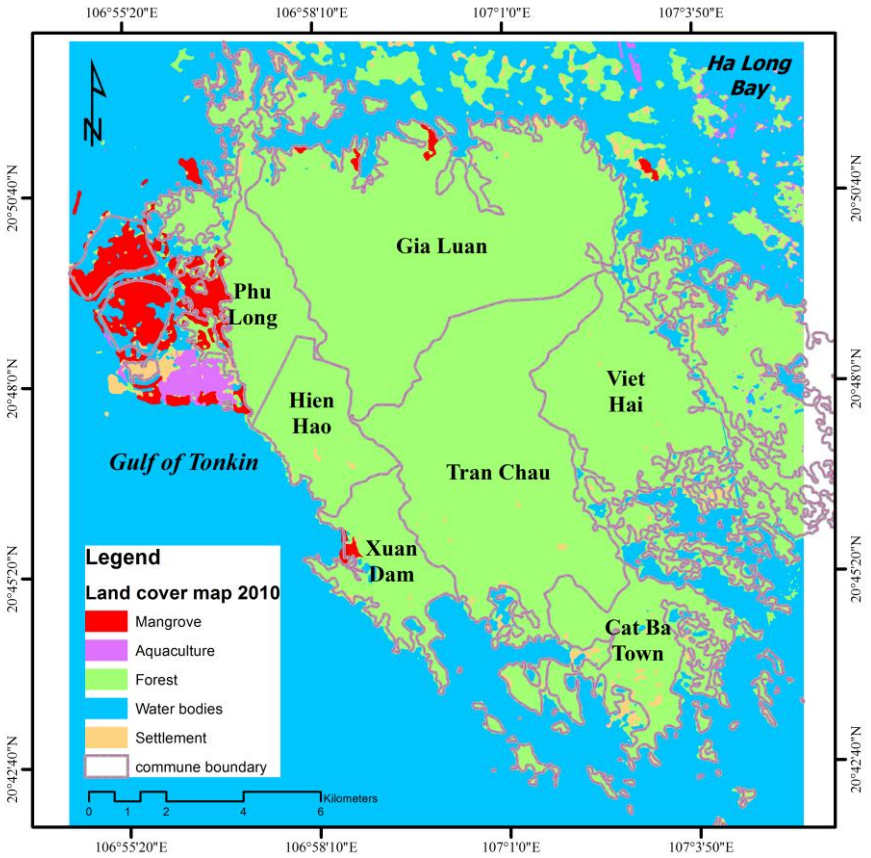

Figure 7.1.4. Mangrove forests mapping of the Cat Ba Biosphere Reserve in 2010.

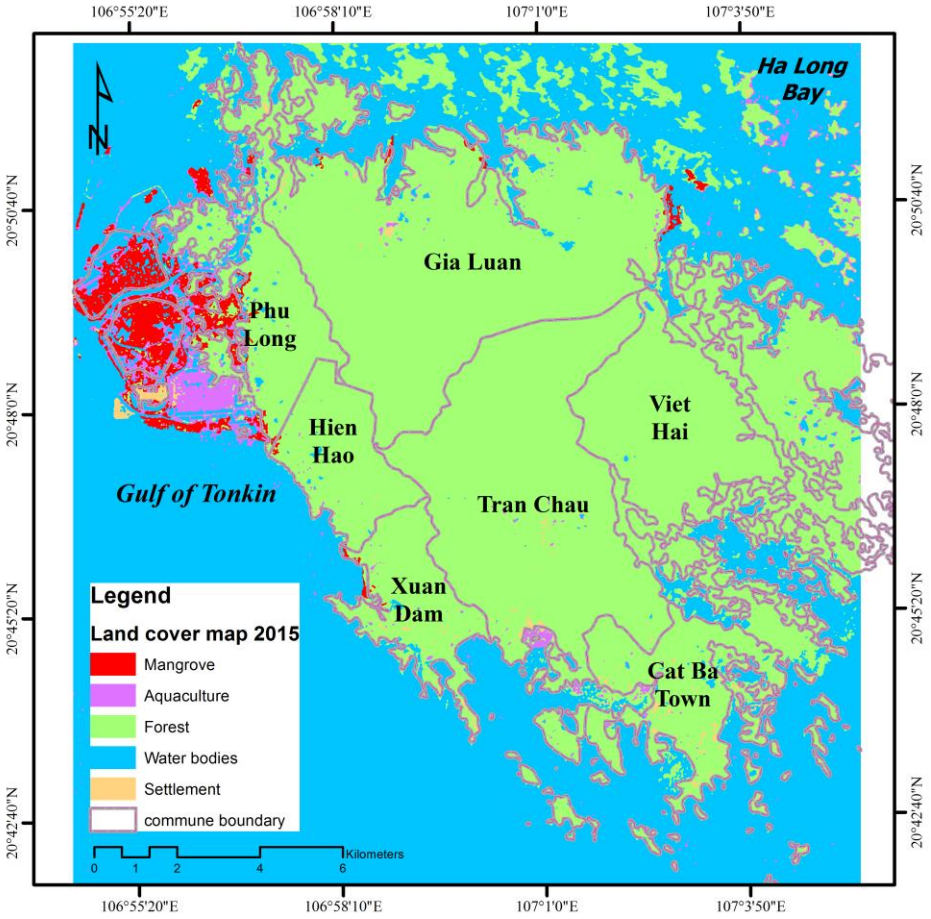

Figure 7.1.5. **Mangrove forests mapping of the Cat Ba Biosphere Reserve in 2015.**

The classification accuracy (Producer, User, and Overall accuracies) and the Kappa coefficients of the SAR image processing are shown in Table 7.1.2. The overall accuracy of SAR data processing for the years 2010 and 2015 are 81%, 85%, and the Kappa indexes are 0.77 and 0.81, respectively. Mangroves, forest and water bodies produced higher user and producer accuracies among the five land cover classes. Settlement class also produced higher user and producer accuracies except for producer accuracy for the year 2010 (62%). Meanwhile, aquaculture class produced lowest user and producer accuracies for both two years 2010 and 2015. The low accuracies observed for the aquaculture class may be attributed to the backscattering coefficients similarity at HH and HV polarizations of aquaculture with water bodies which was reported by Tien Dat and Kunihiko [236]. These may be due to the presence of speckles in ALOS PALSAR images. Speckle is a common problem for SAR sensors, influencing the accuracy of SAR images classification. SAR image despeckling is expected to remove speckle and retain image features. The main limitation of the current work is that we applied the Frost filter for the despeckling of SAR images, which may cause the blurring effect on filtered images, resulting in the changes in information on the smoothed images. Thus, a nonlocal filter for SAR images such as the probabilistic patch-based

filter, the Bayesian nonlocal mean filter, and the SAR block-matching 3D filter [332-334] should be cautiously performed to solve the limitations of speckles in future studies. More research is, therefore, needed to investigate the usability of the nonlocal filters for the preservation of image features for the change detection of SAR data.

Table 7.1.2. Accuracy assessment of the SAR images classification for the years 2010 and 2015

	2010		2015	
Land cover type	**Producer's accuracy (%)**	**User's accuracy (%)**	**Producer's accuracy (%)**	**User's accuracy (%)**
Mangrove	84.6	91.7	76.9	83.3
Aquaculture	70.0	77.8	60.0	85.7
Forest	94.4	73.9	88.9	84.2
Settlement	61.5	88.9	92.3	100
Water bodies	90.9	83.3	100	73.3
Overall accuracy	81.5		84.6	
Kappa coefficient	0.77		0.81	

It can be seen from Table 7.1.2 that the overall accuracy and Kappa coefficient of 2015 are higher than those of 2010. It is likely due to the fact that ALOS-2 PALSAR-2 imagery acquired for 2015 with high sensitivity mode has better spatial resolution than ALOS PALSAR imagery for 2010. The performance of the final images classification using the SVM algorithm with radial functions for both two periods 2010 and 2015 show satisfactory results, compared to previous studies [303, 305, 319].

7.1.4.2 Mangrove forests changes from 2010 to 2015

Figure 7.1.6 shows a mangrove forests change map in the Cat Ba Biosphere Reserve from 2010 to 2015. By overlaying the land-cover maps for two periods within the ArcGIS environment, it can be possibly detected what land cover is currently converted into mangroves. Thus, we also can determine that the past mangrove forest cover has been converted into aquaculture, which a common trend throughout South East Asia [282, 335] in the Mekong Delta [141, 313, 316], and in the Red River Delta of Vietnam [14, 143, 168, 336].

Mangrove forests in the Cat Ba Biosphere Reserve decreased by 14.6% from 2010 to 2015 (Table 7.1.3). It is likely due to over-shrimp aquaculture in the coastal area of Hai Phong. Mangrove forest areas converted to shrimp aquaculture from mangroves by local people in several communes of Cat Hai district including the Cat Ba Biosphere Reserve [291].

Table 7.1.3. Mangroves changes in the Cat Ba Biosphere Reserve from 2010 to 2015.

Period	Onset of period (ha)	End of period (ha)	Change (ha)	% change
2010-2015	856 ± 32	731 ± 21	- 125	-14.6

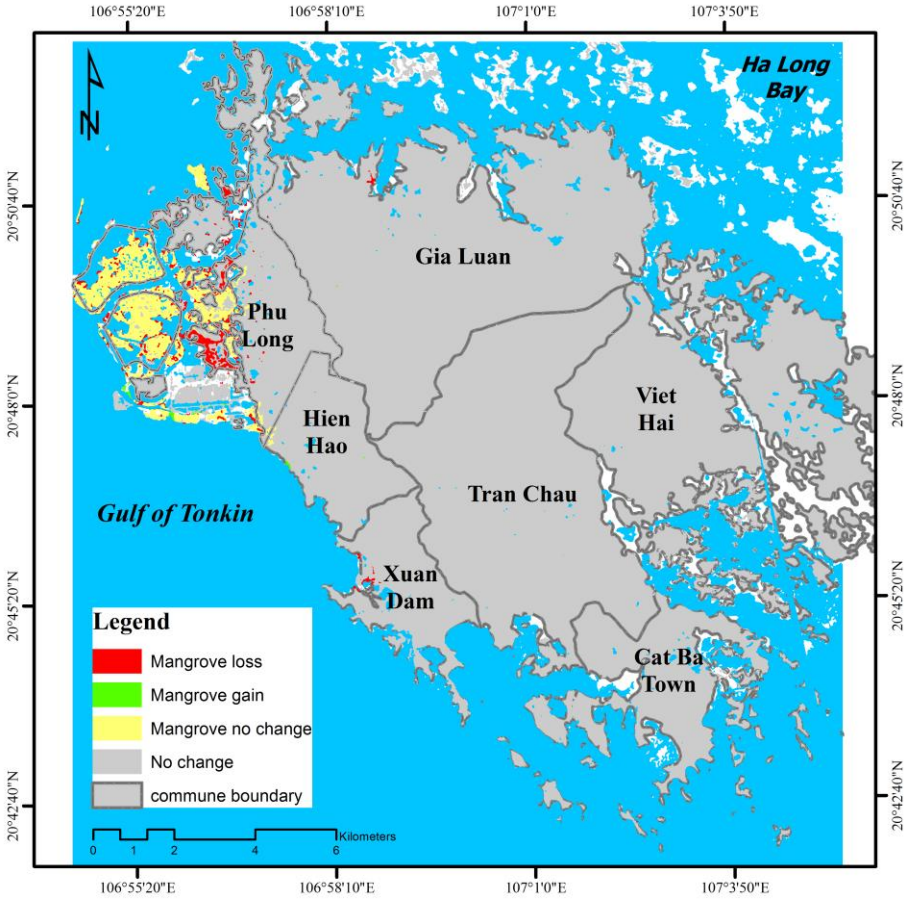

Figure 7.1.6. Mangrove forests change map in the Cat Ba Biosphere Reserve from 2010 to 2015.

The analysis of mangrove changes from 2010 to 2015 using ALOS PALSAR data shows that the mangrove forests area in the Cat Ba Biosphere Reserve, Hai Phong has decreased slightly. However, mangrove area statistics showed significant differences among the three coastal communes of the Cat Ba Biosphere Reserve, Hai Phong (Table 7.1.4).

Table 7.1.4. Mangroves changes per commune in the Cat Ba Biosphere Reserve from 2010-2015.

Period	2010 (ha)	2015 (ha)	Change (ha)	Annual rate loss / gain rate (ha/year)
Phu Long	781.5	632.3	-149.2	-29.8
Gia Luan	45.9	79.0	33.1	6.6
Xuan Dam	28.6	19.7	-8.9	-1.8

Among the three coastal communes, mangrove forests area in Phu Long declined gradually. The annual rate of this loss was about 30 hectares. On the other hand, in Gia Luan, mangroves increased slightly. The annual rate of the gain was just 6.5 hectares. The statistic shows the potential use of ALOS PALSAR imagery in mapping spatial distribution of mangroves and providing a synoptic view of mangrove changes that can be used for prioritizing mangrove restoration and rehabilitation in the Cat Ba Biosphere Reserve. The findings of this study also update the statistical status of the mangroves ecosystem in one of the most well-known islands located on the Northern coast of Vietnam. Our research illustrates that ALOS PALSAR sensor together with a GIS-based SVM classifier provides the promising tool for mapping mangrove forest species and analyzing mangroves changes on a regional scale. This work is essential to support monitoring, reporting, and verification (MRV) work as part of REDD+ program in the developing countries.

7.1.5. Conclusions

Overall, mangroves areas in the Cat Ba Biosphere Reserve, Vietnam have decreased at a moderate rate (15%) from 2010 to 2015. The statistical results of this research are important as a valuable reference to understand the current situation of mangrove forests in the Cat Ba Biosphere Reserve, Hai Phong City of Vietnam. As mangroves can significantly contribute to mitigating climate change impacts and their ecosystem can serve the local communities with ecological and economic services, the local government of Hai Phong City should plan necessary regulations and policies to monitor and conserve mangroves of the Biosphere Reserve.

The results of this chapter show that ALOS PALSAR data and SVM classifier technique can be used to map and assess mangroves changes along the coast of the Cat Ba Biosphere Reserve, Hai Phong, while a GIS can be employed to integrate ancillary information and spatial data of the mangrove forests in order to effectively monitor mangroves in the Cat Ba Biosphere Reserve, Vietnam.

The ALOS-2 PALSAR-2 sensor used for 2015 provides higher overall accuracy and Kappa coefficient in mapping land-cover and mangrove forest than the ALOS PALSAR for 2010. The

ALOS-2 produced the overall accuracy of 85% and the kappa coefficient of 0.81, compared with those of 81% and 0.77, respectively from the ALOS. Therefore, ALOS-2 PALSAR-2 with high sensitive mode should be used for mapping and monitoring mangroves on national and regional scales. This research demonstrates the potential use of ALOS PALSAR data together with a GIS-based SVM algorithm for mapping mangroves and assessing their changes in coastal zones.

7.2. Mangrove Ecosystem Services Valuation in the Context of Climate Change

7.2.1. Introduction

Mangrove forests, which appear in the inter-tidal zones along the coasts in tropical and semi-tropical regions, are considered as one of the most important ecosystems on earth [337]. Mangrove ecosystems can act as highly efficient carbon sinks in tropical climates [7] because they can sequester carbon in both above- and below-ground biomass, as well as in sediments [8, 280]. Despite such benefits, many mangrove forests have been lost in the past 50 years worldwide due to high population growth, rapid urbanization, aquaculture expansion and the impact of other human activities [4]. Among the regions of the world, Asia has suffered the greatest loss (1.9 million hectares) of mangroves [11], with more than 100,000 ha being lost from 2000 to 2012 [282]. Like many other countries in Southeast Asia, the mangrove forests of Vietnam declined dramatically by 400,000 hectares in the early 21st century [12], and are still under severe threat due to high population growth, aquaculture expansion, and migration into coastal areas. For example, the mangrove areas of the northern coast of Vietnam decreased by 17,094 hectares between 1964 and 1997. This loss of mangrove forests was due to over-expansion of shrimp aquaculture [168].

One of the essential steps for planning and implementing restoration and conservation programs in mangrove forests, apart from quantitatively identifying such losses, is to know the economic value of the loss, and the social benefits of restoring the lost resource. The economic valuation of ecosystem services has become more prevalent during the last few decades [203, 338-341]. However, only a few studies have attempted to value mangrove ecosystem services, and to measure WTP to restore the perceived benefits of mangroves in the coastal zone. Previous studies are limited to specific regions in India [342], and in Indonesia [205]. Stone, et al. [342] indicated that the perceived benefits of mangrove restoration are the most significant factor influencing local households' WTP among the fishing communities and rice farmers in the mangrove ecosystems found on the west coast of India. A more recent study of the Mahakam Delta mangroves in

Indonesia by Susilo, et al. [205], showed that the mean WTP estimated using contingent valuation was IDR 35,201 (US$2.71). This study also reported that over 80% of the respondents considered the perceived benefits of mangroves for their livelihood. Nevertheless, these previous studies did not consider the climate change impacts that may affect the success of mangrove restoration projects. As mangroves can significantly contribute to mitigating climate change impacts and protecting dyke systems in the coastal zones, mangrove restoration projects should carefully take this role into consideration [343].

There are a limited number of studies that have estimated WTP for natural resources conservation, and/or respondents' perceptional factors influencing their WTP in Vietnam. Existing studies are restricted to specific regions, such as in marine protected areas [344], or mangrove forests in South Central Vietnam [345]. Kaida and Dang [344] estimated that the mean visitor WTP for conservation programs in the Nha Trang Bay Marine Protected Area in Vietnam was about US$5.99, and reported that income and education of respondents are positively correlated with their WTP. Recently, Tuan, et al. [345] estimated that the mean household WTP for mangrove restoration in a lagoon in South Central Vietnam was around VND 131,670 (US$ 6.08) and indicated that housing condition and attitude of respondents on the future climate scenario are significant factors influencing the household WTP. However, most of the socioeconomic and perceptional factors were not found significantly influencing by the WTP of respondents in these studies. Since mangrove forest restoration and conservation in Vietnam is substantially influenced by the livelihoods available to local communities (i.e., the growing expansion of shrimp aquaculture in mangrove forest areas), and their perceptions toward conservation activities, it is also crucial in policy planning and implementation to identify the socio-demographic and perceptional factors that could affect their WTP for conservation programs.

Our review of the current literature shows that this is the first study that has attempted to estimate respondent WTPs, and to examine the perceptions influencing their WTP for mangrove restoration in a Biosphere Reserve in Vietnam. However, given that the economic valuation of mangrove ecosystem services in the study area can now be established, the present study is able to promote the implementation of mangrove conservation and restoration strategies in climate change mitigation approaches such as the United Nations' REDD+ program. It also provides significant comment regarding PES for developing regional and national blue carbon trading markets, and for guiding mangrove management and conservation for Blue Carbon projects [283, 284].

Thus, the main objectives of the present study were to estimate the WTP for mangrove forest restoration within those households who interact with mangrove forests for their livelihood and who will have to deal with climate change, and to examine socio-demographic and perceptional

factors influencing household WTP for mangrove conservation programs. The present study focused on the payment for sustainable mangrove ecosystem conservation and management in the Cat Ba Biosphere Reserve (CBBR) (buffer and transition zones) located on the northern coast of Vietnam.

7.2.2. Background of mangrove ecosystem of the Cat Ba Biosphere Reserve

Cat Ba is the largest island in the Cat Ba Archipelago in Hai Phong City, located in the north of Vietnam (Fig. 7.2.1). The core ecosystem of the island is tropical forest including tropical rainforests in the lowlands, limestone forests in the mountains, and mangrove forests along the coast. Cat Ba Island has been recognized by UNESCO as a biosphere reserve since 2004. The total area of the CBBR is about 26,241 hectares, and the total population in 2015 was 18,475 persons, or 3695 households [346]. The biosphere is a well-known destination for tourists from not only all parts of Vietnam, but also from around the world. The number of tourists has significantly increased over the last decade [321], and is now about 500,000 annually [322].

Despite the continuing large growth potential in tourism, the CBBR is under serious threat from the degradation of its forest environments. From 1990 to 2001 the tropical rainforest of the CBBR declined by roughly 660 hectares, equaling 4.5% of the total area, while the mangrove forest decreased by almost 600 hectares, or about 50% of its original coverage [323]. The mangrove forest area in the reserve declined largely due to the over-expansion of shrimp aquaculture, which added a further 627 hectares in 2015 [168]. In addition, the marine ecosystem is being polluted at an alarming rate because of the solid and sewage wastes generated from tourism and intensive aquaculture activities, as well as from domestic and industrial activity. Consequently, a large number of environmental parameters, such as the biological and chemical oxygen demand of the marine ecosystem, do not meet national standards [347].

In addition to the biophysical impacts of tourism growth and aquaculture activities, poverty is still persistent within the CBBR. The incidence of poverty in the reserve is still high and around 40% of the population in the CBBR lives in the rural area, where the average annual net income per capita was as low as 4,875 million VND in 2010 (equivalent to US$325 or US$0.89 per capita per day) [348]. The net income in some villages located in the buffer and transition zones of the CBBR, such as Viet Hai and Hien Hao, is even lower at US$0.56 and US$0.64 per capita per day respectively. These numbers are far lower than the poverty level of US$1.25 per capita per day set by the United Nation poverty indicator [349]. Furthermore, many of the rural citizens of Cat Ba Island living in poverty do not benefit from the shrimp aquaculture activities or tourism. The vast

majority of the wealth generated by tourism and aquaculture on the island is instead appropriated by international tourism agencies, hotel operators, and private companies.

The forest and environmental degradation and persistent poverty occurring on Cat Ba Island are clear indications that, although the tourism and aquaculture sectors are growing rapidly and are the largest contributors to the local economy, they are far from being sustainable [321]. In addition, the increasing demand for seafood from a rapidly growing tourism, and the poorly regulated international and domestic markets are exacerbating pressures on the marine ecosystem, especially on the mangrove forests, with further devastating consequences to the local livelihoods that they support.

Over 95% of the mangroves in the CBBR are found in the Phu Long commune, a community with 595 households. There are a total of four villages in Phu Long where mangrove forests are found in the buffer and transitional zones to the CBBR [346]. Three villages are in the transitional zone: Ngoai, Bac, and Nam, while Ao Coi is in the buffer zone. According to the survey carried out in September 2016 for this study, the socio-economic characteristics of these villages were significantly different. In the transitional zone, households are likely to be involved in the aquaculture sector as they have their own shrimp ponds. Conversely, farming and hired labor are the main occupations in Ao Coi as they do not have their own ponds.

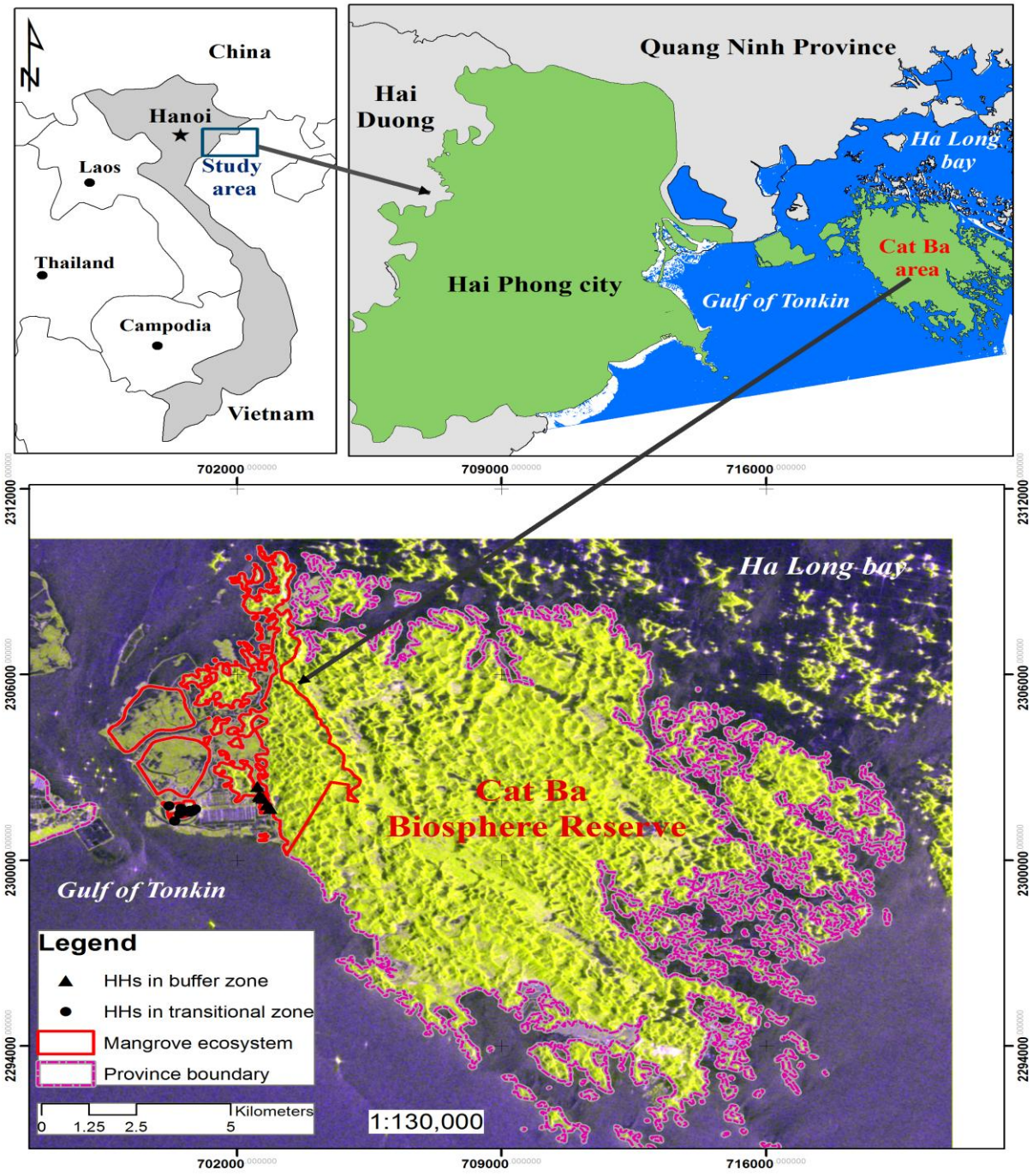

Figure 7.2.1. The study area of the Cat Ba Biosphere Reserve, Vietnam

7.2.3. Method

7.2.3.1. Contingent Valuation Method

CVM is widely used to estimate willingness to pay WTP for environmental conservation and ecosystem services [201-205]. CVM is a survey-based approach, in which an individual independently states his or her willingness to pay (WTP) for the conservation of environmental

services in a particular location [206]. There are two main kinds of willingness to pay (WTP) questions: direct or open-ended, and dichotomous choice. The latter was employed in this study; a single-bounded dichotomous choice WTP question was used, incorporating five bids. Dichotomous choice questions help avoid some biases in answers (such as outliers) but require complicated statistical treatment [207].

In this study, CVM was employed to estimate the WTP for the restoration of the mangrove forest in the CBBR [206]. The DC consists of two formulas: a single-bound (SB) model which offers one question as to whether a bid is "accepted" or "rejected," and a double-bound (DB) model which presents two bids to a respondent. The respondent who has accepted the first bid is offered a higher bid in a second round, and the one that has rejected it is offered a lower bid. The DB model has been widely used because the additional information provides clearer bounds for the respondent in determining their WTP. However, several studies have pointed out that the DB format can induce some biases and inconsistencies through the existence of bound effects [208-210]. To avoid these potential problems, a single-bound dichotomous choice model was considered the appropriate empirical analysis method to determine household WTP in this study.

The two most popular forms of the SB are the logistic function, which is used in logit estimation, and the cumulative normal distribution, which is used in probit estimation. When determining which model to use in this study, logit and probit analysis yielded similar marginal effects in most applications, and the outcomes were similar [350]. In this study, a logit regression model was used to determine household WTP. The formula of this model is as follows:

$$Pr\,(Yes_j) = \frac{1}{1 + \exp\{-(\alpha - \beta.BID + \gamma.\chi\}} \quad (7.2.1)$$

Where α is constant, β is the coefficient of the BID as restoration fee, χ is the vector of explanatory variables influencing the response, and γ is the vector of the corresponding parameters.

Parametric estimation: the parametric method was used to estimate the WTP by using logit regression; in which the dependent variables are the household saying 'yes' to pay for t_i , or 'no' to payment for the t*i* bid level. The list of explanatory or independent variables was subjected to a regression analysis, which was used to estimate the effect of each variable to the WTP of each household including bid amount, the socio-economic characteristics, the participation of respondents in mangrove restoration activities, and the attitude of respondents towards the restoration of mangroves:

$$\alpha_1 Z_j + \beta(Y_j - T_j) + \varepsilon_{1j} = \alpha_0 Z_j + \beta Y_j + \varepsilon_{0j}$$

Therefore, mean WTP is calculated using equation 7.2.2:

$$\text{Mean WTP} = E\,(\text{WTP}|\,\alpha_1, \beta, z_j) = \alpha_1 z_j . \beta^{-1} \quad (7.2.2)$$

We estimated respondent's WTP based on a *yes* or *no* answer to a SBDC question for which five different bidding prices had been prepared. If she/he accepted a bidding price for the single-bounded question, the model can be depicted in a linear or logistic form [207]. In this study, we analyzed which variables (factors) would promote respondent's WTP for mangrove restoration using a binary logistic regression model. The dependent variable indicating the willingness of respondents to pay for mangrove restoration had binary values of 0 and 1, where 0 reflects unwillingness and 1 reflects willingness to pay. There were five bid levels ranging from 20,000 VND (US$0.90) to 300,000 VND (US$ 13.45) per household per year. The variables used in the logit regression model are shown in Table 7.2.1.

Place of residence, gender, age, marital status, income, occupation, the number of household members, house type, and education level were considered as potential explanatory variables. Other variables, including the awareness of the respondents in relation to the perceived benefits of mangrove resources, attitude to the impacts from climate change, and the perceived importance of the mangrove forest restoration programs were also used in the model as perception factors that potentially influence WTP. All statistical analyses were performed using Stata 14 software (Stata Corp).

Regarding the occupation variable, we used dummy variables (binary values of 0 and 1) to examine whether aquaculture influences WTP for mangrove restoration, as the degradation of the mangrove forests in North Vietnam has resulted largely from the over-expansion of shrimp aquaculture [168]. For this purpose, aquaculture was given a value of 1, while other occupations had a value of 0. As to a place of residence, we assumed that the different locations of households might influence their WTP for mangrove restoration, as they would have different perceived benefits in relation to the mangroves resources, different attitudes to the impact of climate change, and differences in their perceived importance of the mangrove forest restoration programs. Thus, the respondents of the village in the buffer zone were given a value of 1, while three villages in the transitional zone of the CBBR were given a value of 0 (See Fig. 7.2.1).

Table 7.2.1. Description of Variables used in the Logit Regression Model

	Variables	Definition	Measurement/unit
1	Probability	The probability of a respondent being willing to pay for mangrove forest restoration	1 = Yes WTP 0 = No WTP
2	Bid	Bid levels (1000 VND)[a]	20, 50, 100, 200, 300
3	Age	Age of respondent	Numeric variables
4	Gender	Gender of respondent	1= Male 0 = Female
5	HH size	Number of family members	Numeric variables
6	Education	If respondent was educated to high-school level or above	1 = High school and above 0 = Otherwise
7	Housetype	The house type of respondent	1 = Permanent house 2 = Otherwise
8	Occupation	Occupation of respondent (main income source)	1= Aquaculture 0 = Otherwise
9	Zone	Place of residence	1 = Buffer zone 0 = Transitional zone
10	Lnincome	Natural logarithm of total household income per month (million VND)	Numeric variables
11	Severe	Respondent attitudes toward the impacts of climate change	1 = Very severe 0 = Otherwise
12	Agreecons	Respondent's decision on mangrove restoration	1 = Strongly agree; 2 = Agree; 3 = No opinion; 4 = Disagree; 5 = Strongly disagree
13	Information	Respondent's knowledge about climate change and its adverse impact on mangrove restoration and the community	1 = Very new information 2 = Knew some news 3 = Knew all
14	Volunteer	Respondent's desire to participate in mangrove restoration activities	1 = Want to join 0 = Otherwise

[a] US$1 is equivalent to VND 22,300.

7.2.3.2. Questionnaire design and survey method

The questionnaire in the present study was predesigned, and was revised based on key informant interviews with the village heads of the four studied communes, the chairmen of farmers' associations (a total of 11 interviewees), and a focus group discussion with the representatives of environmental managers and the village heads of the four communes in the study area. Based on the information exchanged during these sessions, we carefully developed multiple scenarios for the restoration project and the proposed conservation fees as bids for the questionnaire survey, so that these were understood and accepted by the respondents.

The main survey was conducted in September 2016. 205 household responses were collected, all of which were usable. All respondents were asked to answer the questionnaire, which consisted of four main parts. In the first part, respondents were asked general information on the socio-economic characteristics of their households. In the second part, general information on the mangrove ecosystem services of the CBBR was given to the respondents who lived in the four villages located in the buffer and transitions zones of the reserve. They were then asked the reasons for mangrove conservation and protection in the CBBR, and the perceived benefits of mangrove ecosystems for their livelihoods. As a mangrove ecosystem has numerous ecological functions and plays an important role in local livelihoods, mangrove rehabilitation and restoration actions are expected to help the local communities in dealing with climate change in Vietnam [351]. The second section in the questionnaire thus revealed respondent assessments of the proposed mangrove restoration programs and their awareness of these programs.

In the third part, the current situation of mangrove ecosystems in the context of climate change issues and the problems associated with management of the mangrove resource were made known to the respondents. First, information was introduced detailing the current status of the mangroves, reflecting the fact that these forests have decreased due to the rapid increase of extensive shrimp aquaculture. Secondly, the impacts from climate change and predicted sea level rise were also provided to all respondents. They were then asked to evaluate the levels of seriousness of the current conservation scenarios of mangrove ecosystems in the CBBR. Information on the awareness of local people about mangrove restoration under the context of climate change was explored to help respondents understand the agreement levels and motivation for the WTP for mangrove restoration in the CBBR. They were then asked to rate the current conservation scenarios for the mangrove ecosystem in the study site. Respondents were then asked about their opinions on mangrove restoration since the mangrove ecosystem is expected to provide both direct and indirect benefits for local communities [352].

The last part of the questionnaire explored the WTP of respondents for mangrove restoration in the context of the climate change issue. The respondents were asked whether they agree/disagree to pay for mangrove restoration, and to explain the main reasons for their decision. Respondents were also asked about their motivations in relation to mangrove restoration and conservation activities. This involved them giving an answer on the perceived benefits of mangrove forests, and the main reasons for mangrove restoration under the context of climate change. It is noted that a respondent who answered yes/no for his/her WTP also gave a reason for agreeing/not agreeing.

7.2.4. Results

7.2.4.1.Socio-demographic characteristics of the respondents

The socio-demographic characteristics of the respondents are shown in Table 7.2.2. Gender balance was carefully taken into consideration in data collection; thus, we attempted to interview equal numbers of males and females. However, the eventual number of male participants (63% of the 205 respondents) was larger than the number of females. This over representation of males in the present sample reflects the fact that, in general, men tend to be a family representative and are responsible for economic decision-making. This is especially so in relation to the use of the mangrove forests and in aquaculture, which they are substantially engaged in. In the case of the northern coast of Vietnam, the monetary income of a household is in general contributed mainly by men (husbands), while women (wives) are often responsible for taking care of housework and teaching their children.

The age distribution of respondents in the present sample shows they are predominantly aged over 45; this group accounted for over 70% of the total sample. This reflects the local situation that the middle-aged and elderly tend to work in their villages, while younger people (below 45) tend to work outside. Our respondents generally had low educational levels: about 70% of them had completed secondary school or lower, followed by high school (18.5%), and higher education (less than 10%). Approximately 2.9% of the respondents were illiterate.

Table 7.2.2. Socio-Demographic Characteristics of the Respondents

	Category	Frequency	Percentage
Gender	Male	130	63.41
	Female	75	36.59
Age (years old)	18-25	3	1.46
	26-35	18	8.78
	36-45	38	18.54
	46-55	61	29.76
	≥ 56	85	41.46
Education	Under primary school	2	0.98
	Primary school	34	16.59
	Secondary school	109	53.17
	High school	38	18.54
	Technical school	10	4.88
	University	5	2.44
	Post graduate	1	0.49
	Illiterate	6	2.93
Occupation	Aquaculture sector	60	29.27

	Fisherman	37	18.05
	Business owner	34	16.59
	Hired labor	28	13.66
	Farmer	15	7.32
	Retired	17	8.29
	Government Officer	5	2.44
	Disabled	5	2.44
	Babysitter	3	1.46
	Student	1	0.49
House type	Permanent house	120	58.54
	Semi-permanent house	85	41.46
	Temporary house	0	0
Household size (persons)	1	5	2.44
	2	46	22.44
	3	37	18.05
	4	50	24.39
	5	42	20.49
	6	18	8.78
	7	4	1.95
	8	3	1.46
Income (1,000 VND)	< 1,000	13	6.34
	1,100-3,000	54	26.34
	3,100-6,000	75	36.59
	6,100-9,000	25	12.19
	> 9,000	38	18.54

In this study, majority of respondent occupations fell into four categories: working in the aquaculture sector, in fishing, as business owners, or as hired labor; and these four accounted for 78% of the total sample. The remainder were government officers, retirees, farmers, and others. Nearly 50% of the respondents had aquaculture work experience (owning shrimp farms, fishing, employees at private aquaculture companies, and so on). This indicates that the study sample represents typical coastal communes in North Vietnam, where local livelihoods mainly rely on aquaculture activities.

As to house types, there was no respondent that lived in a temporary house in the study area because the Vietnamese Government has attempted to remove slums and temporary housing. About 58% of the respondents had a permanent house, while the rest had a semi-permanent house. Average household size in the sample was 3.79 persons, which is equivalent to the normal family size in Hai Phong City (3.95) [346]. Over one-third of the respondents (37%) had a monthly household income of between 3.1 to 6.0 million VND (about 140-270 US$), followed by 31% receiving more than 6.1 million VND (about 280 US$), and 25% were in the range between 1.1 to 3 million VND (about 49.5-139 US$). About 6.3% are likely to be poor households, similar to the

poverty rate for Hai Phong City, with incomes lower than the poverty level set by the UN poverty indicator (1.25$ per capita per day) [349].

7.2.4.2. Perceived benefits of mangroves in the Cat Ba Biosphere Reserve

Table 7.2.3 shows the responses of respondents in the buffer and transitional zones of the CBBR in terms of the importance of the mangrove ecosystem functions associated with their livelihoods. The results reveal that over 69.4% of respondents understand the function of mangroves as regulating devices in storm prevention, pollution reduction, flood and erosion control, and in carbon storage. In addition, 2.5-18.0% of respondents positively assessed the benefits of mangroves for improving the sustainability of their livelihoods. However, 1.6-2.8% of respondents did not understand the importance of mangrove ecosystem functions.

Table 7.2.3. The Importance of the mangrove ecosystem functions in the CBBR

Mangrove ecosystem function	Ao Coi	Bac	Nam	Ngoai
Unknown	2.8	1.6	0.0	0.0
Improve the sustainability of local livelihoods	11.1	18.0	7.4	2.5
Supporting services	2.8	0.0	0.0	4.9
Provisioning services	11.1	3.3	11.1	6.2
Regulating services	69.4	75.4	77.8	85.2
Help protect biodiversity	0.0	1.6	3.7	1.2
Opportunities and benefits for future generations	2.8	0.0	0.0	0.0

Note: Values are % of total individual responses

Table 7.2.4. Respondent's opinion about the stress on current mangrove ecosystems in the 4 villages

Household opinion	Ao Coi	Bac	Nam	Ngoai
Very severe	45.7	24.6	29.6	30.6
Severe	33.3	49.2	33.3	16.7
Not so severe	21.0	21.3	33.3	41.7
Not at all	0.0	4.9	3.7	11.1

Note: Values are % of total individual responses

Table 7.2.4 shows that many in the four villages believe that the mangrove ecosystems of the CBBR are under very severe stress, ranging from 25% to over 45% of the total respondents. The percentage of respondents in the four villages who consider that the mangrove ecosystems are under severe stress is over 33%, except for the respondents from Ngoai village. In contrast, approximately 42% of the respondents from Ngoai village feel that the current stress on the local mangrove ecosystem is not so severe, while this opinion was held by between 21 and 33% of the

respondents from the other three villages. Overall, the results show that respondents realize that the mangrove ecosystems in the study area have been exposed to destruction through deforestation and biodiversity loss.

7.2.4.3.Bid response

Table 7.2.5 summarizes the WTP bids and the total number of respondents and their responses within a given bid level corresponding to those levels. The proportion of 'yes' votes to the base bid (BD) ranged from 87.8% for VND 20,000, the lowest bid, to 63.4% for VND 300,000, the highest bid.

Table 7.2.5. Distribution of Responses by Bid Amount

Bid level (VND)	Number of respondents	Number of "Yes" votes	Share of "Yes" votes (%)
20,000	41	36	87.8
50,000	41	39	95.1
100,000	41	30	73.2
200,000	41	33	80.5
300,000	41	26	63.4
Total	205	164	100

Note: US$1 was equivalent to VND 22,300 at the time of the study.

7.2.4.4. WTP estimates

The regression results are shown in Table 7.2.6. The bid variable was found to be significant with a negative coefficient (Coef = -0.006, p = 0.004, t = -2.890), indicating that the likelihood of answering yes decreases as the bid is raised. The mean WTP was estimated at 192,780 VND (US$ 8.64), while the median was 134,000 VND (US$ 6.01). There was a significant positive correlation between respondent occupation and WTP for mangrove restoration (Coef = 1.456, p = 0.011, t = 2.530), reflecting that involvement in aquaculture tend to increase their WTP of respondents for mangrove restoration.

The attitude of respondents to the future climate change scenario was found to have a significant positive influence on respondent WTP for mangrove restoration (Coef = 1.064, p = 0.037, t = 2.080), implying that awareness of the likely severity of future climate scenarios leads to a respondent being willing to pay more. In contrast, there was a negative significant correlation between gender and WTP (Coef = -0.976, p = 0.042, t = -2.040), reflecting that men were likely to pay less for mangrove restoration programs. The regression results also indicate that volunteer experience had a positive influence in explaining WTP (Coef = 0.387, p = 0.020, t = 2.330),

showing that respondents were likely to participate in mangrove restoration programs. In addition, educational level was found positively related to WTP (Coef =0.932, p = 0.098, t = 1.660).

Table 7.2.6. Determinants of the WTP for Mangrove Restoration

Variables	Coefficient	Std. error	*t* value
Constant	1.112	1.519	0.730
Bid	-0.006***	0.002	-2.890
Age	0.022	0.016	1.410
Gender	-0.976**	0.479	-2.040
HH size	-0.152	0.138	-1.100
Education	0.932*	0.563	1.660
House type	0.404	0.437	0.920
Occupation	1.456**	0.574	2.530
Zone	-0.288	0.555	-0.520
Lnincome	0.088	0.054	1.610
Severe	1.064**	0.511	2.080
Agreecons	-0.259	0.431	-0.600
Information	-0.144	0.305	-0.470
Volunteer	0.387**	0.166	2.330
Log likelihood	-79.775		
Prob > chi2	0.000		
Pseudo R^2	0.222		
Mean WTP (VND)	192,780		

Note: Significant at p <.1 (*), .05 (**), and .01 (***).

Finally, the total value from the restoration of the mangrove ecosystem in CBBR was calculated by multiplying mean WTP per household and the total number of households living in the CBBR in 2016. The total annual value was calculated at about VND 712.3 million, equivalent to about US$ 31,943 per year. The estimated annual benefits of mangrove restoration per hectare in the CBBR was VND 1.14 million (US$ 49.96).

7.2.4.5.WTP responses and reasons for willing and not willing to pay

Table 7.2.7 gives the main reasons for respondents' being willing or unwilling to pay. The most important reason for WTP for mangrove restoration was their worry about protection from flooding during storm seasons (38.4%). In this context, they believe that mangrove restoration activities are a good protection program (28.6%), and that for this reason it is necessary to conserve the mangrove forests of the CBBR. About 14% of the respondents believed that payment by indicating the bid level set for a respondent is reasonable approach to mangrove restoration. On the other

hand, the main reason for not being willing to pay for the restoration of mangroves was income constraints, accounting for 58.2% of the negative responses; followed by the claim that it is the responsibility of government to pay for mangrove restoration (10.0%). Five percent of the respondents did not agree to pay because they thought that the situation would be better without their contributions, and about 7.5% of respondents did not provide an answer because they did not understand the question.

Table 7.2.7. Reasons for being willing and not willing to pay

Respondent's reasons for being willing to pay	**Percent**
I think the mangrove conservation program is a good case	28.6
I think amount of money to pay is reasonable	14.0
I am concerned about the loss of biodiversity and mangroves in the CBBR	4.3
I am worried about flooding during stormy seasons	38.4
I always comply the community activities	7.4
I want to live in the fresh environment	3.0
I want to protect it for the next generations	1.3
I want the local people could aware environmental protection	2.5
I want to get the natural breeds	0.6
Total	100
Respondent's reasons for not being willing to pay	**Percent**
I do not have the financial capability to pay	58.2
I think it is the government's responsibility	10.0
I think the users should pay	14.4
I believe that the situation will be better without my contribution	5.0
I do not care for the nature conservation issues in the area	2.5
I do not understand the question	7.5
I don't know/not applicable	2.5
Total	100

7.2.4.6.Perceived benefits from mangrove ecosystem and restoration activities

Table 7.2.8 shows respondents' perceived benefits for local communities from mangrove ecosystems. Over 42% of respondents believed that the local communities have benefited from prevention of flooding, storms and soil erosion, as well as improving general environmental protection; reflecting that a predominant number of the respondents have realized the important roles of mangrove ecosystems in their livelihood. They also considered that mangrove forests help to sustain seafood resources for locals.

The results reveal that residents clearly recognize the roles of mangrove forests in their lives as the local communities are currently vulnerable to tropical storms, which appear to be more frequent now due to the impact of climate change. These results are consistent with previous studies reported by Powell, et al. [351] and Tuan, et al. [345].

Table 7.2.8. Perceived benefits from mangrove forests

Benefits from mangrove forest	Percent
1. No benefit	0.9
2. Don't know	0.9
3. Seafood provision	17.4
4. Income from selling seafood	11.3
5. Recreation	3.0
6. Forest products	2.6
7. Research/education	0.4
8. Habitat for wildlife	11.7
9. Flood and storm/soil erosion prevention/environmental protection	42.4
10. Benefit for next generation	5.9
11. Fresh air and harmonize climate	2.6
12. Protect ships, boats	0.9
Total	100

Table 7.2.9. Reasons for mangrove conservation activities

Reason	Percent
Improve sustainable local livelihood	9.4
Provide services: Supporting services	2.5
Provide services: provisioning services	6.9
Provide services: regulating services	79.3
Help protect biodiversity	1.5
Provide opportunities and benefits for future generations	0.5
Total	100

Table 7.2.9 shows that nearly 80% of total respondents agree that the most important reason for supporting conservation of the mangrove ecosystem in the CBBR is to provide a service that helps in regulating the impact of events such as storms and rising sea levels.

7.2.5. Discussion and policy implications

According to the current literature, only a few studies have employed CVM to estimate WTP for valuing mangrove forests as a non-market resource. More importantly, to the best of our knowledge, this is the first study that estimates local community WTP for mangrove restoration in relation to climate change in a biosphere reserve designated by UNESCO. In the present study, we carefully investigated whether and how socio-economic characteristics and the perceived

importance of mangrove ecosystem services among local communities influences their WTP for mangrove restoration in the biosphere reserve. This research also attempted to examine the relationships between respondent attitudes toward future climate change scenarios, and their WTP for mangrove restoration.

The findings revealed that women are likely to be paid more because they realize the important roles of mangrove forests, and they also might be engaged in mangrove restoration more than men. The results of this study can give guidelines and policy recommendations for improving the local livelihoods of female-headed households, or households without men, through participation in conservation and management activities.

The results showed that occupation significantly influenced the WTP of respondents. This was in line with a recent study conducted by Susilo, et al. [205]. However, our findings are different to those from the previous studies reported by Stone, et al. [342] and Tuan, et al. [345], that found that the socio-economic characteristics of respondents in their studies were not significant factors influencing their WTP. This may be because they conducted their studies in relatively high population density areas associated with industrial activities. Our research was conducted in the biosphere reserve of Cat Ba Island, which enjoys a relatively low population density. The results of our study also indicated that education level was found to be significantly positively related to WTP. The respondents with higher education were likely to pay more for the mangrove conservation, and to participate in mangrove restoration through mangrove plantation activities.

In addition, the findings showed that those respondents who consider the impacts of climate change seriously are willing to pay more. Interestingly, our findings suggest that the greater participation of local communities in mangrove restoration activities and enhancing their attitudes toward future climate scenarios, facilitated their appreciation of the mangrove restoration project and allowed them to contribute to the more appropriate economic valuation of mangrove ecosystems. The results confirm the importance of mangrove ecosystems for local communities in dealing with the impact of climate change and providing values not only for current and but also for future generations. Therefore, the mangrove ecosystem of the biosphere reserve must be restored and effectively managed in the context of climate change.

The residents believe that the mangrove restoration program would represent a potential household response to the climate change issue due to the significant roles of the mangrove ecosystem in their livelihoods, if the programs were to be implemented. The results were consistent with previous studies reported by Stone, et al. [342] and Tuan, et al. [345]. The residents thus realize the important role of mangroves in both livelihoods and disaster risk mitigation. Mangrove

restoration projects are expected to provide benefits and satisfaction for locals if they are implemented in the study sites. In 2015, a trial of 100 hectares of the mixture mangrove of *R. stylosa* and *A. marina* was planted, and attracted the involvement of many local community volunteers. The success of this recent trial shows the feasibility of community-based mangrove forest management. Thus, local government may be able to develop full-scale restoration plans to implement similar plantations in different restoration sites in the CBBR; recruiting community volunteers' involvement.

The mean WTP for the respondents within four villages of the CBBR was estimated at 192,780 VND (US$8.64) per year, and the total annual benefits were 712.3 million VND (US$31,943) for the villagers. Thus, the annual environmental benefits estimated in the present study were about 1,140,000 VND (US$ 49.96) per hectare, while financial support for mangrove conservation and management is set at 400,000 VND (US$ 17.95). Using these newly defined benefits, the biosphere reserve may be supported financially and technically more intensively by the government.

The main limitation of the current study is that the increase in the yes category from 100,000 VND to 200,000 VND shown in Table 7.2.5 seems to be a random error. It is noted that different bids should have been randomly assigned to respondents regardless of their income levels, so that a yes vote of about 5-10% would be optimum for the highest bid. However, the present survey did not set the proper truncation point (higher end of the yes curve). Therefore, estimated WTP is likely to have been overestimated. Nevertheless, despite the limitations caused by the present survey design, our findings may boost local livelihoods by assisting government to formulate better policies for sustainable mangrove conservation and management in the biosphere reserve.

This study also promotes the implementation of PES strategies as part of the United Nation's REDD+ program in developing countries, and thus provides support for developing regional and national "Blue Carbon" trading markets, and guiding mangrove management and conservation. Our work may also promote an increased awareness among local people on the role of mangrove restoration in the context of climate change issues, since mangrove forests are expected to contribute significantly to the reduction of climate change impacts. Through this work, local settlements can realize the requirements of a restoration plan for coexistence with natural resources, and avoid their degradation from their long-term use.

7.2.6. Conclusions

This study employed CVM to estimate the WTP for mangrove forest restoration and conservation in the CBBR, Vietnam, and to examine the factors influencing WTP for mangrove forest

restoration in the context of climate change. The estimation using the survey data on local villagers yielded a mean annual WTP at 192,780 VND (US$8.64), and 712.3 million VND (US$31,943) as the total annual benefit for the villagers in the specific study area. The findings show that gender, education level, occupation, the participation of respondents in mangrove restoration activities, and the attitude of respondents toward future climate scenarios were significant factors influencing willingness to pay and participation in the mangrove restoration project. As residents are likely to want to be involved in mangrove restoration activities, local government should consider restoration planning for suitable pilot sites in the mangrove ecosystem of the CBBR; which would in turn encourage the involvement of different stakeholders, and contribute to the ability of local communities to achieve sustainable mangrove conservation and management.

It is suggested that local government should consider the sites for restoration plans while central government should implement mangrove restoration programs (e.g. reforestation and afforestation) in the mangrove forests in the CBBR, based on our findings that local residents are willing to participate in restoration activities, and that mangrove restoration projects are expected to contribute significantly to the ability of local communities to deal with the impact of climate change.

CHAPTER 8

Summary and Future Works

8.1. Summary

8.1.1. Characteristics of mangrove species and their biomass and carbon stock estimation

The first part of current work undertaken to investigate the characteristics of specific mangrove species and estimate their AGB using ALOS PALSAR data during the year 2015 in Hai Phong city, Vietnam. This work illustrates the potential use of ALOS-2 PALSAR-2 with high sensitive mode in characterizing the distribution of mangrove species and determining the relationship between the biophysical parameters of different species and backscattering coefficients at HH and HV polarizations. The findings demonstrate that ALOS-2 PALSAR-2 can be used in estimating AGB of mangrove species using Multiple Linear Regression model. The validation results showed satisfactory correlation between model estimations and field-based measurements R^2 = 0.547 and 0.644 with RMSE = 35.5 Mg ha^{-1} and 41.3 Mg ha^{-1} for *S. caseolaris* and *K. obovata*, respectively. Although the saturation level of AGB for two mangrove species is above 100 Mg ha^{-1}, the use of L-band ALOS-2 PALSAR-2 with high sensitive mode can provide an alternative approach that may allow rapid estimation of AGB for different mangrove species in the tropics in large areas where accessibility is limited.

For second part of this work, we investigated the applicability of using ALOS-2 PALSAR-2 data with the MLPNN model for improving the AGB estimation *S. caseolaris* in the coastal area of Hai Phong city, and compared performance of the MLPNN with other machine learning algorithms. Our findings show that the MLPNN model produced more accurate biomass estimates than other machine learning models. AGB and BGB for this species were estimated from 2.78 to 298.95 Mg ha^{-1} (with an average of 55.8 Mg ha^{-1}) and 4.06 to 436.47 Mg ha^{-1}(with an average of 81.47 Mg ha-1), respectively, using leave-one-out cross-validation with an RMSE of 0.299, an MAE of 0.237, and R^2 of 0.776. The total carbon stock in the study area was estimated between

3.22 to 345.65 Mg C ha^{-1} (with an average of 64.52 Mg C ha^{-1}). We conclude that ALOS-2 PALSAR-2 can be used with MLPNN in estimating mangrove biomass and carbon stock.

8.1.2. Biomass estimation using data integration and machine learning techniques

For improvement of model performance, current work also was undertaken to investigate the applicability of the SVR (Support Vector Regression) model for estimating the AGB in a mangrove plantation with mixed mangrove species using an integration of ALOS-2 PALSAR-2 and Sentinel-2 data at the Do Son and Kien Thuy coastal area of Hai Phong city, Vietnam and compared performance of the SVR with other machine learning algorithms. Our findings show that the SVR model produced better estimations of the AGB for mangrove plantation compared to MLPNN, RBFNN, GP, and RF. The AGB of mangrove forest plantation in the study site was estimated between 36.22 and 230.14 Mg ha^{-1} (average = 87.67 Mg ha^{-1}) using LOO cross-validation with R^2 of 0.596. The findings demonstrate that an integration of ALOS-2 PALSAR-2 and Sentinel-2 data together with machine learning approach can be used for estimating the AGB of mangrove plantations associated with several mangrove species. Despite the limitations caused by the saturation of satellite signals, our findings show significant promise for the use of a combination of L-band ALOS-2 PALSAR-2 and Sentinel-2 together with machine learning techniques as an effective tool for modeling mangrove forest biomass to support the REDD+ program and blue carbon projects.

Our results show that machine learning models provide an alternative method to derive mangrove biomass in a cost-effective and practical way. The machine learning algorithms and methods used in this research can be replicated for other mangrove forest species with similar characteristics, stand structures, and other biophysical parameters. Our approach, using ALOS-2 PALSAR-2 in high sensitive mode together with machine learning algorithms, can be used as a practical guide for the preliminary design of regional and local biomass assessment in other regions of Vietnam. This research was only conducted on the mangrove forests of Hai Phong city, Vietnam. Further research is needed to determine the biomass of other mangrove species and extend this work for entire mangrove forests in Vietnam. The findings will provide useful information regarding the spatial distribution of biomass for mangrove species and their carbon stocks. The findings provide useful information and understanding of spatial distribution of AGB for different mangrove species. This will support provincial decision making on mangrove conservation and management.

The machine learning algorithms and methods used in this research can be used for other mangrove plantations consisted of several mangrove species. Our approach using an integration of

ALOS-2 PALSAR-2 and Sentinel-2 MS together with machine learning algorithms can be used as a practical guide for other mangrove forest regions of Vietnam for the regional and local levels biomass assessment. More research focusing on the integration of optical and SAR data combined with machine learning approach is needed to increase the estimation accuracy of the mangrove AGB and extend this work for entire mangrove forests of Vietnam. The findings provide useful information and understanding of the spatial distribution of the AGB in a mangrove plantation.

8.1.3. Monitoring mangrove forests change from 2010-2015

The last part of current work showed a case study for monitoring mangrove forests change in the Cat Ba Biosphere Reserve, Vietnam. Overall, mangroves areas in this area have decreased at a rate of 15% from 2010 to 2015. The statistical results of this research are important as a valuable reference to understand the current situation of mangrove forests in the Cat Ba Biosphere Reserve, Hai Phong city of Vietnam. The results show that ALOS PALSAR data and SVM classifier technique can be used to map and assess mangroves changes along the coast of the Cat Ba Biosphere Reserve, Hai Phong, while a GIS can be employed to integrate ancillary information and spatial data of the mangrove forests in order to effectively monitor mangroves in the Cat Ba Biosphere Reserve, Vietnam.

The ALOS-2 PALSAR-2 sensor used for 2015 provides higher overall accuracy and Kappa coefficient in mapping land-cover and mangrove forest than the ALOS PALSAR for 2010. The ALOS-2 PALSAR-2 produced the overall accuracy of 85% and the kappa coefficient of 0.81, compared with those of 81% and 0.77, respectively from the ALOS. Therefore, ALOS-2 PALSAR-2 with high sensitive mode should be used for mapping and monitoring mangroves on national and regional scales. This research demonstrates the potential use of ALOS PALSAR data together with a GIS-based SVM algorithm for mapping mangroves and assessing their changes in coastal zones. As mangroves can significantly contribute to mitigating climate change impacts and their ecosystem can serve the local communities with ecological and economic services, the local government of Hai Phong city should plan necessary regulations and policies to monitor and conserve mangroves of the Biosphere Reserve.

8.1.4. Mangrove Ecosystem Services Valuation and Policy Implications

The current study employed CVM to estimate the WTP for mangrove forest restoration and conservation in the CBBR, Vietnam, and to examine the factors influencing WTP in the context of climate change. The estimation using the survey data on local villagers yielded a mean WTP at 192,780 VND (US$8.64), and 712.3 million VND (US$31,943) as the total annual benefit for the

villagers in the specific study area. The findings show that gender, education level, occupation, the participation of respondents in mangrove restoration activities, and the attitude of respondents toward future climate scenarios were significant factors influencing willingness to pay and participation in the mangrove restoration project. As residents are likely to want to be involved in mangrove restoration activities, local government should consider restoration planning for suitable pilot sites in the mangrove ecosystem of the CBBR; which would in turn encourage the involvement of different stakeholders, and contribute to the ability of local communities to achieve sustainable mangrove conservation and management.

It is suggested that local government should consider the sites for restoration plans while central government should implement mangrove restoration programs (e.g. reforestation and afforestation) in the mangrove forests in the CBBR, based on our findings that local residents are willing to participate in restoration activities, and that mangrove restoration projects are expected to contribute significantly to the ability of local communities to deal with the impact of climate change.

8.2. Future works

For the future works, we intend to work on the estimation of Carbon Stocks of Mangrove Ecosystems in Xuan Thuy National Park, Vietnam using Machine Learning Techniques Combined with Remote Sensing Data and Field Measurements

8.2.1. Background of proposed research plan

A large number of studies have been conducted for estimating the AGB and below-ground biomass (BGB) of mangroves [22, 113, 114]. Several studies established their allometric equations to estimate the AGB from field measurements [115] and others using forest inventory data on as stem weights, trees height, and diameter at breast height (DBH) [112, 116]. However, a few studies have quantified above- and below-ground carbon (C) pools including soil organic C stocks, resulting in a lack of up-to-date information and statistical data on the total C stocks and potential C storage of mangrove ecosystems. Thus, development of accurate and cost-efficient models to estimate the total C budget of mangrove ecosystems is necessary to support conservation strategies in climate change mitigation programs such as the United Nations' Reducing Emissions from Deforestation and Forest Degradation (REDD+) program [353] and Blue Carbon projects [284].

Information on the C stocks of mangrove ecosystems and their spatial distribution in Vietnam is still limited. Previous studies have attempted to estimate only the AGB or the BGB of mangroves

in specific regions, such as Ca Mau Peninsula in South Vietnam [141], and Hai Phong in the North [236] However, only a few studies have been conducted to estimate the C storage of mangrove ecosystems such as in Can Gio Biosphere Reserve [354], in Ca Mau National Park [355], in the Mekong Delta [237] and Giao Lac commune of Nam Dinh city [144]. However, up-to-date no study has addressed the C stocks of mangrove ecosystems and their potential C storage using remotely sensed data despite of the fact that the remote sensing data captured for mangrove forests in Vietnam are available from both optical and SAR sensors, resulting in the limited spatial distribution of the total C stocks and C retention potential of mangrove ecosystems in Vietnam. Thus, it is necessary to quantify and assess these variables in a mangrove ecosystem using a practical and cost-effective method.

The literature review shows that methods used to estimate the C stocks of mangrove forests are diversified, from parametric model such as simple regression models [115, 144]; statistical regression models [354, 355] to sophisticated machine learning methods [98, 287]. Compared to parametric methods, machine learning algorithms have been shown to be effective for modeling mangrove biomass using satellite remotely sensed data [238] and soil organic C stocks [356, 357]. Non-parametric statistical models such as Random Forest (RF) algorithm [252], Artificial Neuron Networks (ANN) [98] and Support Vector Machines (SVM) [191] have become more common for estimating the forest biomass and soil organic C stocks with remote sensing dataset because of its potential to outperform than parametric models. Therefore, the investigation of machine learning algorithms for the estimation of the C stocks and C retention potential of mangrove ecosystems is highly necessary to support monitoring, reporting, and verification (MRV) work as part of the REDD+ program and *Blue Carbon* projects in developing nations. Previous studies show that an integration of remote sensing images and GIS may improve the accuracy of forest biomass estimation [133, 289] and soil organic C stocks [337]. However, a limited number of studies have been conducted to develop a model for estimating the C stocks of mangrove forests using an integration of optical and SAR data combined with machine learning techniques for mitigating the impacts of data saturation from these data in the estimation of mangrove C stocks. In this study, we will select an integration of SAR and optical data because SAR data such as ALOS-2 PALSAR-2 has longer wavelengths can penetrate into mangrove forest canopies while optical data such as Landsat 8 OLI or Sentinel-2A and 2B has multispectral bands, reflecting forest stand structures such as biomass volume and soil properties.

Thus, for future works we will attempt to develop a prediction model that uses machine learning techniques with an integration of optical and SAR remote sensing data together field measurements for estimating the C stocks in a mangrove ecosystem at the Xuan Thuy National Park (XTNP) of

Nam Dinh city located in the North of Vietnam. The mangroves in the XTNP are classified into natural and planted forests of which *S. caseolaris*, *K. obovata*, *A. corniculatum*, and *A. marina* are found in the northern area as natural mangrove species while *K. obovata* was dominated in the southern part as planted forests. The XTNP was declared as the first Ramsar Site of Southeast Asian since 1989 (http://www.ramsar.org). Our review of current literature shows that this is the first study that an estimation of the C stocks of mangrove ecosystems using machine learning techniques combined with remote sensing data and field measurements will be conducted for the National Park. Accordingly, a function of mangrove ecosystems in the study area can be established and it may help to elucidate the spatial distribution patterns of the total C storage in tropical and sub-tropical regions. This work also promotes the implementation of REDD+ and Payment for Ecosystem Services (PES) strategies, thus providing practical significances for developing regional and national blue carbon trading markets and guiding mangrove management and conservation.

The objectives of future works are to investigate the capability of machine learning techniques for estimating the carbon stocks in a mangrove ecosystem using a combination of satellite remote sensing data and field measurements in the XTNP of Nam Dinh city, to compare the performance of the selected machine learning techniques for the estimation of the carbon stocks in the mangrove ecosystem of XTNP, and to assess the potential carbon storage of the study site for a baseline of payment for mangrove ecosystem services. Our future works will demonstrate that the usability of remote sensing data combined with machine learning techniques for estimating carbon stocks of mangrove forests has the potential to support improved and sustainable mangrove conservation and management in the tropics.

8.2.2. Purpose of proposed research

For future works, we will propose a novel method by integration of machine learning techniques and remote sensing data to develop estimates of the C stocks of mangrove ecosystems in the XTNP, Vietnam and will provide a baseline of Payment Ecosystems Services (PES) for regional carbon trading markets of mangrove forests. The specific objectives of the future research are as follows:

1. To map and predict carbon stocks including the AGB, the BGB and soil organic carbon stocks of mangroves ecosystems using remote sensing data and field measurements;
2. To investigate the applicability of machine learning techniques and integration of optical and SAR remotely sensed data for estimating the C stocks of mangrove ecosystems;
3. To promote the implementation of PES for a mangrove ecosystem based on the willingness to pay (WTP) for sustainable mangrove ecosystem conservation and management.

8.2.3. Expected results and impacts

It is expected that my future research will provide an alternative method to derive the C stocks of mangrove ecosystems at regional and national levels in a practical and cost-effective way and can easily be replicated for other mangrove ecosystems in Vietnam. The results of my future works may promote an increased awareness of local people on the role of mangroves in the context of climate change issues. Local settlements may also realize the necessities of these plans for coexistence with natural resources and avoiding their degradation for long-term use. Mangrove Payment for Ecosystem Services are intended to improve the income of households in and around the National Park and thereby replace activities that would degrade biodiversity and natural resources. This research will assist policy makers to formulate better mangrove conservation and management policies for a national park in Vietnam.

The results will be disseminated in forms of local meetings with the participation of multiple stakeholders involved in mangrove conservation and management sectors such as local authorities of the XTNP, aquaculture companies. Importantly, the results of this research will be submitted to be considered for publications in the international journals and will be shared in the international conferences. In addition, at least one policy paper will also submitted to related organizations and counterparts for dissemination.

References

[1] M. Reichstein, M. Bahn, P. Ciais, D. Frank, M. D. Mahecha, S. I. Seneviratne, *et al.*, "Climate extremes and the carbon cycle," *Nature,* vol. 500, pp. 287-295, 08/15/print 2013.

[2] T. R. Karl and K. E. Trenberth, "Modern Global Climate Change," *Science,* vol. 302, p. 1719, 2003.

[3] P. Falkowski, R. J. Scholes, E. Boyle, J. Canadell, D. Canfield, J. Elser, *et al.*, "The Global Carbon Cycle: A Test of Our Knowledge of Earth as a System," *Science,* vol. 290, p. 291, 2000.

[4] D. M. Alongi, "Present state and future of the world's mangrove forests," *Environmental Conservation,* vol. 29, pp. 331-349, 2002.

[5] E. B. Barbier and M. Cox, "An Economic Analysis of Shrimp Farm Expansion and Mangrove Conversion in Thailand," *Land Economics,* vol. 80, pp. 391-407, 2004.

[6] F. Danielsen, M. K. Sørensen, M. F. Olwig, V. Selvam, and et al., "The Asian Tsunami: A Protective Role for Coastal Vegetation," *Science,* vol. 310, p. 643, 28 Oct 2005 2005.

[7] D. C. Donato, J. B. Kauffman, D. Murdiyarso, S. Kurnianto, M. Stidham, and M. Kanninen, "Mangroves among the most carbon-rich forests in the tropics," *Nature Geosci,* vol. 4, pp. 293-297, 05//print 2011.

[8] J. B. Kauffman, C. Heider, J. Norfolk, and F. Payton, "Carbon stocks of intact mangroves and carbon emissions arising from their conversion in the Dominican Republic," *Ecological Applications,* vol. 24, pp. 518-527, 2014/04/01 2013.

[9] P. N. Hong and H. T. San, "Mangroves of Vietnam," presented at the IUCN, Bangkok, Thailand, 1993.

[10] L. D. Tuan, T. T. K. Oanh, C. V. Thanh, and N. D. and Quy, *Can Gio Mangrove Biosphere Reserve*. Ho Chi Minh city: Agricultural Publishing house, 2002.

[11] FAO, "The World's mangroves 1980-2005. A thematic study prepared in the framework of the Global Forest Resources Assessment 2005," Food and Agriculture Organization of the United Nations, Rome ISSN 0258-6150, 2007.

[12] L. X. Tuan, Y. Munekage, Q. T. Q. Dao, N. H. Tho, and P. T. A. Dao, "Environmental Management in Mangrove Areas " *Environmental Informatics Archives,* vol. 1, pp. 38-52, 2003.

[13] NEA, "Strategies for Wetland Management in Vietnam," 2003.

[14] P. T. Dat and K. Yoshino, "Monitoring Mangrove Forest using Multi-temporal Satellite Data in the Northern Coast of Vietnam," in *The 32nd Asian Conference on Remote Sensing*, Taipei, Taiwan 2011.

[15] E. F. Lambin, "Modeling and monitoring land-cover change processes in tropical regions," *Progress in Physical Geography,* vol. 21, pp. 375-393, 1997.

[16] P. N. Hong, "Ecology of mangrove vegetation in Vietnam," Doctor, Hanoi Pedagogic University, 1991.

[17] P. N. Hong, D.V.Tan, V.T.Hien, and T.V.Thuy, *Composition and characteristics of mangrove vegetation in Giao Thuy district*: Agricultural Publishing House, 2004.

[18] Rosillo-Calle F., Groot P., Hemstock S.L, and Woods J. (2007). *The Biomass Assessment Handbook: Bioenergy for a Sustainable Environment*.

[19] D. Lu, "The potential and challenge of remote sensing-based biomass estimation," *International Journal of Remote Sensing,* vol. 27, pp. 1297-1328, 2006/04/01 2006.

[20] R. Avtar, R. Suzuki, and H. Sawada, "Natural Forest Biomass Estimation Based on Plantation Information Using PALSAR Data," *PLoS ONE,* vol. 9, p. e86121, 01/21

[21] J. M. B. Carreiras, M. J. Vasconcelos, and R. M. Lucas, "Understanding the relationship between aboveground biomass and ALOS PALSAR data in the forests of Guinea-Bissau (West Africa)," *Remote Sensing of Environment,* vol. 121, pp. 426-442, 6// 2012.

[22] Y. Hirata, R. Tabuchi, P. Patanaponpaiboon, S. Poungparn, R. Yoneda, and Y. Fujioka, "Estimation of aboveground biomass in mangrove forests using high-resolution satellite data," *Journal of Forest Research,* vol. 19, pp. 34-41, 2014/02/01 2014.

[23] O. Hamdan, H. Khali Aziz, and I. Mohd Hasmadi, "L-band ALOS PALSAR for biomass estimation of Matang Mangroves, Malaysia," *Remote Sensing of Environment,* vol. 155, pp. 69-78, 12// 2014.

[24] P. S. Roy and S. Ravan, "Biomass estimation using satellite remote sensing data—An investigation on possible approaches for natural forest," *Journal of Biosciences,* vol. 21, pp. 535-561, 1996/06/01 1996.

[25] G. Sun, K. J. Ranson, and V. I. Kharuk, "Radiometric slope correction for forest biomass estimation from SAR data in the Western Sayani Mountains, Siberia," *Remote Sensing of Environment,* vol. 79, pp. 279-287, 2// 2002.

[26] P. S. Thenkabail, N. Stucky, B. W. Griscom, M. S. Ashton, J. Diels, B. van der Meer, *et al.,* "Biomass estimations and carbon stock calculations in the oil palm plantations of African derived savannas using IKONOS data," *International Journal of Remote Sensing,* vol. 25, pp. 5447-5472, 2004/12/01 2004.

[27] D. Lu and M. Batistella, "Exploring TM image texture and its relationships with biomass estimation in Rondônia, Brazilian Amazon," *Acta Amazonica,* vol. 35, pp. 249-257, 2005.

[28] E. T. A. Mitchard, S. S. Saatchi, I. H. Woodhouse, G. Nangendo, N. S. Ribeiro, M. Williams, *et al.*, "Using satellite radar backscatter to predict above-ground woody biomass: A consistent relationship across four different African landscapes," *Geophysical Research Letters,* vol. 36, pp. n/a-n/a, 2009.

[29] H. Latifi, F. E. Fassnacht, F. Hartig, C. Berger, J. Hernández, P. Corvalán, *et al.*, "Stratified aboveground forest biomass estimation by remote sensing data," *International Journal of Applied Earth Observation and Geoinformation,* vol. 38, pp. 229-241, 6// 2015.

[30] A. M. O. Sousa, A. C. Gonçalves, P. Mesquita, and J. R. Marques da Silva, "Biomass estimation with high resolution satellite images: A case study of Quercus rotundifolia," *ISPRS Journal of Photogrammetry and Remote Sensing,* vol. 101, pp. 69-79, 3// 2015.

[31] M. K. Steininger, "Satellite estimation of tropical secondary forest above-ground biomass: Data from Brazil and Bolivia," *International Journal of Remote Sensing,* vol. 21, pp. 1139-1157, 2000/01/01 2000.

[32] O. Mutanga and A. K. Skidmore, "Narrow band vegetation indices overcome the saturation problem in biomass estimation," *International Journal of Remote Sensing,* vol. 25, pp. 3999-4014, 2004/10/01 2004.

[33] N. R. A. Jachowski, M. S. Y. Quak, D. A. Friess, D. Duangnamon, E. L. Webb, and A. D. Ziegler, "Mangrove biomass estimation in Southwest Thailand using machine learning," *Applied Geography,* vol. 45, pp. 311-321, 12// 2013.

[34] M.-H. Phua and H. Saito, "Estimation of biomass of a mountainous tropical forest using Landsat TM data," *Canadian Journal of Remote Sensing,* vol. 29, pp. 429-440, 2003/08/01 2003.

[35] Y. Wu and A. H. Strahler, "Remote Estimation of Crown Size, Stand Density, and Biomass on the Oregon Transect," *Ecological Applications,* vol. 4, pp. 299-312, 1994.

[36] S. C. Popescu, R. H. Wynne, and R. F. Nelson, "Measuring individual tree crown diameter with lidar and assessing its influence on estimating forest volume and biomass," *Canadian Journal of Remote Sensing,* vol. 29, pp. 564-577, 2003/10/01 2003.

[37] C. Song, M. B. Dickinson, L. Su, S. Zhang, and D. Yaussey, "Estimating average tree crown size using spatial information from Ikonos and QuickBird images: Across-sensor and across-site comparisons," *Remote Sensing of Environment,* vol. 114, pp. 1099-1107, 5/17/ 2010.

[38] J. Lévesque and D. J. King, "Spatial analysis of radiometric fractions from high-resolution multispectral imagery for modelling individual tree crown and forest canopy structure and health," *Remote Sensing of Environment,* vol. 84, pp. 589-602, 4/10/ 2003.

[39] C. Proisy, P. Couteron, and F. Fromard, "Predicting and mapping mangrove biomass from canopy grain analysis using Fourier-based textural ordination of IKONOS images," *Remote Sensing of Environment,* vol. 109, pp. 379-392, 8/15/ 2007.

[40] M. Palace, M. Keller, G. P. Asner, S. Hagen, and B. Braswell, "Amazon Forest Structure from IKONOS Satellite Data and the Automated Characterization of Forest Canopy Properties," *Biotropica,* vol. 40, pp. 141-150, 2008.

[41] A. Leboeuf, A. Beaudoin, R. A. Fournier, L. Guindon, J. E. Luther, and M. C. Lambert, "A shadow fraction method for mapping biomass of northern boreal black spruce forests using QuickBird imagery," *Remote Sensing of Environment,* vol. 110, pp. 488-500, 10/30/ 2007.

[42] S. A. Sader, R. B. Waide, W. T. Lawrence, and A. T. Joyce, "Tropical forest biomass and successional age class relationships to a vegetation index derived from landsat TM data," *Remote Sensing of Environment,* vol. 28, pp. 143-198, 1989/04/01 1989.

[43] D. Zheng, J. Rademacher, J. Chen, T. Crow, M. Bresee, J. Le Moine, *et al.*, "Estimating aboveground biomass using Landsat 7 ETM+ data across a managed landscape in northern Wisconsin, USA," *Remote Sensing of Environment,* vol. 93, pp. 402-411, 11/15/ 2004.

[44] A. Wijaya, S. Kusnadi, R. Gloaguen, and H. Heilmeier, "Improved strategy for estimating stem volume and forest biomass using moderate resolution remote sensing data and GIS," *Journal of Forestry Research,* vol. 21, pp. 1-12, 2010/03/01 2010.

[45] T. M. Basuki, A. K. Skidmore, P. E. van Laake, I. van Duren, and Y. A. Hussin, "The potential of spectral mixture analysis to improve the estimation accuracy of tropical forest biomass," *Geocarto International,* vol. 27, pp. 329-345, 2012/07/01 2012.

[46] G. Zhang, S. Ganguly, R. R. Nemani, M. A. White, C. Milesi, H. Hashimoto, *et al.*, "Estimation of forest aboveground biomass in California using canopy height and leaf area index estimated from satellite data," *Remote Sensing of Environment,* vol. 151, pp. 44-56, 8// 2014.

[47] X. Zhu and D. Liu, "Improving forest aboveground biomass estimation using seasonal Landsat NDVI time-series," *ISPRS Journal of Photogrammetry and Remote Sensing,* vol. 102, pp. 222-231, 4// 2015.

[48] T. Dube and O. Mutanga, "Evaluating the utility of the medium-spatial resolution Landsat 8 multispectral sensor in quantifying aboveground biomass in uMgeni catchment, South

Africa," *ISPRS Journal of Photogrammetry and Remote Sensing,* vol. 101, pp. 36-46, 3// 2015.

[49] T. Hame, A. Salli, K. Andersson, and A. Lohi, "A new methodology for the estimation of biomass of coniferdominated boreal forest using NOAA AVHRR data," *International Journal of Remote Sensing,* vol. 18, pp. 3211-3243, 1997/10/01 1997.

[50] E. Tomppo, M. Nilsson, M. Rosengren, P. Aalto, and P. Kennedy, "Simultaneous use of Landsat-TM and IRS-1C WiFS data in estimating large area tree stem volume and aboveground biomass," *Remote Sensing of Environment,* vol. 82, pp. 156-171, 9// 2002.

[51] G. M. Foody, D. S. Boyd, and M. E. J. Cutler, "Predictive relations of tropical forest biomass from Landsat TM data and their transferability between regions," *Remote Sensing of Environment,* vol. 85, pp. 463-474, 6/15/ 2003.

[52] M. Halme and E. Tomppo, "Improving the accuracy of multisource forest inventory estimates to reducing plot location error — a multicriteria approach," *Remote Sensing of Environment,* vol. 78, pp. 321-327, 12// 2001.

[53] Z. Fazakas, M. Nilsson, and H. Olsson, "Regional forest biomass and wood volume estimation using satellite data and ancillary data," *Agricultural and Forest Meteorology,* vol. 98–99, pp. 417-425, 12/31/ 1999.

[54] A. Baccini, M. A. Friedl, C. E. Woodcock, and R. Warbington, "Forest biomass estimation over regional scales using multisource data," *Geophysical Research Letters,* vol. 31, pp. n/a-n/a, 2004.

[55] G. M. Foody, M. E. Cutler, J. McMorrow, D. Pelz, H. Tangki, D. S. Boyd, *et al.*, "Mapping the biomass of Bornean tropical rain forest from remotely sensed data," *Global Ecology and Biogeography,* vol. 10, pp. 379-387, 2001.

[56] S. Liu, X. Su, S. Dong, F. Cheng, H. Zhao, X. Wu, *et al.*, "Modeling aboveground biomass of an alpine desert grassland with SPOT-VGT NDVI," *GIScience & Remote Sensing,* vol. 52, pp. 680-699, 2015/11/02 2015.

[57] D. Lu, P. Mausel, E. Brondízio, and E. Moran, "Relationships between forest stand parameters and Landsat TM spectral responses in the Brazilian Amazon Basin," *Forest Ecology and Management,* vol. 198, pp. 149-167, 8/23/ 2004.

[58] T. Dube and O. Mutanga, "Investigating the robustness of the new Landsat-8 Operational Land Imager derived texture metrics in estimating plantation forest aboveground biomass in resource constrained areas," *ISPRS Journal of Photogrammetry and Remote Sensing,* vol. 108, pp. 12-32, 10// 2015.

[59] N. Ahmadian, S. Ghasemi, J.-P. Wigneron, and R. Zölitz, "Comprehensive study of the biophysical parameters of agricultural crops based on assessing Landsat 8 OLI and Landsat 7 ETM+ vegetation indices," *GIScience & Remote Sensing*, vol. 53, pp. 337-359, 2016/05/03 2016.

[60] J. R. Jensen, *Introductory Digital Image Processing: A Remote Sensing Perspective* New York: Prentice-Hall, Inc.: Saddle River, 1996.

[61] D. S. Boyd, "The relationship between the biomass of Cameroonian tropical forests and radiation reflected in middle infrared wavelengths (3.0-5.0 mu m)," *International Journal of Remote Sensing*, vol. 20, pp. 1017-1023, 1999/01/01 1999.

[62] P. M. Barbosa, D. Stroppiana, J.-M. Grégoire, and J. M. Cardoso Pereira, "An assessment of vegetation fire in Africa (1981–1991): Burned areas, burned biomass, and atmospheric emissions," *Global Biogeochemical Cycles*, vol. 13, pp. 933-950, 1999.

[63] F. Yan, B. Wu, and Y. Wang, "Estimating spatiotemporal patterns of aboveground biomass using Landsat TM and MODIS images in the Mu Us Sandy Land, China," *Agricultural and Forest Meteorology*, vol. 200, pp. 119-128, 1/15/ 2015.

[64] J. Dong, R. K. Kaufmann, R. B. Myneni, C. J. Tucker, P. E. Kauppi, J. Liski, *et al.*, "Remote sensing estimates of boreal and temperate forest woody biomass: carbon pools, sources, and sinks," *Remote Sensing of Environment*, vol. 84, pp. 393-410, 3// 2003.

[65] S. Sinha, C. Jeganathan, L. K. Sharma, and M. S. Nathawat, "A review of radar remote sensing for biomass estimation," *International Journal of Environmental Science and Technology*, vol. 12, pp. 1779-1792, 2015/05/01 2015.

[66] F. M. Henderson and A. J. Lewis, *Principles and applications of imaging radar. Manual of remote sensing*, 3rd edition ed. vol. Vol 2: Wiley, 1998.

[67] T. Le Toan, S. Quegan, I. Woodward, M. Lomas, N. Delbart, and G. Picard, "Relating Radar Remote Sensing of Biomass to Modelling of Forest Carbon Budgets," *Climatic Change*, vol. 67, pp. 379-402, 2004.

[68] E. E. Sano, L. G. Ferreira, and A. R. Huete, "Synthetic Aperture Radar (L band) and Optical Vegetation Indices for Discriminating the Brazilian Savanna Physiognomies: A Comparative Analysis," *Earth Interactions*, vol. 9, pp. 1-15, 2005/09/01 2005.

[69] S. Englhart, V. Keuck, and F. Siegert, "Aboveground biomass retrieval in tropical forests — The potential of combined X- and L-band SAR data use," *Remote Sensing of Environment*, vol. 115, pp. 1260-1271, 2011.

[70] L. Sarker, J. Nichol, and A. Mubin, "Potential of Multiscale Texture Polarization Ratio of C-band SAR for Forest Biomass Estimation," in *Developments in Multidimensional Spatial*

Data Models, A. Abdul Rahman, P. Boguslawski, C. Gold, and M. N. Said, Eds., ed: Springer Berlin Heidelberg, 2013, pp. 69-83.

[71] K. Thumaty, R. Fararoda, S. Middinti, R. Gopalakrishnan, C. S. Jha, and V. K. Dadhwal, "Estimation of Above Ground Biomass for Central Indian Deciduous Forests Using ALOS PALSAR L-Band Data," *Journal of the Indian Society of Remote Sensing*, pp. 1-9, 2015/07/28 2015.

[72] G. Sandberg, L. M. H. Ulander, J. E. S. Fransson, J. Holmgren, and T. Le Toan, "L- and P-band backscatter intensity for biomass retrieval in hemiboreal forest," *Remote Sensing of Environment*, vol. 115, pp. 2874-2886, 11/15/ 2011.

[73] F. F. Gama, J. R. Dos Santos, and J. C. Mura, "Eucalyptus Biomass and Volume Estimation Using Interferometric and Polarimetric SAR Data," *Remote Sensing*, vol. 2, p. 939, 2010.

[74] V. R. Kubota, T. Yoneda, T. Okuda, and W. R. Kadir, "Suitability of Interferometric Synthetic Aperture Radar (IFSAR) for biomass estimation in a selectively logged tropical rainforest in Peninsular Malaysia," *Tropics*, vol. 24, pp. 101-111, 2015.

[75] N. Ghasemi, M. R. Sahebi, and M. A., "A review on biomass estimation methods using synthetic aperture radar data," *International Journal of Geomatics & Geosciences*, vol. 1, pp. 776-788, 2011.

[76] A. Luckman, J. Baker, T. M. Kuplich, C. da Costa Freitas Yanasse, and A. C. Frery, "A study of the relationship between radar backscatter and regenerating tropical forest biomass for spaceborne SAR instruments," *Remote Sensing of Environment*, vol. 60, pp. 1-13, 4// 1997.

[77] L. Kurvonen, J. Pulliainen, and M. Hallikainen, "Retrieval of biomass in boreal forests from multitemporal ERS-1 and JERS-1 SAR images," *Geoscience and Remote Sensing, IEEE Transactions on*, vol. 37, pp. 198-205, 1999.

[78] K. J. Ranson and S. Guoqing, "Mapping biomass of a northern forest using multifrequency SAR data," *Geoscience and Remote Sensing, IEEE Transactions on*, vol. 32, pp. 388-396, 1994.

[79] T. Le Toan, A. Beaudoin, J. Riom, and D. Guyon, "Relating forest biomass to SAR data," *Geoscience and Remote Sensing, IEEE Transactions on*, vol. 30, pp. 403-411, 1992.

[80] H. H. Shugart, S. Saatchi, and F. G. Hall, "Importance of structure and its measurement in quantifying function of forest ecosystems," *Journal of Geophysical Research: Biogeosciences*, vol. 115, pp. n/a-n/a, 2010.

[81] FAO, "GTOS: biomass assessment of the status of the development of the standards for the terrestrial essential climate variables," Rome, Italy2009.

[82] K. J. Ranson, G. Sun, J. F. Weishampel, and R. G. Knox, "Forest biomass from combined ecosystem and radar backscatter modeling," *Remote Sensing of Environment,* vol. 59, pp. 118-133, 1// 1997.

[83] R. M. Lucas, N. Cronin, M. Moghaddam, A. Lee, J. Armston, P. Bunting, *et al.*, "Integration of radar and Landsat-derived foliage projected cover for woody regrowth mapping, Queensland, Australia," *Remote Sensing of Environment,* vol. 100, pp. 388-406, 2006.

[84] T. M. Kuplich, V. Salvatori, and P. J. Curran, "JERS-1/SAR backscatter and its relationship with biomass of regenerating forests," *International Journal of Remote Sensing,* vol. 21, pp. 2513-2518, 2000/01/01 2000.

[85] J. E. S. Fransson, G. Smith, J. Askne, and H. Olsson, "Stem volume estimation in boreal forests using ERS-1/2 coherence and SPOT XS optical data," *International Journal of Remote Sensing,* vol. 22, pp. 2777-2791, 2001/01/01 2001.

[86] J. R. Santos, M. S. P. Lacruz, L. S. Araujo, and M. Keil, "Savanna and tropical rainforest biomass estimation and spatialization using JERS-1 data," *International Journal of Remote Sensing,* vol. 23, pp. 1217-1229, 2002/01/01 2002.

[87] J. M. Austin, B. G. Mackey, and K. P. Van Niel, "Estimating forest biomass using satellite radar: an exploratory study in a temperate Australian Eucalyptus forest," *Forest Ecology and Management,* vol. 176, pp. 575-583, 3/17/ 2003.

[88] C. S. Jha, M. Rangaswamy, N. Vyjayanthi, and M. S. R. Murthy, "Estimation of forest biomass using Envisat-ASAR data," 2006, pp. 641002-641002-8.

[89] P. Hyde, R. Dubayah, W. Walker, J. B. Blair, M. Hofton, and C. Hunsaker, "Mapping forest structure for wildlife habitat analysis using multi-sensor (LiDAR, SAR/InSAR, ETM+, Quickbird) synergy," *Remote Sensing of Environment,* vol. 102, pp. 63-73, 5/30/ 2006.

[90] K. Navulur. (2007). *Multispectral Image Analysis Using the Object-Oriented Paradigm*. Available: http://www.taylorandfrancis.com

[91] J. Amini and J. Tetuko Sri Sumantyo, "Employing a Method on SAR and Optical Images for Forest Biomass Estimation," *Geoscience and Remote Sensing, IEEE Transactions on,* vol. 47, pp. 4020-4026, 2009.

[92] Y. Yu, S. Saatchi, L. S. Heath, E. LaPoint, R. Myneni, and Y. Knyazikhin, "Regional distribution of forest height and biomass from multisensor data fusion," *Journal of Geophysical Research: Biogeosciences,* vol. 115, pp. n/a-n/a, 2010.

[93] V. Alappat, A. Joshi, and Y. V. N. Krishnamurthy, "Tropical Dry Deciduous Forest Stand Variable Estimation Using SAR Data," *Journal of the Indian Society of Remote Sensing*, vol. 39, pp. 583-589, 2011/12/01 2011.

[94] O. Antropov, Y. Rauste, H. Ahola, and T. Hame, "Stand-Level Stem Volume of Boreal Forests From Spaceborne SAR Imagery at L-Band," *Selected Topics in Applied Earth Observations and Remote Sensing, IEEE Journal of*, vol. 6, pp. 35-44, 2013.

[95] N. Ghasemi, M. R. Sahebi, and A. Mohammadzadeh, "Biomass Estimation of a Temperate Deciduous Forest Using Wavelet Analysis," *Geoscience and Remote Sensing, IEEE Transactions on*, vol. 51, pp. 765-776, 2013.

[96] T. Hame, J. Kilpi, H. A. Ahola, Y. Rauste, O. Antropov, M. Rautiainen, *et al.*, "Improved Mapping of Tropical Forests With Optical and SAR Imagery, Part I: Forest Cover and Accuracy Assessment Using Multi-Resolution Data," *Selected Topics in Applied Earth Observations and Remote Sensing, IEEE Journal of*, vol. 6, pp. 74-91, 2013.

[97] T. D. Pham and K. Yoshino, "Aboveground biomass estimation of mangrove species using ALOS-2 PALSAR imagery in Hai Phong City, Vietnam," *Journal of Applied Remote Sensing*, vol. 11, pp. 026010-026010, 2017.

[98] T. D. Pham, K. Yoshino, and D. T. Bui, "Biomass estimation of Sonneratia caseolaris (l.) Engler at a coastal area of Hai Phong city (Vietnam) using ALOS-2 PALSAR imagery and GIS-based multi-layer perceptron neural networks," *GIScience & Remote Sensing*, vol. 54, pp. 329-353, 2017/05/04 2017.

[99] J. Pulliainen, M. Engdahl, and M. Hallikainen, "Feasibility of multi-temporal interferometric SAR data for stand-level estimation of boreal forest stem volume," *Remote Sensing of Environment*, vol. 85, pp. 397-409, 6/15/ 2003.

[100] J. R. Santos, T. Neeff, L. V. Dutra, L. S. Araujo, F. F. Gama, and M. A. T. Elmiro. (2004, 2015 Nov 27). Tropical forest biomass mapping from dual frequency SAR interferemetry (X and P-Bands). *VII- WG VII/3*, 1133-1136. Available: http://www.isprs.org/proceedings/XXXV/congress/comm7/papers/216.pdf

[101] R. M. Lucas, N. Cronin, A. Lee, M. Moghaddam, C. Witte, and P. Tickle, "Empirical relationships between AIRSAR backscatter and LiDAR-derived forest biomass, Queensland, Australia," *Remote Sensing of Environment*, vol. 100, pp. 407-425, 2/15/ 2006.

[102] M. Neumann, "Remote sensing of vegetation using multi-baseline polarimetric SAR interferometry: theoretical modeling and physical parameter retrieval," PhD, Berlin University of Technology, Germany, 2009.

[103] M. Wollersheim, M. J. Collins, and D. Leckie, "Estimating boreal forest species type with airborne polarimetric synthetic aperture radar," *International Journal of Remote Sensing*, vol. 32, pp. 2481-2505, 2011/05/05 2011.

[104] A. Peregon and Y. Yamagata, "The use of ALOS/PALSAR backscatter to estimate above-ground forest biomass: A case study in Western Siberia," *Remote Sensing of Environment*, vol. 137, pp. 139-146, 10// 2013.

[105] T. Mette, K. Papathanassiou, and I. Hajnsek, "Biomass estimation from polarimetric SAR interferometry over heterogeneous forest terrain," in *Geoscience and Remote Sensing Symposium, 2004. IGARSS '04. Proceedings. 2004 IEEE International*, 2004, pp. 511-514.

[106] D. B. Clark and D. A. Clark, "Landscape-scale variation in forest structure and biomass in a tropical rain forest," *Forest Ecology and Management*, vol. 137, pp. 185-198, 10/15/ 2000.

[107] G. Grimsditch, J. Alder, T. Nakamura, R. Kenchington, and J. Tamelander, "The blue carbon special edition – Introduction and overview," *Ocean & Coastal Management*, vol. 83, pp. 1-4, 10// 2013.

[108] J. Howard, S. Hoyt, K. Isensee, E. Pidgeon, and M. Telszewski, "Coastal Blue Carbon: Methods for assessing carbon stocks and emissions factors in mangroves, tidal salt marshes, and seagrass meadows," Conservation International, Intergovernmental Oceanographic Commission of UNESCO. , International Union for Conservation of Nature. Arlington, Virginia, USA.2014.

[109] B. F. Clough and K. Scott, "Allometric relationships for estimating above-ground biomass in six mangrove species," *Forest Ecology and Management*, vol. 27, pp. 117-127, 1989/05/01 1989.

[110] O. Jin-Eong, G. W. Khoon, and B. F. Clough, "Structure and Productivity of a 20-Year-Old Stand of Rhizophora apiculata Bl. Mangrove Forest," *Journal of Biogeography*, vol. 22, pp. 417-424, 1995.

[111] B. F. Clough, P. Dixon, and O. Dalhaus, "Allometric Relationships for Estimating Biomass in Multi-stemmed Mangrove Trees," *Australian Journal of Botany*, vol. 45, pp. 1023-1031, 1997.

[112] A. Komiyama, V. Jintana, T. Sangtiean, and S. Kato, "A common allometric equation for predicting stem weight of mangroves growing in secondary forests," *Ecological Research*, vol. 17, pp. 415-418, 2002.

[113] A. Komiyama, J. E. Ong, and S. Poungparn, "Allometry, biomass, and productivity of mangrove forests: A review," *Aquatic Botany*, vol. 89, pp. 128-137, 2008.

[114] S. Tamai, T. Nakasuga, R. Tabuchi, and K. Ogino, "Standing Biomass of Mangrove Forests in Southern Thailand," *JOURNAL OF THE JAPANESE FORESTRY SOCIETY*, vol. 68, pp. 384-388, 1986.

[115] J. Chave, C. Andalo, S. Brown, M. A. Cairns, J. Q. Chambers, D. Eamus, *et al.*, "Tree allometry and improved estimation of carbon stocks and balance in tropical forests," *Oecologia*, vol. 145, pp. 87-99, 2005/08/01 2005.

[116] A. Komiyama, S. Poungparn, and S. Kato, "Common allometric equations for estimating the tree weight of mangroves," *Journal of Tropical Ecology*, vol. 21, pp. 471-477, 2005.

[117] M. Ross, P. Ruiz, G. Telesnicki, and J. Meeder, "Estimating above-ground biomass and production in mangrove communities of Biscayne National Park, Florida (U.S.A.)," *Wetlands Ecology and Management*, vol. 9, pp. 27-37, 2001/02/01 2001.

[118] A. Ellison, "Macroecology of mangroves: large-scale patterns and processes in tropical coastal forests," *Trees*, vol. 16, pp. 181-194, 2002/03/01 2002.

[119] E. Mougin, C. Proisy, G. Marty, F. Fromard, H. Puig, J. L. Betoulle, *et al.*, "Multifrequency and multipolarization radar backscattering from mangrove forests," *Geoscience and Remote Sensing, IEEE Transactions on*, vol. 37, pp. 94-102, 1999.

[120] C. Proisy, E. Mougin, F. Fromard, and M. A. Karam, "Interpretation of Polarimetric Radar Signatures of Mangrove Forests," *Remote Sensing of Environment*, vol. 71, pp. 56-66, 2000.

[121] W. Takeuchi, D. V. Tien, V. T. Phuong, A. N. Van, and K. S. Oo, "Above ground biomass mapping of mangrove forest in Vietnam by ALOS PALSAR," in *Synthetic Aperture Radar (APSAR), 2011 3rd International Asia-Pacific Conference on*, 2011, pp. 1-3.

[122] T. D. Vu, W. Takeuchi, and N. A. Van, "Carbon Stock Calculating and Forest Change Assessment Toward REDD+ Activities for The Mangrove Forest in Vietnam," *TRANSACTIONS OF THE JAPAN SOCIETY FOR AERONAUTICAL AND SPACE SCIENCES, AEROSPACE TECHNOLOGY JAPAN*, vol. 12, pp. Pn_23-Pn_31, 2014.

[123] NOAA. (2015, 4 Dec 2015). *LIDAR—Light Detection and Ranging—is a remote sensing method used to examine the surface of the Earth.* Available: http://oceanservice.noaa.gov/facts/lidar.html

[124] M. A. Lefsky, W. B. Cohen, G. G. Parker, and D. J. Harding, "Lidar Remote Sensing for Ecosystem Studies: Lidar, an emerging remote sensing technology that directly measures the three-dimensional distribution of plant canopies, can accurately estimate vegetation structural attributes and should be of particular interest to forest, landscape, and global ecologists," *BioScience*, vol. 52, pp. 19-30, January 1, 2002 2002.

[125] C. J. Gleason and J. Im, "A Review of Remote Sensing of Forest Biomass and Biofuel: Options for Small-Area Applications," *GIScience & Remote Sensing*, vol. 48, pp. 141-170, 2011/04/01 2011.

[126] M. Simard, K. Zhang, V. H. Rivera-Monroy, M. S. Ross, P. L. Ruiz, E. Castañeda-Moya, *et al.*, "Mapping height and biomass of mangrove forests in Everglades National Park with SRTM elevation data," *Photogrammetric Engineering & Remote Sensing*, vol. 72, pp. 299-311, 2006.

[127] D. A. Zimble, D. L. Evans, G. C. Carlson, R. C. Parker, S. C. Grado, and P. D. Gerard, "Characterizing vertical forest structure using small-footprint airborne LiDAR," *Remote Sensing of Environment*, vol. 87, pp. 171-182, 10/15/ 2003.

[128] M. Nilsson, "Estimation of tree heights and stand volume using an airborne lidar system," *Remote Sensing of Environment*, vol. 56, pp. 1-7, 4// 1996.

[129] T. E. Fatoyinbo, M. Simard, R. A. Washington-Allen, and H. H. Shugart, "Landscape-scale extent, height, biomass, and carbon estimation of Mozambique's mangrove forests with Landsat ETM+ and Shuttle Radar Topography Mission elevation data," *Journal of Geophysical Research: Biogeosciences*, vol. 113, pp. n/a-n/a, 2008.

[130] S. J. Lee, J. R. Kim, and Y. S. Choi, "The extraction of forest CO2 storage capacity using high-resolution airborne lidar data," *GIScience & Remote Sensing*, vol. 50, pp. 154-171, 2013/04/01 2013.

[131] D. R. Unger, I. K. Hung, R. Brooks, and H. Williams, "Estimating number of trees, tree height and crown width using Lidar data," *GIScience & Remote Sensing*, vol. 51, pp. 227-238, 2014/05/04 2014.

[132] S. G. Zolkos, S. J. Goetz, and R. Dubayah, "A meta-analysis of terrestrial aboveground biomass estimation using lidar remote sensing," *Remote Sensing of Environment*, vol. 128, pp. 289-298, 1/21/ 2013.

[133] D. Lu, Q. Chen, G. Wang, L. Liu, G. Li, and E. Moran, "A survey of remote sensing-based aboveground biomass estimation methods in forest ecosystems," *International Journal of Digital Earth*, vol. 9, pp. 63-105, 2016/01/02 2016.

[134] M. Sibanda, O. Mutanga, and M. Rouget, "Comparing the spectral settings of the new generation broad and narrow band sensors in estimating biomass of native grasses grown under different management practices," *GIScience & Remote Sensing*, vol. 53, pp. 614-633, 2016/09/02 2016.

[135] S. Luo, C. Wang, X. Xi, F. Pan, D. Peng, J. Zou, *et al.*, "Fusion of airborne LiDAR data and hyperspectral imagery for aboveground and belowground forest biomass estimation," *Ecological Indicators*, vol. 73, pp. 378-387, 2// 2017.

[136] Y. Mazda, M. Magi, M. Kogo, and P. N. Hong, "Mangroves as a coastal protection from waves in the Tong King delta, Vietnam," *Mangroves and Salt Marshes*, vol. 1, pp. 127-135, 1997.

[137] Y. Mazda, M. Magi, Y. Ikeda, T. Kurokawa, and T. Asano, "Wave reduction in a mangrove forest dominated by Sonneratia sp," *Wetlands Ecology and Management*, vol. 14, pp. 365-378, 2006/08/01 2006.

[138] R. McNally, A. McEwin, and T. Holland, "The Potential for Mangrove Carbon Projects in Vietnam," 2011.

[139] T. N. K. D. Binh, Vromant, N., Hung, N.T., Hens, L., Boon, E.K., "Land cover changes between 1968 and 2003 in Cai Nuoc, Ca Mau Peninsula, Vietnam," *Environment, Development and Sustainability*, vol. 7, pp. 519-536, 2005.

[140] V. Tran Thi, A. Tien Thi Xuan, H. Phan Nguyen, F. Dahdouh-Guebas, and N. Koedam, "Application of remote sensing and GIS for detection of long-term mangrove shoreline changes in Mui Ca Mau, Vietnam," *Biogeosciences*, vol. 11, pp. 3781-3795, 2014.

[141] S. Nguyen-Thanh, C. Chi-Farn, C. Ni-Bin, C. Cheng-Ru, C. Ly-Yu, and T. Bui-Xuan, "Mangrove Mapping and Change Detection in Ca Mau Peninsula, Vietnam, Using Landsat Data and Object-Based Image Analysis," *Selected Topics in Applied Earth Observations and Remote Sensing, IEEE Journal of*, vol. 8, pp. 503-510, 2015.

[142] P. Tien Dat and K. Yoshino, "Mangrove analysis using ALOS imagery in Hai Phong City, Vietnam," pp. 85250U-85250U, 2012.

[143] T. D. Pham and K. Yoshino, "Mangrove Mapping and Change Detection Using Multi-temporal Landsat imagery in Hai Phong city, Vietnam," in *International Symposium on Cartography in Internet and Ubiquitous Environments 2015*, The University of Tokyo, Japan, 2015.

[144] H. T. Nguyen, R. Yoneda, I. Ninomiya, K. Harada, T. V. Dao, T. M. Sy, *et al.*, "The effects of stand-age and inundation on carbon accumulation in mangrove plantation soil in Namdinh, Northern Vietnam," *Tropics*, vol. 14, pp. 21-37, 2004.

[145] W. Takeuchi, T. Dien Vu, P. Vu Tan, V. An Ngoc, and O. Kyaw San, "Above ground biomass mapping of mangrove forest in Vietnam by ALOS PALSAR," in *Synthetic Aperture Radar (APSAR), 2011 3rd International Asia-Pacific Conference on*, 2011, pp. 1-3.

[146] M. A. Gilabert, C. Conese, and F. Maselli, "An atmospheric correction method for the automatic retrieval of surface reflectances from TM images," *International Journal of Remote Sensing,* vol. 15, pp. 2065-2086, 1994/07/10 1994.

[147] Y. Kawata, S. Ueno, and T. Kusaka, "Radiometric correction for atmospheric and topographic effects on Landsat MSS images," *International Journal of Remote Sensing,* vol. 9, pp. 729-748, 1988/04/01 1988.

[148] S. Kobayashi and K. Sanga-Ngoie, "The integrated radiometric correction of optical remote sensing imageries," *International Journal of Remote Sensing,* vol. 29, pp. 5957-5985, 2008/10/20 2008.

[149] Z. Gu, X. Shi, L. Li, D. Yu, L. Liu, and W. Zhang, "Using multiple radiometric correction images to estimate leaf area index," *International Journal of Remote Sensing,* vol. 32, pp. 9441-9454, 2011/12/20 2011.

[150] Q. Xu, Z. Hou, and T. Tokola, "Relative radiometric correction of multi-temporal ALOS AVNIR-2 data for the estimation of forest attributes," *ISPRS Journal of Photogrammetry and Remote Sensing,* vol. 68, pp. 69-78, 3// 2012.

[151] X. Pons, L. Pesquer, J. Cristóbal, and O. González-Guerrero, "Automatic and improved radiometric correction of Landsat imagery using reference values from MODIS surface reflectance images," *International Journal of Applied Earth Observation and Geoinformation,* vol. 33, pp. 243-254, 12// 2014.

[152] D. H. Hoekman and J. Reiche, "Multi-model radiometric slope correction of SAR images of complex terrain using a two-stage semi-empirical approach," *Remote Sensing of Environment,* vol. 156, pp. 1-10, 1// 2015.

[153] C. M. Chance, T. Hermosilla, N. C. Coops, M. A. Wulder, and J. C. White, "Effect of topographic correction on forest change detection using spectral trend analysis of Landsat pixel-based composites," *International Journal of Applied Earth Observation and Geoinformation,* vol. 44, pp. 186-194, 2// 2016.

[154] B. Holben and C. Justice, "An examination of spectral band ratioing to reduce the topographic effect on remotely sensed data," *International Journal of Remote Sensing,* vol. 2, pp. 115-133, 1981/04/01 1981.

[155] C. O. Justice, S. W. Wharton, and B. N. Holben, "Application of digital terrain data to quantify and reduce the topographic effect on Landsat data," *International Journal of Remote Sensing,* vol. 2, pp. 213-230, 1981/07/01 1981.

[156] C. Conese, G. Maracchi, and F. Maselli, "Improvement in Maximum Likelihood Classification performance on highly rugged terrain using Principal Components

Analysis," *International Journal of Remote Sensing,* vol. 14, pp. 1371-1382, 1993/05/01 1993.

[157] S. Hantson and E. Chuvieco, "Evaluation of different topographic correction methods for Landsat imagery," *International Journal of Applied Earth Observation and Geoinformation,* vol. 13, pp. 691-700, 10// 2011.

[158] M.-L. Gao, W.-J. Zhao, Z.-N. Gong, H.-L. Gong, Z. Chen, and X.-M. Tang, "Topographic Correction of ZY-3 Satellite Images and Its Effects on Estimation of Shrub Leaf Biomass in Mountainous Areas," *Remote Sensing,* vol. 6, p. 2745, 2014.

[159] M. J. Soja, G. Sandberg, and L. M. H. Ulander, "Topographic correction for biomass retrieval from P-band SAR data in boreal forests," in *Geoscience and Remote Sensing Symposium (IGARSS), 2010 IEEE International*, 2010, pp. 4776-4779.

[160] S. J. Walsh, J. W. Cooper, I. E. Von Essen, and K. R. Gallager, "Image enhancement of Landsat Thematic Mapper data and GIS data integration for evaluation of resource characteristics," *Photogrammetric Engineering and Remote Sensing,* vol. 56, pp. 1135–1141, 1990 1990.

[161] D. A. Yocky, "Multiresolution Wavelet Decomposition I me Merger of Landsat Thematic Mapper and SPOT Panchromatic Data," *Photogrammetric Engineering & Remote Sensing*, vol. 62, pp. 1067-1074, 1996.

[162] B. Garguet-Duport, J. Girel, J.-M. Chassery, and G. Patou, "The use of multiresolution analysis and wavelets transform for merging SPOT panchromatic and multispectral image data," *Photogrammetric Engineering and remote sensing*, vol. 62, pp. 1057-1066, 1996.

[163] M. Shaban and O. Dikshit, "Evaluation of the merging of SPOT multispectral and panchromatic data for classification of an urban environment," *International Journal of Remote Sensing*, vol. 23, pp. 249-262, 2002.

[164] T. M. Basuki, A. K. Skidmore, Y. A. Hussin, and I. Van Duren, "Estimating tropical forest biomass more accurately by integrating ALOS PALSAR and Landsat-7 ETM+ data," *International Journal of Remote Sensing,* vol. 34, pp. 4871-4888, 2013/07/10 2013.

[165] J. L. Dungan, "Toward a Comprehensive View of Uncertainty in Remote Sensing Analysis," in *Uncertainty in Remote Sensing and GIS*, ed: John Wiley & Sons, Ltd, 2006, pp. 25-35.

[166] M. A. Friedl, K. C. McGwire, and D. K. McIver, "An overview of uncertainty in optical remotely sensed data for ecological applications.," in *Spatial Uncertainty in Ecology: Implications for Remote Sensing and GIS Applications*, C. T. Hunsaker, M. F. Goodchild, M. A. Friedl, and T. J. Case, Eds., ed NewYork: Springer, 2001, pp. 258–283.

[167] B. Deepika, K. Avinash, and K. S. Jayappa, "Shoreline change rate estimation and its forecast: remote sensing, geographical information system and statistics-based approach," *International Journal of Environmental Science and Technology,* vol. 11, pp. 395-416, 2014/03/01 2014.

[168] T. D. Pham and K. Yoshino, "Impacts of mangrove management systems on mangrove changes in the Northern Coast of Vietnam," *Tropics,* vol. 24, pp. 141-151, 2016.

[169] ACTMANG, "Mangrove plantation of ACTMANG (Action for Mangrove Reforestation, Japan) in Vietnam " 2006.

[170] S. Attarchi and R. Gloaguen, "Improving the Estimation of Above Ground Biomass Using Dual Polarimetric PALSAR and ETM+ Data in the Hyrcanian Mountain Forest (Iran)," *Remote Sensing,* vol. 6, p. 3693, 2014.

[171] T. Tachikawa, M. Kaku, A. Iwasaki, D. B. Gesch, M. J. Oimoen, Z. Zhang, *et al.*, "ASTER global digital elevation model version 2-summary of validation results," NASA2011.

[172] X. Hu and Q. Weng, "Estimating impervious surfaces from medium spatial resolution imagery using the self-organizing map and multi-layer perceptron neural networks," *Remote Sensing of Environment,* vol. 113, pp. 2089-2102, 2009/10/01/ 2009.

[173] D. Tien Bui, B. Pradhan, O. Lofman, I. Revhaug, and O. B. Dick, "Landslide susceptibility assessment in the Hoa Binh province of Vietnam: A comparison of the Levenberg-Marquardt and Bayesian regularized neural networks," *Geomorphology,* vol. 171–172, pp. 12–29, 2012.

[174] J. F. Mas, "Mapping land use/cover in a tropical coastal area using satellite sensor data, GIS and artificial neural networks," *Estuarine, Coastal and Shelf Science,* vol. 59, pp. 219-230, 2004.

[175] D. L. Civco, "Artificial neural networks for land-cover classification and mapping," *International journal of geographical information systems,* vol. 7, pp. 173-186, 1993/03/01 1993.

[176] S. Haykin, *Neural Networks: A Comprehensive Foundation (2nd Edition)*. Upper Saddle River, NJ, USA: Prentice Hall, 1998.

[177] H. Drucker, C. J. Burges, L. Kaufman, A. J. Smola, and V. Vapnik, "Support vector regression machines," in *Advances in neural information processing systems*, 1997, pp. 155-161.

[178] A. J. Smola and B. Schölkopf, "A tutorial on support vector regression," *Statistics and computing,* vol. 14, pp. 199-222, 2004.

[179] D. Tien Bui, B. Pradhan, O. Lofman, and I. Revhaug, "Landslide Susceptibility Assessment in Vietnam Using Support Vector Machines, Decision Tree, and Naïve Bayes Models," *Mathematical Problems in Engineering,* vol. 2012, p. 26, 2012.

[180] D. Tien Bui, T. A. Tuan, H. Klempe, B. Pradhan, and I. Revhaug, "Spatial prediction models for shallow landslide hazards: a comparative assessment of the efficacy of support vector machines, artificial neural networks, kernel logistic regression, and logistic model tree," *Landslides,* vol. 13, pp. 361-378, 2016.

[181] B. T. Pham, D. Tien Bui, M. B. Dholakia, I. Prakash, and H. V. Pham, "A Comparative Study of Least Square Support Vector Machines and Multiclass Alternating Decision Trees for Spatial Prediction of Rainfall-Induced Landslides in a Tropical Cyclones Area," *Geotechnical and Geological Engineering,* pp. 1-18, 2016.

[182] G. P. Petropoulos, C. Kalaitzidis, and K. Prasad Vadrevu, "Support vector machines and object-based classification for obtaining land-use/cover cartography from Hyperion hyperspectral imagery," *Computers & Geosciences,* 2011.

[183] G. P. Petropoulos, K. Arvanitis, and N. Sigrimis, "Hyperion hyperspectral imagery analysis combined with machine learning classifiers for land use/cover mapping," *Expert Systems with Applications,* 2011.

[184] A. Okujeni, S. van der Linden, L. Tits, B. Somers, and P. Hostert, "Support vector regression and synthetically mixed training data for quantifying urban land cover," *Remote Sensing of Environment,* vol. 137, pp. 184-197, 2013/10/01/ 2013.

[185] C. Wu, H. Shen, A. Shen, J. Deng, M. Gan, J. Zhu, *et al.*, "Comparison of machine-learning methods for above-ground biomass estimation based on Landsat imagery," *Journal of Applied Remote Sensing,* vol. 10, pp. 035010-035010, 2016.

[186] C. Wu, H. Tao, M. Zhai, Y. Lin, K. Wang, J. Deng, *et al.*, "Using nonparametric modeling approaches and remote sensing imagery to estimate ecological welfare forest biomass," *Journal of Forestry Research,* May 11 2017.

[187] G. Mountrakis, J. Im, and C. Ogole, "Support vector machines in remote sensing: A review," *ISPRS Journal of Photogrammetry and Remote Sensing,* vol. 66, pp. 247-259, 2011/05/01/ 2011.

[188] S. S. Durbha, R. L. King, and N. H. Younan, "Support vector machines regression for retrieval of leaf area index from multiangle imaging spectroradiometer," *Remote Sensing of Environment,* vol. 107, pp. 348-361, 2007/03/15/ 2007.

[189] J. Verrelst, J. Muñoz, L. Alonso, J. Delegido, J. P. Rivera, G. Camps-Valls, *et al.*, "Machine learning regression algorithms for biophysical parameter retrieval: Opportunities for Sentinel-2 and-3," *Remote Sensing of Environment,* vol. 118, pp. 127-139, 2012.

[190] V. Vapnik, *The nature of statistical learning theory*: Springer science & business media, 2013.

[191] P. M. López-Serrano, C. A. López-Sánchez, J. G. Álvarez-González, and J. García-Gutiérrez, "A Comparison of Machine Learning Techniques Applied to Landsat-5 TM Spectral Data for Biomass Estimation," *Canadian Journal of Remote Sensing,* vol. 42, pp. 690-705, 2016/11/01 2016.

[192] L. Breiman, "Random forests," *Machine Learning,* vol. 45, pp. 5-32, Oct 2001.

[193] D. R. Cutler, T. C. Edwards, K. H. Beard, A. Cutler, K. T. Hess, J. Gibson, *et al.*, "RANDOM FORESTS FOR CLASSIFICATION IN ECOLOGY," *Ecology,* vol. 88, pp. 2783-2792, 2007.

[194] C. Pelletier, S. Valero, J. Inglada, N. Champion, and G. Dedieu, "Assessing the robustness of Random Forests to map land cover with high resolution satellite image time series over large areas," *Remote Sensing of Environment,* vol. 187, pp. 156-168, 2016/12/15/ 2016.

[195] J. Friedman, T. Hastie, and R. Tibshirani, *The elements of statistical learning* vol. 1: Springer series in statistics New York, 2001.

[196] O. Mutanga, E. Adam, and M. A. Cho, "High density biomass estimation for wetland vegetation using WorldView-2 imagery and random forest regression algorithm," *International Journal of Applied Earth Observation and Geoinformation,* vol. 18, pp. 399-406, 2012/08/01/ 2012.

[197] V. F. Rodriguez-Galiano, B. Ghimire, J. Rogan, M. Chica-Olmo, and J. P. Rigol-Sanchez, "An assessment of the effectiveness of a random forest classifier for land-cover classification," *ISPRS Journal of Photogrammetry and Remote Sensing,* vol. 67, pp. 93-104, 2012/01/01/ 2012.

[198] C. E. Rasmussen and C. K. Williams, *Gaussian processes for machine learning* vol. 1: MIT press Cambridge, 2006.

[199] J. Verrelst, C. van der Tol, F. Magnani, N. Sabater, J. P. Rivera, G. Mohammed, *et al.*, "Evaluating the predictive power of sun-induced chlorophyll fluorescence to estimate net photosynthesis of vegetation canopies: A SCOPE modeling study," *Remote Sensing of Environment,* vol. 176, pp. 139-151, 2016/04/01/ 2016.

[200] M. Campos-Taberner, F. J. García-Haro, G. Camps-Valls, G. Grau-Muedra, F. Nutini, A. Crema, *et al.*, "Multitemporal and multiresolution leaf area index retrieval for operational

local rice crop monitoring," *Remote Sensing of Environment,* vol. 187, pp. 102-118, 2016/12/15/ 2016.

[201] C. Zhang, D. Robinson, J. Wang, J. Liu, X. Liu, and L. Tong, "Factors Influencing Farmers' Willingness to Participate in the Conversion of Cultivated Land to Wetland Program in Sanjiang National Nature Reserve, China," *Environmental Management,* vol. 47, pp. 107-120, 2011.

[202] B. Alves, R. Rigall-I-Torrent, R. Ballester, J. Benavente, and Ó. Ferreira, "Coastal erosion perception and willingness to pay for beach management (Cadiz, Spain)," *Journal of Coastal Conservation,* vol. 19, pp. 269-280, 2015.

[203] R. Brouwer, S. Brouwer, M. A. Eleveld, M. Verbraak, A. J. Wagtendonk, and H. J. van der Woerd, "Public willingness to pay for alternative management regimes of remote marine protected areas in the North Sea," *Marine Policy,* vol. 68, pp. 195-204, 6// 2016.

[204] J. C. Trujillo, B. Carrillo, C. A. Charris, and R. A. Velilla, "Coral reefs under threat in a Caribbean marine protected area: Assessing divers' willingness to pay toward conservation," *Marine Policy,* vol. 68, pp. 146-154, 6// 2016.

[205] H. Susilo, Y. Takahashi, and M. Yabe, "Evidence for Mangrove Restoration in the Mahakam Delta, Indonesia, Based on Households' Willingness to Pay," *2017,* vol. 9, 2017-02-13 2017.

[206] R. C. Mitchell and R. T. Carson, *Using surveys to value public goods: the contingent valuation method*: Resources for the Future, 1989.

[207] J. Cooper and J. Loomis, "Sensitivity of willingness-to-pay estimates to bid design in dichotomous choice contingent valuation models," *Land economics,* pp. 211-224, 1992.

[208] D. McFadden, "Contingent Valuation and Social Choice," *American Journal of Agricultural Economics,* vol. 76, pp. 689-708, 1994.

[209] I. J. Bateman, I. H. Langford, A. P. Jones, and G. N. Kerr, "Bound and path effects in double and triple bounded dichotomous choice contingent valuation," *Resource and Energy Economics,* vol. 23, pp. 191-213, 7// 2001.

[210] R. T. Carson, N. E. Flores, and N. F. Meade, "Contingent Valuation: Controversies and Evidence," *Environmental and Resource Economics,* vol. 19, pp. 173-210, 2001.

[211] B. G. Long and T. D. Skewes, "A Technique for Mapping Mangroves with Landsat TM Satellite Data and Geographic Information System," *Estuarine, Coastal and Shelf Science,* vol. 43, pp. 373-381, 1996.

[212] V. Pasqualini, J. Iltis, N. Dessay, M. Lointier, O. Guelorget, and L. Polidori, "Mangrove mapping in North-Western Madagascar using SPOT-XS and SIR-C radar data," *Hydrobiologia,* vol. 413, pp. 127-133, 1999.

[213] G. Conchedda, L. Durieux, and P. Mayaux, "An object-based method for mapping and change analysis in mangrove ecosystems," *ISPRS Journal of Photogrammetry and Remote Sensing,* vol. 63, pp. 578-589, 9// 2008.

[214] S. Nandy and S. Kushwaha, "Study on the utility of IRS 1D LISS-III data and the classification techniques for mapping of Sunderban mangroves," *Journal of Coastal Conservation,* vol. 15, pp. 123-137, 2011.

[215] J. B. Long and C. Giri, "Mapping the Philippines' Mangrove Forests Using Landsat Imagery," *Sensors,* vol. 11, pp. 2972-2981, 2011.

[216] R. M. Lucas, A. L. Mitchell, A. Rosenqvist, C. Proisy, A. Melius, and C. Ticehurst, "The potential of L-band SAR for quantifying mangrove characteristics and change: case studies from the tropics," *Aquatic Conservation: Marine and Freshwater Ecosystems,* vol. 17, pp. 245-264, 2007.

[217] Y. Zhu, K. Liu, L. Liu, S. Wang, and H. Liu, "Retrieval of Mangrove Aboveground Biomass at the Individual Species Level with WorldView-2 Images," *Remote Sensing,* vol. 7, p. 12192, 2015.

[218] T. D. Pham, K. Yoshino, and D. T. Bui, "Biomass estimation of Sonneratia caseolaris (l.) Engler at a coastal area of Hai Phong city (Vietnam) using ALOS-2 PALSAR imagery and GIS-based multi-layer perceptron neural networks," *GIScience & Remote Sensing,* pp. 1-25, 2016.

[219] JAXA, "ALOS-2/PALSAR-2 Level 1.1/1.5/2.1/3.1 CEOS SAR Product " Japan Aerospace Exploration Agency May 23, 2014 2014.

[220] M. R. de Leeuw and L. M. T. de Carvalho, "Performance evaluation of several adaptive speckle filters for SAR imaging," *Anais XIV Simpósio Brasileiro de Sensoriamento Remoto,* pp. 7299-7305, 2009.

[221] Y. Wang and M. L. Imhoff, "Simulated and observed L-HH radar backscatter from tropical mangrove forests," *International Journal of Remote Sensing,* vol. 14, pp. 2819-2828, 1993/10/01 1993.

[222] Y. Wang, L. L. Hess, S. Filoso, and J. M. Melack, "Understanding the radar backscattering from flooded and nonflooded Amazonian forests: Results from canopy backscatter modeling," *Remote Sensing of Environment,* vol. 54, pp. 324-332, 1995/12/01 1995.

[223] N. H. Phan and D. T. Vu, "The role of mangroves in mitigating natural disasters," 2007.

[224] J. W. Fourqurean, B. Johnson, J. B. Kauffman, H. Kennedy, C. Lovelock, and N. Saintilan. (2014, 2015/01/6). *Field sampling of vegetative carbon pools in coastal ecosystems*.

[225] R. Lucas, J. Armston, R. Fairfax, R. Fensham, A. Accad, J. Carreiras, *et al.*, "An Evaluation of the ALOS PALSAR L-Band Backscatter - Above Ground Biomass Relationship Queensland, Australia: Impacts of Surface Moisture Condition and Vegetation Structure," *Selected Topics in Applied Earth Observations and Remote Sensing, IEEE Journal of,* vol. 3, pp. 576-593, 2010.

[226] A. W. Moore, "Cross-validation for detecting and preventing overfitting," *School of Computer Science Carneigie Mellon University,* 2001.

[227] H. Viana, J. Aranha, D. Lopes, and W. B. Cohen, "Estimation of crown biomass of Pinus pinaster stands and shrubland above-ground biomass using forest inventory data, remotely sensed imagery and spatial prediction models," *Ecological Modelling,* vol. 226, pp. 22-35, 2/10/ 2012.

[228] K. B. Byrd, J. L. O'Connell, S. Di Tommaso, and M. Kelly, "Evaluation of sensor types and environmental controls on mapping biomass of coastal marsh emergent vegetation," *Remote Sensing of Environment,* vol. 149, pp. 166-180, 6// 2014.

[229] S. Darmawan, W. Takeuchi, Y. Vetrita, G. Winarso, K. Wikantika, and D. K. Sari, "Characterization of mangrove forest types based on ALOS-PALSAR in overall Indonesian archipelago," *IOP Conference Series: Earth and Environmental Science,* vol. 20, p. 012051, 2014.

[230] M. Marchand, "Mangrove restoration in Vietnam: Key considerations and a practical guide," Deltares2008.

[231] R. M. Lucas, P. Bunting, D. Clewley, C. Proisy, P. W. M. Souza Filho, K. Viergever, *et al.*, "Characterisation and monitoring of mangroves using ALOS PALSAR data," 2009.

[232] M. N. Khan, R. Suwa, and A. Hagihara, "Biomass and aboveground net primary production in a subtropical mangrove stand of Kandelia obovata (S., L.) Yong at Manko Wetland, Okinawa, Japan," *Wetlands Ecology and Management,* vol. 17, pp. 585-599, 2009/12/01 2009.

[233] D. A. Freedman, *Statistical models: theory and practice*: cambridge university press, 2009.

[234] N. C. Duke, J.-O. Meynecke, S. Dittmann, A. M. Ellison, K. Anger, U. Berger, *et al.*, "A World Without Mangroves?," *Science,* vol. 317, pp. 41-42, July 6, 2007 2007.

[235] P. Tien Dat and K. Yoshino, "Impacts of mangrove management systems on mangrove changes in the Northern Coast of Vietnam," *Tropics,* vol. 24, 2016.

[236] P. Tien Dat and Y. Kunihiko, "Characterization of mangrove species using ALOS-2 PALSAR in Hai Phong city, Vietnam," *IOP Conference Series: Earth and Environmental Science,* vol. 37, p. 012036, 2016.

[237] V. N. Nam, S. D. Sasmito, D. Murdiyarso, J. Purbopuspito, and R. A. MacKenzie, "Carbon stocks in artificially and naturally regenerated mangrove ecosystems in the Mekong Delta," *Wetlands Ecology and Management,* vol. 24, pp. 231-244, 2016.

[238] L. Wang, J. L. Silván-Cárdenas, and W. P. Sousa, "Neural Network Classification of Mangrove Species from Multi-seasonal Ikonos Imagery," *Photogrammetric Engineering & Remote Sensing,* vol. 74, pp. 921-927, // 2008.

[239] B. W. Heumann, "Satellite remote sensing of mangrove forests: Recent advances and future opportunities," *Progress in Physical Geography,* vol. 35, pp. 87-108, February 1, 2011 2011.

[240] M. Hall, E. Frank, G. Holmes, B. Pfahringer, P. Reutemann, and I. H. Witten, "The WEKA data mining software: an update," *SIGKDD Explor. Newsl.,* vol. 11, pp. 10-18, 2009.

[241] F. Pedregosa, G. Varoquaux, A. Gramfort, V. Michel, B. Thirion, O. Grisel, *et al.*, "Scikit-learn: Machine learning in Python," *Journal of Machine Learning Research,* vol. 12, pp. 2825-2830, 2011.

[242] M. Valipour, M. E. Banihabib, and S. M. R. Behbahani, "Comparison of the ARMA, ARIMA, and the autoregressive artificial neural network models in forecasting the monthly inflow of Dez dam reservoir," *Journal of Hydrology,* vol. 476, pp. 433-441, 1/7/ 2013.

[243] M. Valipour, "Optimization of neural networks for precipitation analysis in a humid region to detect drought and wet year alarms," *Meteorological Applications,* vol. 23, pp. 91-100, 2016.

[244] M. Valipour, "Sprinkle and trickle irrigation system design using tapered pipes for pressure loss adjusting," *Journal of Agricultural Science,* vol. 4, p. 125, 2012.

[245] M. Valipour, M. A. G. Sefidkouhi, and S. Eslamian, "Surface irrigation simulation models: a review," *International Journal of Hydrology Science and Technology,* vol. 5, pp. 51-70, 2015.

[246] M. Mahdizadeh Khasraghi, M. A. Gholami Sefidkouhi, and M. Valipour, "Simulation of open- and closed-end border irrigation systems using SIRMOD," *Archives of Agronomy and Soil Science,* vol. 61, pp. 929-941, 2015/07/03 2015.

[247] P. N. Hong, H. T. San, and P. T. A. and Dao, "The role of mangrove ecosystem in the environment and the life of people in coastal mangrove areas," in *Proceedings of the*

national workshop on"Socio-economic status of women in coastal mangrove areas - Trends to improve their lives and environment", Hanoi, 1998, pp. 13-46.

[248] M. Shimada, O. Isoguchi, T. Tadono, and K. Isono, "PALSAR Radiometric and Geometric Calibration," *Geoscience and Remote Sensing, IEEE Transactions on,* vol. 47, pp. 3915-3932, 2009.

[249] S. Darmawan, W. Takeuchi, Y. Vetrita, K. Wikantika, and D. K. Sari, "Impact of Topography and Tidal Height on ALOS PALSAR Polarimetric Measurements to Estimate Aboveground Biomass of Mangrove Forest in Indonesia," *Journal of Sensors,* vol. 2015, p. 13, 2015.

[250] C. Beh Boon, M. Z. M. Jafri, and S. Lim Hwee, "Mangrove mapping in Penang Island by using Artificial Neural Network technique," in *Open Systems (ICOS), 2011 IEEE Conference on*, 2011, pp. 245-249.

[251] X. Yu, H.-b. Shao, and X.-h. a. Z. Liu, D.-z, "Applying Neural Network Classification to Obtain Mangrove Landscape Characteristics for Monitoring the Travel Environment Quality on the Beihai Coast of Guangxi, P. R. China," *CLEAN – Soil, Air, Water,* vol. 38, pp. 289-295, 2010.

[252] S. Sasikala, S. Appavu alias Balamurugan, and S. Geetha, "Multi Filtration Feature Selection (MFFS) to improve discriminatory ability in clinical data set," *Applied Computing and Informatics*, 2014.

[253] O. Şenkal and T. Kuleli, "Estimation of solar radiation over Turkey using artificial neural network and satellite data," *Applied Energy,* vol. 86, pp. 1222-1228, 7// 2009.

[254] T. Chai and R. R. Draxler, "Root mean square error (RMSE) or mean absolute error (MAE)?–Arguments against avoiding RMSE in the literature," *Geoscientific Model Development,* vol. 7, pp. 1247-1250, 2014.

[255] D. Tien Bui, B. Pradhan, H. Nampak, T. Quang Bui, Q.-A. Tran, and Q. P. Nguyen, "Hybrid Artificial Intelligence Approach Based on Neural Fuzzy Inference Model and Metaheuristic Optimization for Flood Susceptibility Modelling in A High-Frequency Tropical Cyclone Area using GIS," *Journal of Hydrology*, vol. 540, pp. 317-330, 2016.

[256] W. Zucchini, "An Introduction to Model Selection," *Journal of Mathematical Psychology,* vol. 44, pp. 41-61, 3// 2000.

[257] G. Claeskens and N. L. Hjort, *Model selection and model averaging* vol. 330: Cambridge University Press Cambridge, 2008.

[258] C. J. Schwarz, "Sampling, regression, experimental design and analysis for environmental scientists, biologists, and resource managers," *Department of Statistics and Actuarial Science, Simon Fraser University,* vol. 57, 2011.

[259] K. P. Burnham and D. R. Anderson, "Multimodel inference understanding AIC and BIC in model selection," *Sociological methods & research,* vol. 33, pp. 261-304, 2004.

[260] K. P. Burnham, D. R. Anderson, and K. P. Huyvaert, "AIC model selection and multimodel inference in behavioral ecology: some background, observations, and comparisons," *Behavioral Ecology and Sociobiology,* vol. 65, pp. 23-35, 2011.

[261] E. K. Kelloway, *Using Mplus for structural equation modeling: a researcher's guide*: Sage Publications, 2014.

[262] G. Vaglio Laurin, Q. Chen, J. A. Lindsell, D. A. Coomes, F. D. Frate, L. Guerriero, *et al.*, "Above ground biomass estimation in an African tropical forest with lidar and hyperspectral data," *ISPRS Journal of Photogrammetry and Remote Sensing,* vol. 89, pp. 49-58, 3// 2014.

[263] C. Ibanez, B. Carcellar III, E. Paringit, R. Argamosa, R. Faelga, M. Posilero, *et al.*, "Estimating Dbh of Trees Employing Multiple Linear Regression of the best Lidar-Derived Parameter Combination Automated in Python in a Natural Broadleaf Forest in the Philippines," *ISPRS-International Archives of the Photogrammetry, Remote Sensing and Spatial Information Sciences,* pp. 657-662, 2016.

[264] S. G. Tesfamichael and C. Beech, "Combining Akaike's Information Criterion and discrete return LiDAR data to estimate structural attributes of savanna woody vegetation," *Journal of Arid Environments,* vol. 129, pp. 25-34, 6// 2016.

[265] M. S. Wisz, R. J. Hijmans, J. Li, A. T. Peterson, C. H. Graham, A. Guisan, *et al.*, "Effects of sample size on the performance of species distribution models," *Diversity and Distributions,* vol. 14, pp. 763-773, 2008.

[266] M. J. Patel, A. Khalaf, and H. J. Aizenstein, "Studying depression using imaging and machine learning methods," *NeuroImage: Clinical,* vol. 10, pp. 115-123, // 2016.

[267] K. Were, D. Tien Bui, Ø. B. Dick, and B. R. Singh, "A comparative assessment of support vector regression, artificial neural networks, and random forests for predicting and mapping soil organic carbon stocks across an Afromontane landscape," *Ecological Indicators,* vol. 52, pp. 394-403, 2015.

[268] A. Smola and V. Vapnik, "Support vector regression machines," *Advances in neural information processing systems,* vol. 9, pp. 155-161, 1997.

[269] N.-D. Hoang, D. Tien Bui, and K.-W. Liao, "Groutability estimation of grouting processes with cement grouts using Differential Flower Pollination Optimized Support Vector Machine," *Applied Soft Computing,* vol. 45, pp. 173-186, 8// 2016.

[270] T. Chen and H. Chen, "Approximation capability to functions of several variables, nonlinear functionals, and operators by radial basis function neural networks," *IEEE Transactions on Neural Networks,* vol. 6, pp. 904-910, 1995.

[271] H. Hong, C. Xu, I. Revhaug, and D. Tien Bui, "Spatial Prediction of Landslide Hazard at the Yihuang Area (China): A Comparative Study on the Predictive Ability of Backpropagation Multi-layer Perceptron Neural Networks and Radial Basic Function Neural Networks," in *Cartography - Maps Connecting the World*, C. Robbi Sluter, C. B. Madureira Cruz, and P. M. Leal de Menezes, Eds., ed Cham, Switzerland: Springer International Publishing, 2015, pp. 175-188.

[272] B. Scholkopf, K.-K. Sung, C. J. Burges, F. Girosi, P. Niyogi, T. Poggio, *et al.*, "Comparing support vector machines with Gaussian kernels to radial basis function classifiers," *IEEE transactions on Signal Processing,* vol. 45, pp. 2758-2765, 1997.

[273] O. Hamdan, M. R. Khairunnisa, A. A. Ammar, I. M. Hasmadi, and H. K. Aziz, "MANGROVE CARBON STOCK ASSESSMENT BY OPTICAL SATELLITE IMAGERY," *Journal of Tropical Forest Science,* vol. 25, pp. 554-565, 2013.

[274] T. Dube, O. Mutanga, A. Elhadi, and R. Ismail, "Intra-and-Inter Species Biomass Prediction in a Plantation Forest: Testing the Utility of High Spatial Resolution Spaceborne Multispectral RapidEye Sensor and Advanced Machine Learning Algorithms," *Sensors,* vol. 14, p. 15348, 2014.

[275] I. Ali, F. Greifeneder, J. Stamenkovic, M. Neumann, and C. Notarnicola, "Review of Machine Learning Approaches for Biomass and Soil Moisture Retrievals from Remote Sensing Data," *Remote Sensing,* vol. 7, p. 15841, 2015.

[276] İ. Güneralp, A. M. Filippi, and J. Randall, "Estimation of floodplain aboveground biomass using multispectral remote sensing and nonparametric modeling," *International Journal of Applied Earth Observation and Geoinformation,* vol. 33, pp. 119-126, 12// 2014.

[277] J. Carreiras, J. Melo, and M. Vasconcelos, "Estimating the Above-Ground Biomass in Miombo Savanna Woodlands (Mozambique, East Africa) Using L-Band Synthetic Aperture Radar Data," *Remote Sensing,* vol. 5, p. 1524, 2013.

[278] S. Shataee Joibary, "Forest Attributes Estimation Using Aerial Laser Scanner and TM Data," *2013,* vol. 22, p. 13, 2013-12-01 2013.

[279] J. E. Anderson, L. C. Plourde, M. E. Martin, B. H. Braswell, M.-L. Smith, R. O. Dubayah, *et al.*, "Integrating waveform lidar with hyperspectral imagery for inventory of a northern temperate forest," *Remote Sensing of Environment,* vol. 112, pp. 1856-1870, 4/15/ 2008.

[280] D. M. Alongi, "Carbon sequestration in mangrove forests," *Carbon Management,* vol. 3, pp. 313-322, 2012/06/01 2012.

[281] C. Giri and J. Muhlhausen, "Mangrove Forest Distributions and Dynamics in Madagascar (1975–2005)," *Sensors,* vol. 8, pp. 2104-2117, 2008.

[282] D. R. Richards and D. A. Friess, "Rates and drivers of mangrove deforestation in Southeast Asia, 2000–2012," *Proceedings of the National Academy of Sciences,* vol. 113, pp. 344-349, 2016.

[283] L. Pendleton, D. C. Donato, B. C. Murray, S. Crooks, W. A. Jenkins, S. Sifleet, *et al.*, "Estimating Global "Blue Carbon" Emissions from Conversion and Degradation of Vegetated Coastal Ecosystems," *PLoS ONE,* vol. 7, p. e43542, 09/04

[284] N. Ahmed and M. Glaser, "Coastal aquaculture, mangrove deforestation and blue carbon emissions: Is REDD+ a solution?," *Marine Policy,* vol. 66, pp. 58-66, 4// 2016.

[285] F. Rocha de Souza Pereira, M. Kampel, and M. Cunha-Lignon, "Mapping of mangrove forests on the southern coast of São Paulo, Brazil, using synthetic aperture radar data from ALOS/PALSAR," *Remote Sensing Letters,* vol. 3, pp. 567-576, 2012/12/10 2011.

[286] Y. Maeda, A. Fukushima, Y. Imai, Y. Tanahashi, E. Nakama, S. Ohta, *et al.*, "ESTIMATING CARBON STOCK CHANGES OF MANGROVE FORESTS USING SATELLITE IMAGERY AND AIRBORNE LiDAR DATA IN THE SOUTH SUMATRA STATE, INDONESIA," *ISPRS-International Archives of the Photogrammetry, Remote Sensing and Spatial Information Sciences,* pp. 705-709, 2016.

[287] L. T. H. Pham and L. Brabyn, "Monitoring mangrove biomass change in Vietnam using SPOT images and an object-based approach combined with machine learning algorithms," *ISPRS Journal of Photogrammetry and Remote Sensing,* vol. 128, pp. 86-97, 6// 2017.

[288] X. Huang, L. Zhang, and L. Wang, "Evaluation of Morphological Texture Features for Mangrove Forest Mapping and Species Discrimination Using Multispectral IKONOS Imagery," *IEEE Geoscience and Remote Sensing Letters,* vol. 6, pp. 393-397, 2009.

[289] J. Goh, J. Miettinen, A. S. Chia, P. T. Chew, and S. C. Liew, "Biomass estimation in humid tropical forest using a combination of ALOS PALSAR and SPOT 5 satellite imagery," *Asian Journal of Geoinformatics,* vol. 13, 2014.

[290] H. Nemmour and Y. Chibani, "Multiple support vector machines for land cover change detection: An application for mapping urban extensions," *ISPRS Journal of Photogrammetry and Remote Sensing,* vol. 61, pp. 125-133, 11// 2006.

[291] P. T. Dat and K. Yoshino, "Comparing Mangrove Forest Management in Hai Phong City, Vietnam towards Sustainable Aquaculture," *Procedia Environmental Sciences,* vol. 17, pp. 109-118, 2013.

[292] M. Drusch, U. Del Bello, S. Carlier, O. Colin, V. Fernandez, F. Gascon, *et al.*, "Sentinel-2: ESA's Optical High-Resolution Mission for GMES Operational Services," *Remote Sensing of Environment,* vol. 120, pp. 25-36, 5/15/ 2012.

[293] S. Manna, S. Nandy, A. Chanda, A. Akhand, S. Hazra, and V. K. Dadhwal, "Estimating aboveground biomass in Avicennia marina plantation in Indian Sundarbans using high-resolution satellite data," *Journal of Applied Remote Sensing,* vol. 8, pp. 083638-083638, 2014.

[294] J. B. Kauffman, H. Hernandez Trejo, M. del Carmen Jesus Garcia, C. Heider, and W. M. Contreras, "Carbon stocks of mangroves and losses arising from their conversion to cattle pastures in the Pantanos de Centla, Mexico," *Wetlands Ecology and Management,* vol. 24, pp. 203-216, 2016.

[295] P. Wicaksono, P. Danoedoro, Hartono, and U. Nehren, "Mangrove biomass carbon stock mapping of the Karimunjawa Islands using multispectral remote sensing," *International Journal of Remote Sensing,* vol. 37, pp. 26-52, 2016/01/02 2016.

[296] N. Patel and A. Majumdar, "Biomass estimation of Shorea robusta with principal component analysis of satellite data," *Journal of Forestry Research,* vol. 21, pp. 469-474, 2010.

[297] C. J. Tucker, "Red and photographic infrared linear combinations for monitoring vegetation," *Remote Sensing of Environment,* vol. 8, pp. 127-150, 1979/05/01 1979.

[298] J. W. Rouse Jr, R. Haas, J. Schell, and D. Deering, "Monitoring vegetation systems in the Great Plains with ERTS," 1974.

[299] Z. Jiang, A. R. Huete, K. Didan, and T. Miura, "Development of a two-band enhanced vegetation index without a blue band," *Remote Sensing of Environment,* vol. 112, pp. 3833-3845, 10/15/ 2008.

[300] A. R. Huete, "A soil-adjusted vegetation index (SAVI)," *Remote Sensing of Environment,* vol. 25, pp. 295-309, 1988/08/01 1988.

[301] J. Qi, A. Chehbouni, A. R. Huete, Y. H. Kerr, and S. Sorooshian, "A modified soil adjusted vegetation index," *Remote Sensing of Environment,* vol. 48, pp. 119-126, 1994/05/01 1994.

[302] A. J. Richardson and J. H. Everitt, "Using spectral vegetation indices to estimate rangeland productivity," *Geocarto International,* vol. 7, pp. 63-69, 1992/03/01 1992.

[303] B. W. Heumann, "An Object-Based Classification of Mangroves Using a Hybrid Decision Tree—Support Vector Machine Approach," *Remote Sensing,* vol. 3, pp. 2440-2460, 2011.

[304] S. K. Singh, P. K. Srivastava, M. Gupta, J. K. Thakur, and S. Mukherjee, "Appraisal of land use/land cover of mangrove forest ecosystem using support vector machine," *Environmental Earth Sciences,* vol. 71, pp. 2245-2255, 2014.

[305] K. Kanniah, A. Sheikhi, A. Cracknell, H. Goh, K. Tan, C. Ho, *et al.*, "Satellite Images for Monitoring Mangrove Cover Changes in a Fast Growing Economic Region in Southern Peninsular Malaysia," *Remote Sensing,* vol. 7, p. 14360, 2015.

[306] P. Zhao, D. Lu, G. Wang, L. Liu, D. Li, J. Zhu, *et al.*, "Forest aboveground biomass estimation in Zhejiang Province using the integration of Landsat TM and ALOS PALSAR data," *International Journal of Applied Earth Observation and Geoinformation,* vol. 53, pp. 1-15, 12// 2016.

[307] A. Aslan, A. F. Rahman, M. W. Warren, and S. M. Robeson, "Mapping spatial distribution and biomass of coastal wetland vegetation in Indonesian Papua by combining active and passive remotely sensed data," *Remote Sensing of Environment,* vol. 183, pp. 65-81, 9/15/ 2016.

[308] P. Zhao, D. Lu, G. Wang, C. Wu, Y. Huang, and S. Yu, "Examining Spectral Reflectance Saturation in Landsat Imagery and Corresponding Solutions to Improve Forest Aboveground Biomass Estimation," *Remote Sensing,* vol. 8, p. 469, 2016.

[309] Y. Su, Q. Guo, B. Xue, T. Hu, O. Alvarez, S. Tao, *et al.*, "Spatial distribution of forest aboveground biomass in China: Estimation through combination of spaceborne lidar, optical imagery, and forest inventory data," *Remote Sensing of Environment,* vol. 173, pp. 187-199, 2// 2016.

[310] X. Tian, Z. Li, Z. Su, E. Chen, C. van der Tol, X. Li, *et al.*, "Estimating montane forest above-ground biomass in the upper reaches of the Heihe River Basin using Landsat-TM data," *International Journal of Remote Sensing,* vol. 35, pp. 7339-7362, 2014/11/02 2014.

[311] C. Giri, E. Ochieng, L. L. Tieszen, Z. Zhu, A. Shingh, and T. Loveland, "Status and distribution of mangrove forests of the world using earth observation satellite data," *Global Ecology and Biogeography,* vol. 20, pp. 154-159, 2011.

[312] P. H. S. Tong, Y. Auda, J. Populus, M. Aizpuru, A. A. Habshi, and F. Blasco, "Assessment from space of mangroves evolution in the Mekong Delta, in relation to extensive shrimp

farming," *International Journal of Remote Sensing,* vol. 25, pp. 4795-4812, 2004/11/01 2004.

[313] P. M. Thu and J. Populus, "Status and changes of mangrove forest in Mekong Delta: Case study in Tra Vinh, Vietnam," *Estuarine, Coastal and Shelf Science,* vol. 71, pp. 98-109, 2007.

[314] L. X. Tran and A. Fischer, "Spatiotemporal changes and fragmentation of mangroves and its effects on fish diversity in Ca Mau Province (Vietnam)," *Journal of Coastal Conservation,* pp. 1-14, 2017.

[315] M. Béland, K. Goïta, F. Bonn, and T. T. H. Pham, "Assessment of land-cover changes related to shrimp aquaculture using remote sensing data: a case study in the Giao Thuy District, Vietnam," *International Journal of Remote Sensing,* vol. 27, pp. 1491-1510, 2006/04/01 2006.

[316] Q. Vo, N. Oppelt, P. Leinenkugel, and C. Kuenzer, "Remote Sensing in Mapping Mangrove Ecosystems — An Object-Based Approach," *Remote Sensing,* vol. 5, pp. 183-201, 2013.

[317] J. Rogan, J. Franklin, D. Stow, J. Miller, C. Woodcock, and D. Roberts, "Mapping land-cover modifications over large areas: A comparison of machine learning algorithms," *Remote Sensing of Environment,* vol. 112, pp. 2272-2283, 5/15/ 2008.

[318] C. Kamusoko, J. Gamba, and H. Murakami, "Mapping Woodland Cover in the Miombo Ecosystem: A Comparison of Machine Learning Classifiers," *Land,* vol. 3, p. 524, 2014.

[319] G. P. Petropoulos, C. Kalaitzidis, and K. Prasad Vadrevu, "Support vector machines and object-based classification for obtaining land-use/cover cartography from Hyperion hyperspectral imagery," *Computers & Geosciences,* vol. 41, pp. 99-107, 4// 2012.

[320] M. Ustuner, F. B. Sanli, and B. Dixon, "Application of Support Vector Machines for Landuse Classification Using High-Resolution RapidEye Images: A Sensitivity Analysis," *European Journal of Remote Sensing,* vol. 48, pp. 403-422, 2015/01/01 2015.

[321] T. Mai and C. Smith, "Addressing the threats to tourism sustainability using systems thinking: a case study of Cat Ba Island, Vietnam," *Journal of Sustainable Tourism,* vol. 23, pp. 1504-1528, 2015/11/26 2015.

[322] T. Le Viet, M. Choisy, J. E. Bryant, D. Vu Trong, T. Pham Quang, P. Horby, *et al.*, "A dengue outbreak on a floating village at Cat Ba Island in Vietnam," *BMC Public Health,* vol. 15, pp. 1-8, 2015.

[323] V. Hoang and C. K. Lin, "Cat Ba National Park," *Bangkok, Thailand: Asian Institute of Technology,* 2001.

[324] M. C. Hansen, P. V. Potapov, R. Moore, M. Hancher, S. A. Turubanova, A. Tyukavina, *et al.*, "High-Resolution Global Maps of 21st-Century Forest Cover Change," *Science*, vol. 342, p. 850, 2013.

[325] J. Neha, T. A. M. Edward, W. Natalia, T. Jorge, M.-R. Julian, E. Andrea, *et al.*, "Mapping dynamics of deforestation and forest degradation in tropical forests using radar satellite data," *Environmental Research Letters*, vol. 10, p. 034014, 2015.

[326] E. S. Kasischke, M. A. Tanase, L. L. Bourgeau-Chavez, and M. Borr, "Soil moisture limitations on monitoring boreal forest regrowth using spaceborne L-band SAR data," *Remote Sensing of Environment*, vol. 115, pp. 227-232, 2011/01/17/ 2011.

[327] D. Nong, J. Fox, T. Miura, and S. Saksena, "Built-up Area Change Analysis in Hanoi Using Support Vector Machine Classification of Landsat Multi-Temporal Image Stacks and Population Data," *Land*, vol. 4, p. 1213, 2015.

[328] C. Huang, K. Song, S. Kim, J. R. G. Townshend, P. Davis, J. G. Masek, *et al.*, "Use of a dark object concept and support vector machines to automate forest cover change analysis," *Remote Sensing of Environment*, vol. 112, pp. 970-985, 2008/03/18/ 2008.

[329] E. U. s. Guide, "ENVI on-line software user's manual," *ITT Visual Information Solutions*, 2008.

[330] S. V. Stehman, "Selecting and interpreting measures of thematic classification accuracy," *Remote Sensing of Environment*, vol. 62, pp. 77-89, 1997/10/01 1997.

[331] R. G. Congalton and K. Green, *Assessing the accuracy of remotely sensed data - Principles and Practices*. New York: Lewis Publishers, 1999.

[332] F. Qiu, J. Berglund, J. R. Jensen, P. Thakkar, and D. Ren, "Speckle Noise Reduction in SAR Imagery Using a Local Adaptive Median Filter," *GIScience & Remote Sensing*, vol. 41, pp. 244-266, 2004/09/01 2004.

[333] H. Zhong, Y. Li, and L. Jiao, "SAR Image Despeckling Using Bayesian Nonlocal Means Filter With Sigma Preselection," *IEEE Geoscience and Remote Sensing Letters*, vol. 8, pp. 809-813, 2011.

[334] H. M. Zhu, W. Q. Zhong, and L. C. Jiao, "Combination of Target Detection and Block-matching 3D Filter for Despeckling SAR Images," *Electronics Letters*, vol. 49, pp. 495-497, 2013.

[335] C. Giri, J. Long, S. Abbas, R. M. Murali, F. M. Qamer, B. Pengra, *et al.*, "Distribution and dynamics of mangrove forests of South Asia," *Journal of Environmental Management*, vol. 148, pp. 101-111, 1/15/ 2015.

[336] K. C. Seto and M. Fragkias, "Mangrove conversion and aquaculture development in Vietnam: A remote sensing-based approach for evaluating the Ramsar Convention on Wetlands," *Global Environmental Change,* vol. 17, pp. 486-500, 2007.

[337] B. B. Edward and S. Suthawan, *Shrimp Farming and Mangrove Loss in Thailand*: Edward Elgar Publisher, 2004.

[338] E. B. Barbier, M. C. Acreman, and D. Knowler, *Economic valuation of wetlands: A guide for policy markets and planners*. Gland: Ramsar Convention Bureau, Switzerland, 1997.

[339] M. Gunawardena and J. S. Rowan, "Economic valuation of a mangrove ecosystem threatened by shrimp aquaculture in Sri Lanka," *Environ Manage,* vol. 36, 2005.

[340] A. Ekka and A. Pandit, "Willingness to pay for restoration of natural ecosystem: A study of Sundarban mangroves by contingent valuation approach," *Indian Journal of Agricultural Economics,* vol. 67, p. 323, 2012.

[341] K. N. Ninan and A. Kontoleon, "Valuing forest ecosystem services and disservices – Case study of a protected area in India," *Ecosystem Services,* vol. 20, pp. 1-14, 8// 2016.

[342] K. Stone, M. Bhat, R. Bhatta, and A. Mathews, "Factors influencing community participation in mangroves restoration: A contingent valuation analysis," *Ocean & Coastal Management,* vol. 51, pp. 476-484, // 2008.

[343] R. R. Lewis, "Methods and Criteria for Successful Mangrove Forest Restoration," in *Coastal Wetlands: An integrated ecosystem approach*, G. M. E. Perillo, E. Wolanski, D. R. Cahoon, and M. M. Brinson, Eds., ed Oxford: Elsevier, 2009.

[344] N. Kaida and N. A. Dang, "Economic Valuation of the Nha Trang Bay Marine Protected Area: A Willingness to Pay Survey on the Conservation Programs " *Journal of Environmental Information Sciences,* vol. 24, pp. 33-40, 2014.

[345] T. H. Tuan, N. H. D. My, L. T. Q. Anh, and N. V. Toan, "Using contingent valuation method to estimate the WTP for mangrove restoration under the context of climate change: A case study of Thi Nai lagoon, Quy Nhon city, Vietnam," *Ocean & Coastal Management,* vol. 95, pp. 198-212, 7// 2014.

[346] Hai Phong Statistical Office, *Hai Phong Statistics yearbook 2015*. Hai Phong, Vietnam, 2015.

[347] N. T. Son, J. J. Pigram, and B. A. Rugendyke, "Cat Ba Island National Park, Vietnam," *Contemporary issues in tourism development,* vol. 6, p. 209, 1999.

[348] N. C. Nguyen and O. J. Bosch, "A systems thinking approach to identify leverage points for sustainability: a case study in the Cat Ba Biosphere Reserve, Vietnam," *Systems Research and Behavioral Science,* vol. 30, pp. 104-115, 2013.

[349] World Bank *World Development Indicators 2012*: World Bank Publications, 2012.

[350] T. C. Haab and K. E. McConnell, *Valuing environmental and natural resources: the econometrics of non-market valuation*: Edward Elgar Publishing, 2002.

[351] N. Powell, M. Osbeck, S. B. Tan, and V. C. Toan, "Mangrove restoration and rehabilitation for climate change adaptation in Vietnam," *World Resources Report Case Study. World Resources Report, Washington DC. URL: http://www.worldresourcesreport.org*, 2011.

[352] C. Kuenzer, A. Bluemel, S. Gebhardt, T. V. Quoc, and S. Dech, "Remote Sensing of Mangrove Ecosystems: A Review," *Remote Sensing*, vol. 3, pp. 878-928, 2011.

[353] K. G. Holly, B. Sandra, O. N. John, and A. F. Jonathan, "Monitoring and estimating tropical forest carbon stocks: making REDD a reality," *Environmental Research Letters*, vol. 2, p. 045023, 2007.

[354] L. V. Dung, N. T. Tue, M. T. Nhuan, and K. Omori, "Carbon storage in a restored mangrove forest in Can Gio Mangrove Forest Park, Mekong Delta, Vietnam," *Forest Ecology and Management*, vol. 380, pp. 31-40, 11/15/ 2016.

[355] N. T. Tue, L. V. Dung, M. T. Nhuan, and K. Omori, "Carbon storage of a tropical mangrove forest in Mui Ca Mau National Park, Vietnam," *CATENA*, vol. 121, pp. 119-126, 10// 2014.

[356] K. O. Were, B. D. Tien, Ø. B. Dick, and B. R. Singh, "A novel evolutionary genetic optimization-based adaptive neuro-fuzzy inference system and GIS predict and map soil organic carbon stocks across an Afromontane landscape," *Pedosphere*, 2017/08/05/ 2017.

[357] K. Were, D. T. Bui, Ø. B. Dick, and B. R. Singh, "A comparative assessment of support vector regression, artificial neural networks, and random forests for predicting and mapping soil organic carbon stocks across an Afromontane landscape," *Ecological Indicators*, vol. 52, pp. 394-403, 2015/05/01/ 2015.

Appendices

Appendix 1: Household Questionnaire

Willingness to pay for Mangrove Ecosystem Services:
A case study in Cat Ba Biosphere Reserve, Vietnam

We want to know your experiences, thoughts and choices about Cat Ba Biosphere Reserve and Mangrove Ecosystem Services

My name is Pham Tien Dat. I am a research fellow at the Center for Agricultural Research and Ecological Studies (CARES), Vietnam National University of Agriculture. Currently, I am doing a PhD in Environmental Policy at Graduate School of Systems and Information Engineering, the University of Tsukuba, Japan. I would like to seek your points of view on the mangrove conservation and management of this Biosphere Reserve. Your response in this survey will provide useful insights to policy making regarding the design of effective mangrove conservation programs in Cat Ba Biosphere Reserve. I would be highly appreciated if you could take your time to answer this questionnaire. Responses are strictly confidential and there are no correct or wrong answers. I just want to know your opinion. Thank you very much for your cooperation and your time.

Name of Enumerator: _____
Date: _____
Time started: _____
Time Ended: _____

Part I: Information about yourself

1. Age _____

2. Gender: Male _____ Female_____

3. Nationality: _____

If local citizen, skip question #4 and proceed to #5.

4. 1) I am a permanent resident 2) I am a tourist

5. Occupation

1) Governmental official
2) Own business
3) Private sector
4) Laborer
5) Farmer
6) Student
7) Retirement
8) Other (please specify)

6. Number of members in your family _____

7. Do you have children? Yes _____ No _____

8. Which is the highest level of education you have completed or you are in process of completing?

1) Less than primary school
2) Primary school
3) Secondary school
4) High school
5) Technical school
6) University
7) Postgraduate

9. How much for households monthly income? _____VND/_____USD

10. What is the status of your house?

1) Permanent house 2) Semi-permanent house 3) Temporary house

11. What are your household's assets?

Yes	Name of asset	Yes	Name of asset
1	Motorbike	5	TV
2	Refrigerator	6	Computer/Laptop
3	Air conditioning	7	Cooking stove (Microwave oven)
4	Telephone/mobile phones	8	Other (please specify)

12. Which nature park in Vietnam have you been in your life?

1) Cat Ba Biosphere Reserve 2) Cat Tien National Park 3) Can Gio Biosphere Reserve
4) Cu Lao Cham- Hoi An 5) Kien Giang Reserve 6) Red River Delta
7) West Nghe An 8) Ca Mau Reserve

13. How many times have you been in Cat Ba Biosphere Reserve?

14. Did you know about Cat Ba Biosphere Reserve before the visit?

Yes _____ No _____

15. If you have already been in Cat Ba Biosphere Reserve, what are the main purposes of the visit (you can circle more than one)

1) Swimming _____ 2) Bird watching_____ 3) Mount Climbing _____
4) Cave sightseeing _____ 5) Community meeting _____ 6) Support conservation _____
7) Other (please specify) _____

16. Have you ever been in mangrove forests of Cat Ba Biosphere Reserve? What are the main purposes?

1) Collect NTFPs (non-timber forest products) _____ 2) Sea crab and other resources catching_____
3) Forestry products (charcoal, poles) _____ 4) Support conservation _____
5) Other (please specify)_____

Part 2: General Information on Mangroves in Cat Ba National Biosphere Reserve

In this section, we provide information about the current status of Cat Ba National Biosphere Reserve and the future proposed conditions also known as improved scenarios. Please read this well and then answer the follow up questions.

Mangroves in Cat Ba Biosphere Reserve is primary forest and their ecosystems are considered as high biodiversity and provide a wide range of benefits to humans including supporting local likelihoods for local communities. They also provide various ecosystem services such as: supporting services (nutrient cycling, nursing seedlings, primary production), provisioning services (food, fiber and fuel), regulating services (storm prevention, pollution reduction, flood and erosion control, carbon/climate storage), and cultural services (education and recreational).

17. Please let us know your opinion on mangrove conservation and protection

1) strongly agree 2) agree
3) no opinion neither agree nor disagree 4) disagree
5) strongly disagree

18. There are some reasons for mangrove conservation and protection in Cat Ba Biosphere Reserve Please let us know your idea

Reasons for mangrove conservation	**Not very important**	**Not important**	**No opinion**	**Important**	**Very important**
	1	2	3	4	5
- Improve sustainable local livelihood					
- Provide recreational value					
- Provide services: Supporting services					
- Provide services: provisioning services					
- Provide services: regulating services					
- Provide services: culture services					
- Help protect biodiversity					
- Provide opportunities and benefits for future generations					

19. What are benefits do you currently receive from mangrove forests and their resources? Choose any

1) No benefit 2) do know
3) Seafood collection: sea crab, fish 4) income from seafood
5) Recreation 6) forestry products (poles/charcoal)
7) research/education 8) habitat for wildlife
9) Flood and storm prevention/soil erosion/ environmental protection
10) Benefit for next generation
11) Other (please specify)

20. Are you likely to visit the mangrove forests in the next 5 years?

1. Yes/ 0. No/unlikely

Part 3: Problems associated with mangrove resources and management

The area mangrove forests in Cat Ba Biosphere Reserve decreased significantly over the past 20 years due to government policies that encouraged conversion to shrimp aquaculture for export and over expansion of tourism services to attract more tourists. Therefore, the local community is more vulnerable to climate change impacts especially during stormy seasons.

One of the greatest risks is the impact of climate change and rising sea levels. The flooded area is located on some villages of Phu Long and Gia Luan communes. The flooded areas have a high density which is likely due to tropical cyclones.

Cat Ba Biosphere Reserve is directly vulnerable to hazards caused by the impacts of climate change such as: storm, flooding, coastal erosion and pollution. These hazards can result in disasters involving damage to property, facilities and infrastructure for communities and households. The biggest challenge therefore is how to sustainably manage the importance of mangrove forests in dealing with climate change impacts.

Recognizing the problems, Department of Natural Resources and Environment and Management Board of Cat Ba Biosphere Reserve together with Center for Agricultural Research and Ecological Studies, VN National University of Agriculture proposed a mangrove conservation and management plan in some communes of Cat Ba National Park.

The main objectives of this conservation program include:

- Raising awareness of local community on the importance of mangrove forests.
- Preventing illegal logging
- Promoting mangrove planting and maintenance of recreational facilities to reduce impacts of climate change
- Contributing to ecologically sustainable and climate resilient

Please see the pictures attached in the first page and answer the questions

21. Is this information listed above new to you?

1) Yes. Very new
2) Only some of it is new
3) I already know all information

22. How severe in your opinion is the likely damage to the mangroves of Cat Ba Biosphere Reserve if the trend highlighted above continues?

1) Very severe
2) Severe
3) Not so severe
4) Not at all

23. Mangrove Conservation activities in Cat Ba Biosphere Reserve: Options.

This section provides options of mangrove conservation activities proposed to improve the status of mangrove forests in Cat Ba Biosphere Reserve.
Please read the alternatives thoroughly and choose only one option from the possible 5 options by ticking below the option (√).

Please keep in mind that in this kind of surveys people often tend to overstate their willingness to pay to contribute to the proposed project.

Activities of Mangroves in Cat Ba Biosphere Reserve	**OPTION 1**	**OPTION 2**	**OPTION 3**	**OPTION 4**	**OPTION 5**
Entrance fee (USD)	1	2	4	3	
Afforestation and catchment protection					
Protection from illegal logging					STATUS QUO = NEITHER OPTIONS
Maintenance of recreation facilities					
Planting Mangrove and protection to reduce impacts of Climate change					
(Please select one) (√)	☐	☐	☐	☐	☐

Part 3. WILLINGNES TO PAY

Cat Ba Biosphere Reserve conservation faces a severe funding limitation to implement various activities such as mangrove conservation and protection, maintenance of recreational facilities and biodiversity conservation among others.
To generate revenues for the implementation of these activities, Cat Ba Biosphere Reserve Management Board through the Department of Natural Resource and Environment would want to introduce an entrance fee or Biodiversity fund in order to protect and restore the mangroves of CBBR

Suppose the money raised by the fund will **only** be used to protect and conserve the mangroves of Cat Ba Biosphere Reserve. Please keep it in mind:

- This interview is about mangroves of Cat Ba Biosphere Reserve and not about other environmental problems or other mangroves around the country.
- There are no right or wrong answers, we would like to know your points of view

Please answer question 24, to show your willingness to pay.

24. Are you willing to pay **(bid level)** a year to protect and conserve the mangroves of Cat Ba Biosphere Reserves? (Bid levels will be designed via focus group discussions and key informant interviews)

Yes ☐ No ☐

25. If YES, what was it that made you willing to vote for the conservation programs? (Check the most appropriate answer)

I think the mangrove conservation program is a good case	1
I think this is a reasonable amount of money to pay	2
I am considered about the loss of biodiversity and mangroves in the Cat Ba Biosphere Reserve	3
I am worried about flooding during stormy seasons	4
I wish I could pay but I am not sure	5
I don't know/not applicable	6
Other (please specify)	7

26. If NO, can you please tell me why you would vote against the conservation programs? (Check the most appropriate answer)

I do not have the financial capability to pay	1
I think it is the government's responsibility	2
I think the users should pay	3
I think tourist company should pay	4
I believe that the situation will be better without my contribution	5
I feel that mangrove conservation programs in Cat Ba Biosphere Reserve is unimportant	6
I do not care for the nature conservation issues in the area	7
I do not have enough information about mangrove conservation measures	8
Don't know/not application	9
Other (please specify)	10

27. Under the current situation instead of paying anything to the biodiversity fund, would you be willing to be a volunteer to help or contribute to conservation actives of mangroves in Cat Ba Biosphere Reserve?
If yes, how many hours per month you could be involved in as a volunteer?
If No, please tell why?

28. Do you have any comments/suggestions about this interview?

END OF QUESTIONAIRE
THANKS SO MUCH FOR YOUR COOPERATION